

11/10/96
11/10/96

NASA Contractor Report 195480

Improved NASA-ANOPP Noise Prediction
Computer Code for Advanced Subsonic
Propulsion Systems
Volume 1: ANOPP Evaluation and Fan Noise Model
Improvement

K. B. Kontos, B. A. Janardan, and P. R. Gliebe
GE Aircraft Engines
Cincinnati, OH

August, 1996

Prepared for
NASA Lewis Research Center
Under Contract NAS3-26617
Task Order Number 24

NASA

Table of Contents

List of Figures.....	iv
List of Tables.....	v
Nomenclature.....	vi
1.0 Summary.....	1
2.0 Introduction.....	2
3.0 Results and Discussion -- ANOPP Evaluation.....	3
3.1 Overall Results.....	6
3.2 Fan Inlet Noise.....	10
3.3 Fan Exhaust Noise.....	12
3.4 Jet Noise.....	14
3.5 Combustor Noise.....	16
3.6 Turbine Noise.....	18
4.0 Results and Discussion -- Fan Noise Model Improvements.....	21
4.1 Fan Inlet Broadband Noise.....	22
4.2 Fan Exhaust Broadband Noise.....	25
4.3 Fan Inlet Discrete Tone Noise.....	27
4.4 Fan Exhaust Discrete Tone Noise.....	32
4.5 Directivity.....	34
4.6 Combination Tone Noise.....	37
4.7 Summary of Fan Noise Methodology Changes.....	43
5.0 Concluding Remarks.....	45
Appendix A. Sample ANOPP Input.....	46
Appendix B. Fan Inlet Noise Spectral Comparisons - CF6-80C2.....	50
Appendix C. Fan Inlet Noise Spectral Comparisons - E ³	63
Appendix D. Fan Inlet Noise Spectral Comparisons - QCSEE.....	70
Appendix E. Fan Exhaust Noise Spectral Comparisons - CF6-80C2.....	77
Appendix F. Fan Exhaust Noise Spectral Comparisons - E ³	102
Appendix G. Fan Exhaust Noise Spectral Comparisons - QCSEE.....	109
Appendix H. Jet Noise Spectral Comparisons, 150 degrees.....	116
Appendix I. Combustor Noise Spectral Comparisons, 120 degrees.....	120
Appendix J. Turbine Noise Spectral Comparisons, 120 degrees.....	124
Appendix K. Directivity, CF6-80C2 and QCSEE.....	128
Appendix L. Combination Tone Noise Spectra - CFM56.....	133
Appendix M. Combination Tone Noise Spectra - CF6-80C2.....	142
6.0 References.....	147

List of Figures

Figure 3.0.1 CF6-80C2 Engine.....	3
Figure 3.0.2 E ³ Engine.....	3
Figure 3.0.3 QCSEE Engine.....	4
Figure 3.0.4 Sample E ³ Component Noise Spectrum.....	6
Figure 3.1.1 ANOPP Summary, CF6-80C2, forward peak angle.....	7
Figure 3.1.2 ANOPP Summary, E ³ , forward peak angle.....	7
Figure 3.1.3 ANOPP Summary, QCSEE, forward peak angle.....	8
Figure 3.1.4 ANOPP Summary, CF6-80C2, aft peak angle.....	8
Figure 3.1.5 ANOPP Summary, E ³ , aft peak angle.....	9
Figure 3.1.6 ANOPP Summary, QCSEE, aft peak angle.....	9
Figure 3.2.1 Fan Inlet Noise Spectrum, CF6-80C2.....	11
Figure 3.2.2 Fan Inlet Noise Spectrum, E ³	11
Figure 3.2.3 Fan Inlet Noise Spectrum, QCSEE.....	12
Figure 3.3.1 Fan Exhaust Noise Spectrum, CF6-80C2.....	13
Figure 3.3.2 Fan Exhaust Noise Spectrum, E ³	13
Figure 3.3.3 Fan Exhaust Noise Spectrum, QCSEE.....	14
Figure 3.4.1 Jet Noise Spectrum, CF6-80C2.....	15
Figure 3.4.2 Jet Noise Spectrum, E ³	15
Figure 3.4.3 Jet Noise Spectrum, QCSEE.....	16
Figure 3.5.1 Combustor Noise Spectrum, CF6-80C2.....	17
Figure 3.5.2 Combustor Noise Spectrum, E ³	17
Figure 3.5.3 Combustor Noise Spectrum, QCSEE.....	18
Figure 3.6.1 Turbine Noise Spectrum, CF6-80C2.....	19
Figure 3.6.2 Turbine Noise Spectrum, E ³	19
Figure 3.6.3 Turbine Noise Spectrum, QCSEE.....	20
Figure 3.6.4 Turbine Noise Adjustment.....	20
Figure 4.1.1 “Figure 4a” CF6-80C2 Fan Inlet Broadband Noise.....	23
Figure 4.1.2 “Figure 4a” E ³ Fan Inlet Broadband Noise.....	24
Figure 4.1.3 “Figure 4a” QCSEE Fan Inlet Broadband Noise.....	24
Figure 4.2.1 “Figure 4b” CF6-80C2 Fan Exhaust Broadband Noise.....	25
Figure 4.2.2 “Figure 4b” E ³ Fan Exhaust Broadband Noise.....	26
Figure 4.2.3 “Figure 4b” QCSEE Fan Exhaust Broadband Noise.....	27
Figure 4.3.1 “Figure 10a” CF6-80C2 Fan Inlet Tone.....	28
Figure 4.3.2 “Figure 10a” E ³ Fan Inlet Tone.....	29
Figure 4.3.3 “Figure 10a” QCSEE Fan Inlet Tone.....	29

List of Figures (continued)

Figure 4.4.1 “Figure 10b” CF6-80C2 Fan Exhaust Tone.....	32
Figure 4.4.2 “Figure 10b” E3 Fan Exhaust Tone.....	33
Figure 4.4.3 “Figure 10b” QCSEE Fan Exhaust Tone.....	33
Figure 4.5.1 “Figure 7a” Fan Inlet Broadband Directivity Correction.....	34
Figure 4.5.2 “Figure 13a” Fan Inlet Tone Directivity Correction.....	35
Figure 4.5.3 “Figure 7b” Fan Exhaust Broadband Directivity Correction.....	35
Figure 4.5.4 “Figure 13b” Fan Exhaust Tone Directivity Correction.....	36
Figure 4.6.1 “Figure 14” Combination Tone Noise Spectrum Content.....	37
Figure 4.6.2 Combination Tone Noise Spectra, CFM56, $M_q = 1.2$	38
Figure 4.6.3 Combination Tone Noise Spectra, CFM56, $M_q = 1.32$	39
Figure 4.6.4 Combination Tone Noise Spectra, CFM56, $M_q = 1.43$	39
Figure 4.6.5 “Figure 15” Combination Tone Noise, $f/f_b = 1/2$	40
Figure 4.6.6 “Figure 15” Combination Tone Noise, $f/f_b = 1/4$	41
Figure 4.6.7 “Figure 15” Combination Tone Noise, $f/f_b = 1/8$	41

List of Tables

Table 3.0.1 Engine Summary - Typical Takeoff Condition.....	4
Table 3.2.1 Rotor Tip Relative Inlet Mach Number	10
Table 4.3.1 Flight Cleanup Suppression Table.....	31
Table 4.6.1 Combination Tone Noise Levels.....	42

Nomenclature

ANOPP.....	Aircraft Noise Prediction Program
B.....	number of fan blades
BPF.....	blade passing frequency
dB.....	decibel
E ³	Energy Efficient Engine
f/f_b	ratio of frequency to BPF frequency
F _n	normalized SPL
GE.....	General Electric
IGV.....	inlet guide vane
k.....	harmonic order
L _c	characteristic peak SPL, dB
L _n	normalized peak sound pressure level, dB
m.....	airflow, lb/s
m _o	reference airflow, lb/s
M _t	fan blade tip Mach number
M _t or MTR.....	rotor tip relative inlet Mach number
M _{td} or MTRD.....	rotor tip relative inlet Mach number at fan design point
MPT.....	multiple pure tone
NASA.....	National Aeronautics and Space Administration
RSS.....	Rotor/Stator Spacing (in % of blade chord length)
SPL.....	Sound Pressure Level, dB
ΔT.....	delta T (total temperature rise across fan stage), deg R
ΔT _o	reference value of ΔT, 1 deg R
TCS.....	turbulence control screen
UHB.....	Ultra High Bypass
V.....	number of stator vanes
QCSEE.....	Quiet, Clean, Short Haul Experimental Engine
δ.....	fan inlet tone cutoff ratio
θ.....	Angle relative to engine inlet, deg.

1.0 Summary

Recent experience using ANOPP (Aircraft Noise Prediction Program) to predict turbofan engine flyover noise suggests that it over-predicts overall EPNL by a significant amount. An improvement in this prediction method is desired for system optimization and assessment studies of advanced UHB engines.

An assessment of the ANOPP fan inlet, fan exhaust, jet, combustor, and turbine noise prediction methods was made using static engine component noise data from the CF6-80C2, E³, and QCSEE turbofan engines. It was shown that the ANOPP prediction results are generally higher than the measured GE data, and that the fan inlet noise prediction method (Heidmann method) is the most significant source of this overprediction. Fan noise spectral comparisons show that improvements to the fan tone, broadband, and combination tone noise models are required to yield results that more closely simulate the GE data.

Suggested changes that yield improved fan noise predictions but preserve the Heidmann model structure were identified and are described herein. These changes are based on the engine data sets mentioned above, as well as additional CFM56 engine data that was used to expand the combination tone noise database. It should be noted that the recommended changes are based on an analysis of engines that are limited to single stage fans with design tip relative mach numbers greater than one.

2.0 Introduction

The purpose of the Aircraft Noise Prediction Program is to predict aircraft noise with the best currently available methods (Gillian, 1982). The task of predicting the aircraft noise is divided into four areas within ANOPP:

1. Aircraft Flight Definition
2. Source Noise Modeling
3. Propagation and Ground Effects
4. Noise Calculations

The work described in this report is concerned entirely with the Source Noise Modeling portion of the ANOPP program. In keeping with the promise of ANOPP to contain the best methods available, an industry-established reputation for over-prediction, and the need to refine ANOPP for the completion of advanced UHB studies, GE was provided with the task of evaluating the engine source noise models in ANOPP. The evaluation of ANOPP was made by comparing fan, jet, combustor, and turbine noise prediction model results with GE data on a static, single engine basis.

The results of these comparisons identified that the Heidmann fan noise model contained in ANOPP was contributing significantly to the trend of noise over-prediction, and under the existing contract, GE was given the task of resolving this problem. Rather than replace the fan noise model in its entirety, it was recommended by NASA that the basic Heidmann model be retained, but modified to yield results that would more closely predict the commercial turbofan noise.

Each part of the Heidmann fan noise prediction model was carefully evaluated relative to three GE databases -- CF6-80C2, E³, and QCSEE. A CFM engine database was also used to expand the combination tone database in order to evaluate that part of the model. Volume 1 of this report presents the results of the ANOPP fan, jet, combustor, and turbine noise module assessment. Also included are specific recommendations for changes to the Heidmann fan noise model (Heidmann, 1979) that were determined to yield results in closer agreement with these databases.

Volume 2 of this report (to be published at a later date) will describe the results of ongoing work relative to the correlation of fan inlet and fan exhaust noise suppression with various treatment design parameters. This follow-on work is an enhancement to the Heidmann method, which currently predicts noise for only hardwall engine nacelles.

3.0 Results and Discussion -- ANOPP Evaluation

An assessment of ANOPP was carried out to evaluate the ability of ANOPP to predict engine component noise of high bypass ratio engines. Predictions were made for representative engines for which detailed noise measurements were available. These engines were the CF6-80C2 (Biebel, J., and Hoerst, D., "Acoustic Data Report for CF6-80C2", GE TM #87-80, 1987, private communication), The Energy Efficient Engine (E³) (Lavin et al., 1978), and the Quiet Clean Short-Haul Experimental Engine (QCSEE) (Stimpert, 1979). Cross-sections of each engine are shown in Figures 3.0.1, 3.0.2, and 3.0.3. A summary of general cycle and geometry information for these three engines is given in Table 3.0.1.

Figure 3.0.1 CF6-80C2 Engine

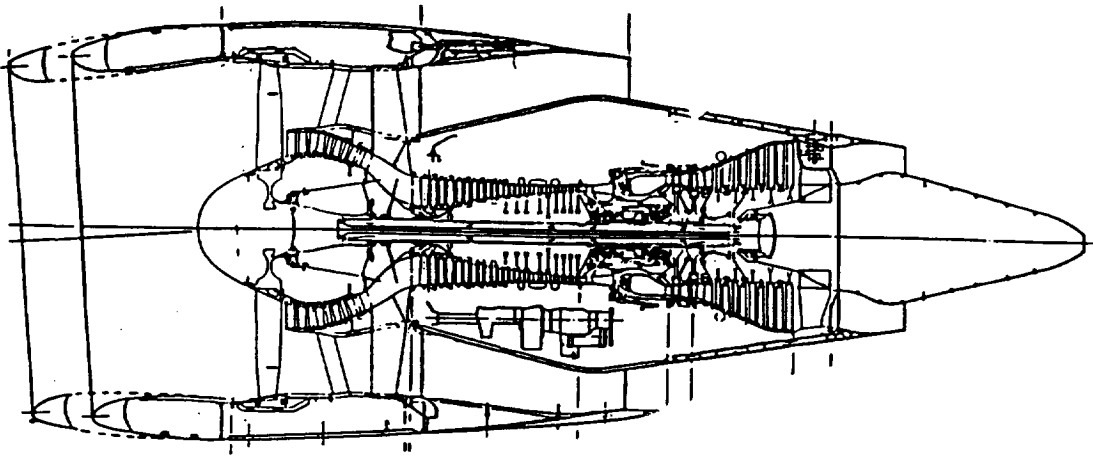


Figure 3.0.2 E³ Engine

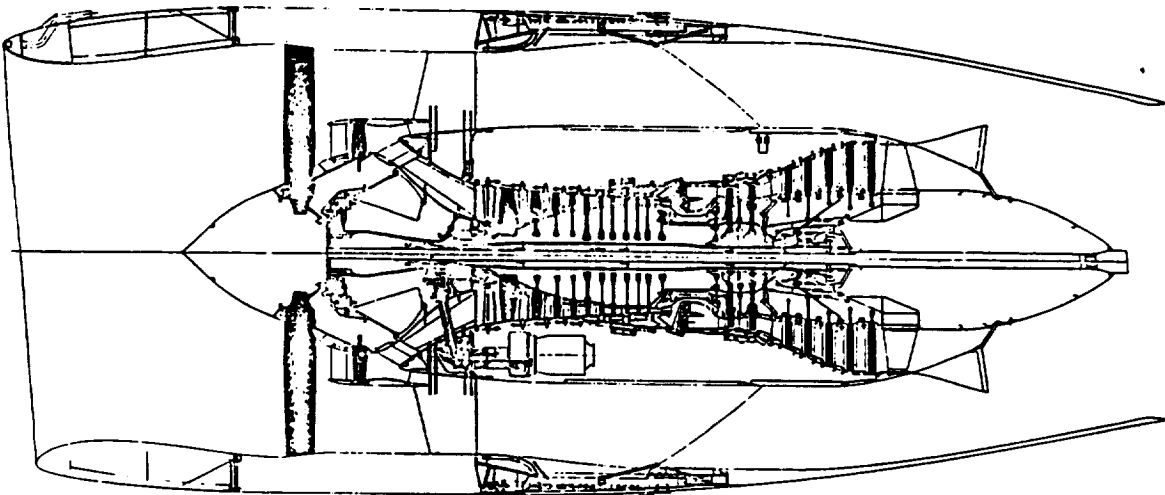


Figure 3.0.3 QCSEE UTW (Under The Wing) Engine

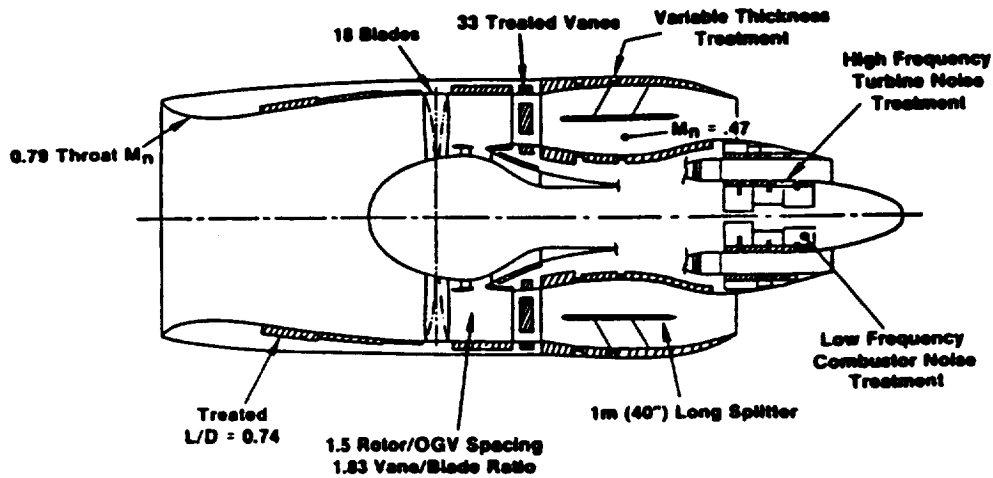


Table 3.0.1 Engine Summary -Typical Takeoff Condition

	<u>CF6</u>	<u>E³</u>	<u>QCSEE</u>
FN	57	32	19 K lbs
BPR	5.0	7.7	12.1
tip speed	1434	1123	956 ft/s
Core jet velocity	1577	889	868 ft/s
Exhaust type	separate	mixed	separate
PR	1.8	1.4	1.3
Fan Treatment	hardwall	hardwall	hardwall

In order to assess the ANOPP source noise models, the following component noise predictions were made:

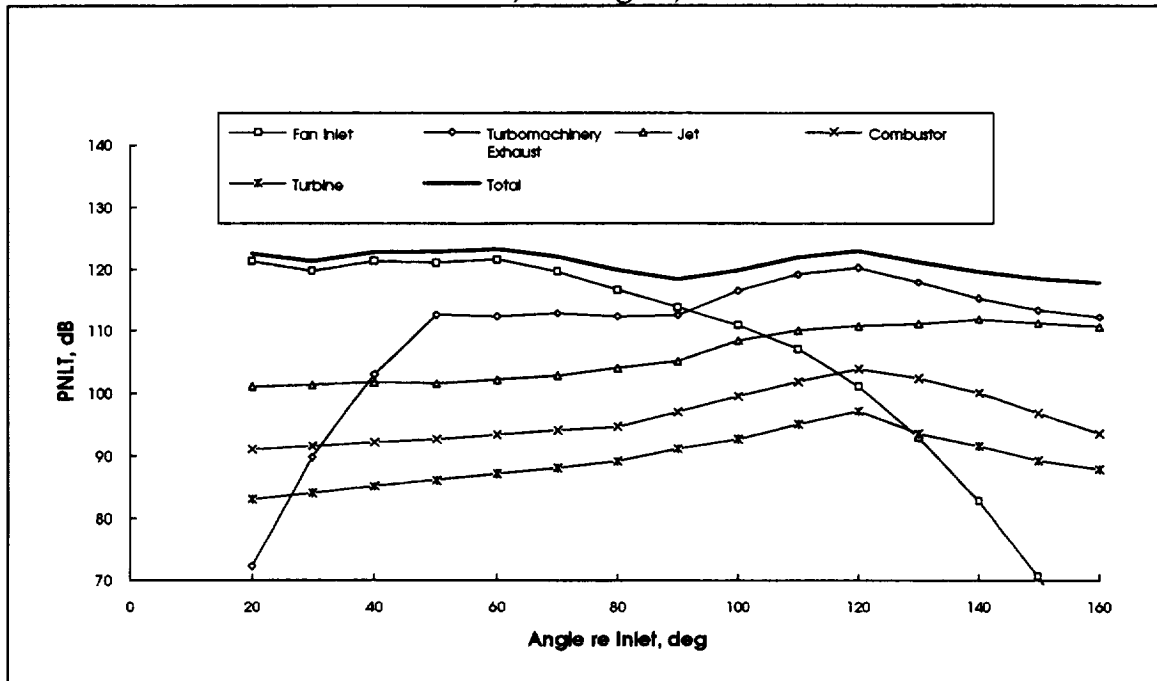
<u>Component</u>	<u>ANOPP Module</u>
fan	- HDNFAN
jet	- STNJET
combustor	- GECOR
turbine	- GETUR

Predictions were made for each of three engines: the CF6-80C2, E³, and QCSEE.

All predictions were made for a static, single engine on a 150 ft arc, and were made on the VAX system using ANOPP version 03/02/10. For each engine, typical takeoff, cutback, and approach conditions were predicted. These conditions were selected to facilitate comparison with the existing GE engine component noise database. A sample ANOPP input listing (E³ takeoff case) is given in Appendix A.

The GE in-house component noise databases are created by using engine geometry and cycle information in order to split the measured static acoustic data into jet, fan inlet, and turbomachinery exhaust components. Figure 3.0.4 shows a typical E³ component database generated for the takeoff condition. The combustor and turbine noise predictions shown were made using GE in-house prediction methods.

**Figure 3.0.4 Sample E' Component Noise
150 ft arc, one engine, Takeoff**



For the E³ and QCSEE engines, the GE database used was for a hardwall fan inlet and fan exhaust. For the CF6-80C2, a treated fan inlet and fan exhaust database was used (a hardwall fan exhaust database did not exist at the time this work was completed). In order to compare the ANOPP predictions with the CF6-80C2 database, calculated treatment suppressions were applied to the ANOPP fan inlet and fan exhaust component results.

3.1 Overall Results

Figures 3.1.1 -- 3.1.6 show summaries on a spectral basis of the ANOPP component predictions for all three engines at the takeoff condition. For each engine, there are separate plots for both the peak forward and peak aft angles. The heavy, solid line represents the total measured engine noise, and the solid squares represent a static SPL sum of all of the ANOPP components. These plots show how well ANOPP predicts total engine noise, and indicate where particular ANOPP component predictions are yielding noise levels greater than the total engine noise.

Figure 3.1.1 ANOPP Component Summary, CF6-80C2, forward angle, takeoff, 150 ft arc, one engine

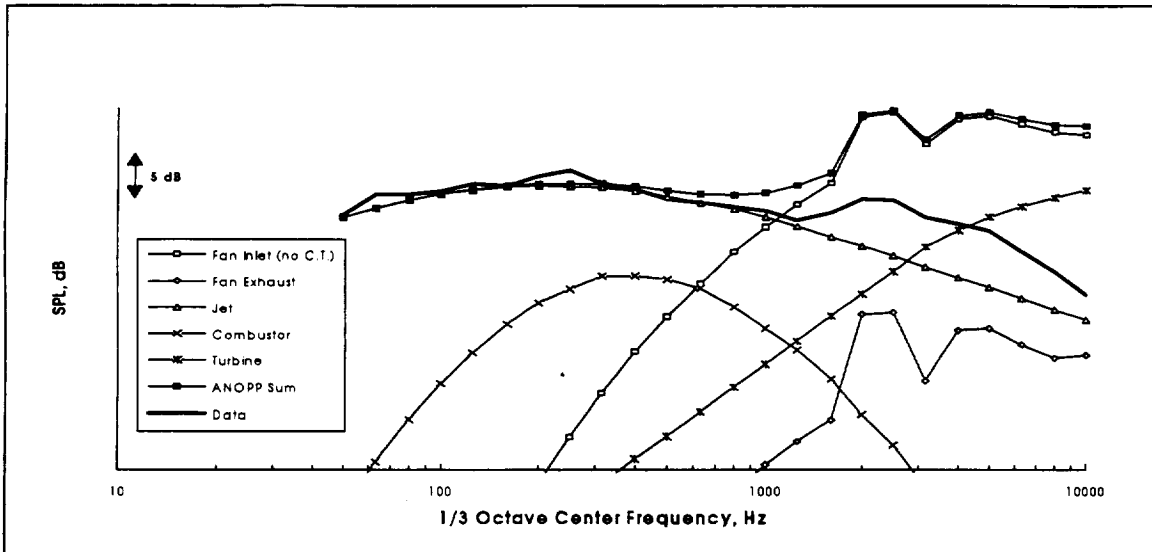


Figure 3.1.2 ANOPP Component Summary, E3, forward peak angle, takeoff, 150 ft arc, one engine

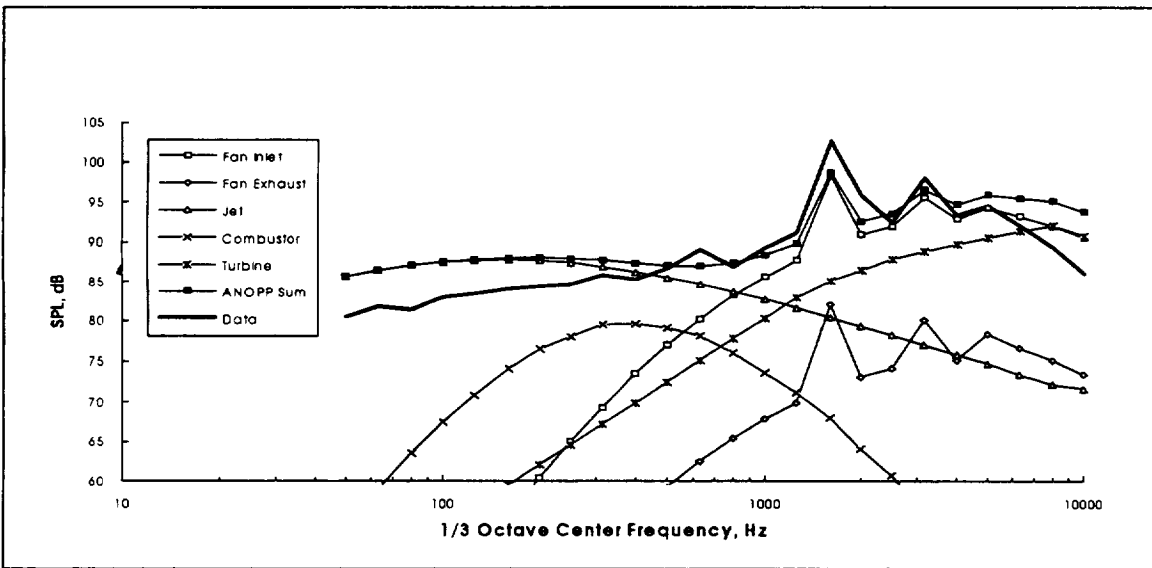


Figure 3.1.3 ANOPP Component Summary, QCSEE, forward angle, takeoff, 150 ft arc, one engine

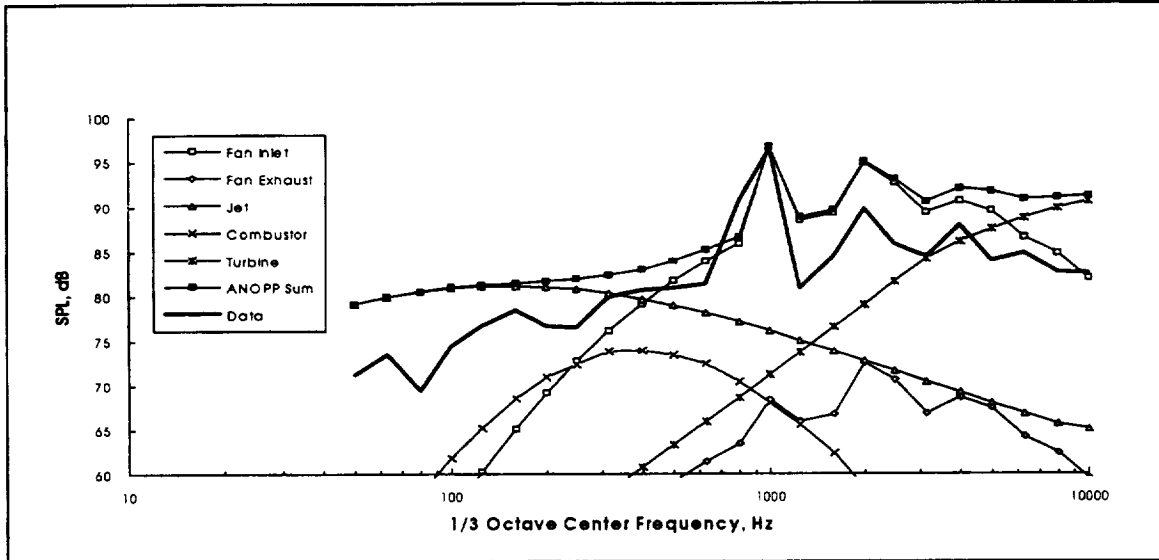


Figure 3.1.4 ANOPP Component Summary, CF6-80C2, aft angle, takeoff, 150 ft arc, one engine

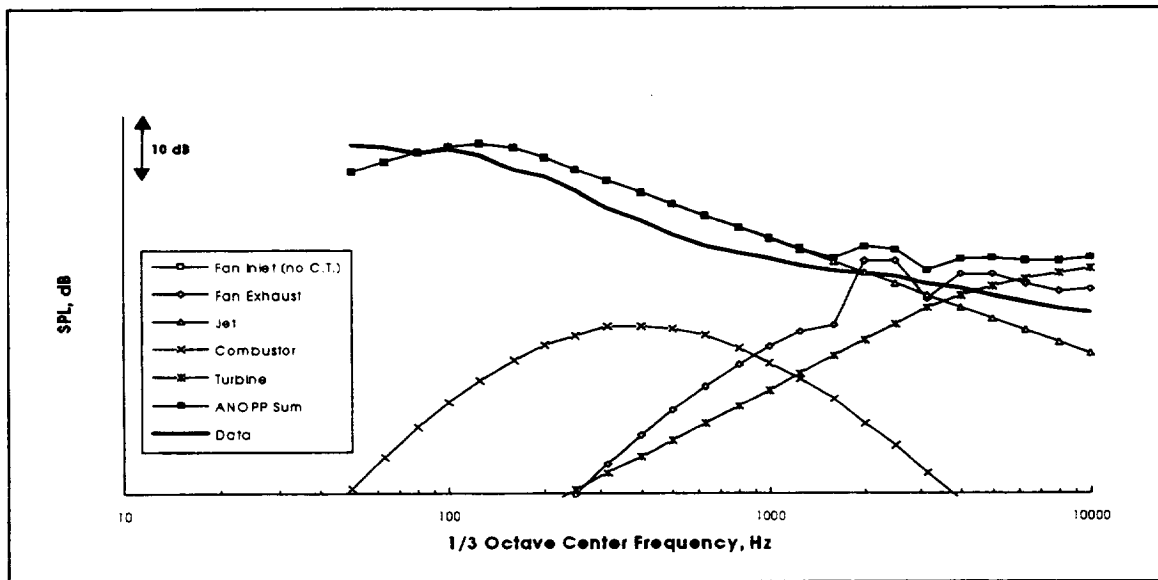


Figure 3.1.5 ANOPP Component Summary, E³, aft angle, takeoff, 150 ft arc, one engine

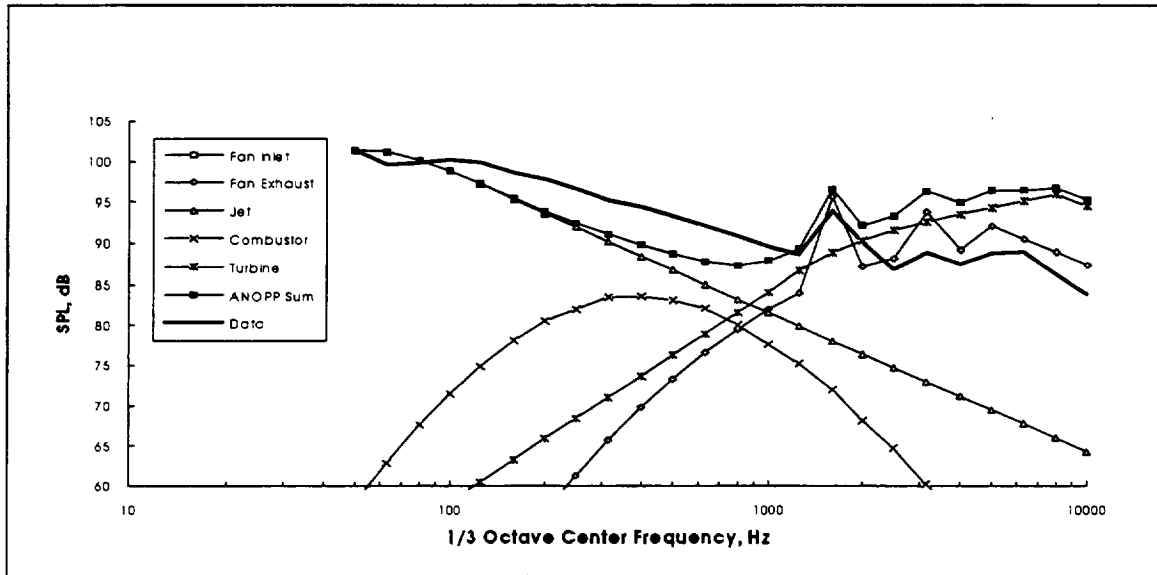
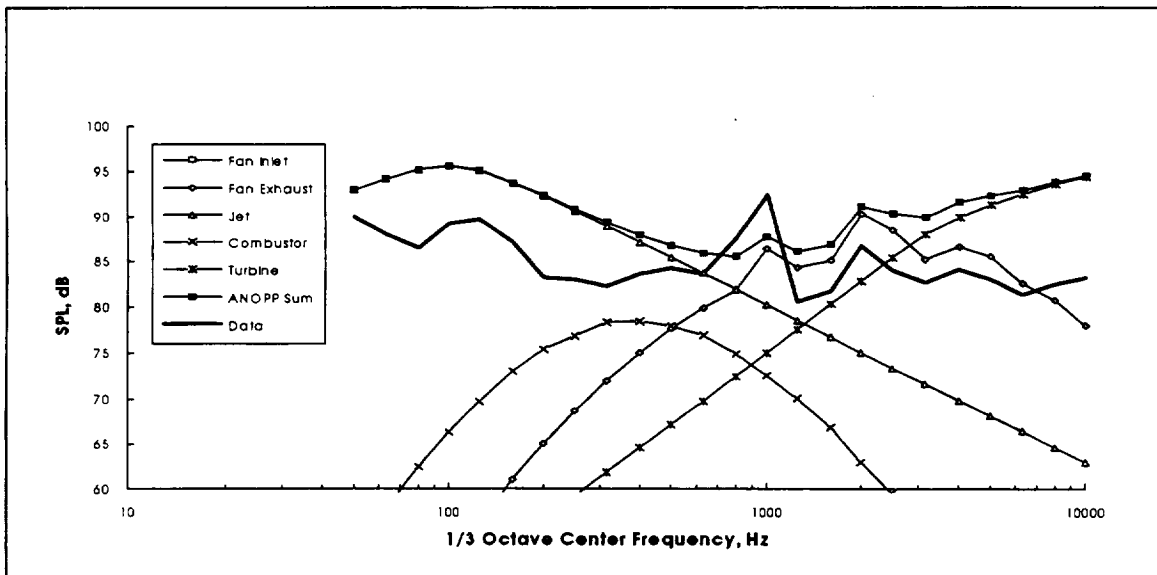


Figure 3.1.6 ANOPP Component Summary, QCSEE, aft angle, takeoff, 150 ft arc, one engine



The general results for each noise component are presented in the following subsections. Because of the large amount of data, only selected charts are shown in this section. For each component, a peak angle spectrum at the takeoff condition for each of the three engines is shown. Additional charts are given in Appendices B-J.

3.2 Fan Inlet Noise

General Results

The data show that the fan inlet noise ANOPP results depend heavily on the fan tip relative Mach number (M_{tr}). At a subsonic value ($M_{tr} < 1$), ANOPP shows a slight underprediction relative to the GE component database (0.5 - 5 dB). At higher tip speeds (such as for the CF6-80C2 engine at typical takeoff and cutback conditions), the ANOPP results show a significant overprediction (11 - 19 dB). This overprediction is due largely to the combination tone noise model in ANOPP. The amount of overprediction seems related to the value of M_{tr} ; the greater the value, the greater the degree of overprediction. M_{tr} values and the range of M_{tr} values covered in the databases are as follows:

Table 3.2.1 Rotor Tip Relative Inlet Mach Number

Engine	M_{tr}	M_{tr} Range
CF6-80C2	1.53	0.65 -- 1.53
E ³	1.14	0.64 -- 1.14
QCSEE	1.01	0.89 -- 1.01

Results -- Takeoff

One-third octave spectra from the peak forward angle are shown in Figures 3.2.1, 3.2.2, and 3.2.3 for takeoff conditions of the CF6-80C2, E³, and QCSEE engines, respectively. A large overprediction by ANOPP is shown relative to the CF6-80C2 engine data (Figure 3.2.1). Since there was such a large difference, an inlet noise prediction was made which excluded the contribution of the combination tone noise portion of the fan noise model in ANOPP. Relative to the CF6-80C2 data, the ANOPP method is shown to overpredict in this case as well. The ANOPP E³ prediction (Figure 3.2.2) also shows that the fan inlet noise is overpredicted when the combination tone noise model is included. If the combination tone noise calculation is excluded, the engine noise is actually slightly underpredicted. An overprediction is shown relative to the QCSEE engine data (Figure 3.2.3) -- but in this case the combination tone noise model does not significantly contribute to the prediction due to the lower tip relative Mach number. Detailed information regarding the combination tone noise model is given in Section 4.6.

Note that the CF6-80C2 ANOPP prediction does not include the inflow distortion noise effect, since the GE data was measured using a turbulence control screen (TCS). The ANOPP E³ and QCSEE predictions do include the inflow distortion effect, since this data was measured without a TCS.

Results -- Cutback, and Approach

The same trends are shown for each engine for the cutback and approach conditions as were demonstrated at the takeoff condition. Spectra plots for all engine conditions and at all angles of interest are given in Appendix B for CF6-80C2, Appendix C for E³, and Appendix D for QCSEE.

Figure 3.2.1 Fan Inlet Noise Spectrum, CF6-80C2, takeoff, 40 deg, 150 ft arc

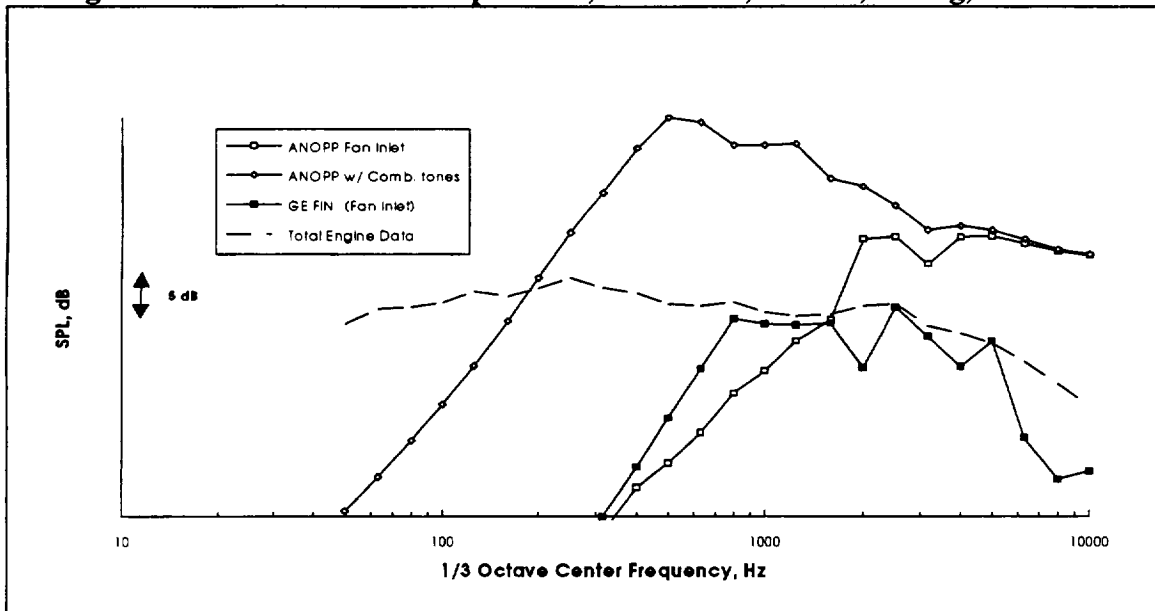


Figure 3.2.2 Fan Inlet Noise Spectrum, E3, takeoff, 40 deg, 150 ft arc

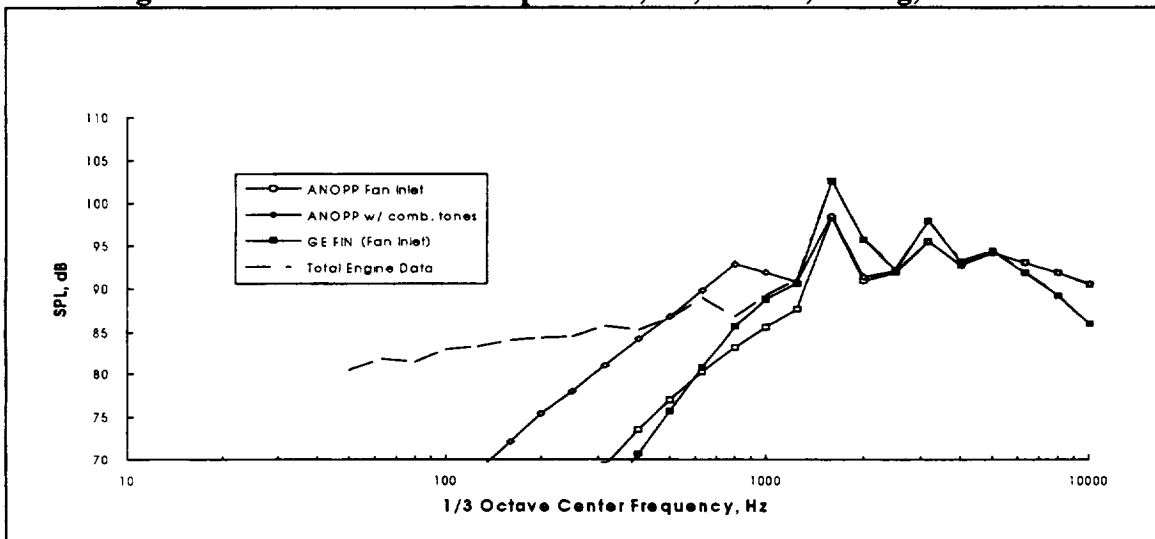
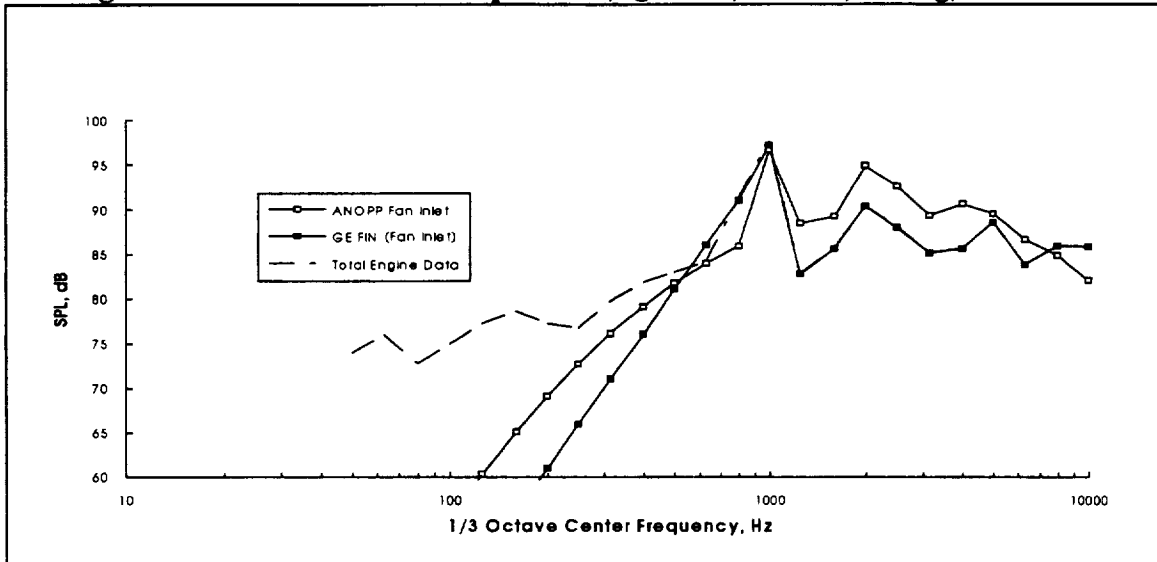


Figure 3.2.3 Fan Inlet Noise Spectrum, QCSEE, takeoff, 30 deg, 150 ft arc



3.3 Fan Exhaust Noise

Results -- Takeoff, Cutback, and Approach

The fan exhaust noise ANOPP predictions vary with the type of engine as well as condition. Peak aft angle spectra of takeoff fan exhaust noise are shown in Figures 3.3.1, 3.3.2, and 3.3.3 for the CF6-80C2, E³, and QCSEE engines. The spectral content and amplitudes for the CF6-80C2 and the E³ ANOPP predictions (Figures 3.3.1 and 3.3.2) show a slight overprediction relative to the GE component database, while the QCSEE prediction is well below the measured engine data. Additional spectra plots at other angles and for the other cycle conditions are given in Appendices E, F, and G for the CF6-80C2, E³, and QCSEE data respectively. The same trends demonstrated at takeoff are shown in the cutback and approach conditions for the E³ and QCSEE Engines. The CF6-80C2 results vary from overprediction at takeoff to underprediction at approach.

Figure 3.3.1 Fan Exhaust Noise Spectrum, CF6-80C2, peak aft angle, 150 ft arc

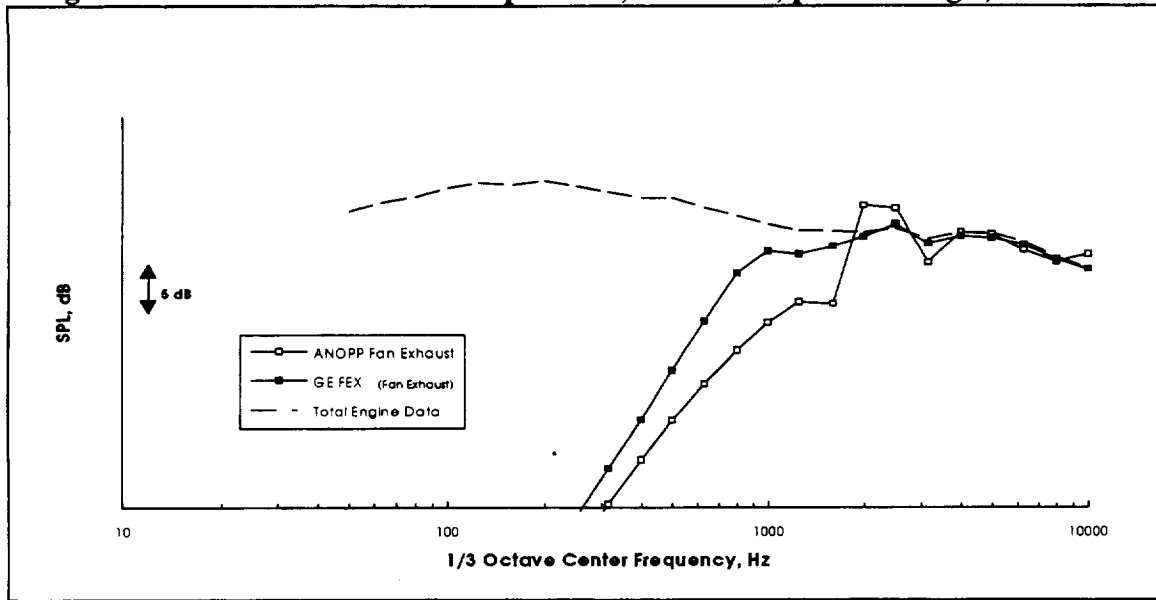


Figure 3.3.2 Fan Exhaust Noise Spectrum, E3, peak aft angle, 150 ft arc

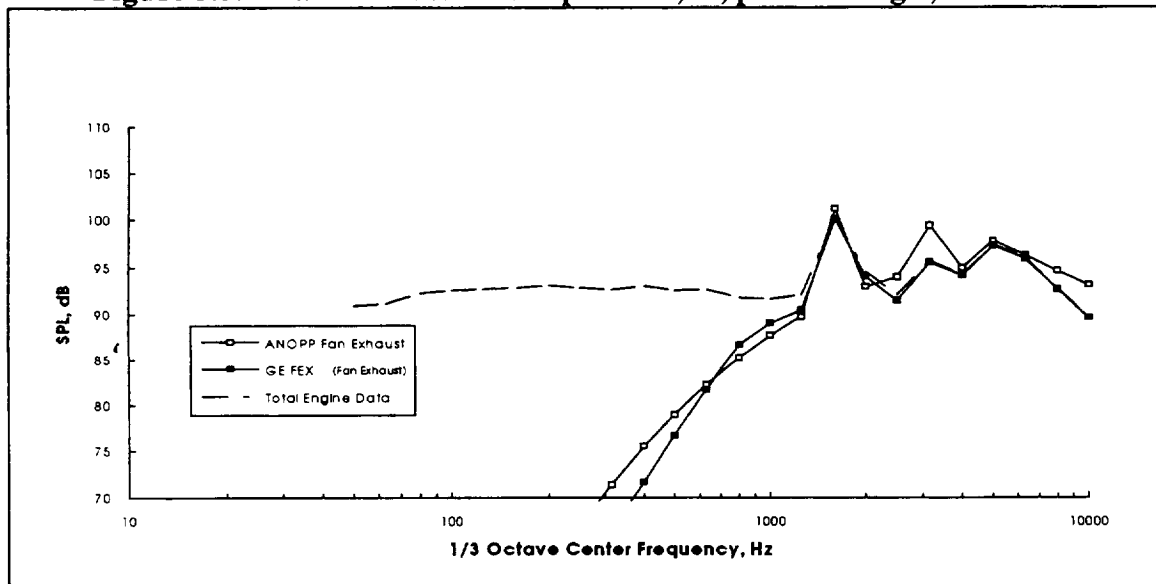
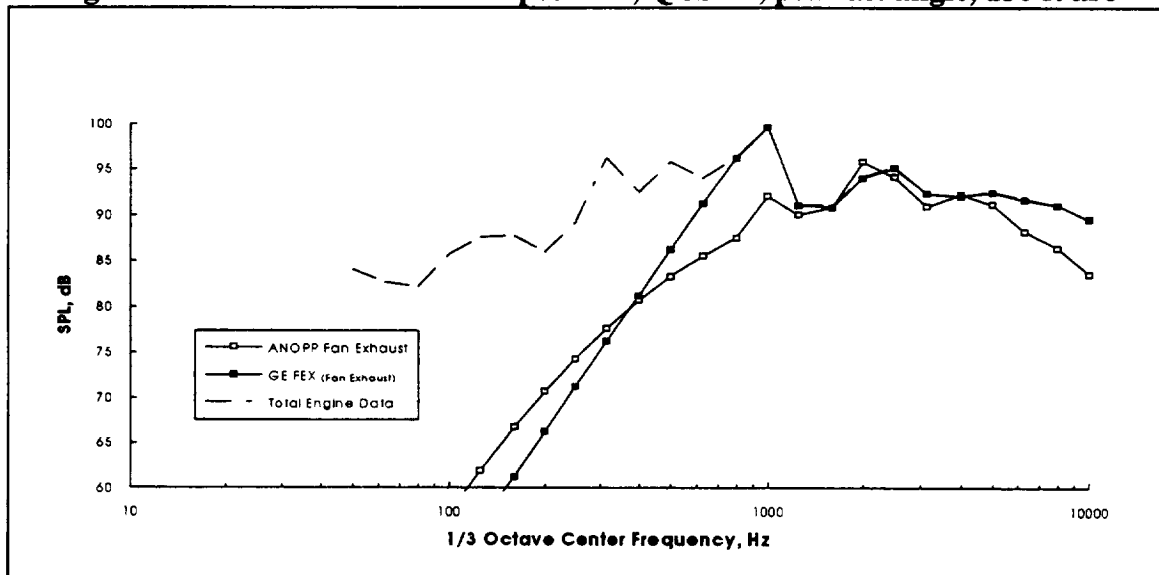


Figure 3.3.3 Fan Exhaust Noise Spectrum, QCSEE, peak aft angle, 150 ft arc



3.4 Jet Noise

Figures 3.4.1, 3.4.2, and 3.4.3 show the ANOPP predictions and GE jet noise database spectra at takeoff conditions for the CF6-80C2, E³, and QCSEE engines. Additional jet noise spectra for the other engine conditions are shown in Appendix H. The ANOPP-predicted amplitudes are generally above those of the GE database, especially for predictions of the lower velocity jets. A clear trend of overprediction (1-6 dB) is indicated in the CF6-80C2 and the QCSEE predictions (Figure 3.4.1 and 3.4.3). The peak frequency is quite different between data and prediction for the CF6-80C2 and QCSEE engines. The ANOPP and GE jet noise component results are closer in agreement in terms of peak noise (amplitude and frequency) for the mixed flow E³ engine at takeoff (Figure 3.4.2) and cutback, but show a slight underprediction at approach.

Figure 3.4.1 Jet Noise Spectrum, CF6-80C2, takeoff, 150 deg, 150 ft arc

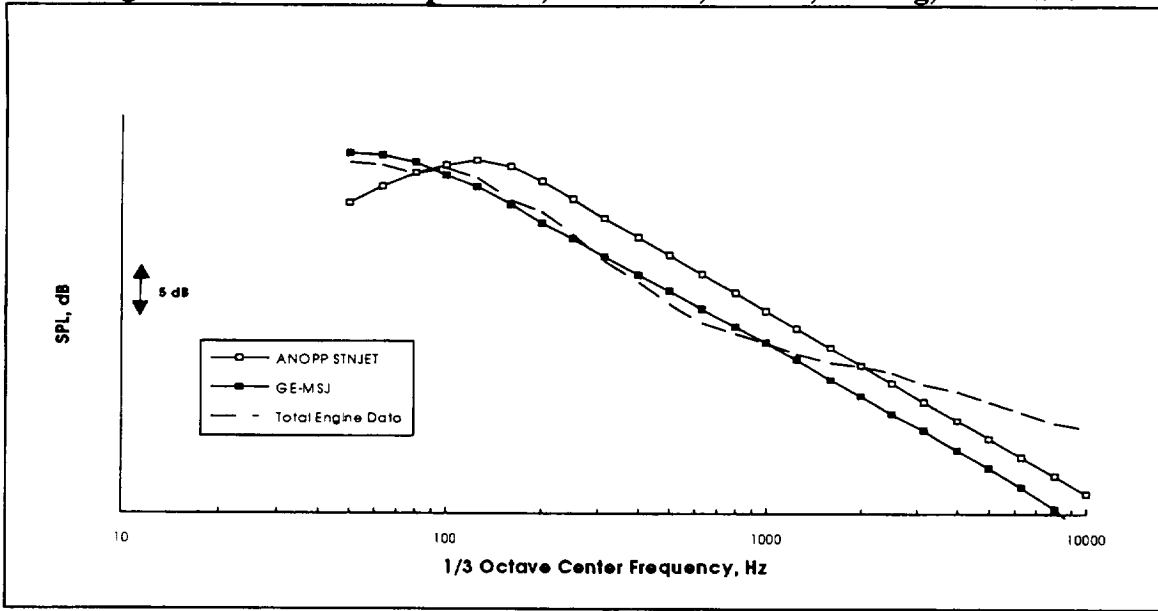


Figure 3.4.2 Jet Noise Spectrum, E3, takeoff, 150 deg, 150 ft arc

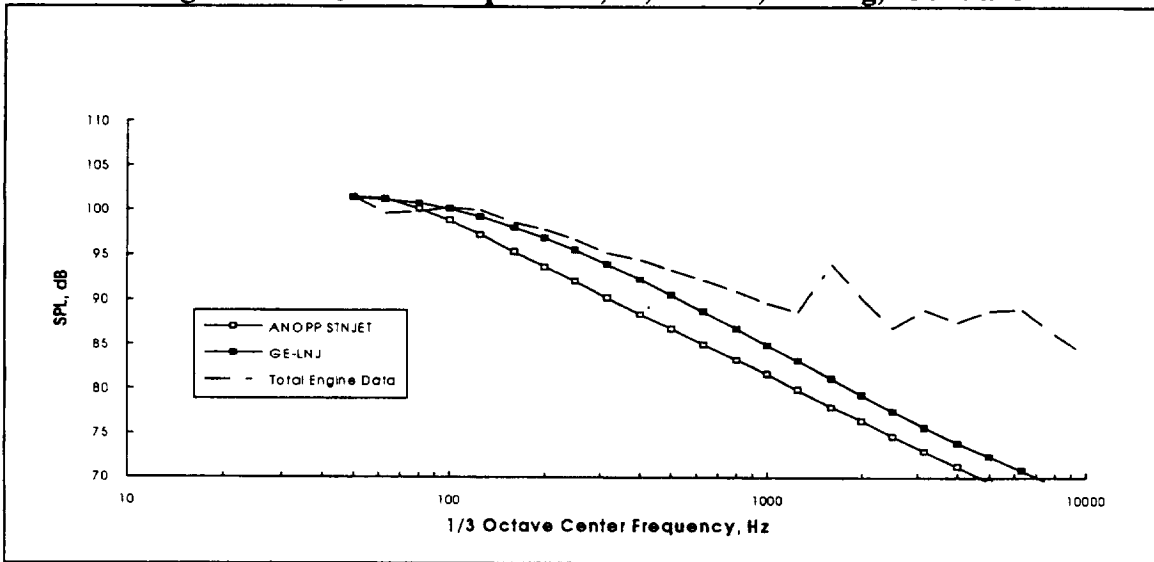
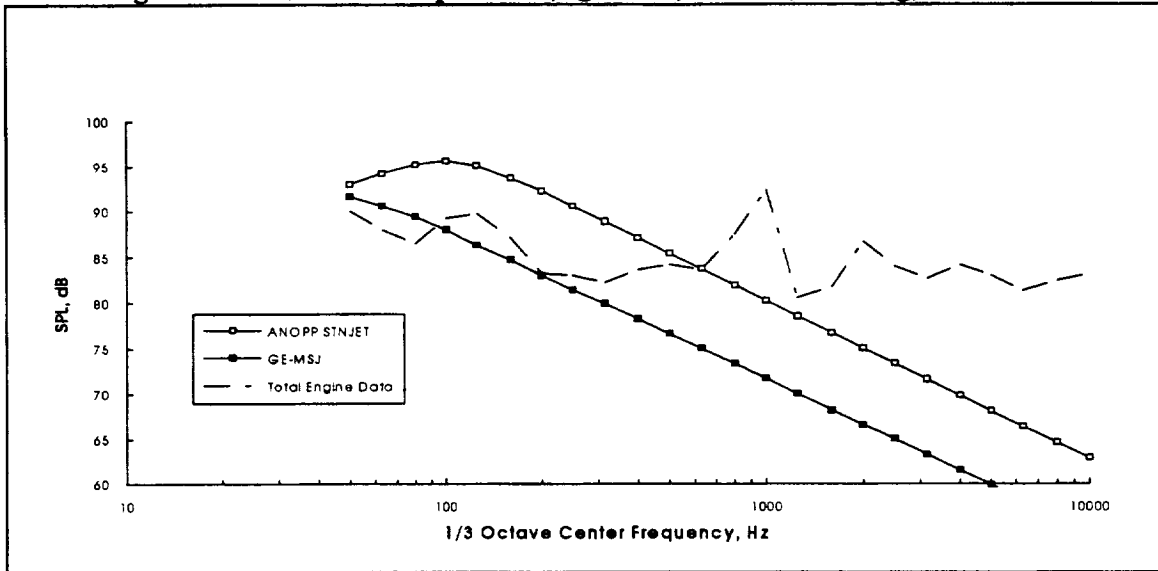


Figure 3.4.3 Jet Noise Spectrum, QCSEE, takeoff, 150 deg, 150 ft arc



3.5 Combustor Noise

ANOPP combustor noise predictions agree closely with the GE predictions (the two prediction methods are identical, except that the cycle input parameters are slightly different). The discrepancies observed in the QCSEE predictions are attributable to the QCSEE cycle estimations that were made. Figures 3.5.1, 3.5.2, and 3.5.3 show the combustor noise spectra at the peak noise angle for each of the three engines at takeoff power. Spectra for the other engine conditions can be found in Appendix I.

Although the ANOPP and GE combustor noise predictions agree, it is difficult to assess the absolute accuracy of the predicted levels and peak frequency. It can at least be stated that the combustor noise predictions do not cause the total predicted engine noise to assume an unreasonable spectral shape or to exceed the level of total measured engine noise.

Figure 3.5.1 Combustor Noise Spectrum, CF6-80C2, takeoff, 120 deg, 150 ft arc

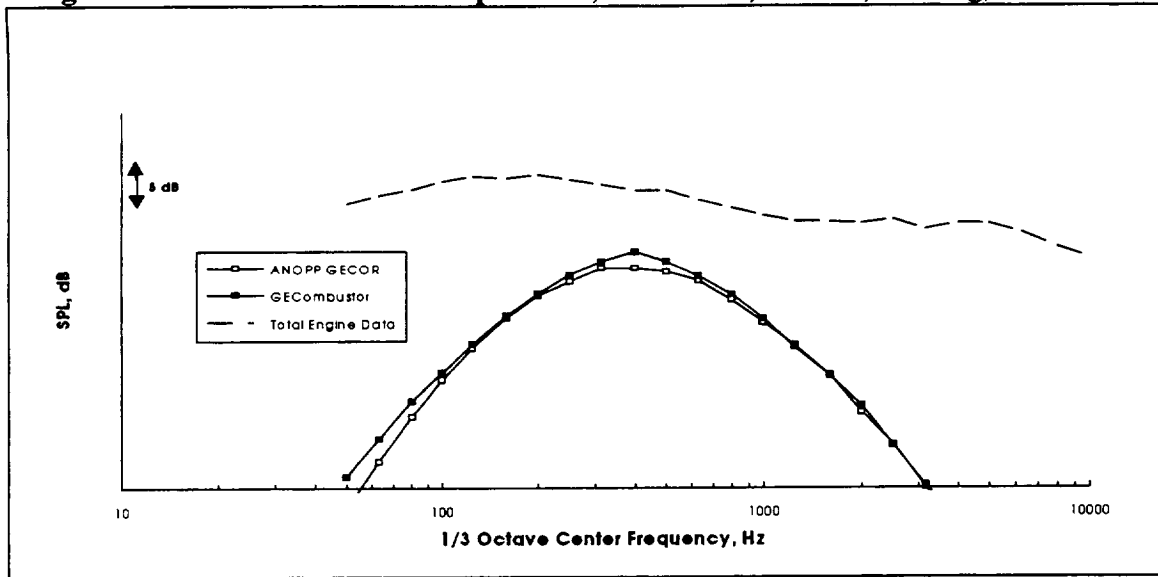


Figure 3.5.2 Combustor Noise Spectrum, E3, takeoff, 120 deg, 150 ft arc

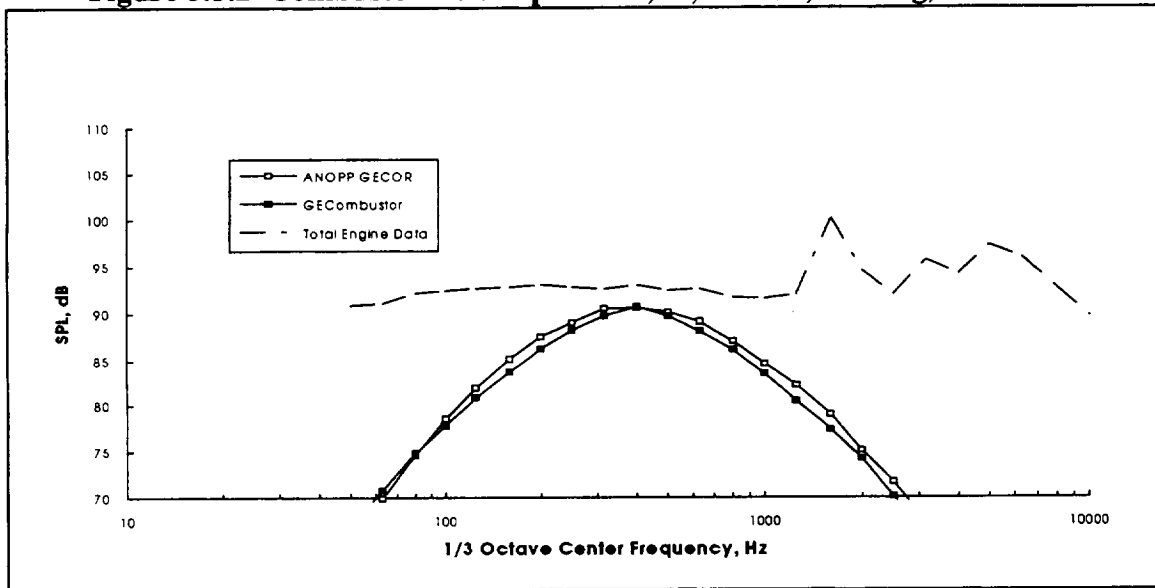
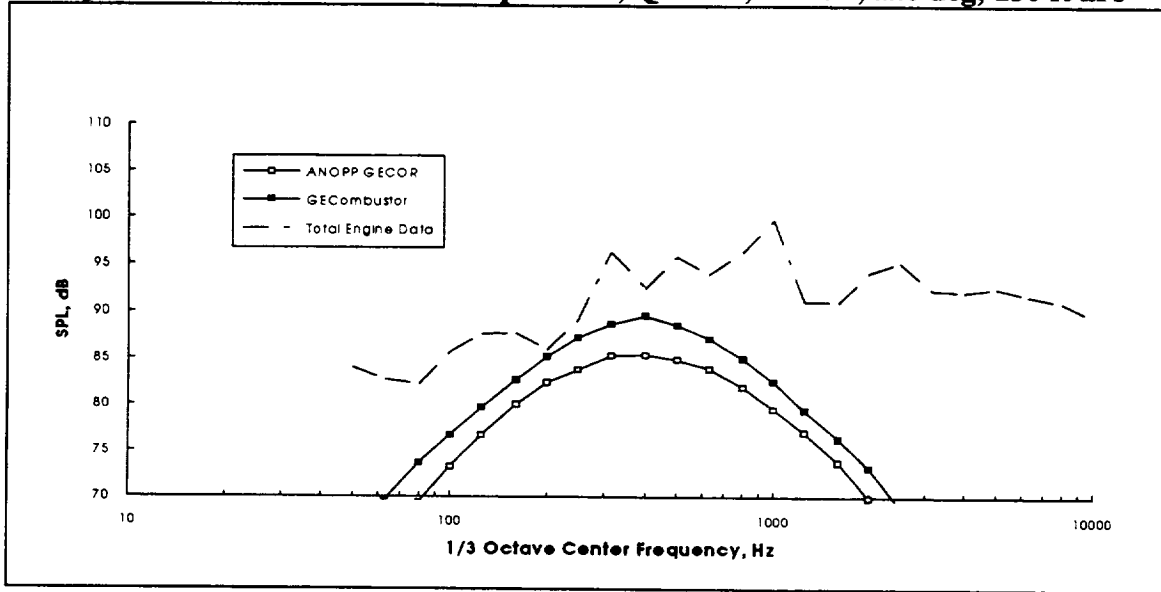


Figure 3.5.3 Combustor Noise Spectrum, QCSEE, takeoff, 120 deg, 150 ft arc



3.6 Turbine Noise

The ANOPP turbine noise predictions are on the order of 30 dB greater than the corresponding GE predictions. Figures 3.6.1, 3.6.2, and 3.6.3 show the spectra for all three engines at takeoff power. Additional peak noise spectra for the other engine conditions are in Appendix J. All of these plots show an unusual turbine noise spectral shape (no tones), and that the ANOPP component predictions are much greater than the turbine noise data.

There are several reasons for the differences observed. On the basis of previous engine experience, GE turbine noise predictions assume that there is one dominant stage (usually the last stage) of the low pressure turbine that significantly contributes to the turbine noise component. Input parameters for the GE turbine noise prediction are adjusted accordingly. If these adjustments are not made, the turbine noise component prediction increases dramatically, nearly matching the ANOPP prediction in magnitude. Figure 3.6.4 demonstrates these results.

Although this "adjustment" seems to explain a significant portion of the large differences observed, the discrepant spectral content of the ANOPP predictions still requires explanation. (It should be noted that the ANOPP prediction method, despite the name "GETUR", is in no way related to the GE turbine noise prediction method used.)

Figure 3.6.1 Turbine Noise Spectrum, CF6-80C2, takeoff, 120 deg, 150 ft arc

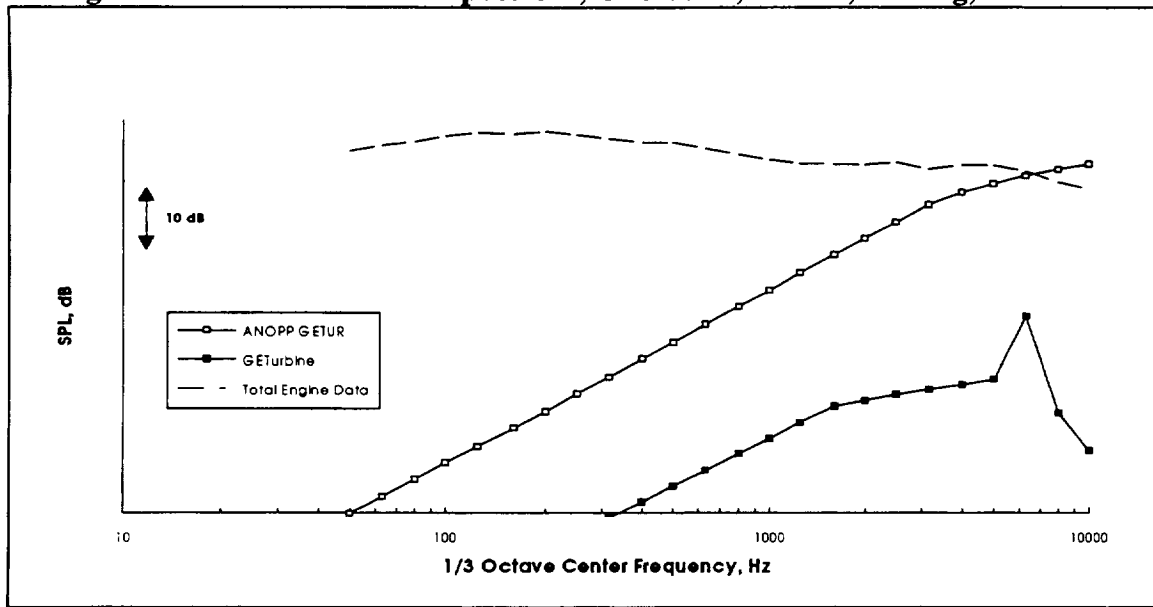


Figure 3.6.2 Turbine Noise Spectrum, E3, takeoff, 120 deg, 150 ft arc

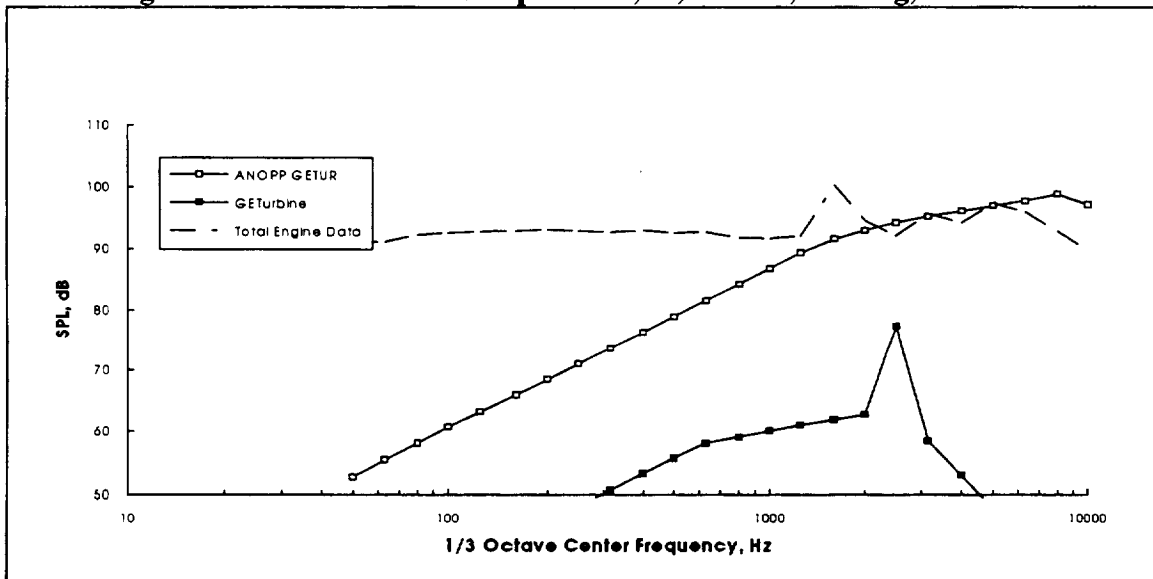


Figure 3.6.3 Turbine Noise Spectrum, QCSEE, takeoff, 120 deg, 150 ft arc

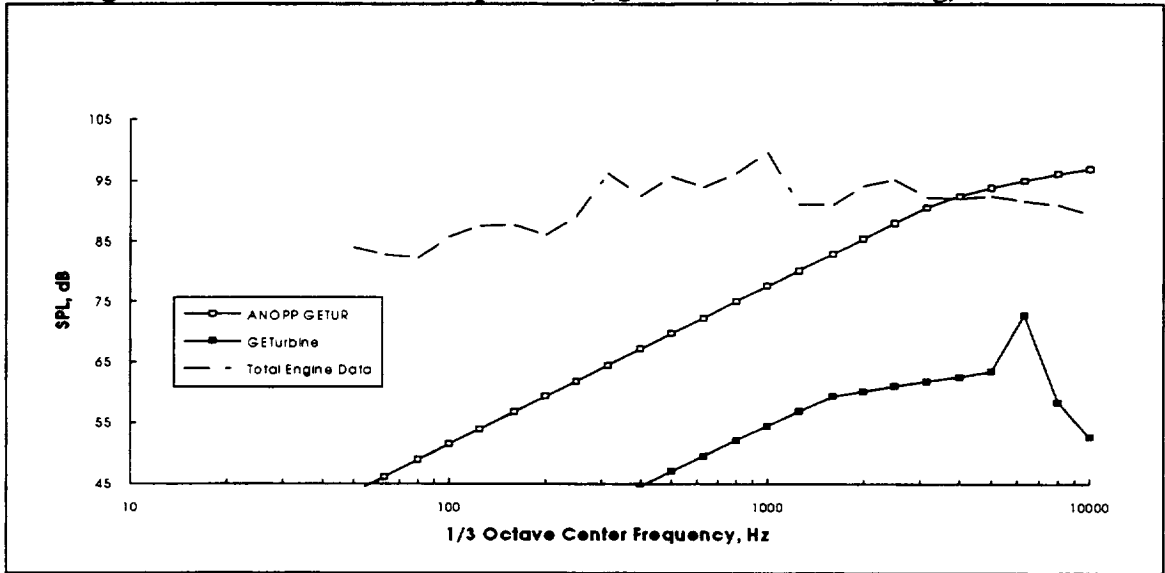
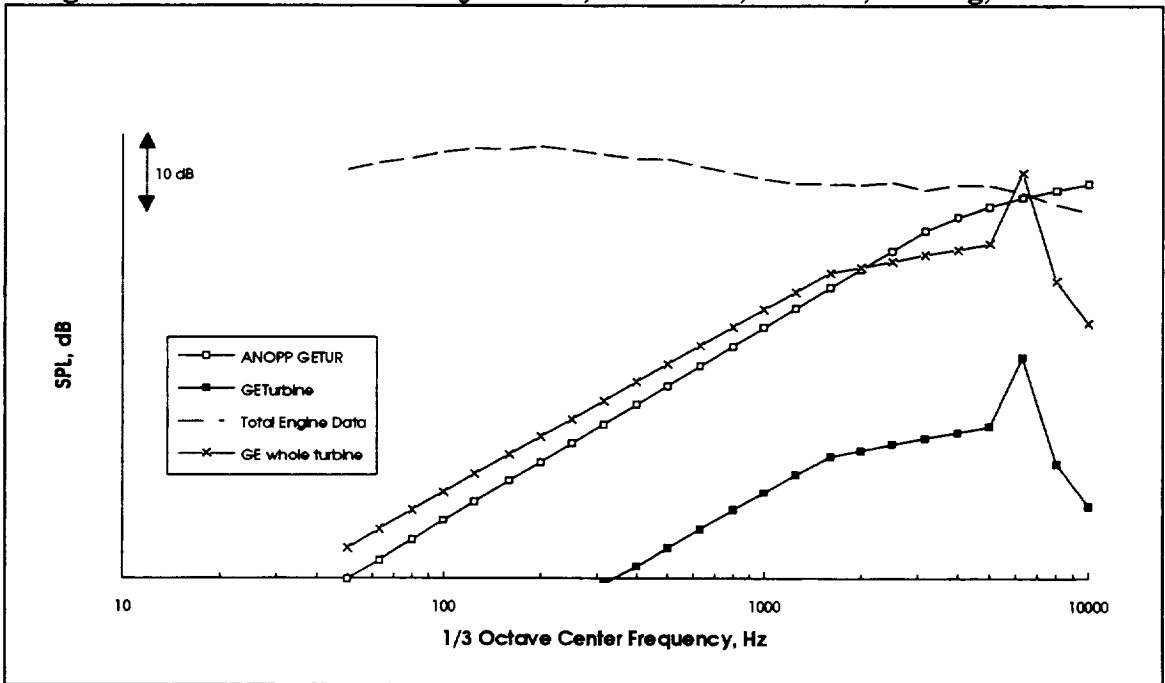


Figure 3.6.4 Turbine Noise Adjustment, CF6-80C2, Takeoff, 120 deg, 150 ft arc



4.0 Results and Discussion -- Fan Noise Model Improvements

This section, which describes all of the recommended changes to the Heidmann fan noise model, refers extensively to the Interim Prediction Method for Fan and Compressor Source Noise (Heidmann, 1979). Complete understanding of the content of this section requires familiarity with the Heidmann fan noise model.

A detailed description of the model would be impossible to give within the context of this report. However, in order to help the reader who may be unfamiliar with the method, a brief summary of the Heidmann model is attempted in the following paragraph (excerpted from Heidmann, 1979).

The Heidmann procedure predicts one-third octave band levels of the free-field noise pattern. The prediction method was initially developed by The Boeing Company, under contract with NASA Ames Research Center. Heidmann made modifications to this method, based on correlations and interpretations of the acoustic data from full-scale fan tests performed at NASA Lewis (Heidmann, 1973). The noise predictions applicable to one- and two-stage turbofans with or without inlet guide vanes (IGVs). The procedure involves predicting spectrum shape, spectrum level, and free-field directivity for each of the following components:

- fan inlet broadband noise
- fan inlet tone noise
- fan inlet combination-tone noise
- fan exhaust noise
- fan exhaust tone noise

Four parameters are required to predict the basic spectrum levels: mass flow rate (m), total temperature rise across the fan stage (ΔT), and the design and operating point values of the rotor tip relative inlet Mach number (M_{rd} , M_r). The basic levels are then corrected for presence of IGV, rotor-stator spacing (RSS), inlet flow distortions, and cutoff.

In order to compare with the Heidmann model, tone and broadband noise components for the fan inlet and fan exhaust were separated for all three engine databases. Using the Heidmann method normalization (fan temperature rise and mass flow), the GE data was corrected and plotted relative to each appropriate Heidmann method correlation. Using the CF6-80C2 data, the Heidmann method was adjusted to agree with the data, as necessary. These adjustments were then further evaluated using the E³ and QCSEE data. Since these databases did not contain much combination tone noise information, a typical CFM56 noise database was also used to provide additional direction for the combination tone noise model adjustments.

In the following sections, the specific results for each of the noise models are described. The figures make reference in the title to the corresponding figure numbers in the original Heidmann method documentation.

4.1 Fan Inlet Broadband Noise

Fan inlet broadband, fan exhaust broadband, fan inlet tone, and fan exhaust tone noise components are each described by the following equation (Heidmann, 1979)

$$L_c = 20\log(\Delta T/\Delta T_o) + 10\log(m/m_o) + F_1(M_{trd}, M_{tr}) + F_2(RSS) + F_3(\theta) \quad (1)$$

where:

L_c is the peak characteristic sound pressure level of the noise component, $\Delta T/\Delta T_o$ is the temperature rise across the fan stage normalized by a reference delta temperature, m/m_o is the mass flow through the fan relative to a reference mass flow, F_1 is a function of rotor tip relative inlet mach numbers at the design and operating points, F_2 is a function of the rotor to stator spacing, and F_3 is a function of observer angle relative to the engine inlet. Values for F_1 , F_2 , and F_3 vary for each noise component.

In the initial stages of the Heidmann method evaluation, comparisons of the GE data with the Heidmann method predictions did not show consistent results for the different engines. It was found that when the F_2 term (rotor-stator spacing effect) was eliminated, more consistent results were predicted. Elimination of this term is in accord with prior GE commercial engine experience, in which no effect of rotor-stator spacing on fan inlet broadband noise is observed.

Figure 4.1.1 shows the "Figure 4a" (Heidmann, 1979) fan inlet broadband noise curve for the design tip relative Mach number (M_{trd}) of 1.53 for the CF6-80C2 engine. The CF6 inlet broadband data shown by the triangles indicate that a steeper slope on the Heidmann prediction curve is required. This can be accomplished by using -50 log instead of -20 log such that the new curve for normalized inlet broadband peak noise level, L_n , (F_1 in equation (1)) is given by:

$$L_n = 58.5 + 20 \log(M_{trd}) - 50 \log(M_{tr}/0.9); M_{trd} > 1, M_{tr} > 0.9 \quad (2)$$

The solid line in Figure 4.1.1 represents the original Heidmann curve, the dotted line indicates the change described in equation (2). Similarly, Figures 4.1.2 and 4.1.3 show the results for the E³ (M_{td} = 1.14) and QCSEE(M_{td} = 1.01) engine data, respectively. The data generally show close agreement with the new Heidmann method curve.

One-third octave spectra for the inlet angles are given in Appendix B for the CF6-80C2 engine. Each plot shows the measured engine noise, the original Heidmann prediction, and the new prediction (the new prediction reflects all of the changes that have not yet been explained, but will be described later in this section). E³ inlet spectra are shown in Appendix C, and QCSEE inlet spectra are in Appendix D. These plots generally show close agreement between the new broadband prediction and the measured data.

The directivity correction, F₃ in equation (1), remains unchanged (see Section 4.5).

Figure 4.1.1 “Figure 4a”, CF-80C2 Fan Inlet Broadband Noise

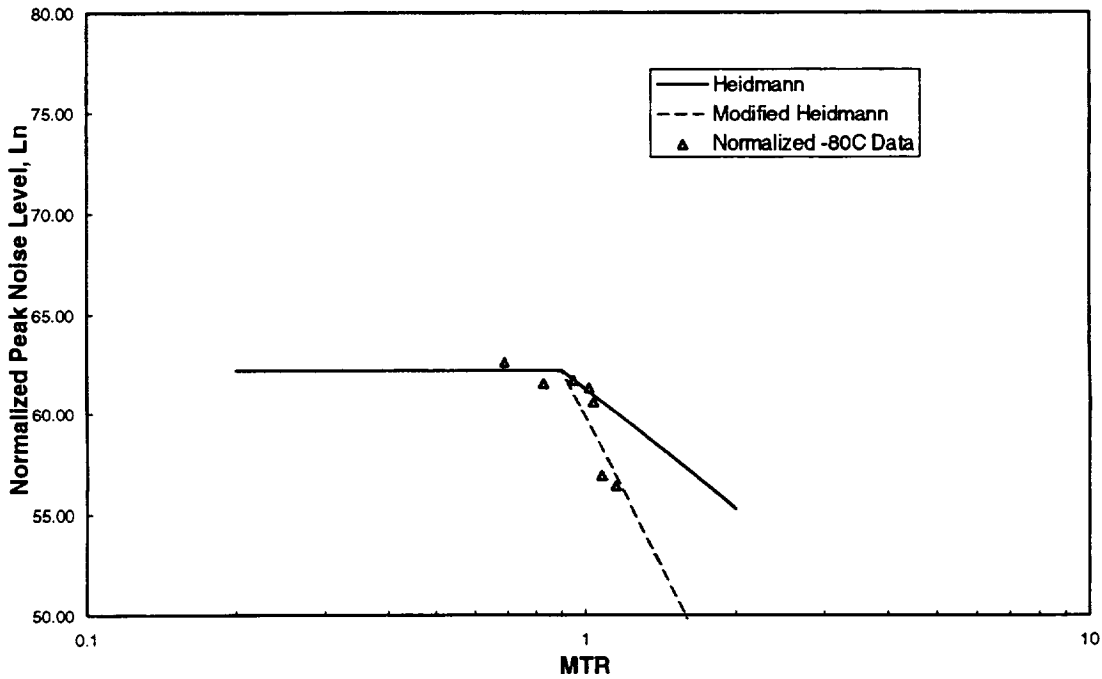


Figure 4.1.2 "Figure 4a", E' Fan Inlet Broadband Noise

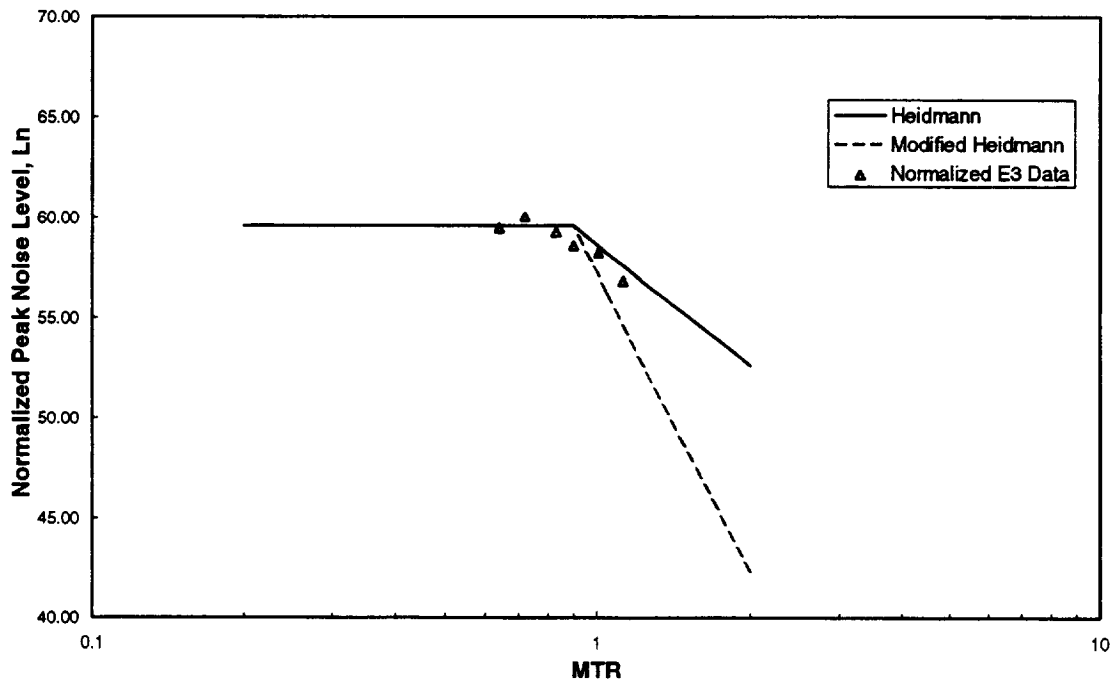
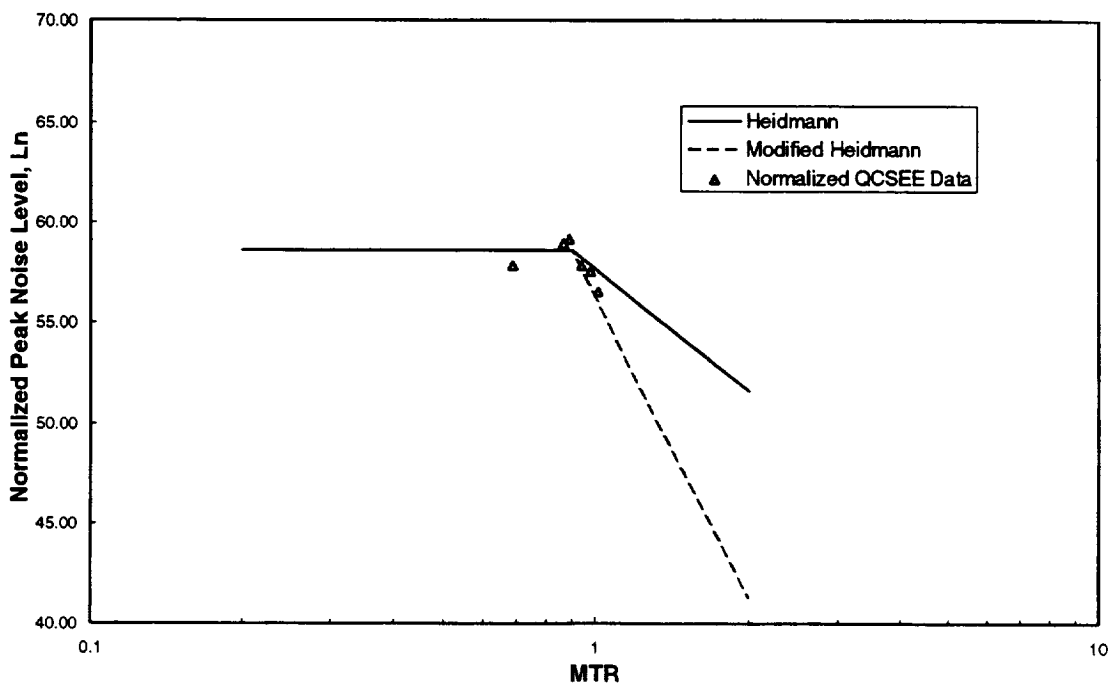


Figure 4.1.3 "Figure 4a", QCSEE Fan Inlet Broadband Noise



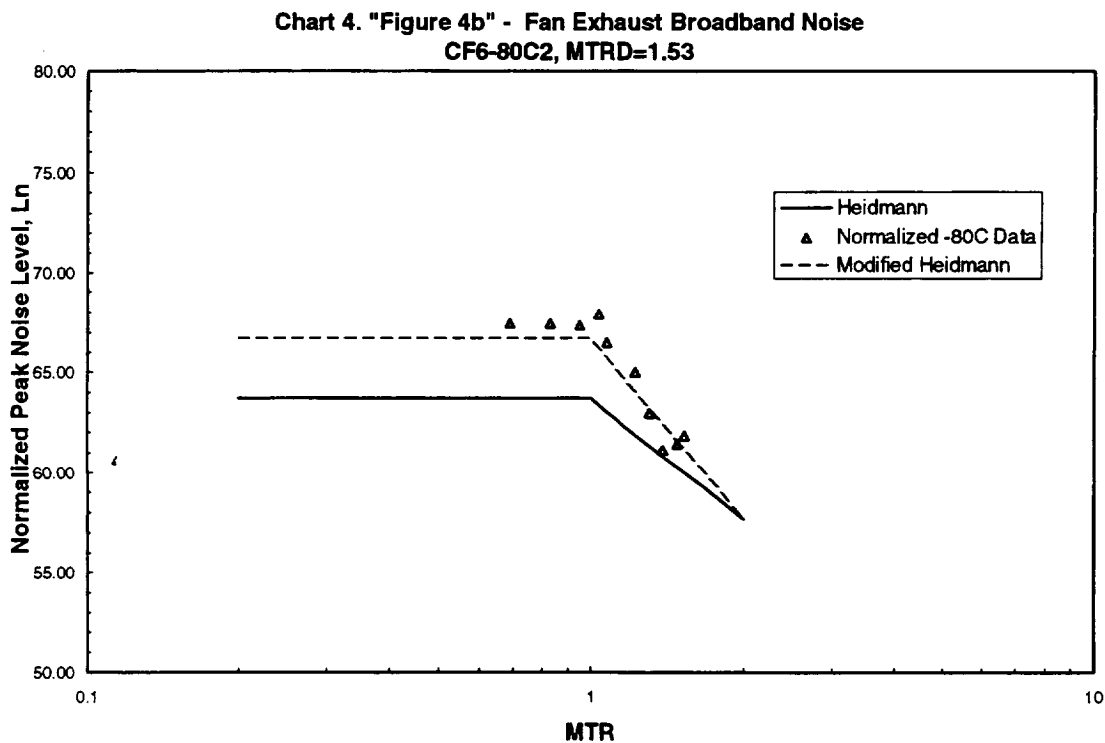
4.2 Fan Exhaust Broadband Noise

Fan exhaust broadband noise is also described by equation (1), with different values for F_1 , F_2 , and F_3 . Figure 4.2.1 shows the "Figure 4b" (Heidmann, 1979) fan exhaust broadband noise curve for a design tip relative Mach number (M_{trd}) of 1.53 (CF6-80C2). The CF6-80C2 exhaust broadband data shown by the triangles indicate that an increased level as well as a steeper slope on the Heidmann prediction curve are required. Accordingly, the base level of the "Figure 4b" curves for $M_{trd} > 1$ is increased by 3 dB. The slope of these curves is increased by using $-30 \log$ instead of $-20 \log$. The new equations for peak normalized broadband noise levels (F_1 in equation (1)) are:

$$L_n = 63 + 20 \log(M_{trd}); M_{trd} > 1, M_{tr} \leq 1.0 \quad (3a)$$

$$L_n = 63 + 20 \log(M_{trd}) - 30 \log(M_{tr}); M_{trd} > 1, M_{tr} > 1.0 \quad (3b)$$

Figure 4.2.1 "Figure 4b", CF6-80C2 Fan Exhaust Broadband Noise



Figures 4.2.2 and 4.2.3 show the results for the E³ (M_{trd} = 1.14) and QCSEE (M_{trd} = 1.01) engine data, respectively. The E³ data do not agree well with the new Heidmann curve. However, the E³ is a mixed flow exhaust engine and the fan exhaust component extracted from the measured engine noise is much lower in this case (not true for other mixed flow exhaust databases) than for the separate flow engines at comparable speeds. The QCSEE results generally agree with those of the CF6-80C2 in that an increase in the Heidmann curve level is desirable.

One-third octave spectra for the exhaust angles are given in Appendix E for the CF6-80C2 engine. Each plot shows the measured engine noise, the original Heidmann prediction, and the new prediction (The new prediction reflects all of the changes that have not yet been explained, but will be described later in this section). E³ inlet spectra are shown in Appendix F, and QCSEE inlet spectra are in Appendix G. The E³ charts show that the new Heidmann noise method is overpredicting the fan exhaust noise, as expected. The QCSEE charts generally show close agreement between the new broadband prediction and the measured data.

Figure 4.2.2 “Figure 4b”, E³ Fan Exhaust Broadband Noise

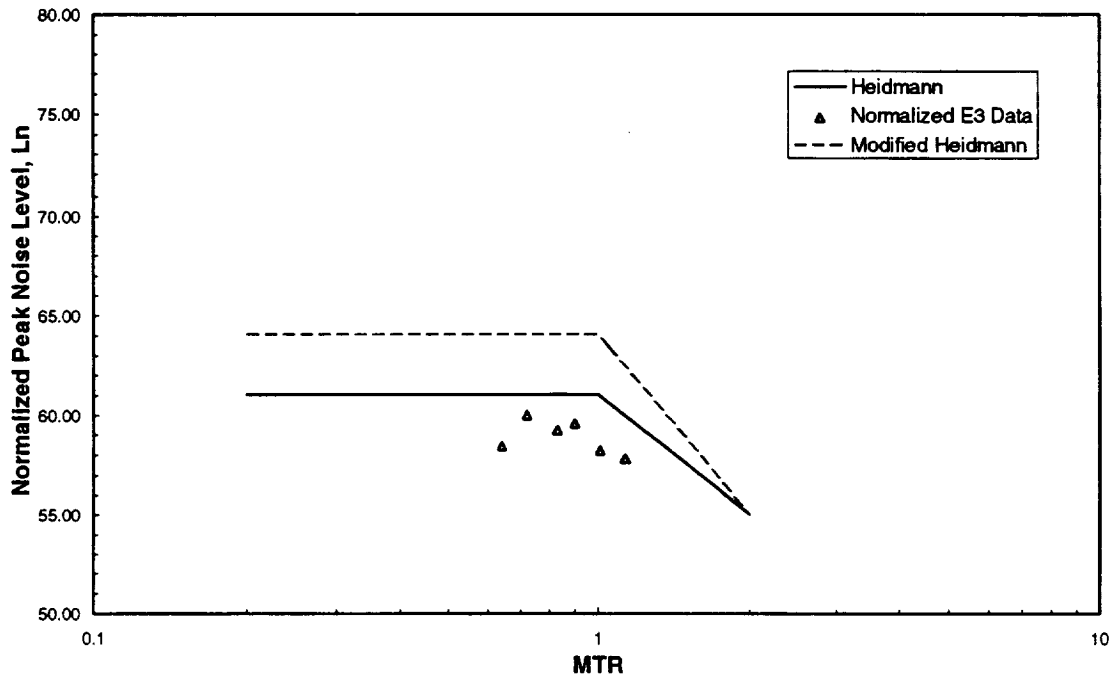
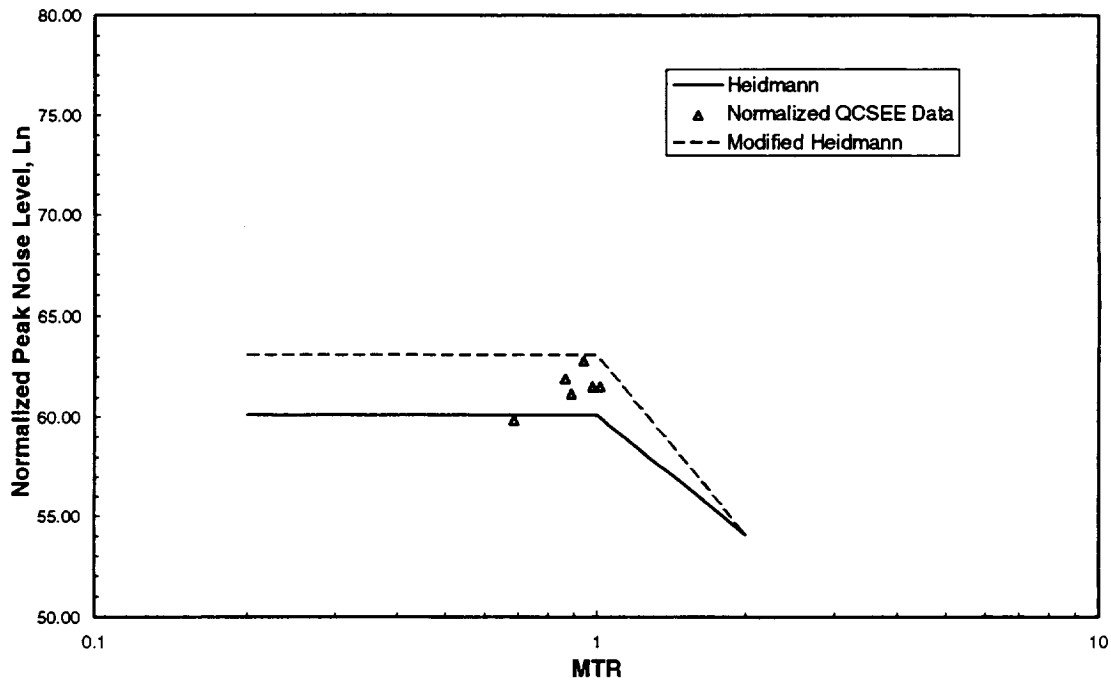


Figure 4.2.3 “Figure 4b”, QCSEE Fan Exhaust Broadband Noise



F_2 , the rotor-stator spacing (RSS) correction term, should always be calculated using the equation labeled “no inlet distortion” in “Figure 6 -- Rotor Stator Spacing Correction For Broadband Noise” (Heidmann, 1979), given by:

$$F_2 = -5 \log(\text{RSS}/300) \quad (4)$$

The directivity correction, F_3 in equation (1), remains unchanged (see Section 4.5).

4.3 Fan Inlet Discrete Tone Noise

Figure 4.3.1 shows the “Figure 10a” (Heidmann, 1979) fan inlet discrete tone noise curve for a design tip relative Mach number (M_{trd}) of 1.53 (CF6-80C2). The CF6 inlet tone data shown by the triangles indicate that an increased level as well as “shift to the right” of the Heidmann prediction curve are required. Accordingly, “Figure 10a” curves were adjusted. The new equation for normalized peak fan inlet discrete tone noise, L_n , (F_1 in equation (1)) is:

$$L_n = 64.5 + 80 \log(M_{trd}/M_{tr}); L_n = 60.5 + 20 \log(M_{trd}) + 50 \log(M_{tr}/0.72) \quad (5)$$

for $M_{trd} > 1$, $M_{tr} > 0.72$ (choose lesser value)

Figure 4.3.1 "Figure 10a", CF6-80C2 Fan Inlet Tone
 $M_{\text{trd}} = 1.53$

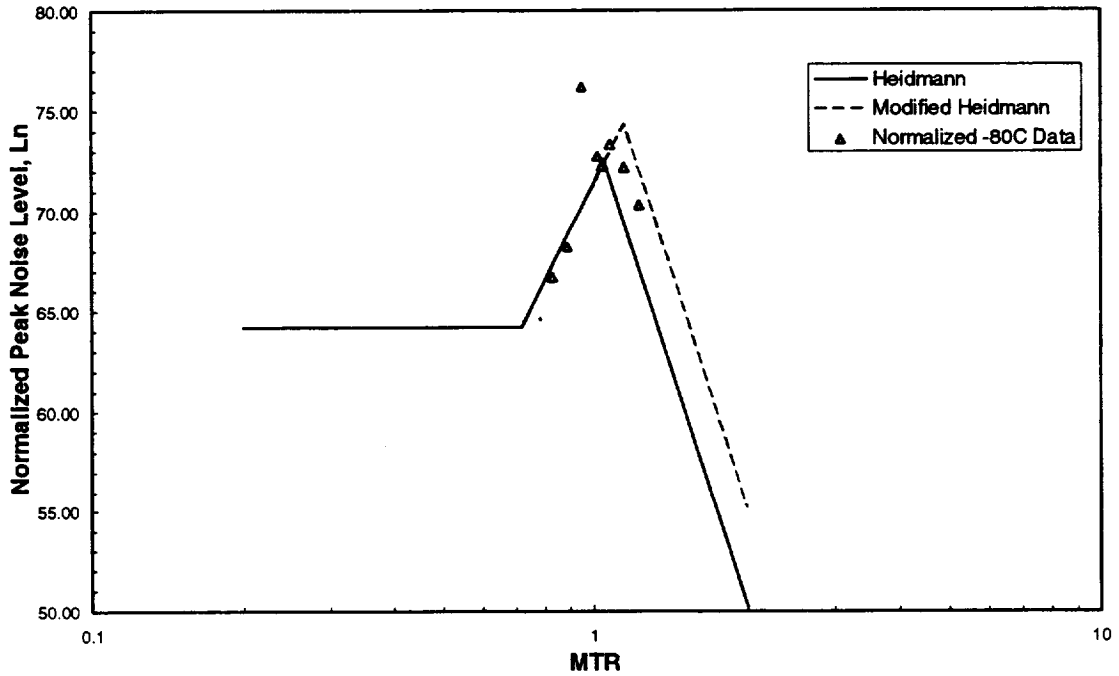


Figure 4.3.2 shows the E³ engine results. This plot shows that the new curve will yield a slight overprediction for the higher speed points that were previously underpredicted. Figure 4.3.3, the QCSEE results, show very good agreement between the data and the new Heidmann curve.

Figure 4.3.2 "Figure 10a", E³ Fan Inlet Tone
 $M_{trd} = 1.14$

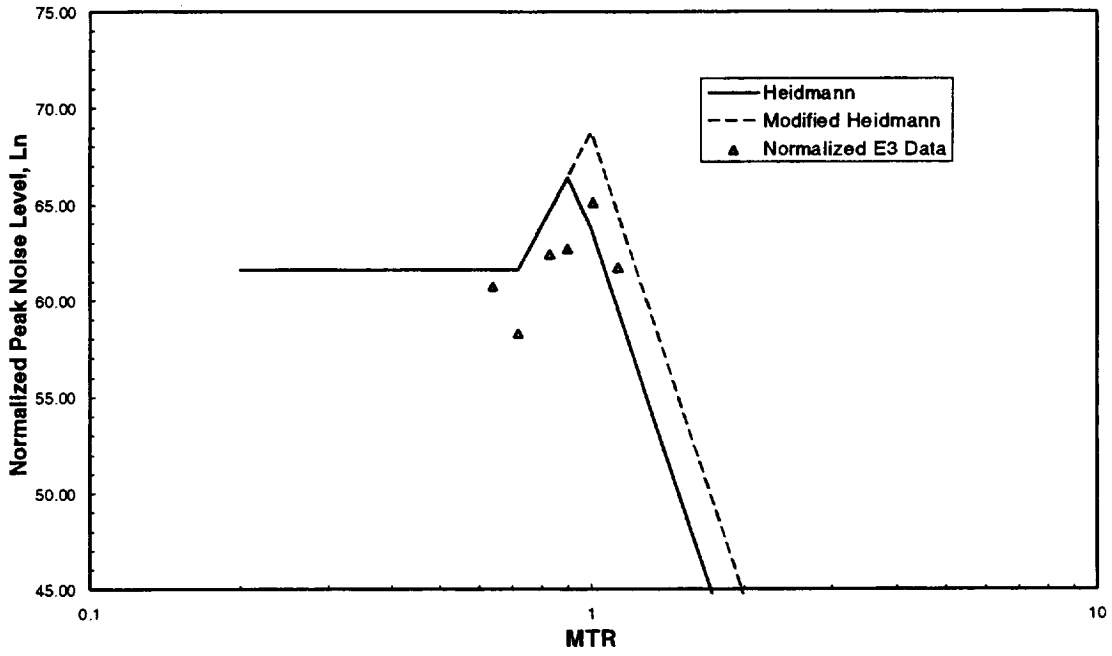
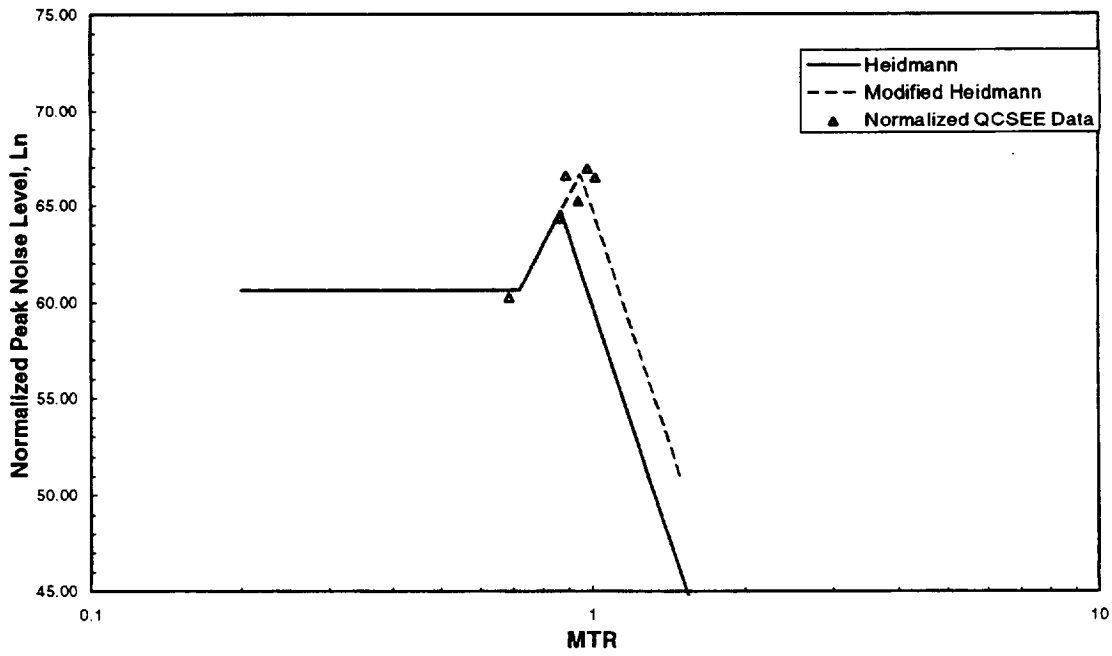


Figure 4.3.3 "Figure 10a", QCSEE Fan Inlet Tone
 $M_{trd} = 1.01$



The cutoff factor, δ , for the fundamental tone is given by:

$$\delta = |M_t / (1 - V/B)| \quad (6)$$

where M_t is the blade tip Mach number, V is the number of stator vanes, and B is the number of rotor blades. If the cutoff factor is less than or equal to the critical value of 1.05, then the fundamental tone level is reduced by 8 dB (“Figure 8a”, Heidmann, 1979). Based on the GE databases, it is recommended that the amount of tone reduction, L , due to cutoff become a function of the rotor tip relative Mach number, as shown by equation sets 7 and 8. The correction at cutoff remains 8 dB, but the harmonic fall-off rates are increased from 3 dB as follows:

For $M_{tr} < 1.15$:		For $M_{tr} \geq 1.15$:	
$L = 6 - 6k; \delta > 1.05$	(7a)	$L = 9 - 9k; \delta > 1.05$	(8a)
$L = -8; k = 1$	(7b)	$L = -8; k = 1$	(8b)
$L = 6 - 6k; k \geq 2$	(7c)	$L = 9 - 9k; k \geq 2$	(8c)

Refer to the data in Appendices B-D for the spectra plots for each of the three engines. The “modified Heidmann method curves” generally show better agreement at the BPF harmonics (reduced/eliminated over-prediction) relative to the measured engine data.

No changes are recommended to “Figure 8b”, the cutoff correction curve for fans with inlet guide vanes, since this effect could not be evaluated with the given commercial engines that do not have inlet guide vanes.

It should be noted that the BPF cutoff factor is being incorrectly calculated in ANOPP due to an error in the computer code. The vane/blade ratio is defined in the code as an integer value, but must be defined as a real number to yield the proper value of δ that determines cutoff.

The F_2 term (rotor-stator spacing effect), in accord with prior GE commercial engine experience in which no effect of rotor-stator spacing on fan inlet tone noise is observed, should be set equal to zero. The directivity correction, F_3 in equation (1), remains unchanged (see Section 4.5).

During ground static test, inflow disturbances drawn into the engine and interact with the fan to cause rotor-turbulence interaction noise. A Turbulence Control Structure (TCS) is a test apparatus that is used to clean-up the airflow disturbances in static engine tests. The Heidmann model was developed from data that was taken without the benefit of such a structure. GE initially developed a set of “flight cleanup” values based on the CF6-50/A300 aircraft flight test and engine static test data (Ho, Patrick Y., GE Design Practice # 1935, 1987, private communication). Table 4.3.1 shows the suppressions that should be applied to the Heidmann fan inlet tone predictions at the fundamental (BPF) and second harmonic (2BPF) frequencies to remove the effects of inflow disturbances in the model.

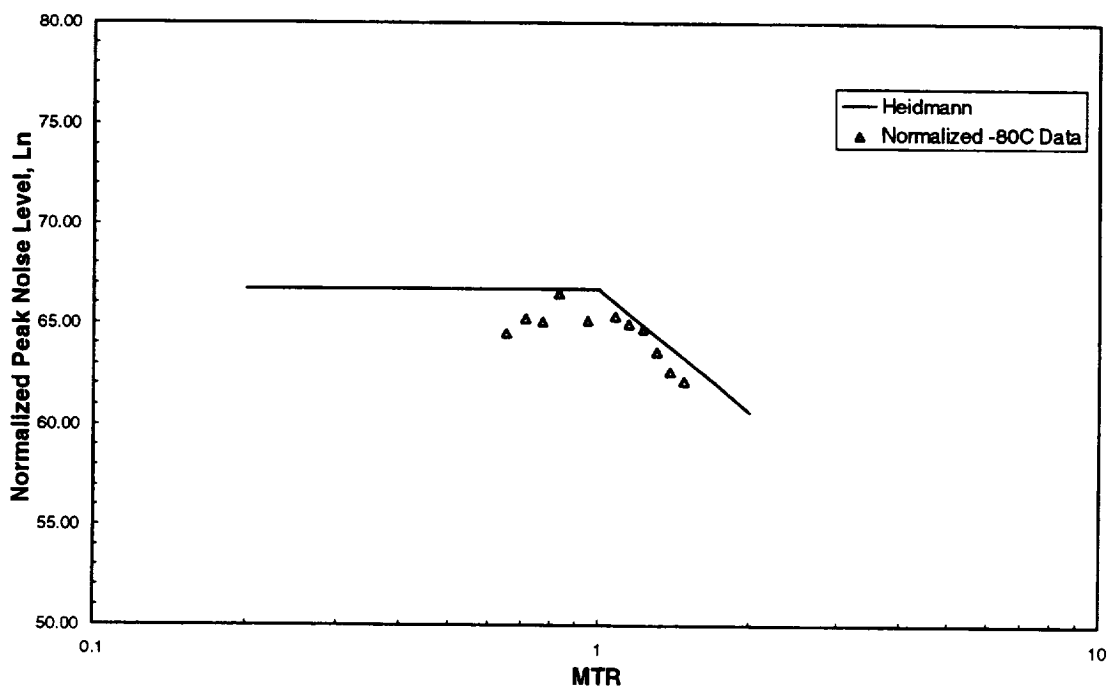
Table 4.3.1 GE “Flight Cleanup” -- TCS Suppression

Angle	Approach		Takeoff	
	BPF	2BPF	BPF	2BPF
10	5.6	5.4	4.8	5.8
20	5.8	4.3	5.5	3.8
30	4.7	3.4	5.5	5.3
40	4.6	4.1	5.3	6.4
50	4.9	2.0	5.3	3.5
60	5.1	2.9	5.1	3.0
70	2.9	1.6	4.4	2.1
80	3.2	1.3	3.9	2.1
90	1.6	1.5	2.6	1.1
100	1.6	1.1	2.3	1.4
110	1.8	1.4	1.8	0.9
120	2.1	1.5	2.1	0.7
130	2.4	1.0	1.7	0.7
140	2.2	1.8	1.7	0.4
150	2.0	1.6	2.6	0.6
160	2.8	1.6	3.5	0.8

4.4 Fan Exhaust Discrete Tone Noise

Figures 4.4.1, 4.4.2, and 4.4.3 show the “Figure 10b” (Heidmann, 1979) normalized fan exhaust noise levels representative of the CF6-80C2, E³, and QCSEE engines, respectively. The CF6-80C2 data show fairly good agreement with the Heidmann curve. The E³ and QCSEE data do not show any trends that resemble the Heidmann fan exhaust tone curve, nor do they suggest any alternative correlation. For these reasons, it is recommended that the original curve be retained.

Figure 4.4.1 “Figure 10b” CF6-80C2 Fan Exhaust Tone



F_2 , the rotor-stator spacing (RSS) correction term, should always be calculated using the equation labeled “no inlet distortion” in “Figure 12 -- Rotor Stator Spacing Correction For Discrete Tone Noise” (Heidmann, 1979), given by:

$$F_2 = -10 \log(\text{RSS}/300) \quad (9)$$

The directivity correction, F_3 in equation (1), remains unchanged (see Section 4.5).

Figure 4.4.2 “Figure 10b” E³ Fan Exhaust Tone

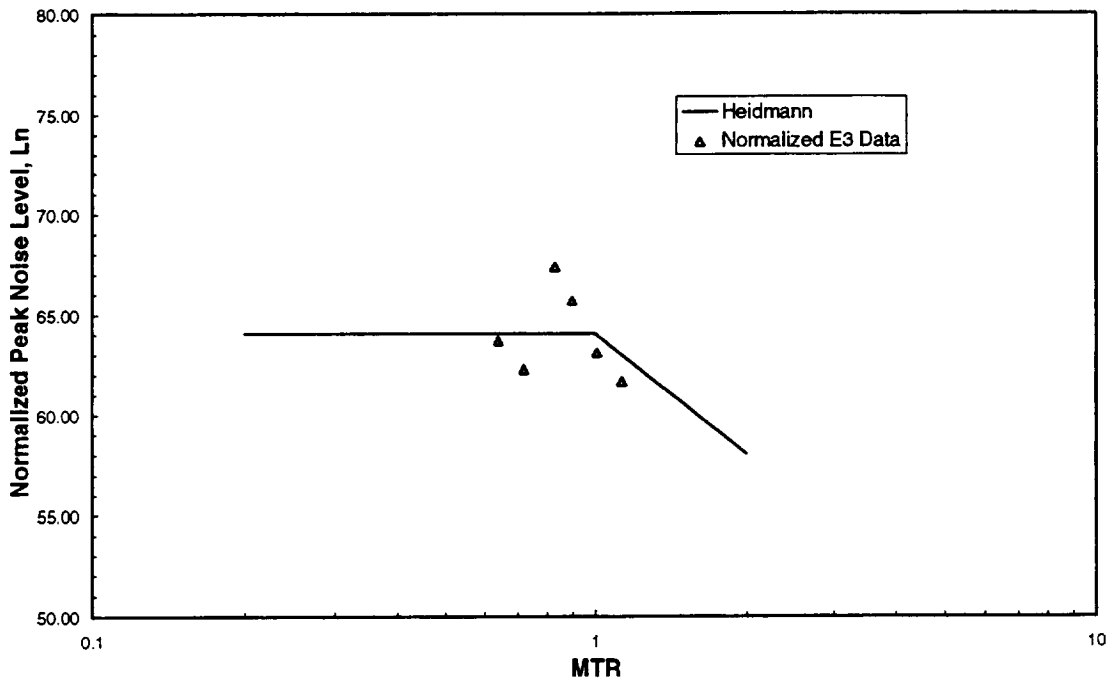
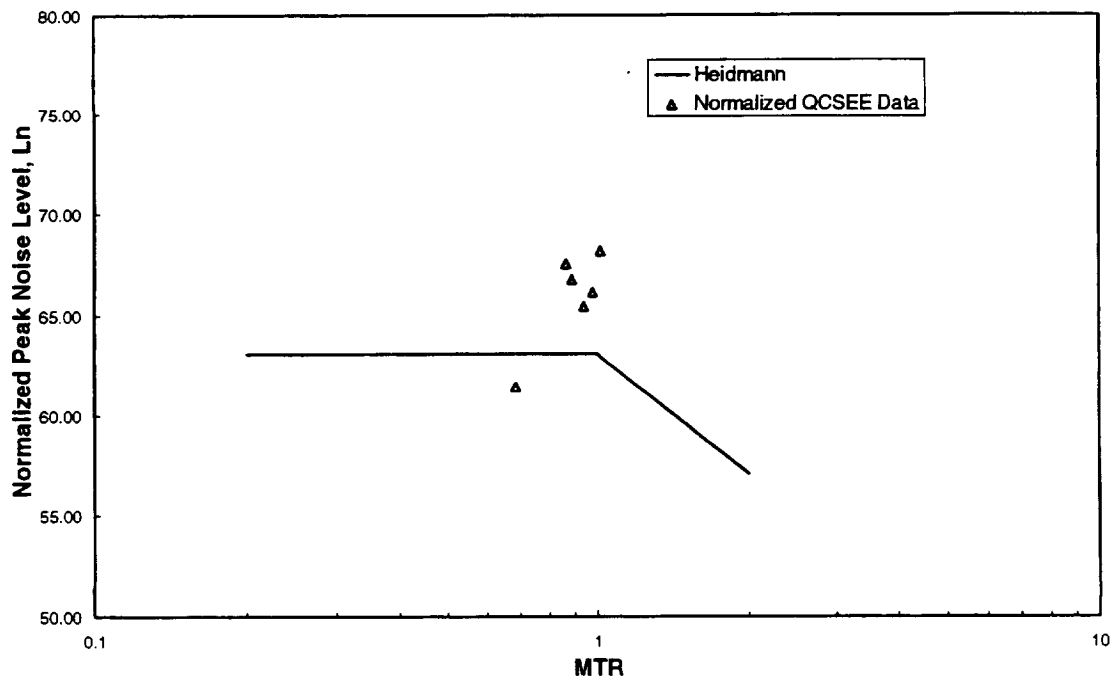


Figure 4.4.3 “Figure 10b” QCSEE Fan Exhaust Tone



4.5 Directivity

The directivity correction “L”, (F_3 in equation 1) for fan inlet broadband, fan inlet tone, fan exhaust broadband, and fan exhaust tone noise fit the GE measured data reasonably well. The data were normalized by subtracting the peak one-third octave level from all angles. Peak angles therefore have a directivity correction equal to zero, and off-peak angles have correction values less than zero. The Heidmann directivity curves for each of the four noise components are shown in comparison to the normalized E^3 data in Figures 4.5.1 - 4.5.4. Directivity comparisons relative to the CF6-80C2 and QCSEE engines are given in Appendix K. Since the data generally show a close relationship to the directivity curves in the Heidmann model, no changes are recommended.

Figure 4.5.1 “Figure 7a” Fan Inlet Broadband Directivity Correction -- E^3 Data

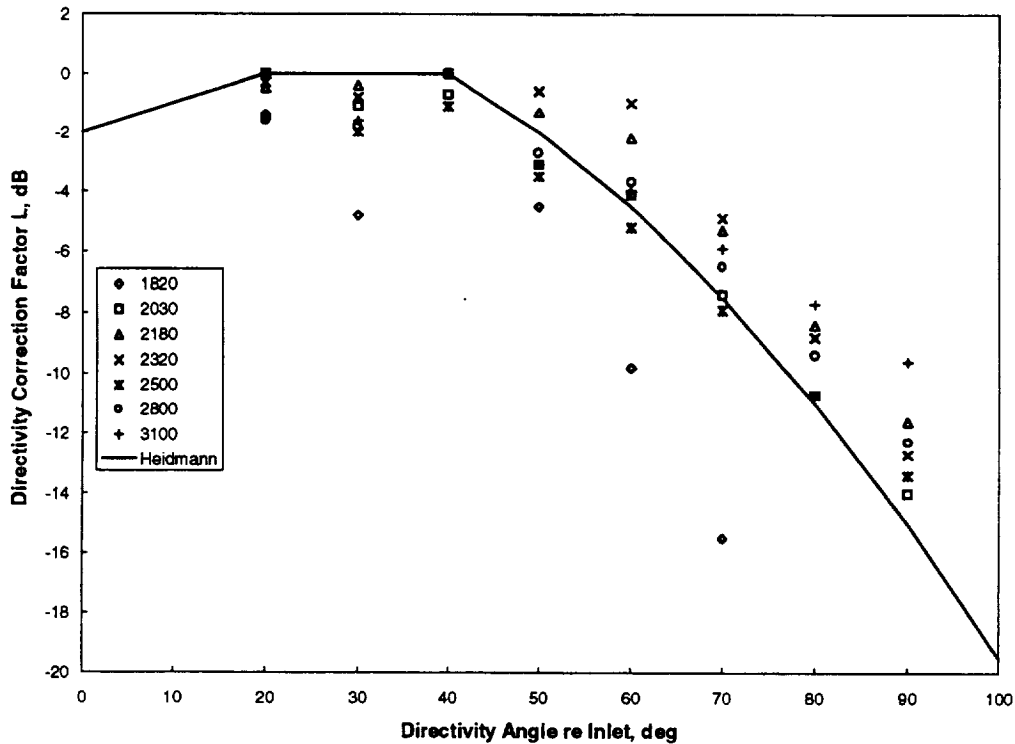


Figure 4.5.2 "Figure 13a: Fan Inlet Tone Directivity Correction -- E³ Data

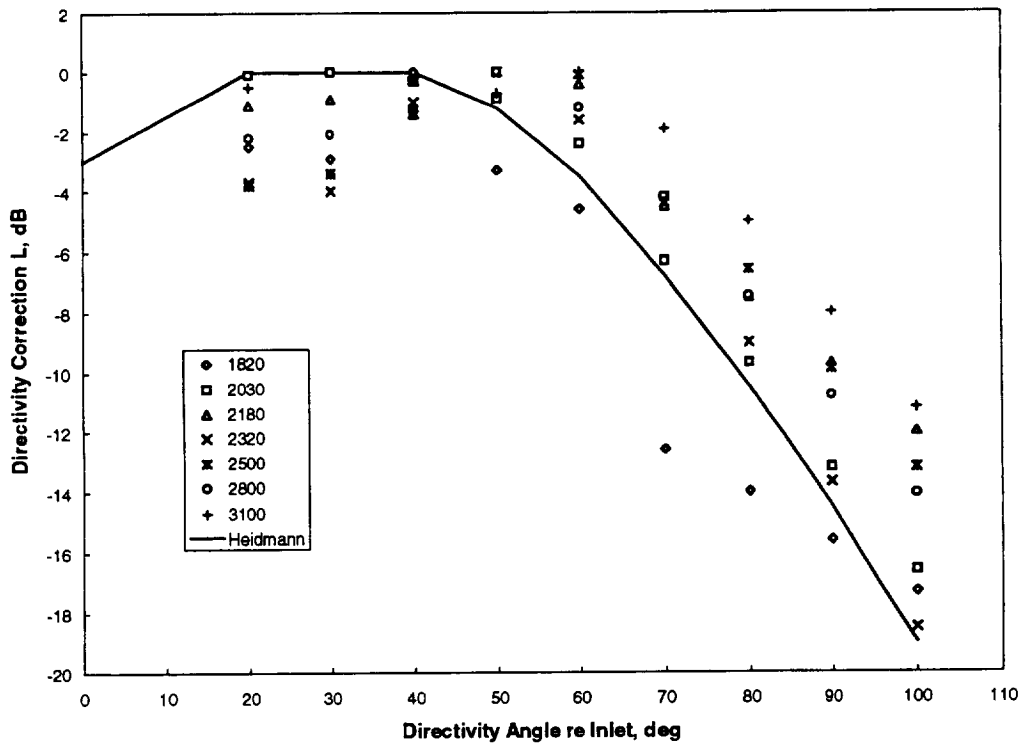


Figure 4.5.3 "Figure 7b" Fan Exhaust Broadband Directivity Correction -- E³ Data

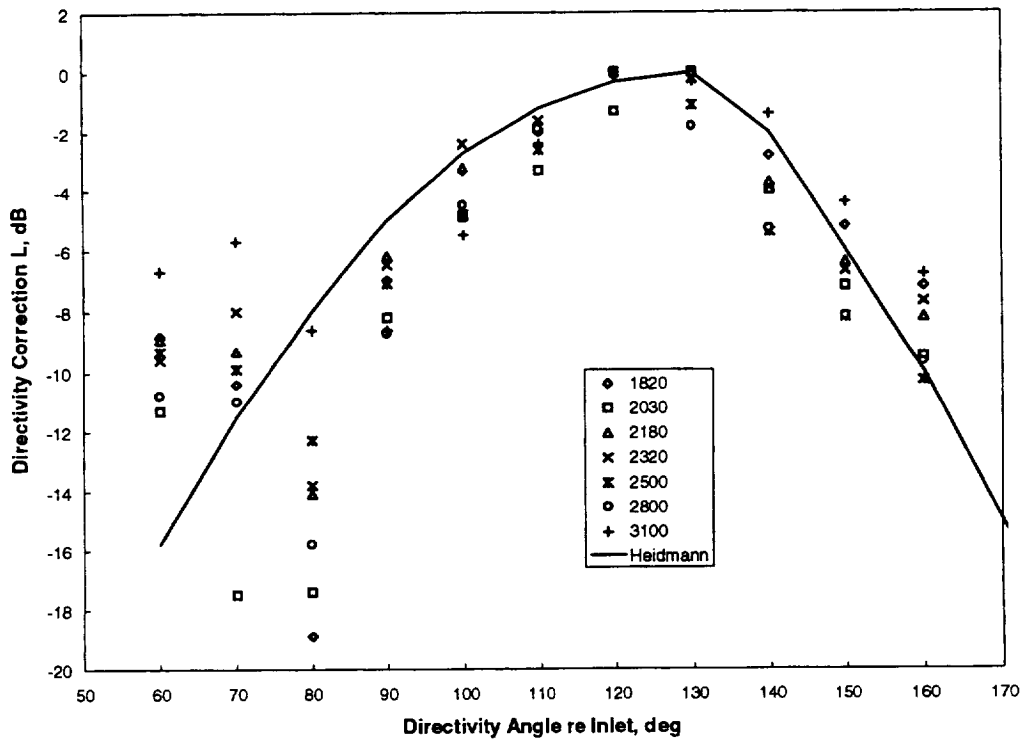
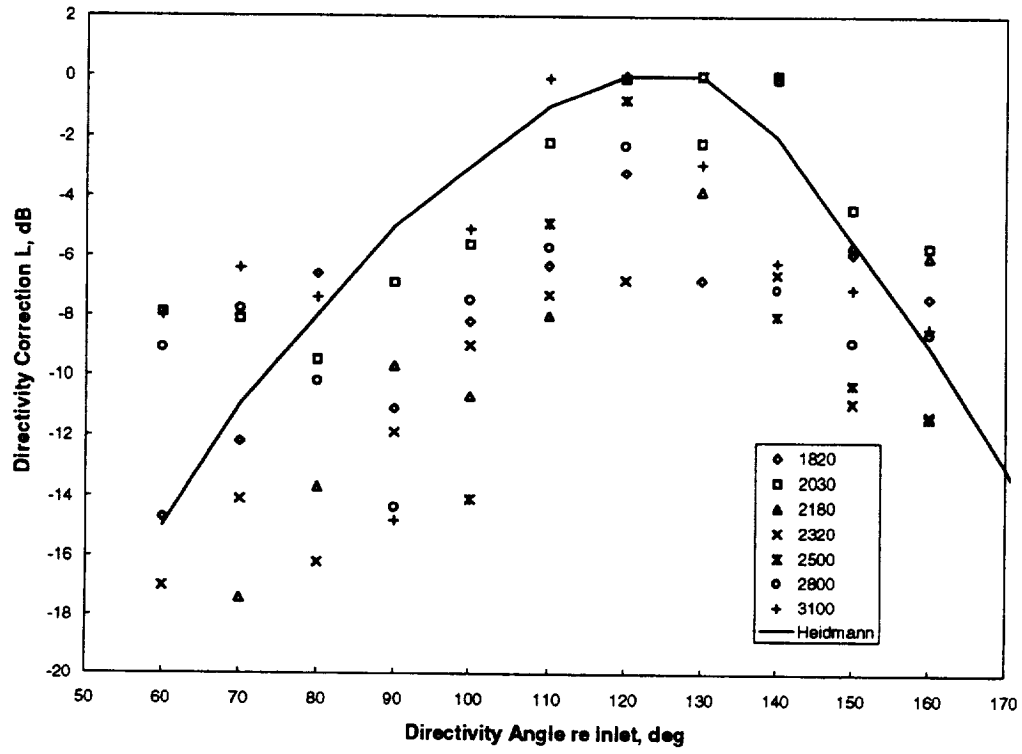


Figure 4.5.4 "Figure 13b" Fan Exhaust Tone Directivity Correction -- E³ Data



4.6 Combination Tone Noise

The Heidmann method contains a model for predicting combination tone noise, a noise source that occurs only at supersonic tip speeds. It is also commonly referred to as “buzz-saw” noise or Multiple Pure Tone (MPT) noise. “At supersonic tip speeds, shock waves are formed at the leading edge of each rotor blade. These shocks move upstream and decay into a system of Mach waves which propagate out of the inlet duct. Ideally, these shocks would contribute to the BPF tone, but small blade-to-blade manufacturing variations result in a redistribution of the energy into various harmonics of the shaft rotational speed” (Heidmann, 1979).

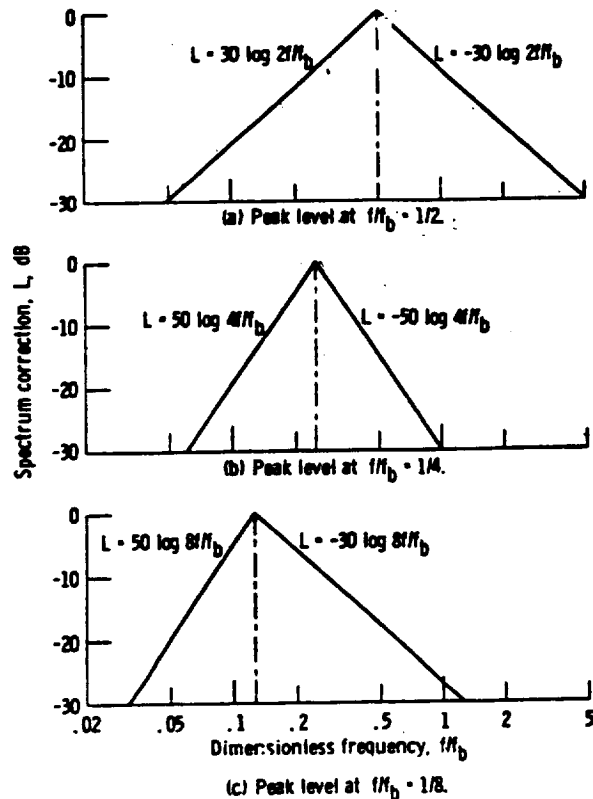
The characteristic peak level at center frequencies one-half, one-fourth, and one-eighth of the fundamental blade passage frequency f_b is given by

$$L_c = 20 \log(\Delta T/\Delta T_o) + 10 \log(m/m_o) + F_1(M_{tr}) + F_2(\theta) + C \quad (10)$$

($C = -5$ dB for fans with inlet guide vanes, $C = 0$ for fans without IGV)

F_1 is characterized by three separate spectra, which have peaks at one-half, one-fourth, and one-eighth of the fundamental blade passage frequency of the fan stage, respectively. These curves appear in Figure 4.6.1. (“Figure 14”, Heidmann, 1979).

Figure 4.6.1. “Figure 14.” Combination Tone Noise Spectrum Content



The changes recommended for the combination tone model are largely based on GE CFM56 data comparisons. Use of this data was required since the CF6-80C2 data contain relatively little combination tone noise. There is no discernible MPT noise in either the E³ or QCSEE databases.

Figures 4.6.2, 4.6.3, and 4.6.4 show how well the spectral content of the combination tone noise is predicted by the modified Heidmann method, relative to the CFM56 data at various tip speeds. These charts indicate that the spectral distribution shapes with peaks at one-half, one-fourth, and one-eighth of the blade passage frequency ($f/f_b = 1/2, 1/4,$ and $1/8$) are not characteristic of the combination tone noise. In fact, there are no clear trends shown for the spectral distribution, and therefore no changes can be recommended.

Figure 4.6.2 Combination Tone Noise Spectrum, CFM56 engine, $M_{tr} = 1.2$

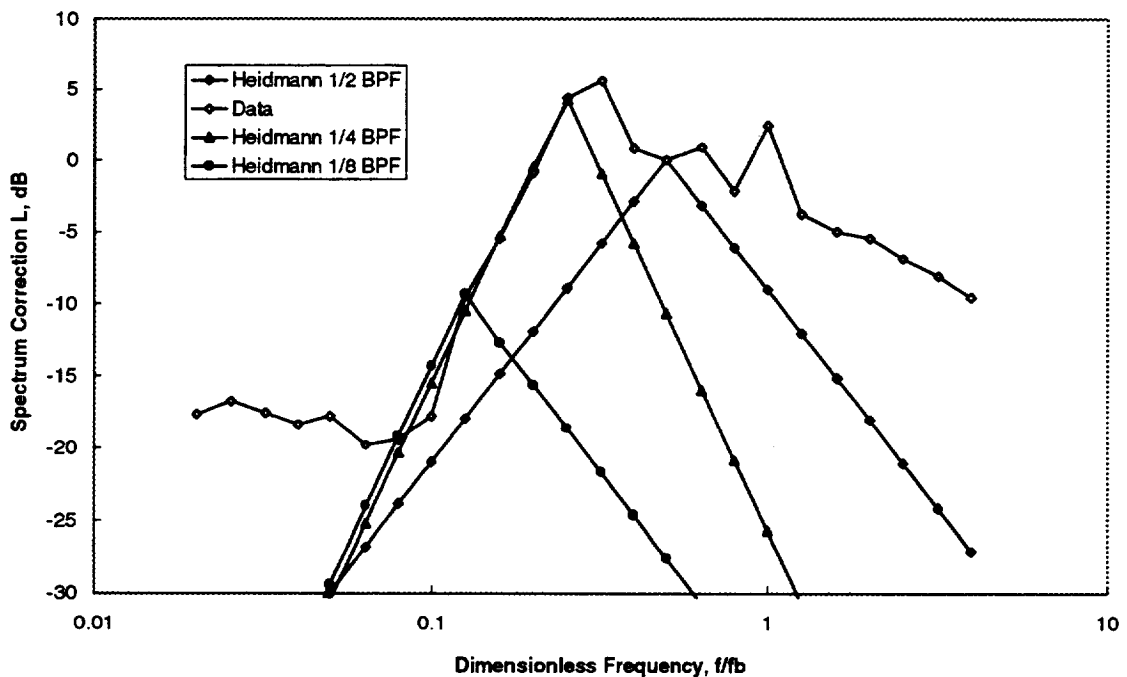


Figure 4.6.3 Combination Tone Noise Spectrum, CFM56 engine, $M_{tr} = 1.32$

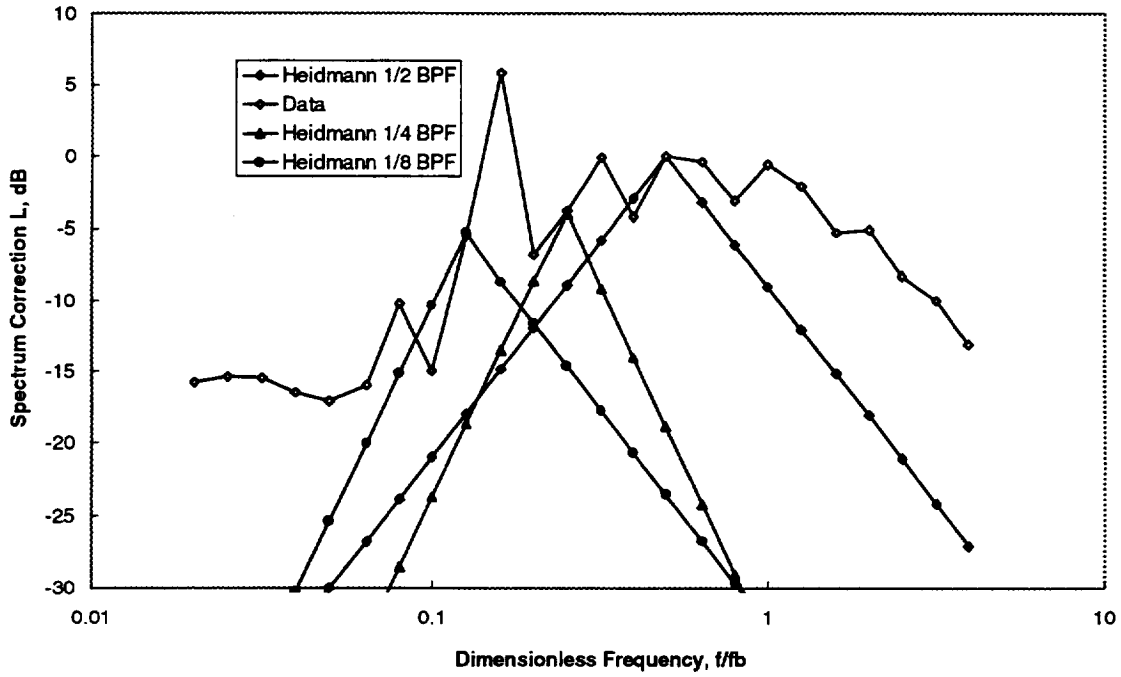
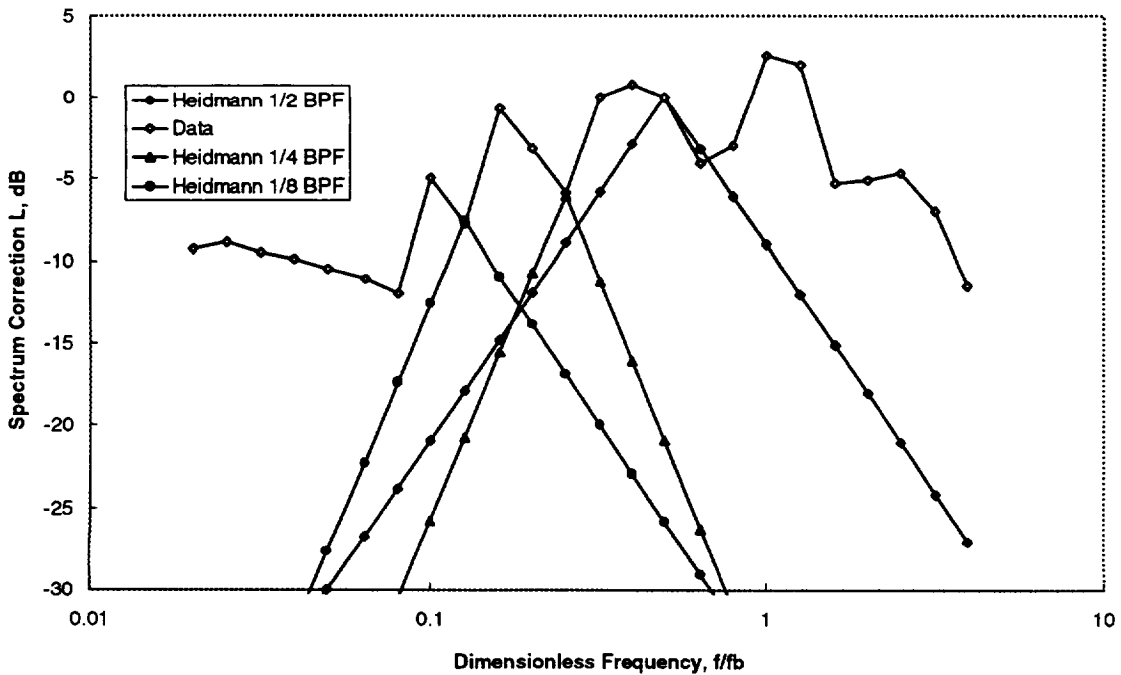


Figure 4.6.4 Combination Tone Noise Spectrum, CFM56 engine, $M_{tr} = 1.43$



The levels of the three spectra are determined by a set of curves that are labeled "Heidmann" in Figures 4.6.5 - 4.6.7 (taken from "Figure 15", Heidmann, 1979). Figure 4.6.5 shows the new combination tone noise level curve that is recommended for $f/f_b = 1/2$ (shown by the dashed line), based on the comparison made with the CFM56 and CF6-80C2 data. Similarly, Figures 4.6.6 and 4.6.7 show the recommended shapes for the $f/f_b = 1/4$ and $1/8$ curves. In the case of the $1/2$ and $1/4$ BPF curves, the modification was determined by a best fit with the CFM56 data (the CF6-80C2 data was ignored since the MPT content is relatively low in this engine). For the $1/8$ BPF peak curve, the CFM56 and CF6-80C2 data agree, but there is not enough data to support definition of a new curve. In this case, the slope of the ascending curve was modified according to the data, and the slope of the descending curve was maintained.

Spectral comparisons of the old and new Heidmann method predictions relative to the GE data are given in Appendix L for the CFM56 and Appendix M for the CF6-80C2. Exact definition of the new normalized combination tone levels (F_1) is given in Table 4.6.1.

Figure 4.6.5 "Figure 15" Combination Tone Noise, $f/f_b = 1/2$

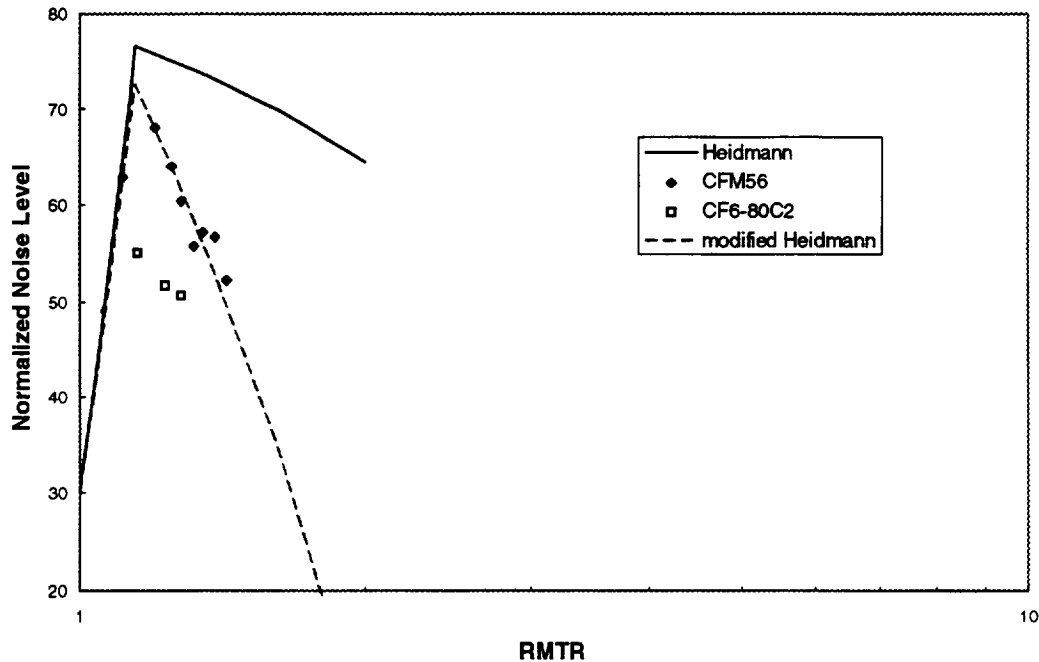


Figure 4.6.6 "Figure 15" Combination Tone Noise, $f/f_b = 1/4$

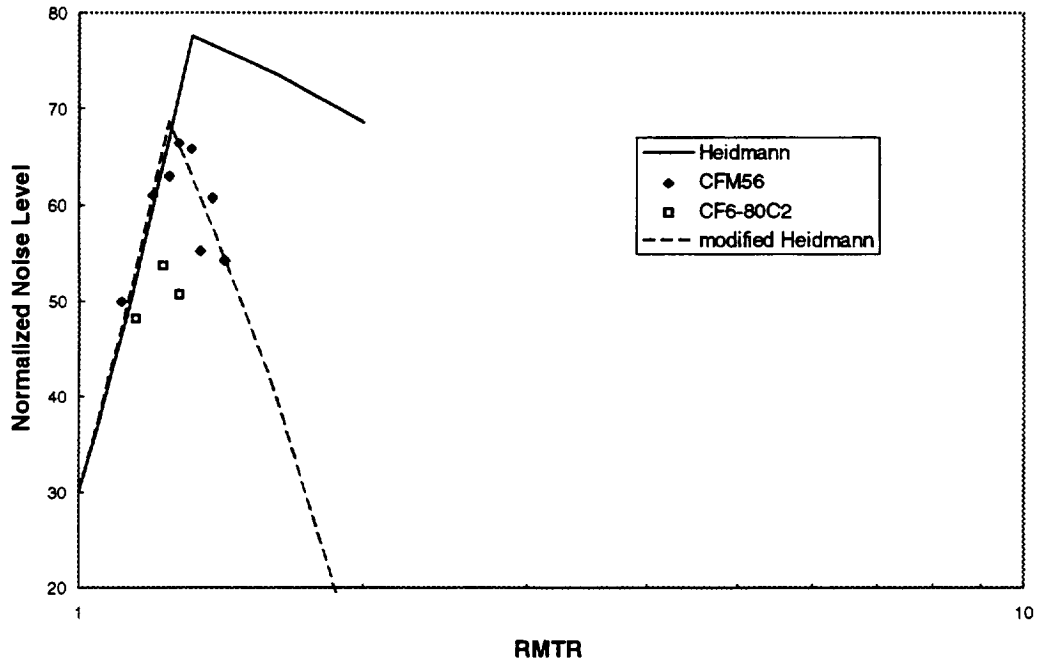


Figure 4.6.7 "Figure 15" Combination Tone Noise, $f/f_b = 1/8$

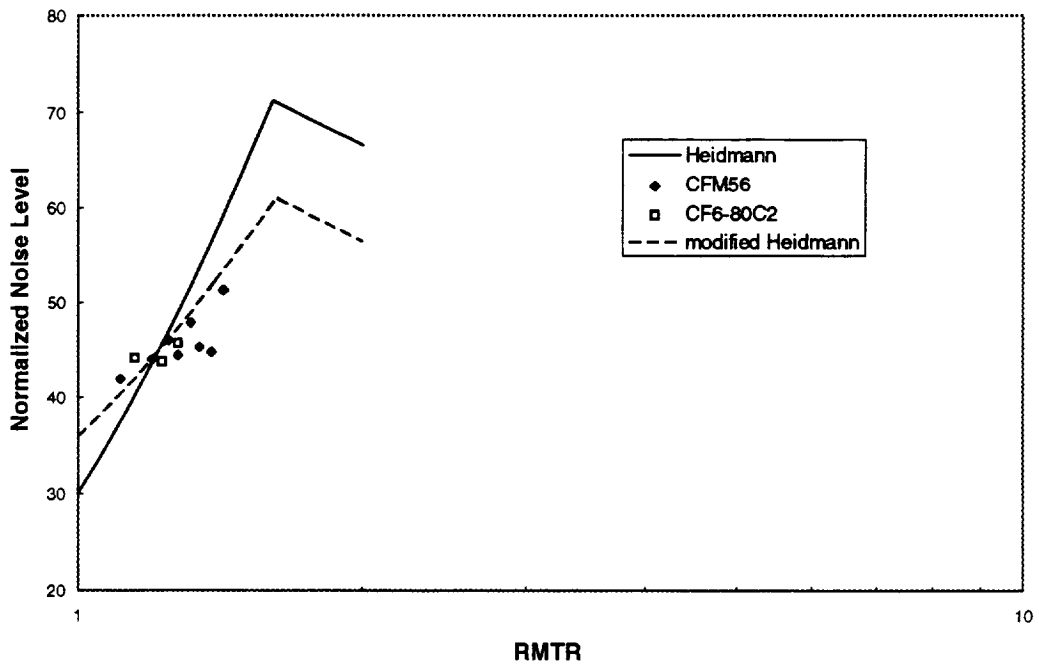


Table 4.6.1 Combination Tone Noise Levels

f/fb	MTR	Ln
1/2	1	30
	1.14	72.5
	2	4.4
1/4	1	30
	1.25	68.6
	2	10.5
1/8	1	36
	1.61	60.6
	2	56.5

4.7 Summary of Fan Noise Methodology Changes

The following section is an outline of all recommended changes to the Heidmann fan noise model, based on the results of correlations made with the CF6-80C2, E³, and QCSEE engine data.

Inlet Broadband Noise

Inlet broadband noise is given by Heidmann as:

$$L_c = 20 \log(\Delta T/\Delta T_o) + 10 \log(m/m_o) + F_1(M_{trd}, M_{tr}) + F_2(RSS) + F_3(\theta)$$

Modify F_1 such that:

$$F_1 = 58.5 + 20 \log(M_{trd}) - 50 \log(M_{tr}/0.9); M_{trd} > 1, M_{tr} > 0.9$$

Modify F_2 such that:

$$F_2 = 0$$

Fan Exhaust Broadband Noise

Fan exhaust broadband noise is given by Heidmann as:

$$L_c = 20 \log(\Delta T/\Delta T_o) + 10 \log(m/m_o) + F_1(M_{trd}, M_{tr}) + F_2(RSS) + F_3(\theta)$$

Modify F_1 such that:

$$L_n = 63 + 20 \log(M_{trd}); M_{trd} > 1, M_{tr} \leq 1.0$$

$$L_n = 63 + 20 \log(M_{trd}) - 30 \log(M_{tr}); M_{trd} > 1, M_{tr} > 1.0$$

Always calculate F_2 by:

$$F_2 = -5 \log(RSS/300)$$

Inlet Tone Noise

Fan inlet tone noise is given by Heidmann as:

$$L_c = 20 \log(\Delta T/\Delta T_o) + 10 \log(m/m_o) + F_1(M_{trd}, M_{tr}) + F_2(RSS) + F_3(\theta)$$

Modify F_1 such that:

$$L_n = 64.5 + 80 \log(M_{trd}/M_{tr}); L_n = 60.5 + 20 \log(M_{trd}) + 50 \log(M_{tr}/0.72)$$

for $M_{trd} > 1, M_{tr} > 0.72$ (choose lesser value)

Modify F_2 such that:

$$F_2 = 0$$

Cutoff Correction

Increase the harmonic fall-off rate for cutoff correction and make it a function of M_{tr} as follows:

For $M_{tr} < 1.15$:

$$L = 6 - 6k; \delta > 1.05$$

$$L = -8; k = 1$$

$$L = 6 - 6k; k \geq 2$$

For $M_{tr} \geq 1.15$:

$$L = 9 - 9k; \delta > 1.05$$

$$L = -8; k = 1$$

$$L = 9 - 9k; k \geq 2$$

Flight Cleanup

Apply following suppressions to fan inlet fundamental (BPF) and second harmonic (2BPF) tones for “flight cleanup” effect:

Angle	Approach		Takeoff	
	BPF	2BPF	BPF	2BPF
10	5.6	5.4	4.8	5.8
20	5.8	4.3	5.5	3.8
30	4.7	3.4	5.5	5.3
40	4.6	4.1	5.3	6.4
50	4.9	2.0	5.3	3.5
60	5.1	2.9	5.1	3.0
70	2.9	1.6	4.4	2.1
80	3.2	1.3	3.9	2.1
90	1.6	1.5	2.6	1.1
100	1.6	1.1	2.3	1.4
110	1.8	1.4	1.8	0.9
120	2.1	1.5	2.1	0.7
130	2.4	1.0	1.7	0.7
140	2.2	1.8	1.7	0.4
150	2.0	1.6	2.6	0.6
160	2.8	1.6	3.5	0.8

Fan Exhaust Tone Noise

Always calculate F_2 by:

$$F_2 = -10 \log(\text{RSS}/300)$$

Combination Tone Noise

Fan combination tone noise is given by Heidmann as:

$$L_c = 20 \log(\Delta T/\Delta T_o) + 10 \log(m/m_o) + F_1(M_{tr}) + F_2(\theta) + C$$

Revise normalized combination tone noise levels (F_1) as follows:

f/fb	MTR	Ln
1/2	1	30
	1.14	72.5
	2	4.4
1/4	1	30
	1.25	68.6
	2	10.5
1/8	1	36
	1.61	60.6
	2	56.5

5.0 Concluding Remarks

The fan noise model in ANOPP is based on noise correlations developed from fan rig tests at NASA Lewis. The recommendations that have been made relative to commercial engine data have now helped the method to achieve results that are a better indication of full-scale fan noise from large commercial turbofan engines. No assessments related to multiple stage fans or fans with inlet guide vanes were made, since this is outside of the task of developing ANOPP as a tool for advanced UHB studies.

The recommendations intentionally are structured to retain the form of the Heidmann model. Generally, no need to change the structure of the models was demonstrated, since many of the original correlations showed some relationship to the engine data. An exception to this was the combination tone noise model. In this case, it was demonstrated that the structure of the model did not reflect the nature of the data, both in magnitude and in frequency. The engine combination tone noise data does not fit the one-half, one-fourth, and one-eighth blade passage frequency spectrum model. It is therefore suggested that the current Heidmann method for combination tone noise prediction be replaced with a new methodology.

The assessment of the other components of engine noise (jet, combustor, and turbine) identified some other areas for potential model improvements, especially to the turbine noise method. This model was shown to give tremendously high predictions of turbine noise, and a spectral content that was much different from that of the engine data.

Follow-on work to this task is in progress to add fan inlet and fan exhaust noise models of acoustic treatment suppression. This will be an enhancement to the current Heidmann model, which predicts only hardwall fan noise. Such a tool will enable comparisons of engine configurations with different treatment designs.

Appendix A
Sample ANOPP Input

```

ANOPP JECHO=.TRUE.  JLOG=.FALSE.  NLPPM=60  $
STARTCS  $
SETSYS JECHO=.FALSE.  JCON=.TRUE.  $
CREATE SCRATCH ATM HDNFAN STNJET GECOR GETUR SFIELD  $
CREATE FANIN FANEX  $
$
$ DEFINE FREQUENCY AND DIRECTIVITY ANGLE ARRAYS
$
UPDATE NEWU=SFIELD SOURCE=* $
  -ADDR OLDM=*  NEWM=FREQ  FORMAT=5H24RS$  $
    50. 63. 80. 100. 125. 160. 200. 250. 315. 400. 500. 630. 800. 1000
    1250. 1600. 2000. 2500. 3150. 4000. 5000. 6300. 8000. 10000. $
  -ADDR OLDM=*  NEWM=THETA  FORMAT=5H17RS$  $
    10. 20. 30. 40. 50. 60. 70. 80. 90. 100. 110. 120. 130. 140.
    150. 160. 170. $
  -ADDR OLDM=*  NEWM=PHI  FORMAT=3HRS$  $
    90. $
END* $
$
PARAM IUNITS=7HENGLISH $
PARAM RS = 150.  $ RADIAL DISTANCE FROM SOURCE TO OBSERVER, M
PARAM IOUT=1  $ REQUEST dB OUTPUT
PARAM AE=33.2  $ ENGINE REFERNCE AREA, ft**2
PARAM NENG=1  $ NUMBER OF ENGINES
PARAM IPRINT=2  $ INPUT PRINT ONLY
$
$ LOAD SYSTEM PROCEDURE LIBRARY
$
LOAD /LIBRARY/STNTBL $
LOAD /LIBRARY/ LIB=PROCLIB $
$
$ BUILD ATMOSPHERIC AND ATMOSPHERIC ABSORPTION TABLES
$
PARAM DELH=100.  $ ALTITUDE INCREMENT FOR OUTPUT, M
PARAM H1=0.  $ GROUND LEVEL ALTITUDE
PARAM NAI=1  $
PARAM NHO=11  $ NUMBER OF ALTITUDES FOR OUTPUT
PARAM P1=1936.08  $ ATMOSPHERIC PRESSURE AT GROUND LEVEL, LB/FT^2
PARAM ABSINT=10  $ # OF INTEGRATION STEPS FOR ABS
$
$ DEFINE MEMBER ATM(IN) - ALTITUDE.  TEMPERATURE.  RELATIVE HUMIDITY
$
UPDATE NEWU=ATM SOURCE=* LIST=ES $
  -ADDR OLDM=*  NEWM=IN  FORMAT=4H3RS$  $
    0.  536.67  70.  $
END*  $
$
$ EXECUTE ATM $
$ EXECUTE ABS $
$
$ SET UP INPUT FOR GEO
$
PARAM DELT=0.5  $ RECEPTION TIME INCREMENT
PARAM ENGAM=3HXXX  $ MATCH DEFAULT NAMES IN OTHER MODULES
PARAM START=0.0  $ START TIME FOR GEOMETRY
PARAM STOP=40.  $ STOP TIME FOR GEOMETRY
PARAM ICOORD=1  $ REQUEST BODY AXIS ONLY

```

```

PARAM DIRECT=.FALSE. $ INTERPOLATE FROM FLI (TAKOFF) OBSERVER RECEPTION
$ TIMES AND GEOMETRY BASED ON USER PARAMS
PARAM DELTH=10. $ MAXIMUM POLAR DIRECTIVITY ANGLE
PARAM CTK=1. $ CHARACTERISTIC TIME CONSTANT
PARAM DELDB=10. $ LIMITING NOISE LEVEL DOWN FROM PEAK
$
$
$ PUT OBSERVER AT LOCATION 0,0,0
$
UPDATE NEWU=OBSERV SOURCE=* $
-ADDR OLDM=* NEWM=COORD FORMAT=4H3RS$ $
0. 0. 0. $
END* $
$
$
PARAM RHOA=.00222 $
PARAM MA=0.00 $
$
$
$ DEFINE ENGINE CYCLE PARAMETERS FOR FAN NOISE
$
PARAM CA= 1135.6 $ AMBIENT SPEED OF SOUND
PARAM DIAM=1.2 $ FAN ROTOR DIAMETER, RE AE
PARAM MDOT=.443 $ MASS FLOW RATE, RE RHOA*CA*AE
PARAM N=0.320 $ ROTATIONAL SPEED, RE CA/DIAM
PARAM DELTAT=0.123 $ TOTAL TEMPERATURE RISE ACROSS FAN, RE TA
PARAM NB=32 $ NUMBER OF BLADES
PARAM MD=0.989 $ FAN ROTOR REL. TIP MACH NO. AT DESIGN POINT
PARAM AFAN=1.0 $ FAN INLET X-SECT AREA, RE AE
PARAM RSS=2.600 $ ROTOR-STATOR SPACING, RE MEAN BLADE CHORD
PARAM NV=34 $ NUMBER OF VANES
PARAM IGV=1 $ NO INLET GUIDE VANES
PARAM DIS=2 $ INLET FLOW DISTORTION
PARAM INRS=.TRUE. $ ROTOR STATOR INTERACTION TONES ON
PARAM INCT=.FALSE. $ COMBINATION TONES ON
PARAM INDIS=.TRUE. $ INLET DISTORTION TONES OFF
PARAM IDRS=.FALSE. $ DISCHARGE ROTOR-STATOR TONES ON
PARAM IDBB=.FALSE. $ DISCHARGE BROADBAND ON
PARAM INBB=.TRUE. $ INLET BROADBAND ON
$
EXECUTE HDNFAN HDNFAN=FANIN $
$
PARAM IDBB=.TRUE. IDRS=.TRUE. INBB=.FALSE. INCT=.FALSE. INRS=.FALSE. $
PARAM INDIS=.FALSE. $
$
EXECUTE HDNFAN HDNFAN=FANEX $
$
$
$ DEFINE INPUT PARAMETERS FOR JET NOISE MODULE
$
PARAM CIRCLE=.TRUE. $ IMPLIES CIRCULAR NOZZLE
PARAM PLUG=.TRUE. $ EXHAUST PLUG OPTION ON
PARAM SUPER=.FALSE. $ SUPERSONIC JET OPTION OFF
PARAM DELTA=0. $ ANGLE BETWEEN FLIGHT VECTOR AND ENGINE AXIS
PARAM M1=.707 $ PRIMARY STREAM MACH NO
PARAM V1=0.783 $ " " JET VELOCITY, RE CA
PARAM T1=1.341 $ " " TOTAL TEMP, RE TA
PARAM MA=0.0 $ AIRCRAFT MACH NO.
PARAM RHO1=.819 $ PRIMARY STREAM JET DENSITY, RE RHOA
PARAM DE1=.912 $ ACTUAL PRIMARY STREAM EQUIVALENT DIAMETER

```

```

PARAM DH1=DE1          $ PRIMARY STREAM HYDRAULIC DIAMETER
PARAM A1=.653          $ PRIMARY STREAM FULLY EXPANDED JET AREA
$
EXECUTE STNJET $
$
$ DEFINE PARAMETERS FOR COMBUSTION NOISE MODULE
$
PARAM MDOT=.037        $ COMBUSTOR ENTRANCE MASS FLOW RATE, RE RHOA*CA*AE
PARAM PI=25.09         $ " " TOTAL PRESSURE, RE TA
PARAM TI=2.709         $ " " TEMPERATURE, RE TA
PARAM TCJ=5.707        $ " EXIT TOTAL TEMPERATURE, RE TA
PARAM TDDELTA=2.8      $ DESIGN TURBINE TEMPERATURE RISE, RE TA
PARAM A=.01            $ COMBUSTOR ENTRANCE AREA, RE AE
$
EXECUTE GECOR $
$
$ DEFINE PARAMETERS FOR TURBINE NOISE MODULE
$
PARAM AREA=.213        $ TURBINE INLET CROSS-SECTIONAL AREA, RE AE
PARAM NBLADE=48        $ # OF ROTOR BLADES
PARAM D= .351          $ TURBINE ROTOR DIAMETER, RE SQRT AE
PARAM ROTSPD=.32       $ ROTATIONAL SPEED, RE CA/D
PARAM TTI=3.786        $ ENTRANCE TOTAL TEMPERATURE, RE TA
PARAM TSJ=2.875        $ EXIT STATIC TEMPERATURE, RE TA
$
EXECUTE GETUR $
$
$
PARAM PROPRT=2 $
$
ENDCS $

```

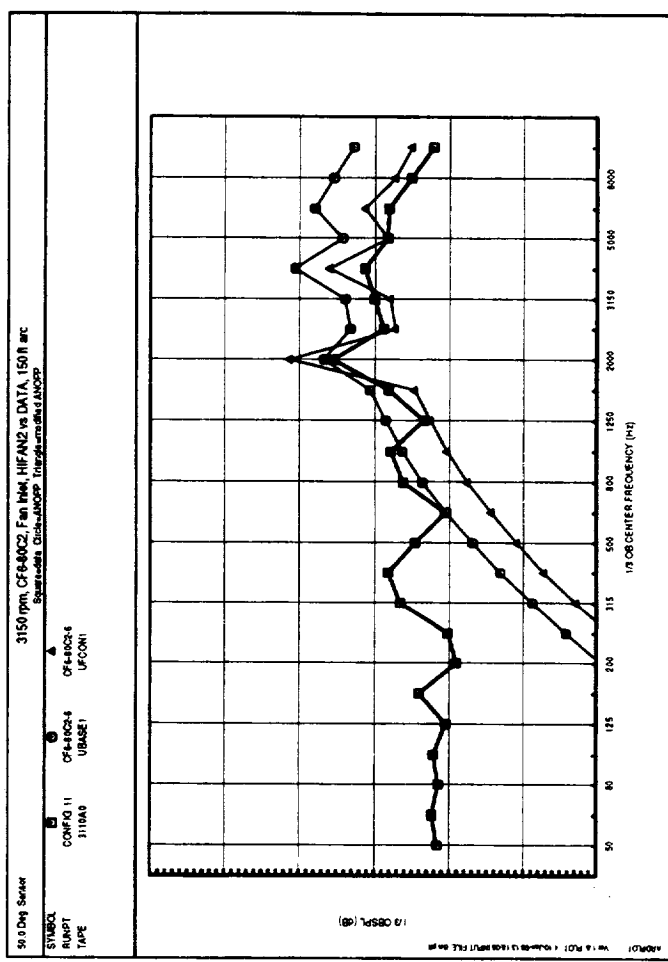
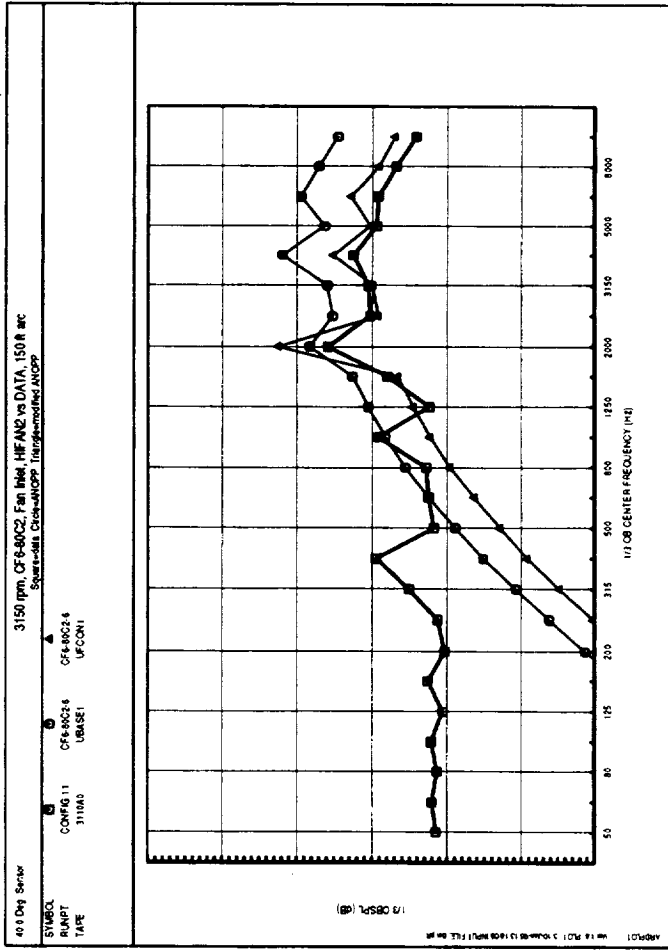
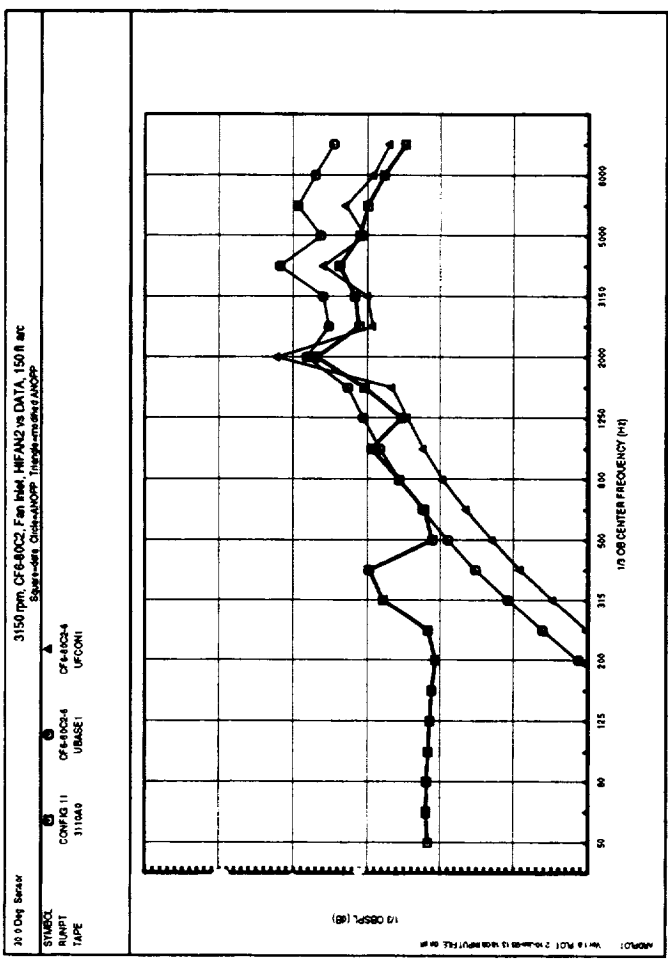
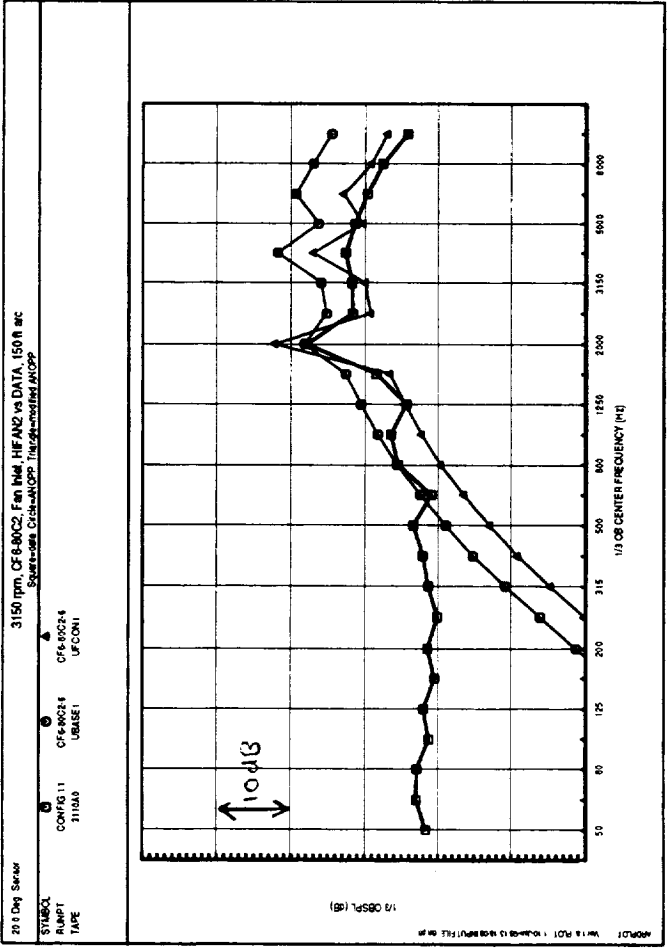
Appendix B
Fan Inlet Noise Spectral Comparisons - CF6-80C2

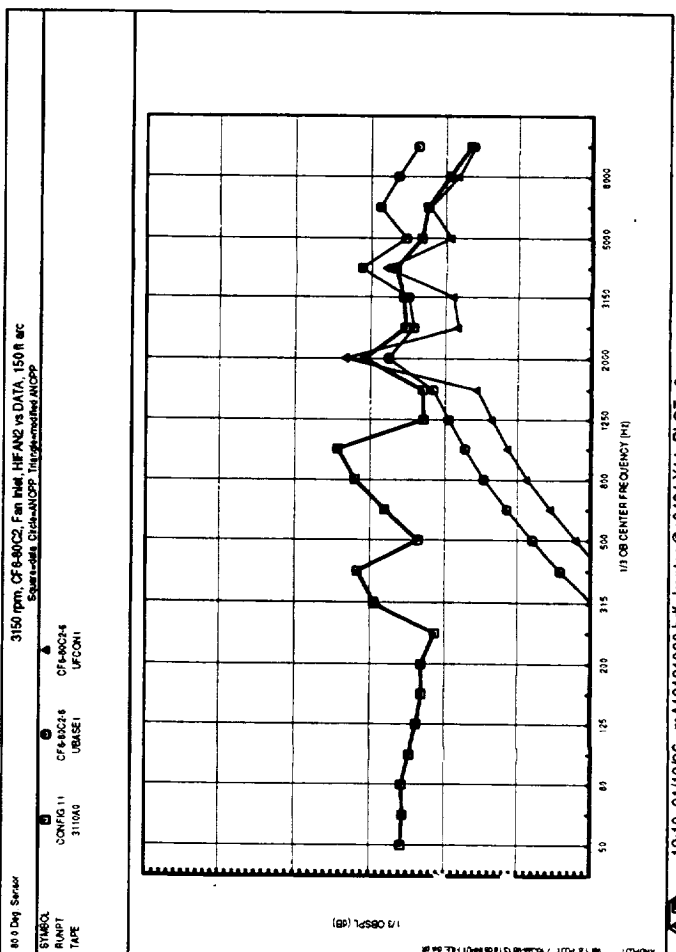
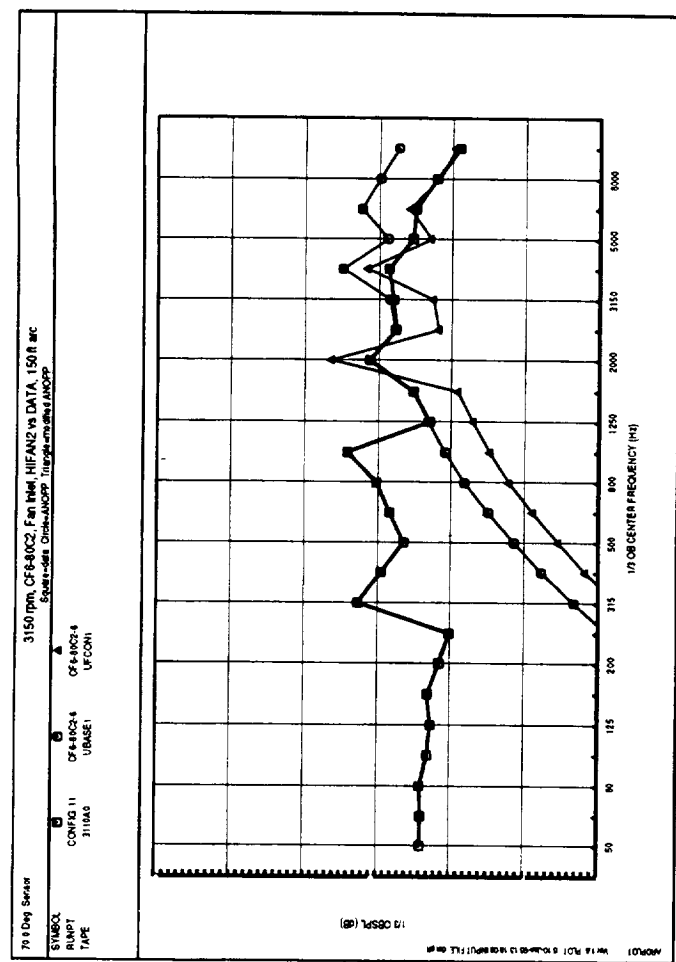
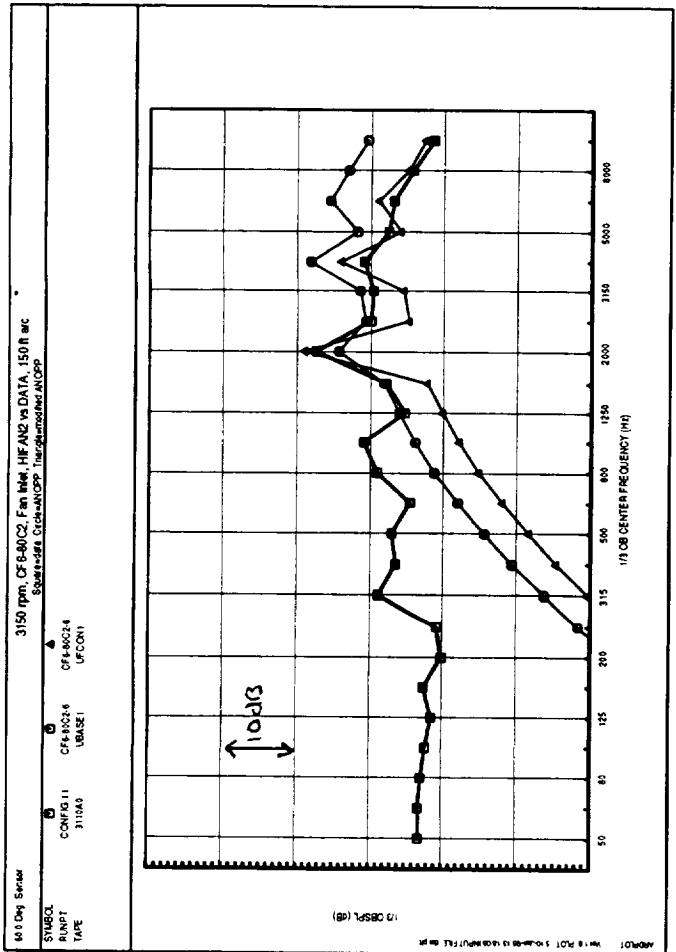
Appendix B Contents

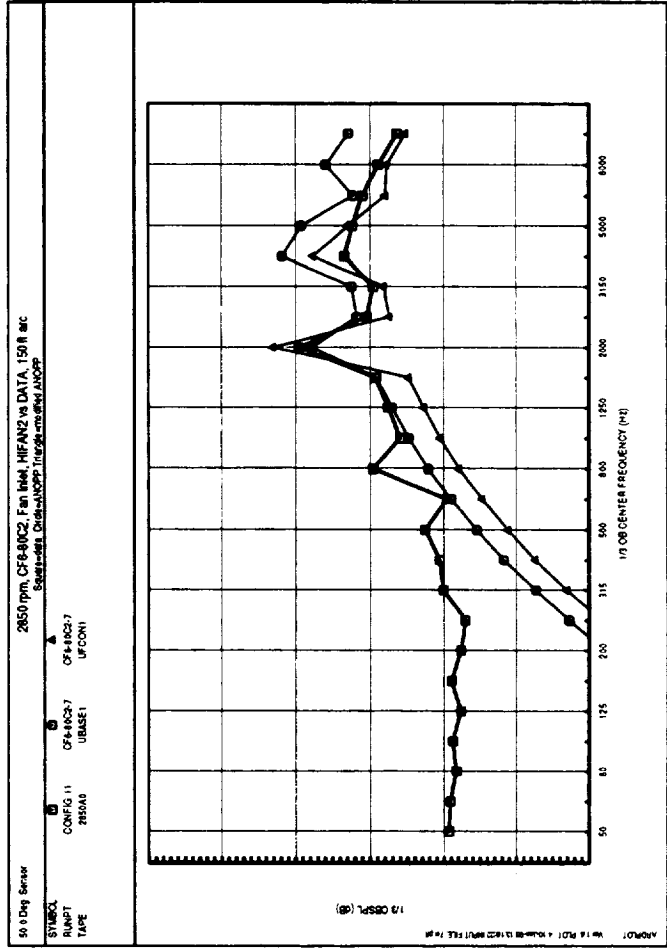
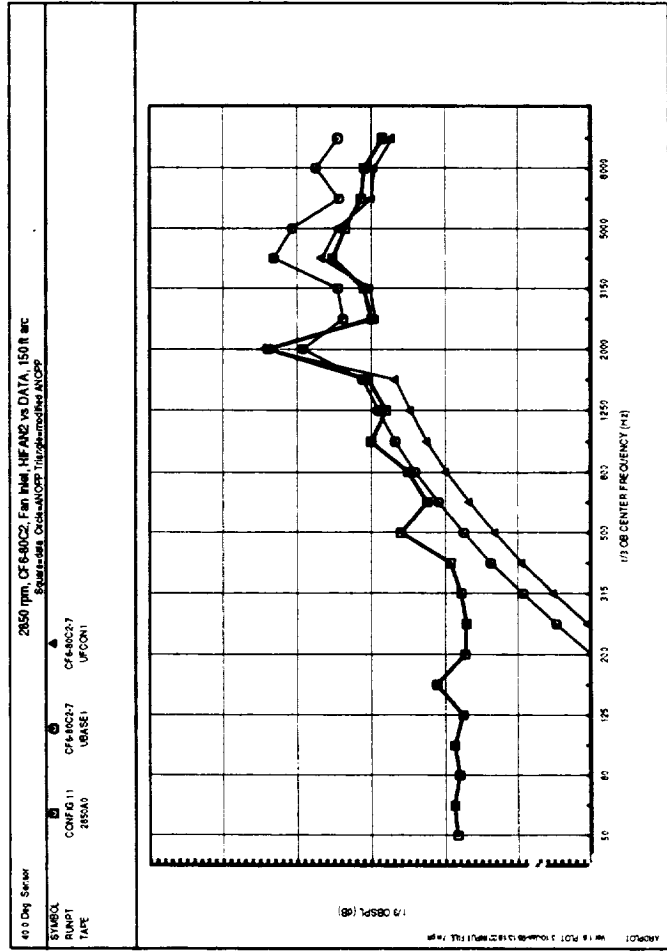
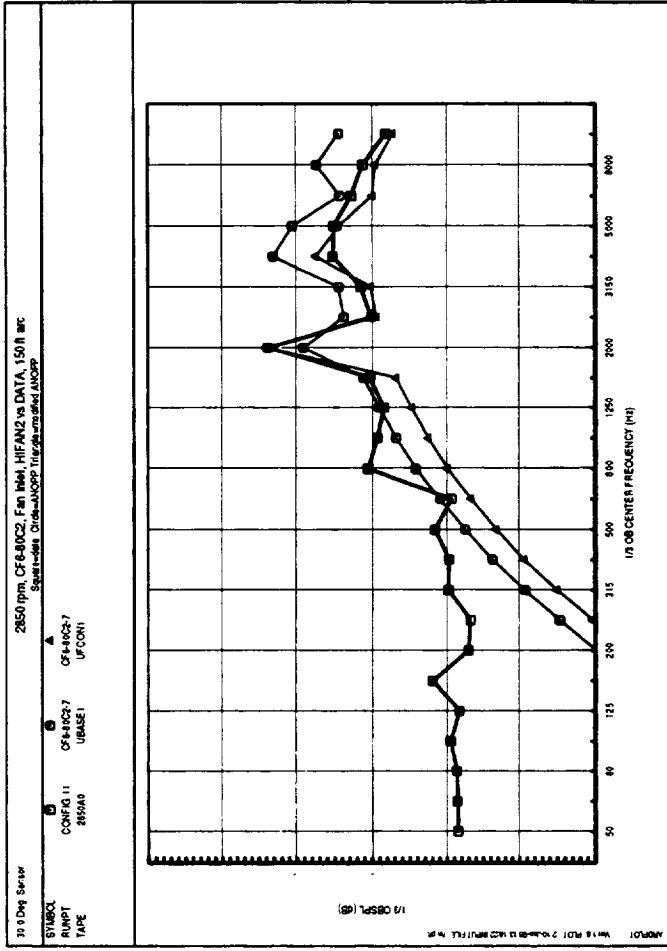
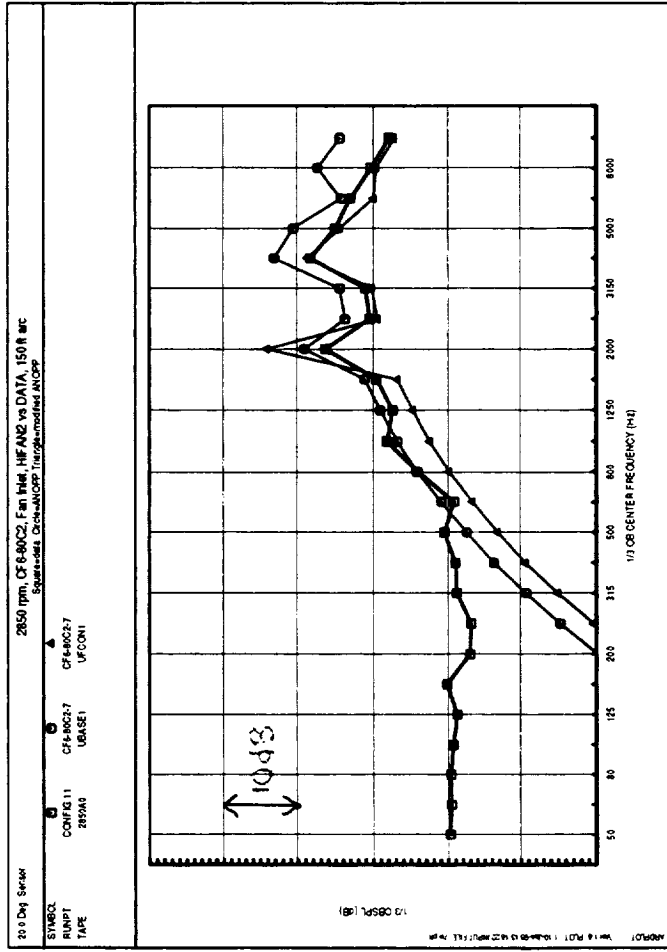
Page	Fan Speed, rpm	Angles, deg
51	3150 (takeoff)	20-50
52	3150 (takeoff)	60-80
53	2850 (cutback)	20-50
54	2850 (cutback)	60-80
55	2700	20-50
56	2700	60-80
57	2550	20-50
58	2550	60-80
59	2250	20-50
60	2250	60-80
61	2100 (approach)	20-50
62	2100 (approach)	60-80

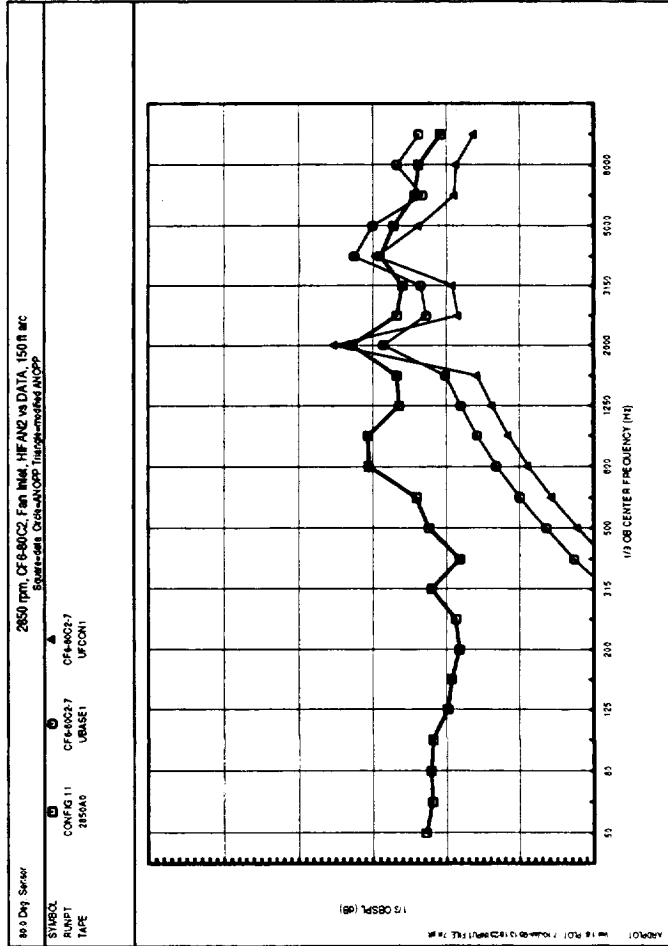
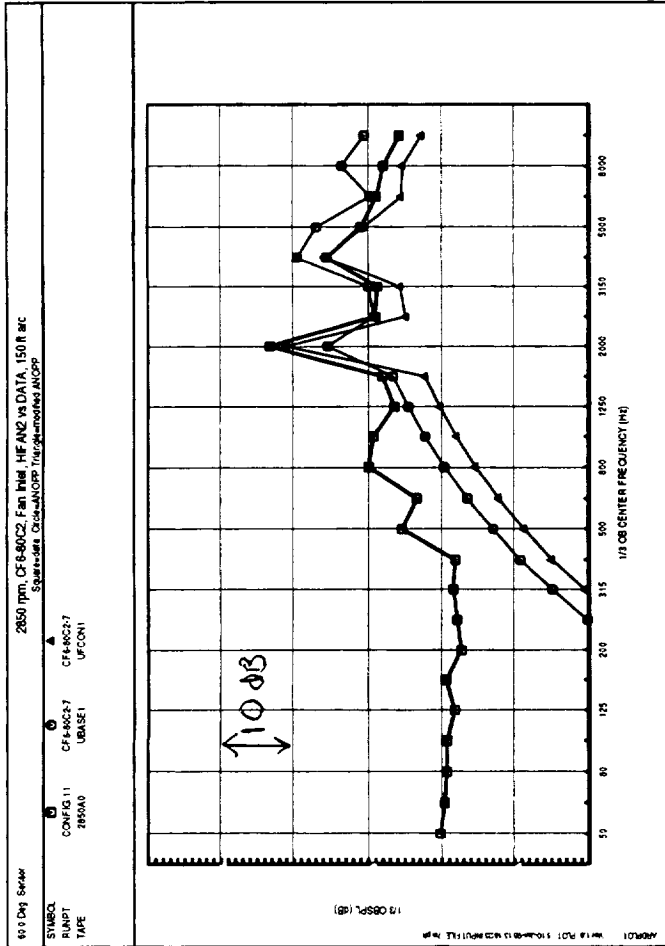
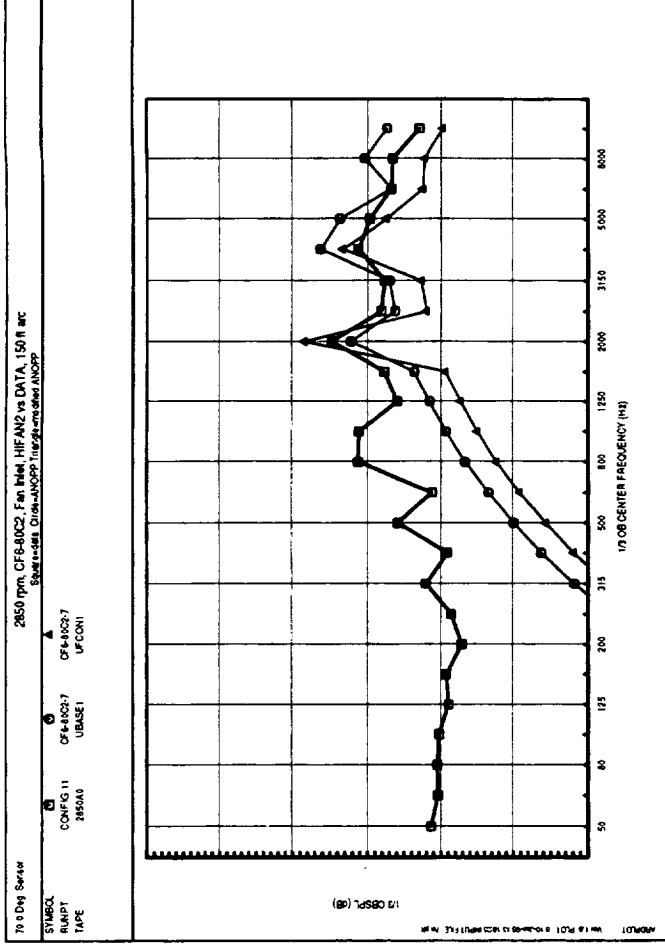
Key to Plots:

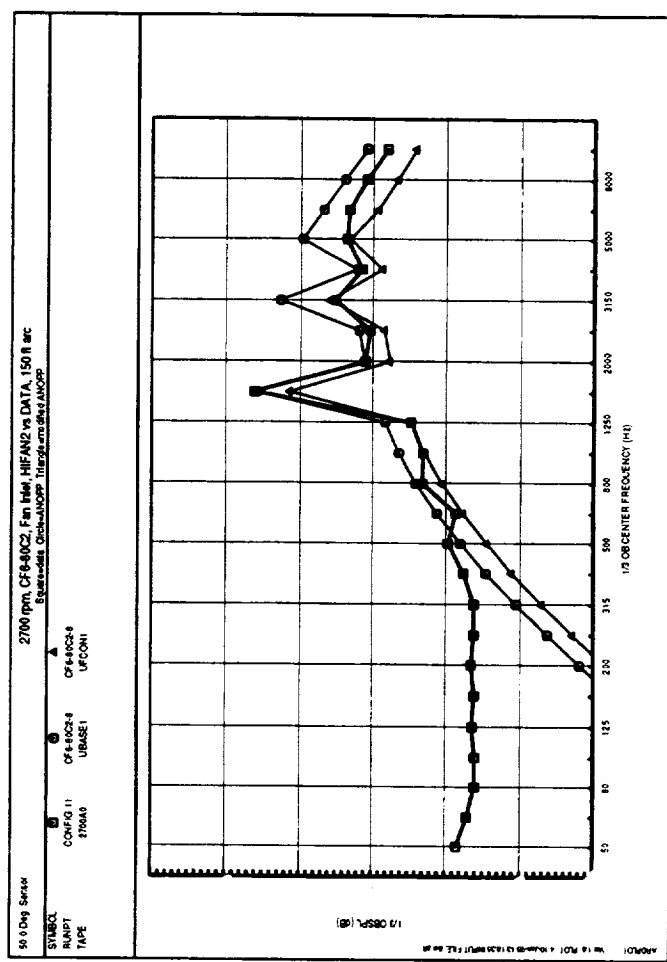
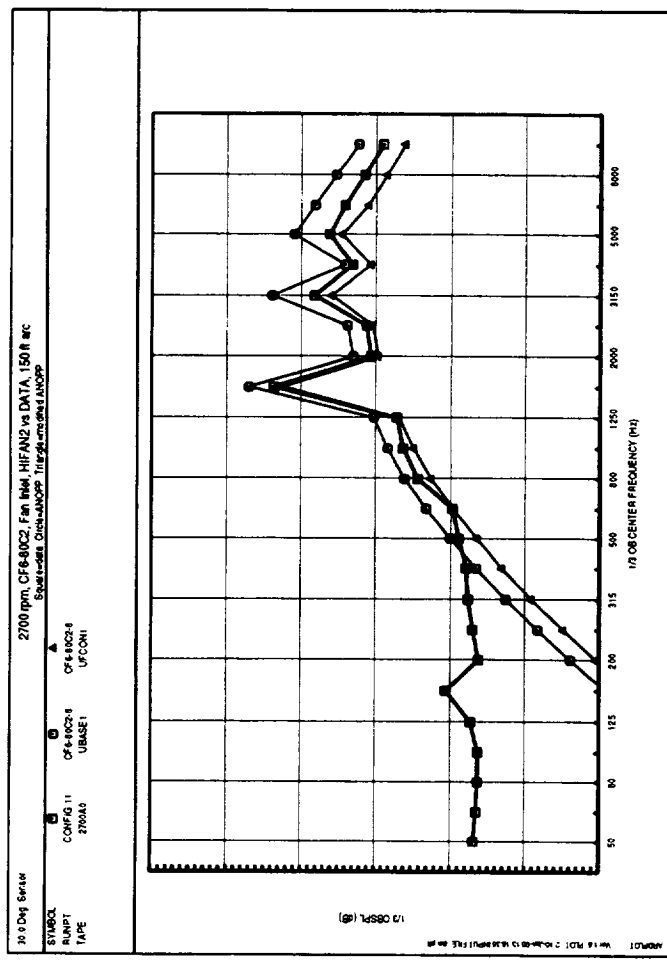
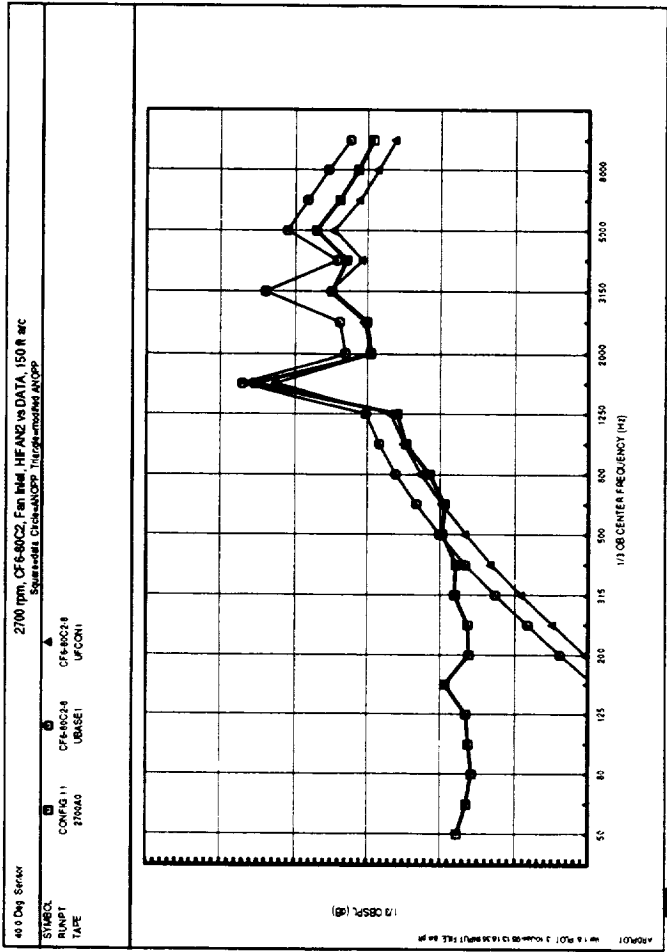
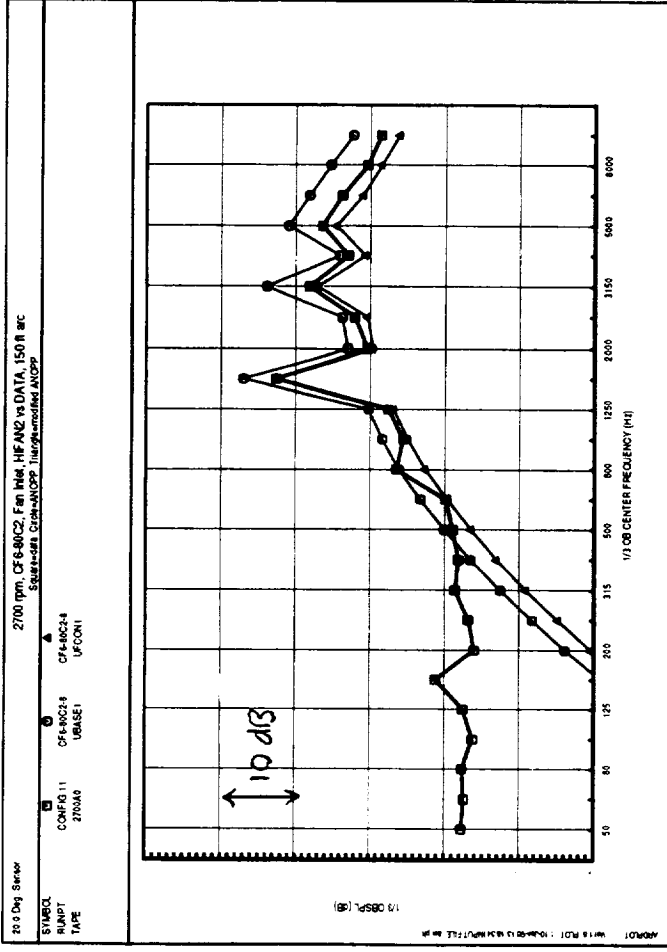
squares = total measured engine data
circles = Heidmann method prediction
triangles = modified Heidmann method prediction (see Section 4)

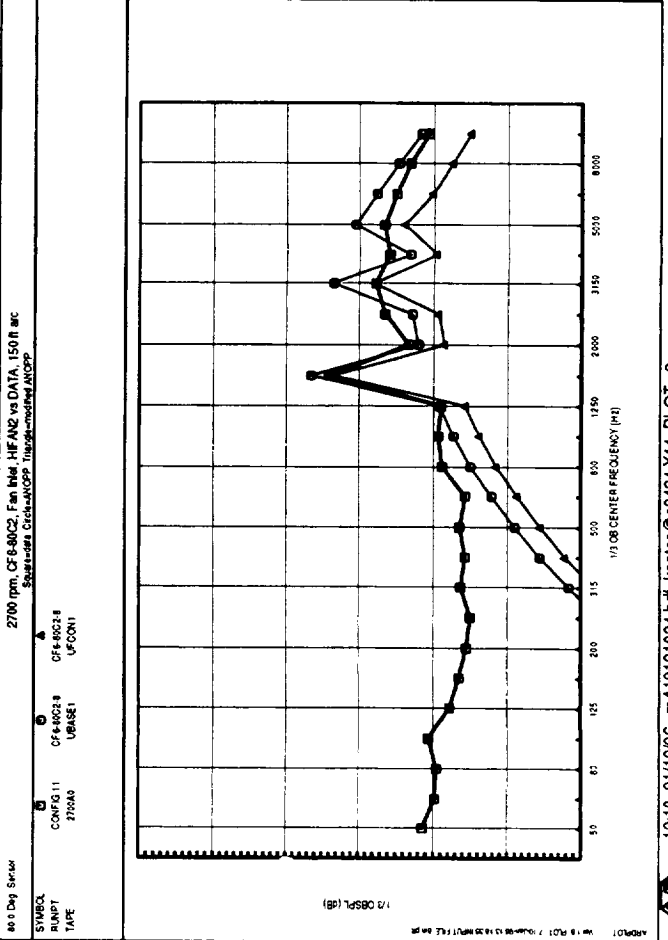
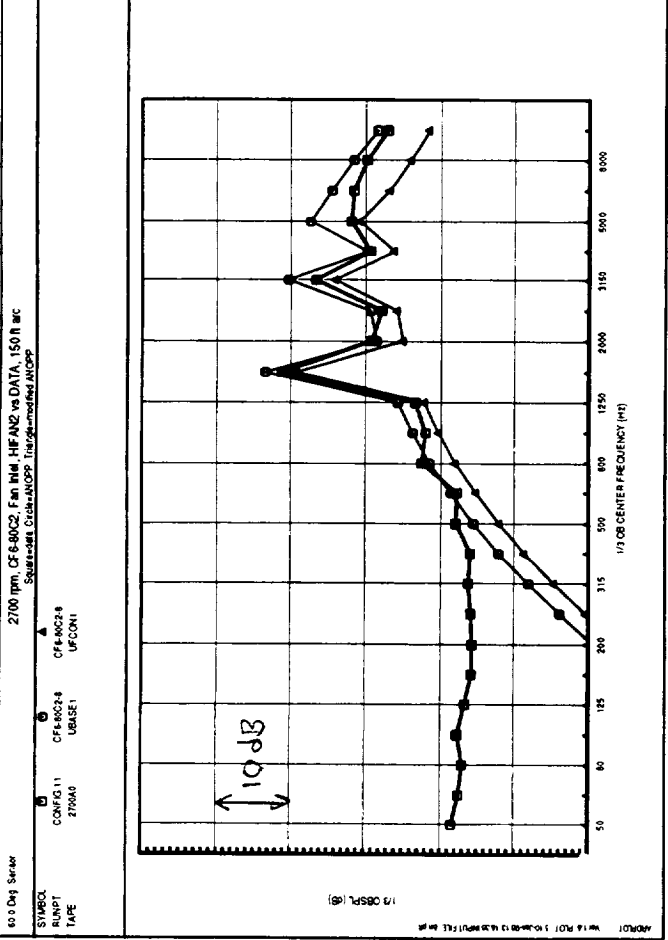
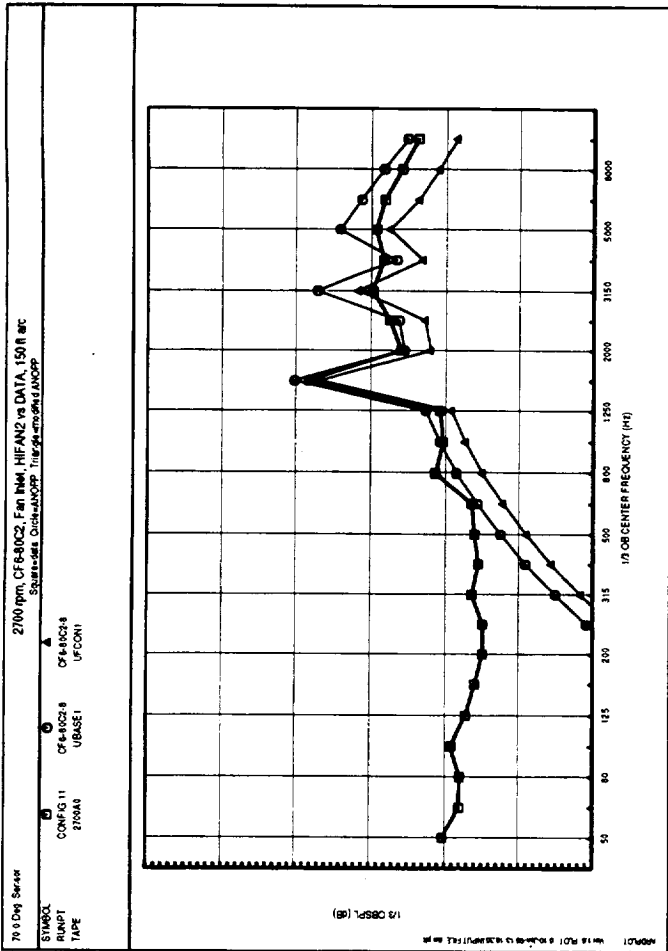






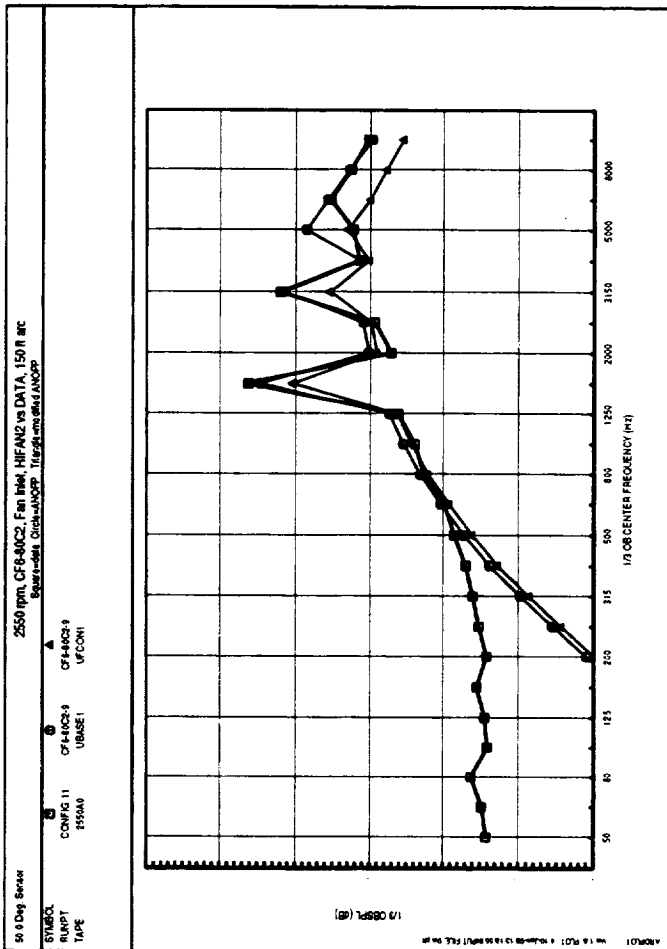
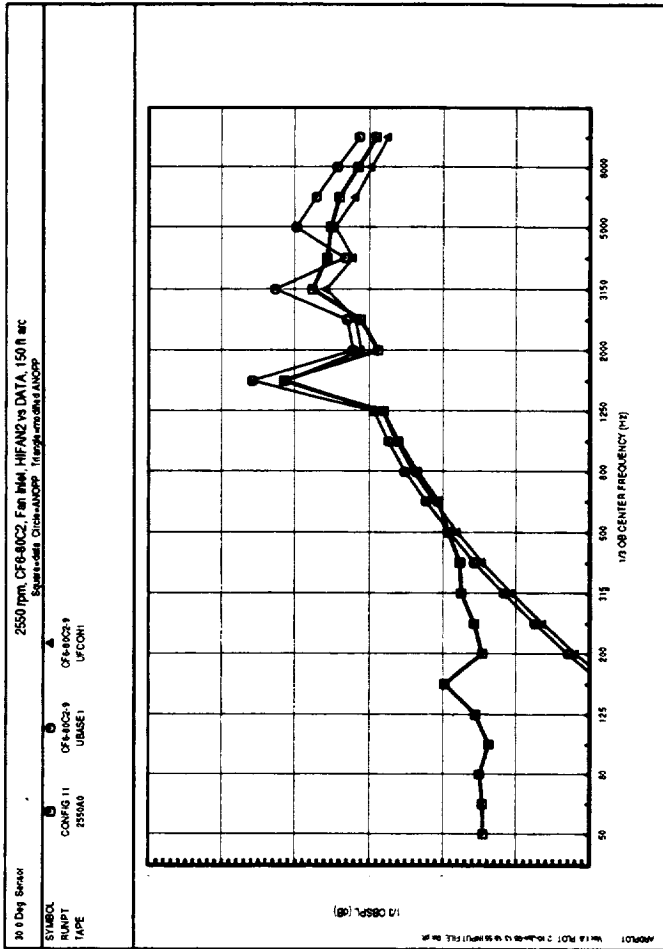
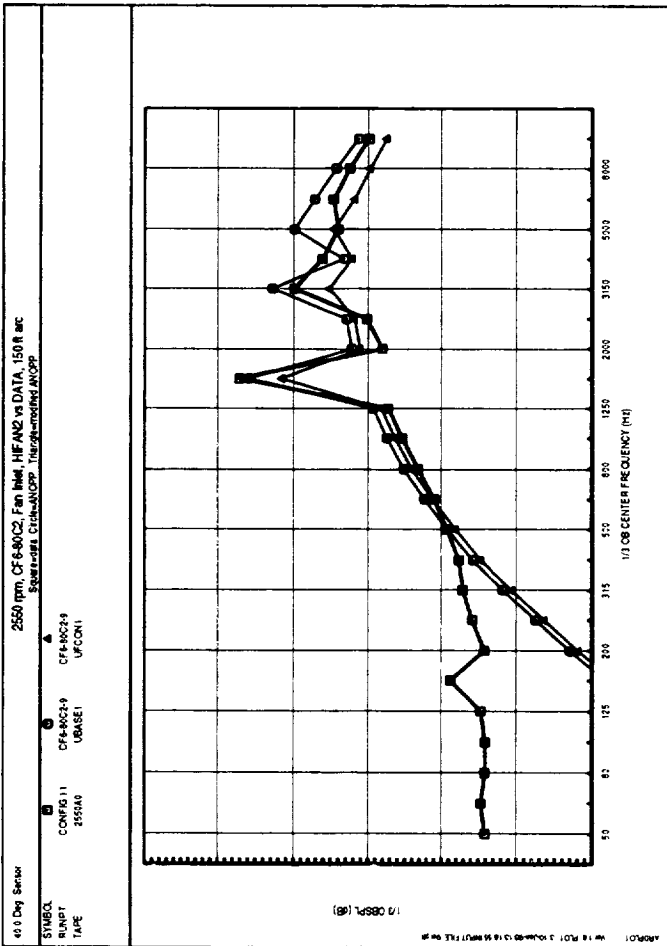
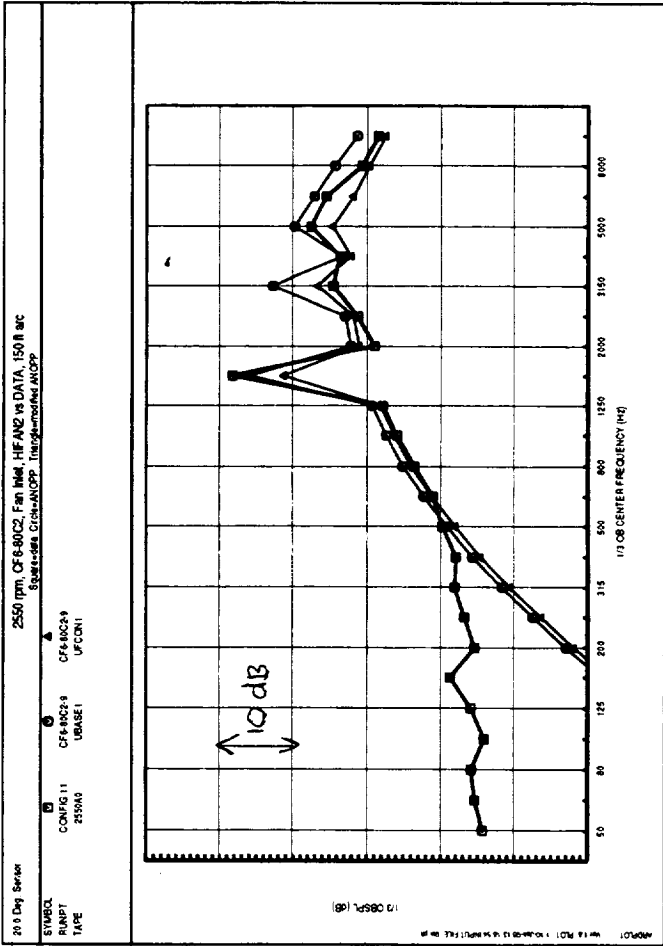


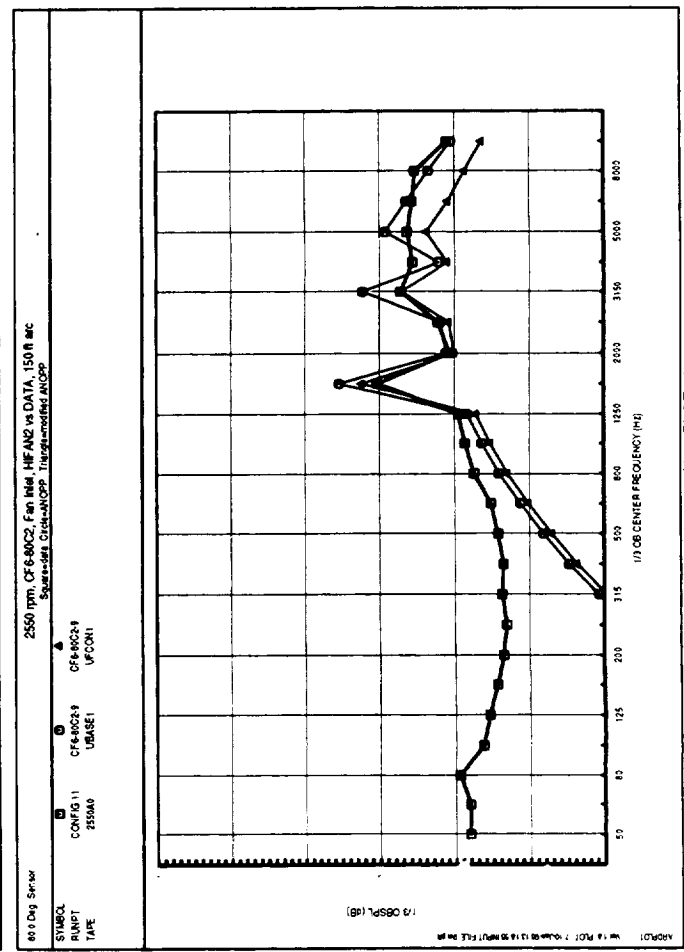
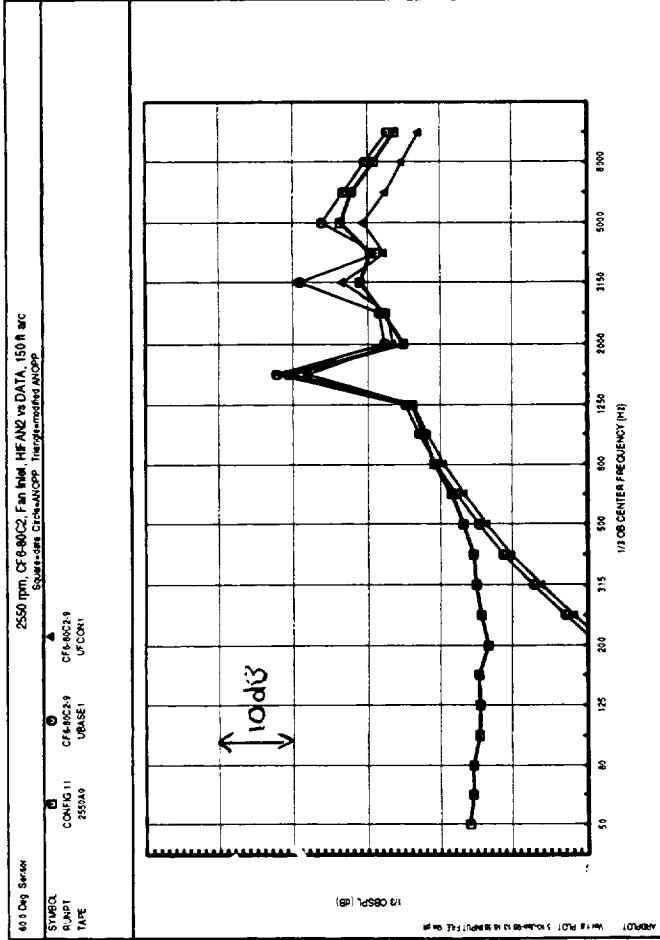
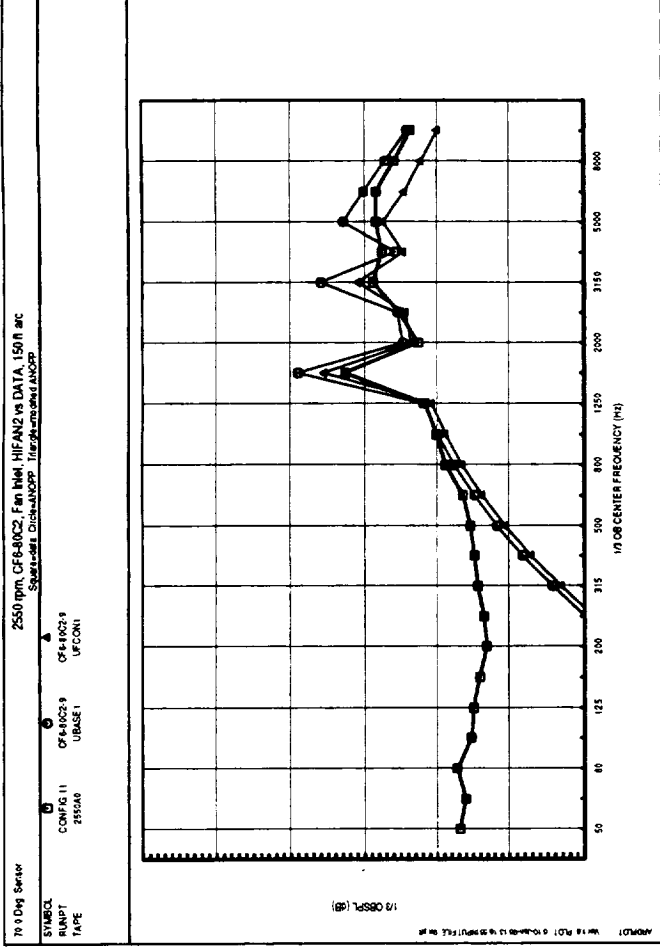


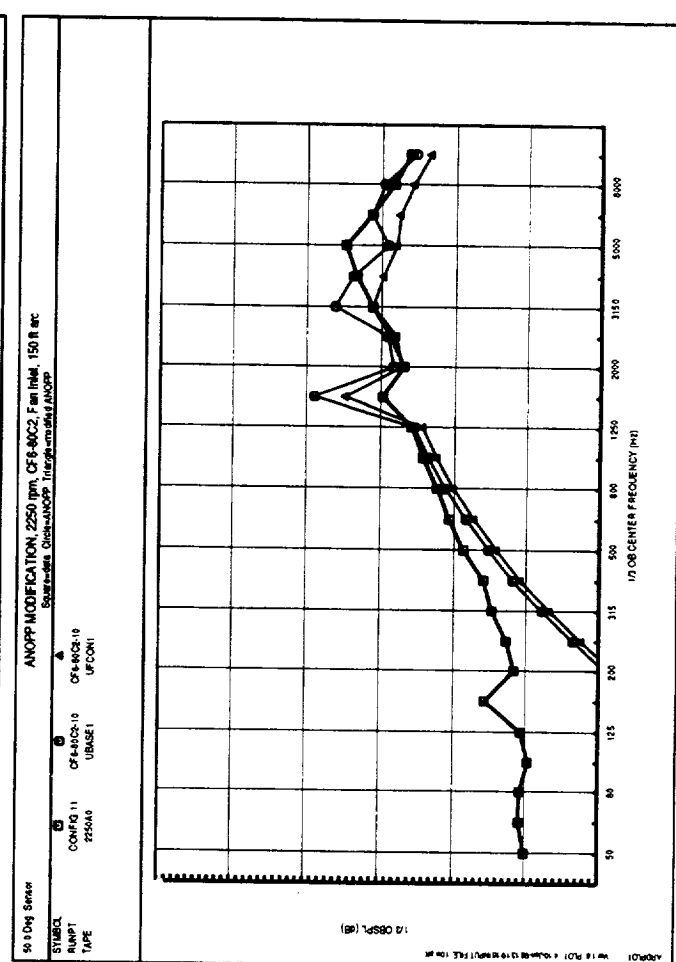
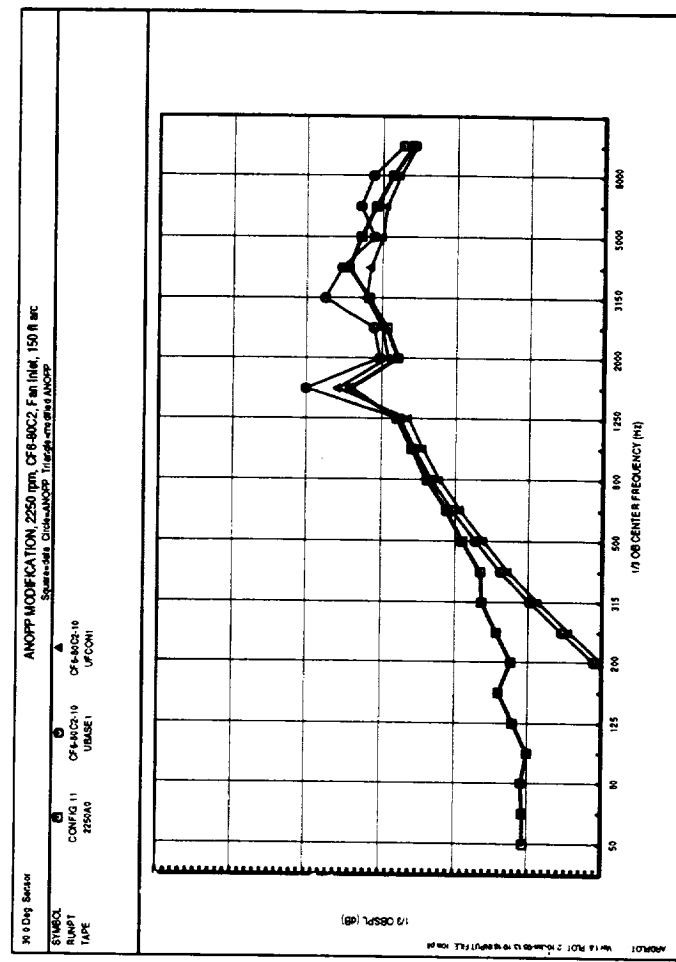
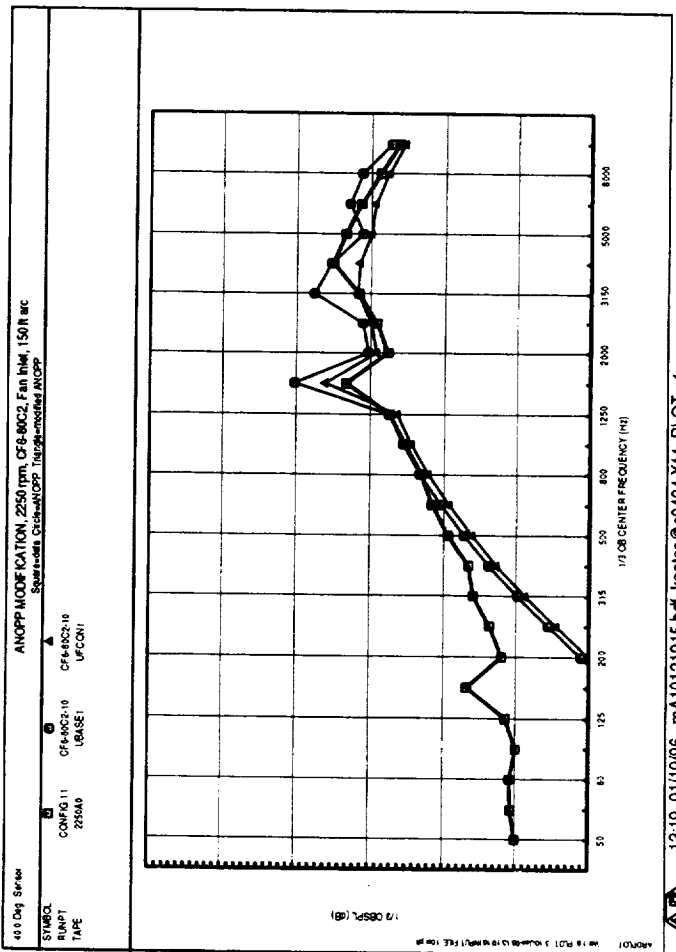
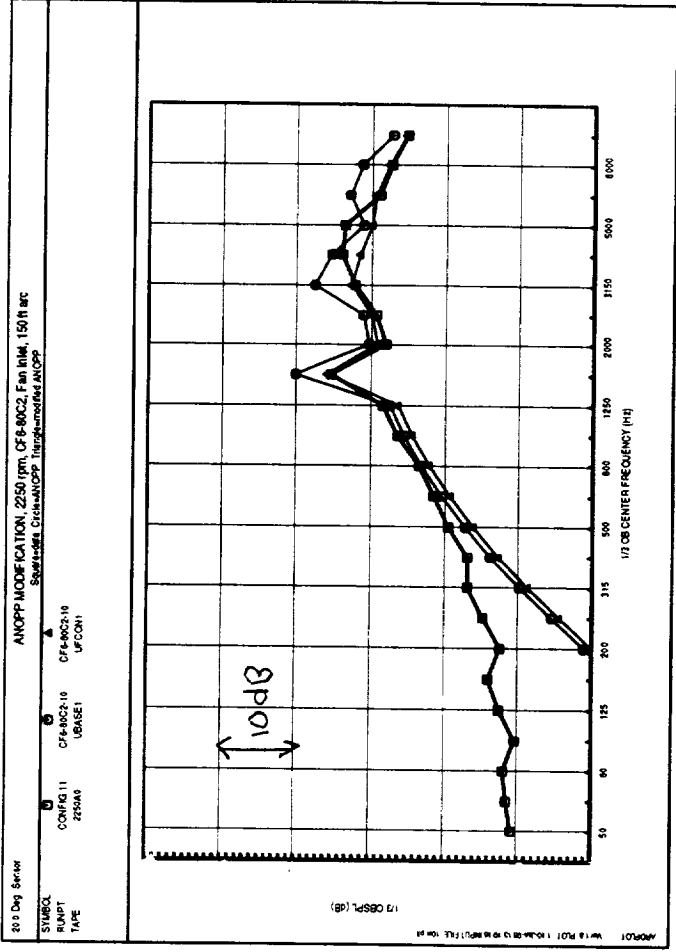


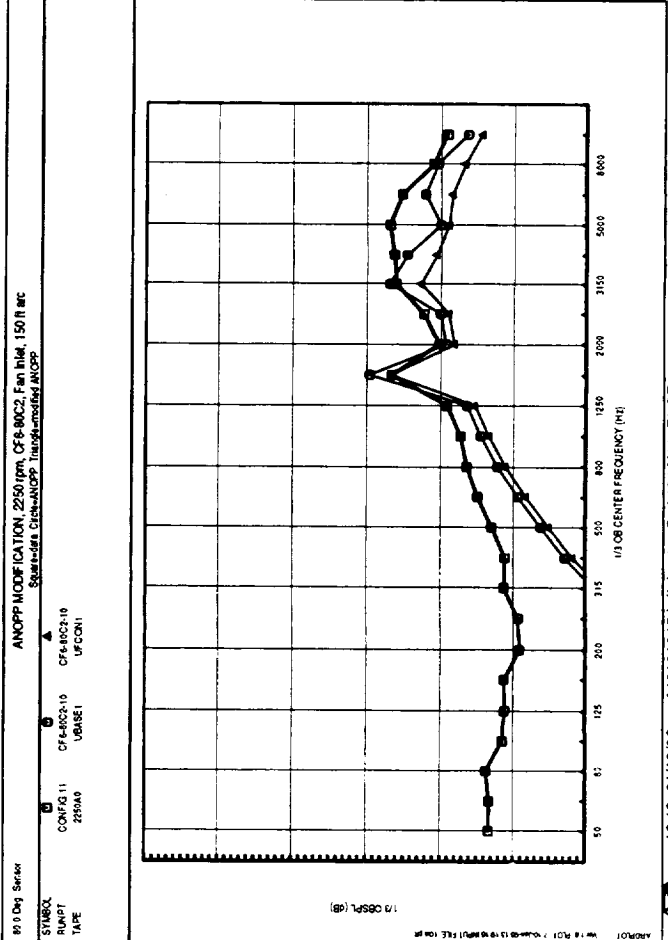
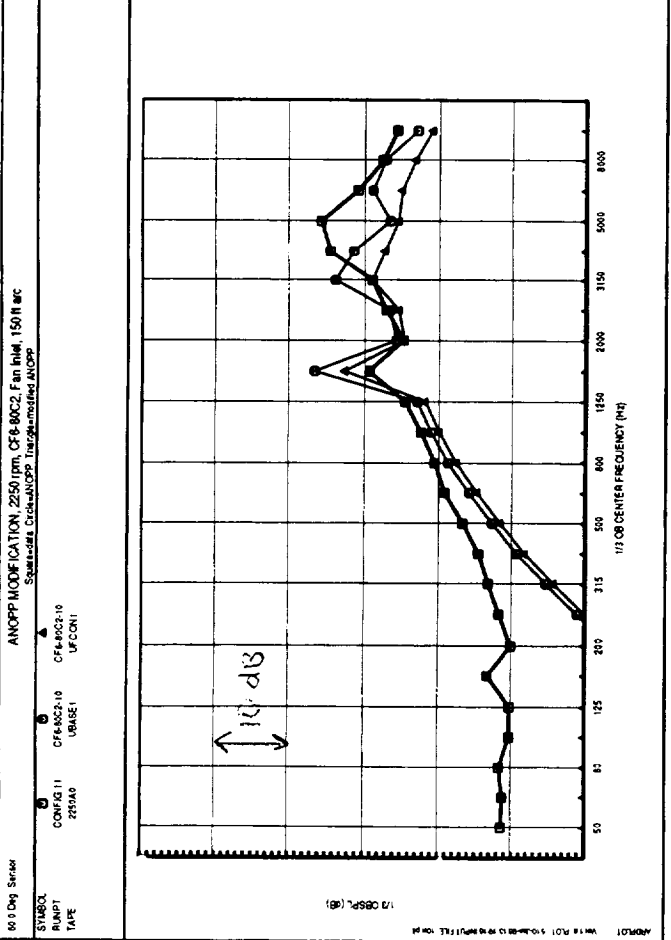
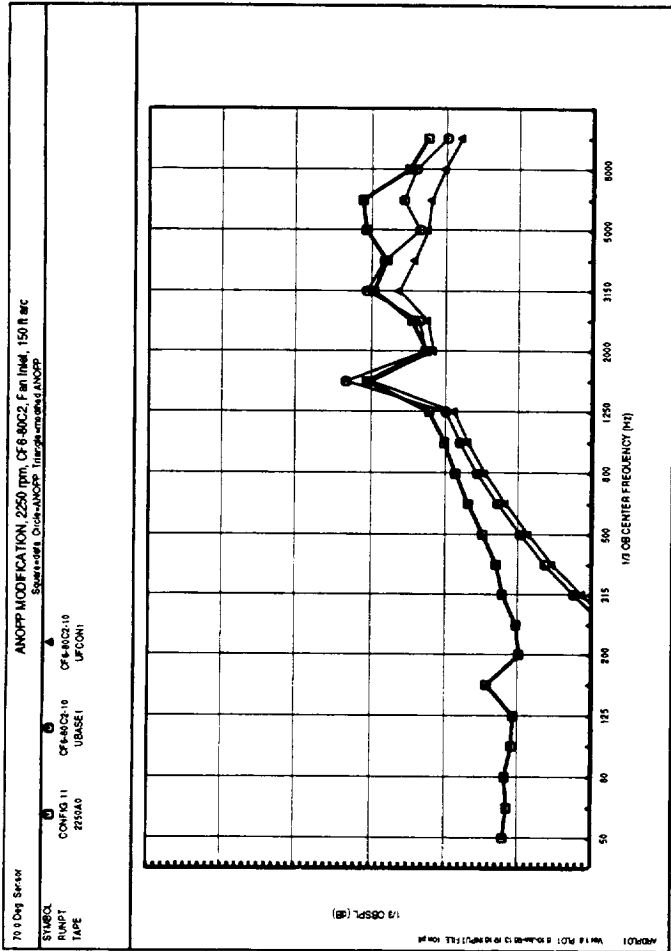
13:18 01/10/96 MA10131834.D\F1 K0105@c0424 X11 PLOT 2
 EGS LIB 5.112/1495 LEGSREP.XPOST 5.1 12/14/95 on c0424
 (NO PROG. VER. SPECIFIED)

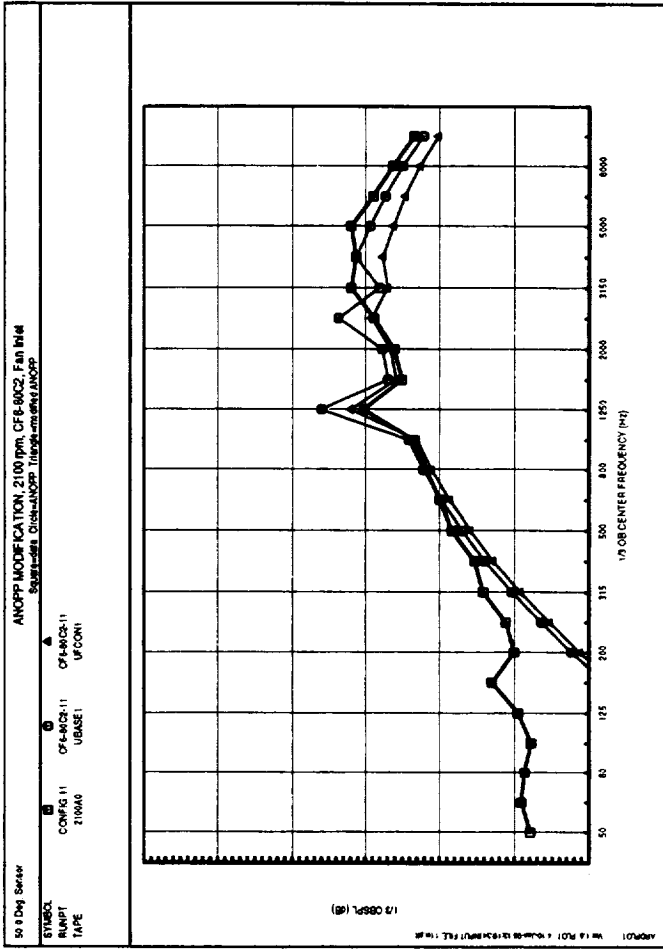
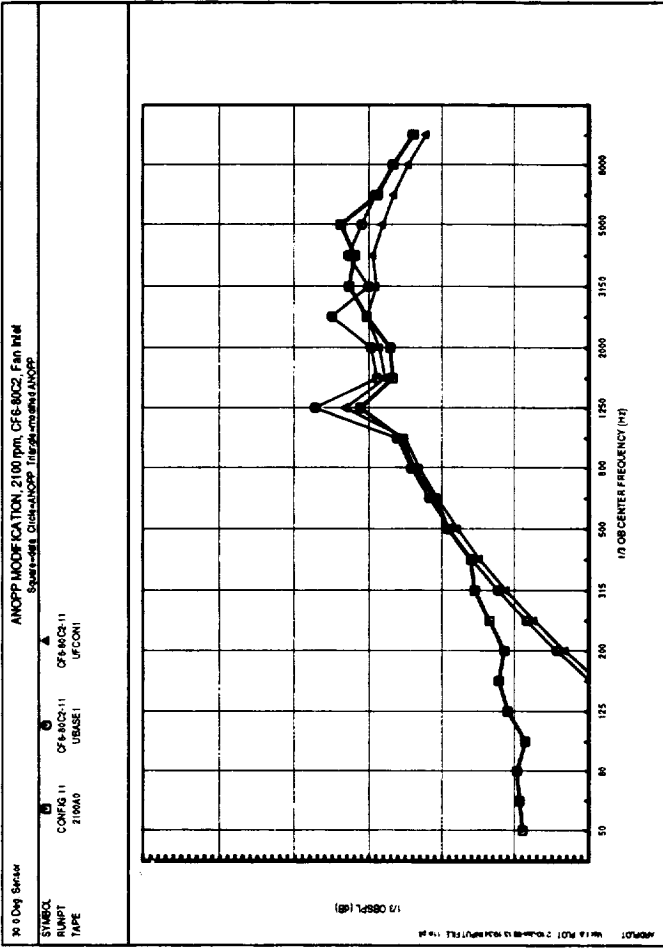
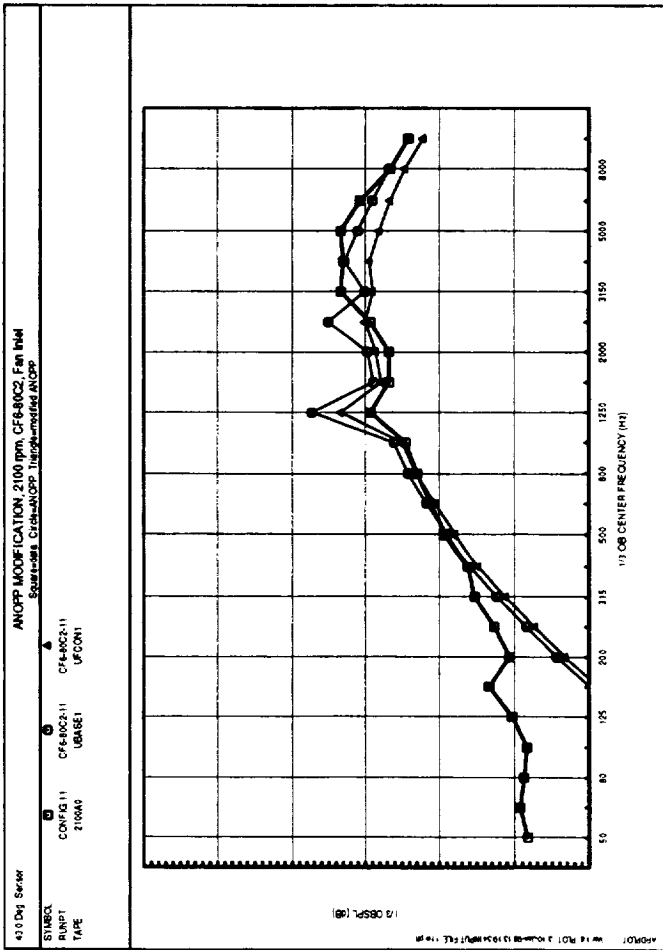
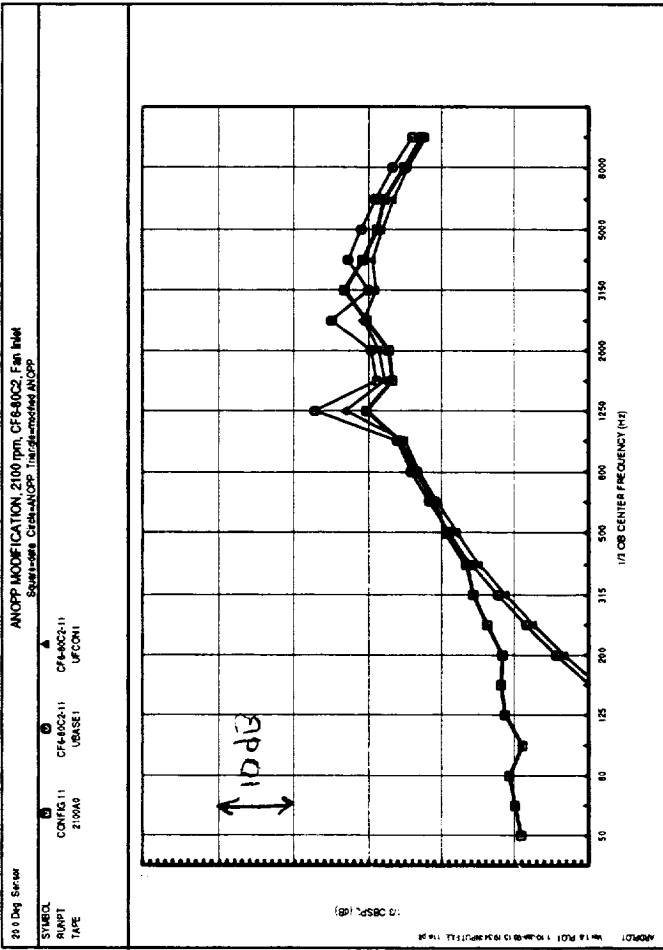


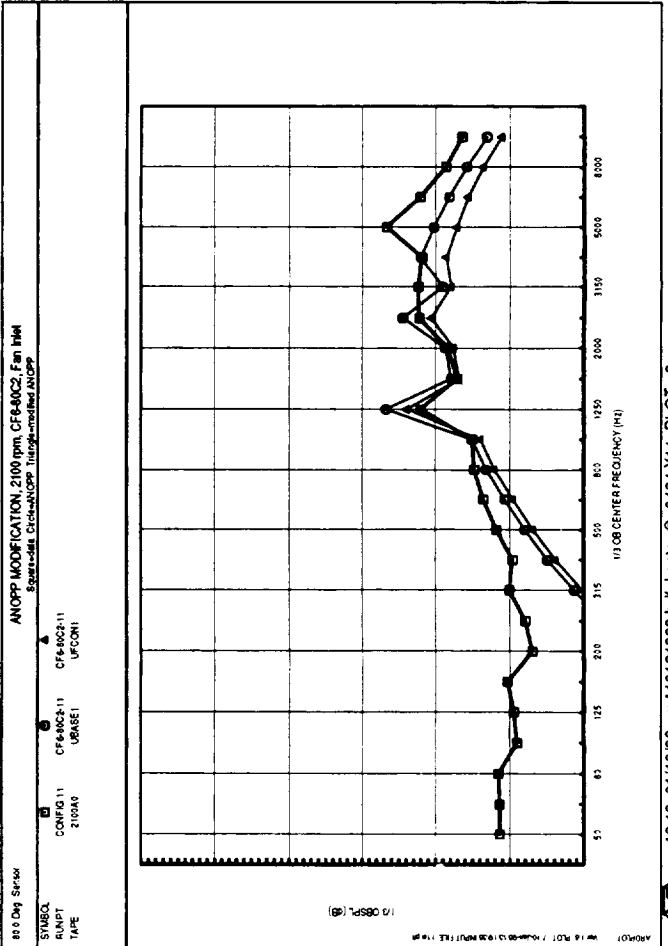
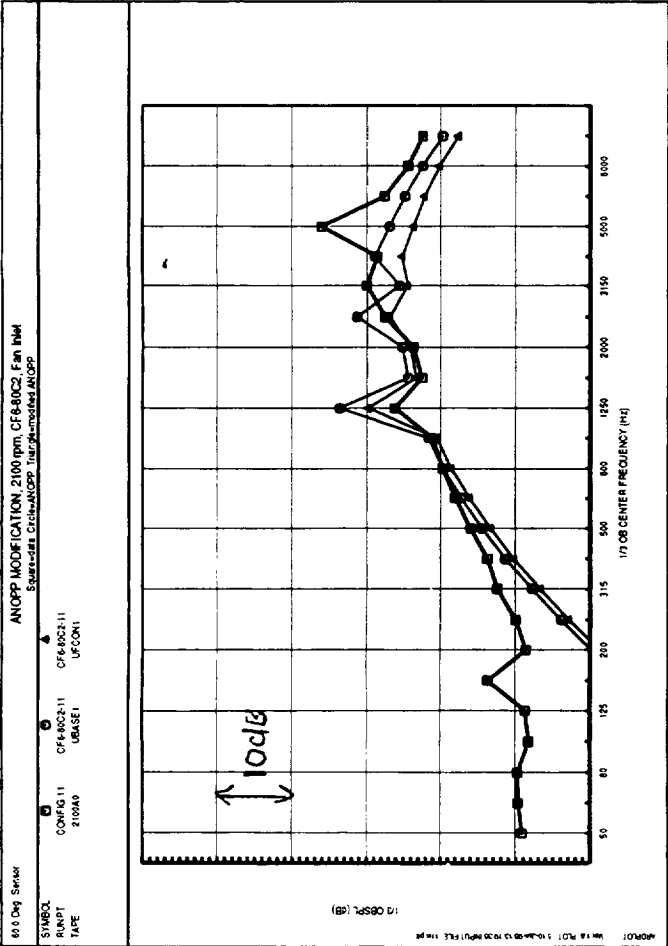
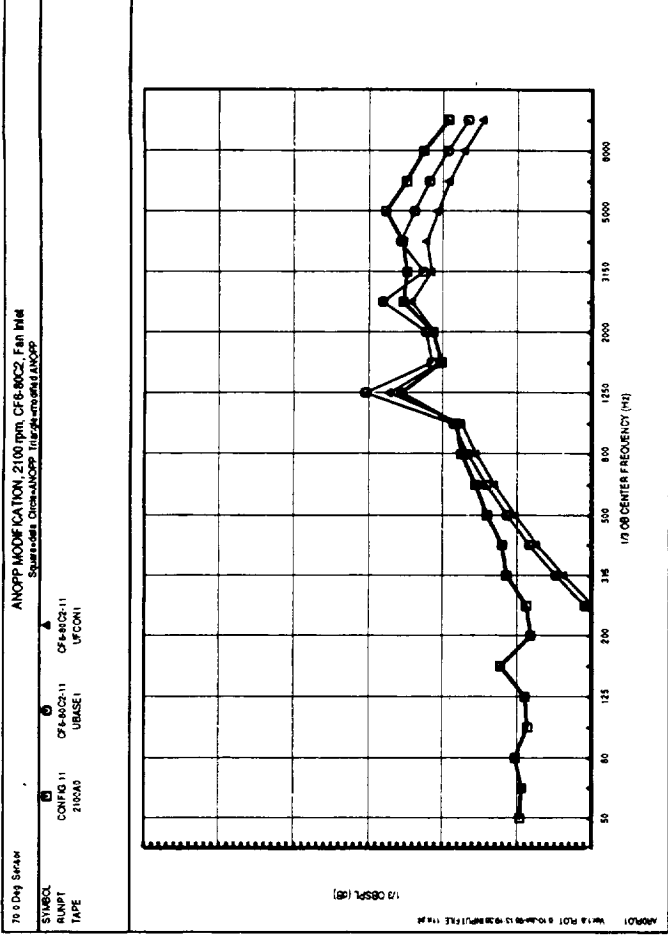












13.19 01/10/96 MA10131933.bdf Konlos@c0424.X11.PLOT_2
 EGS LIB 5.1 12/14/95 EGSREP.XPOST 5.1 12/14/95 on c0424)
 (NO PROG. VER. SPECIFIED)



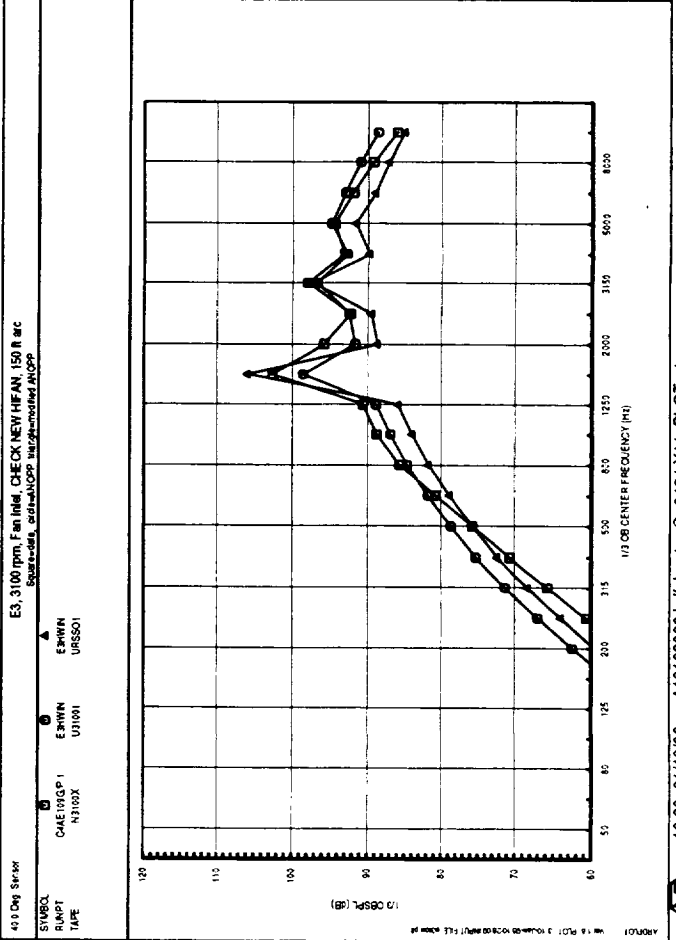
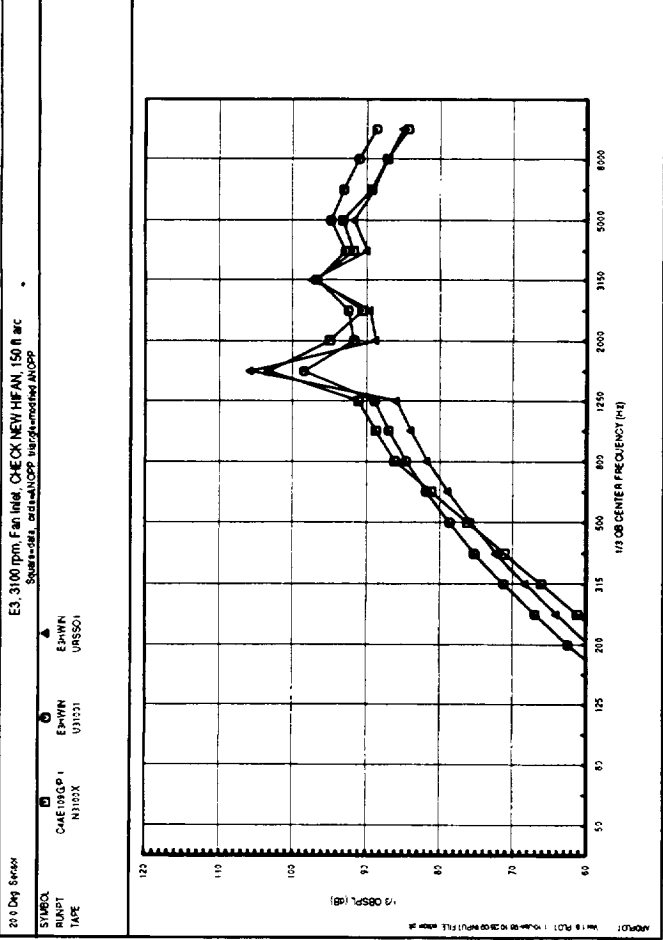
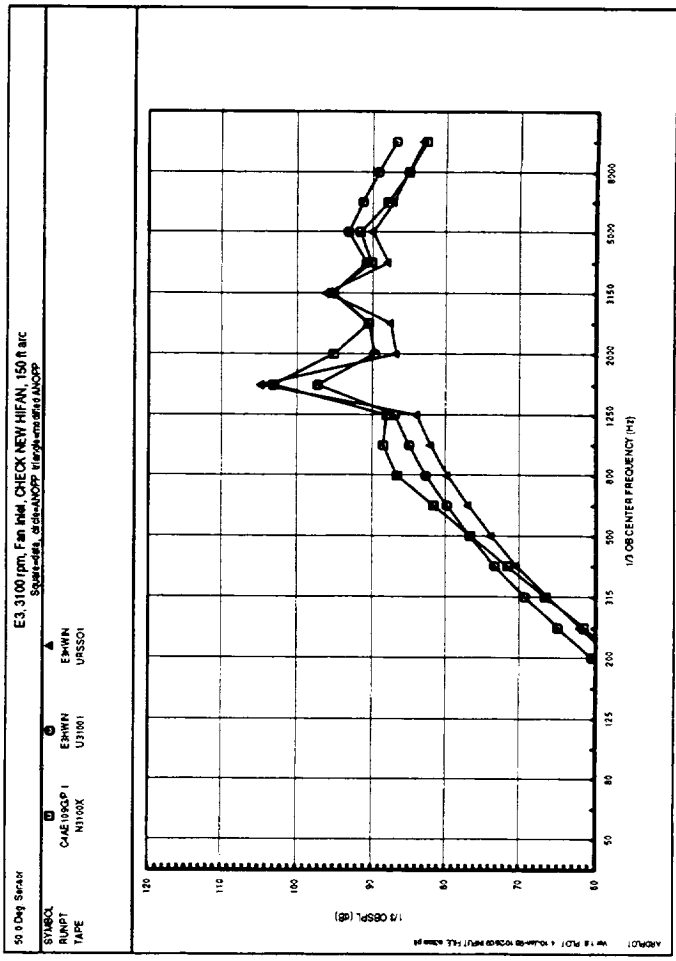
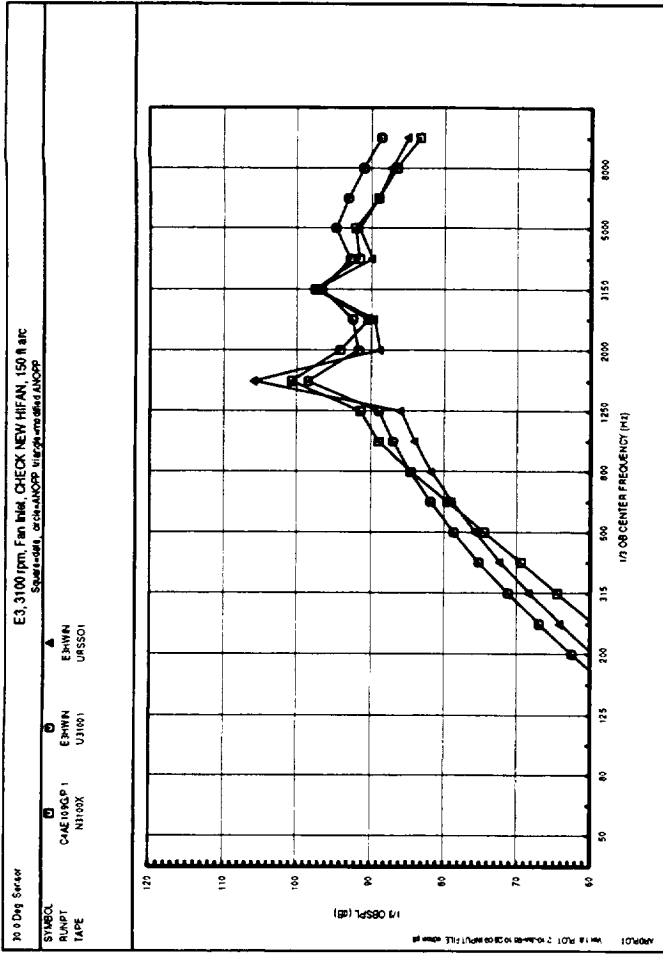
Appendix C
Fan Inlet Noise Spectral Comparisons - E³

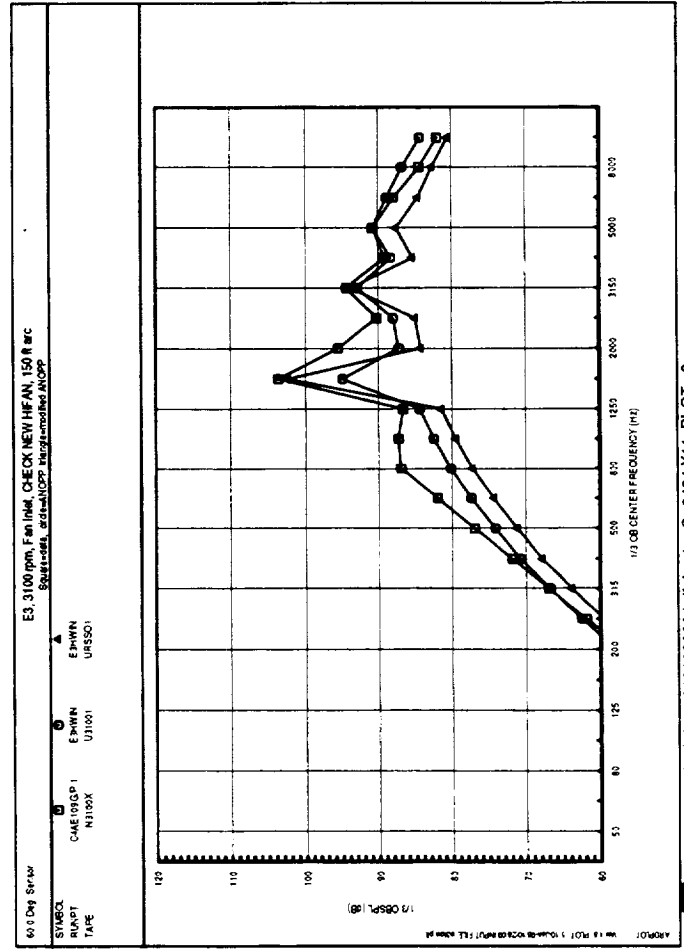
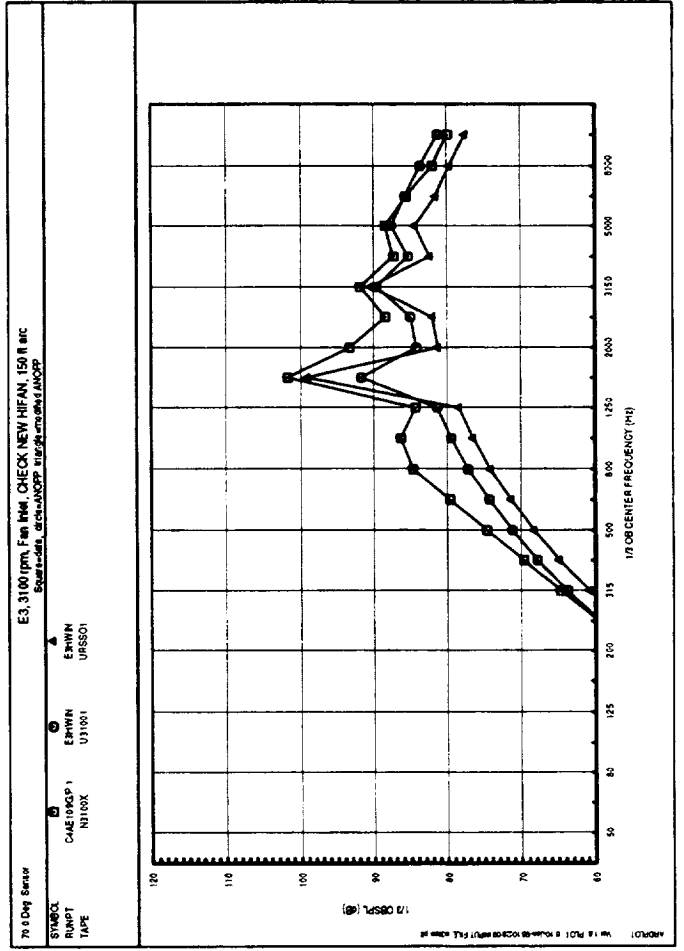
Appendix C Contents

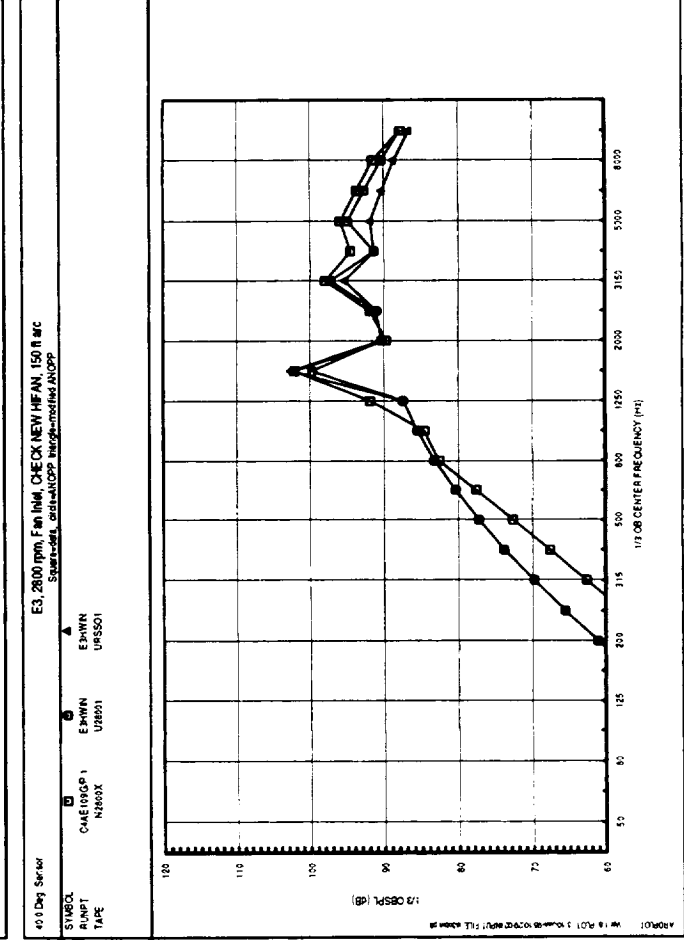
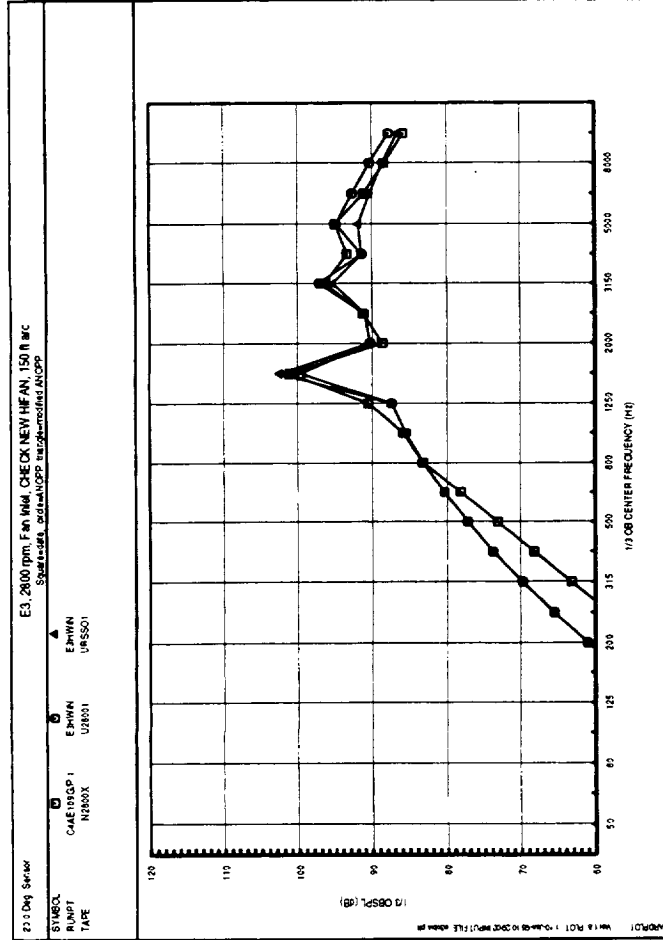
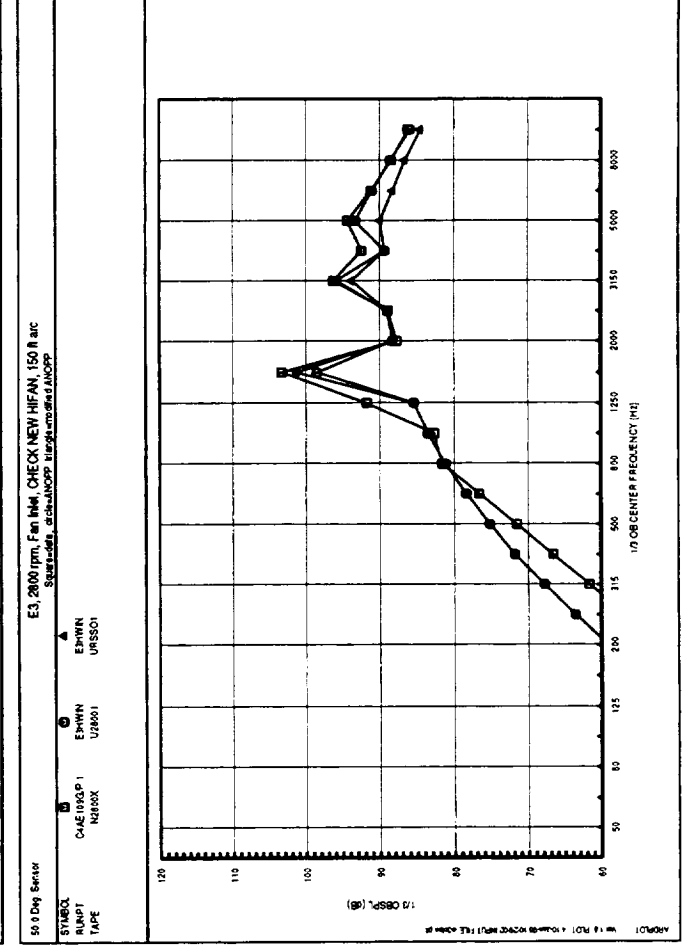
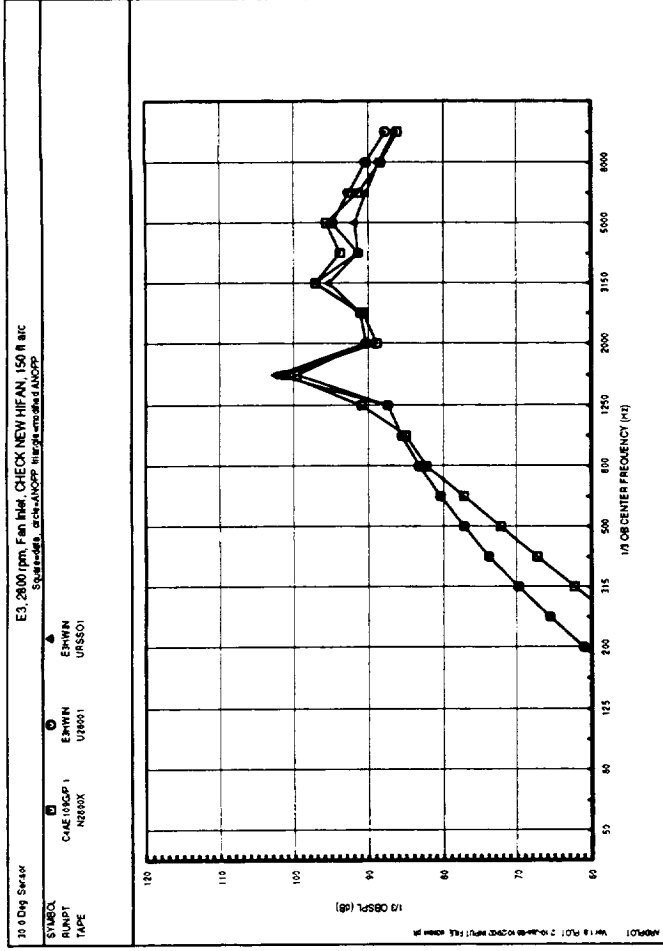
Page	Fan Speed, rpm	Angles, deg
64	3100 (takeoff)	20-50
65	3100 (takeoff)	60-70
66	2800 (cutback)	20-50
67	2800 (cutback)	60-70
68	1820 (approach)	20-50
69	1820 (approach)	60-70

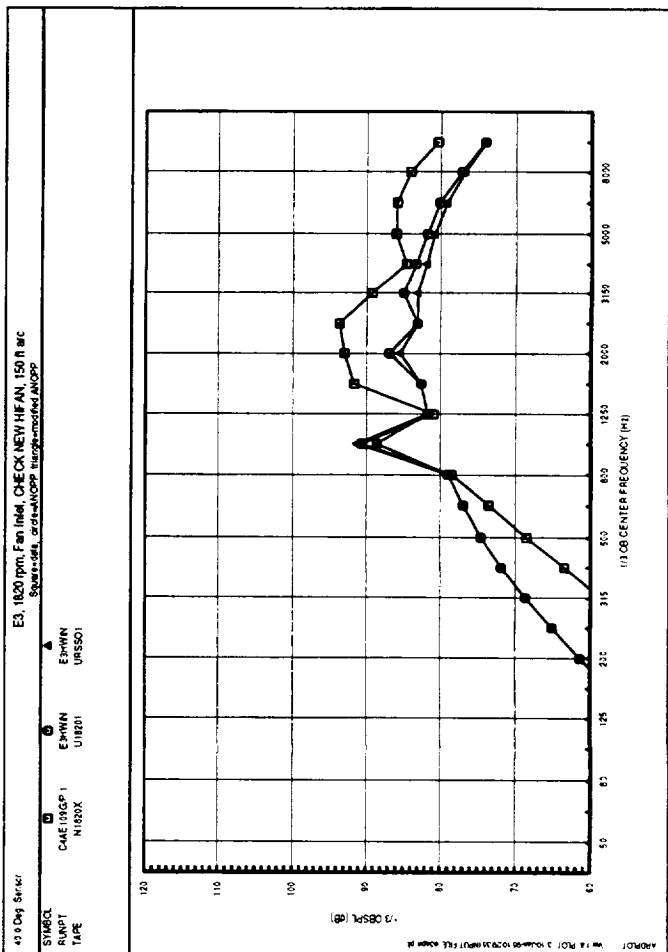
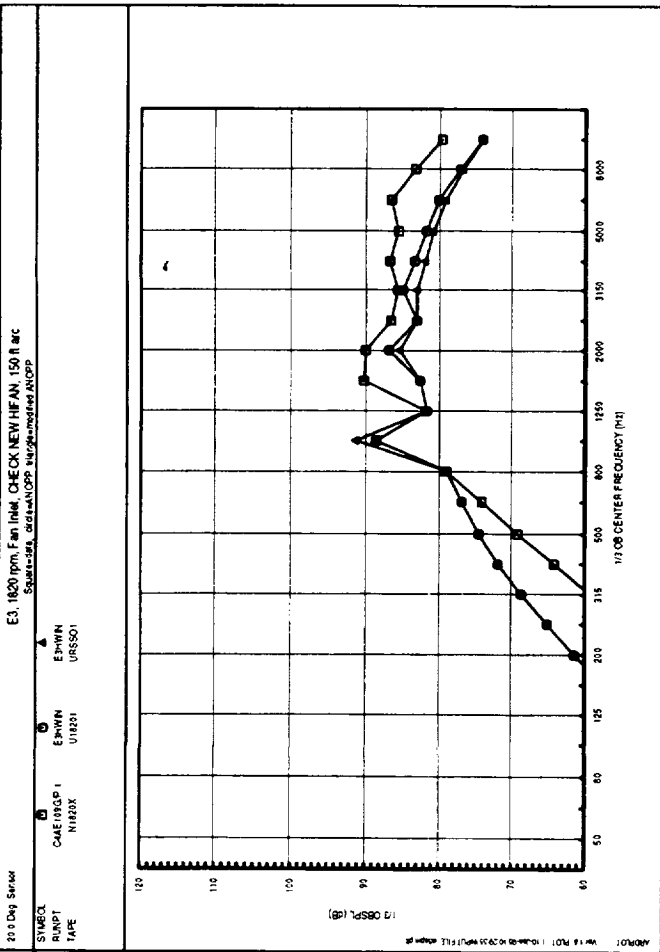
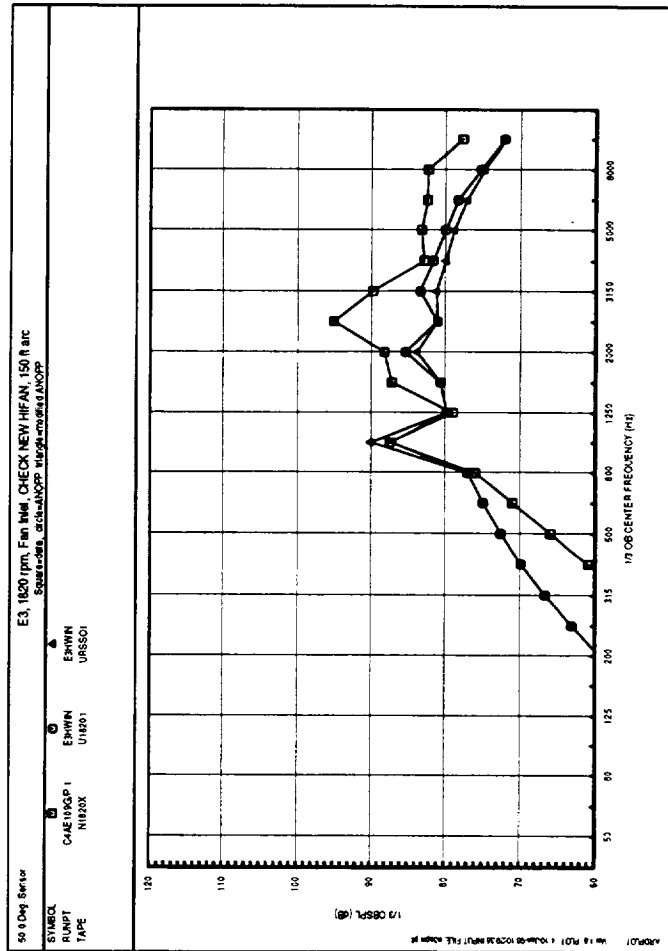
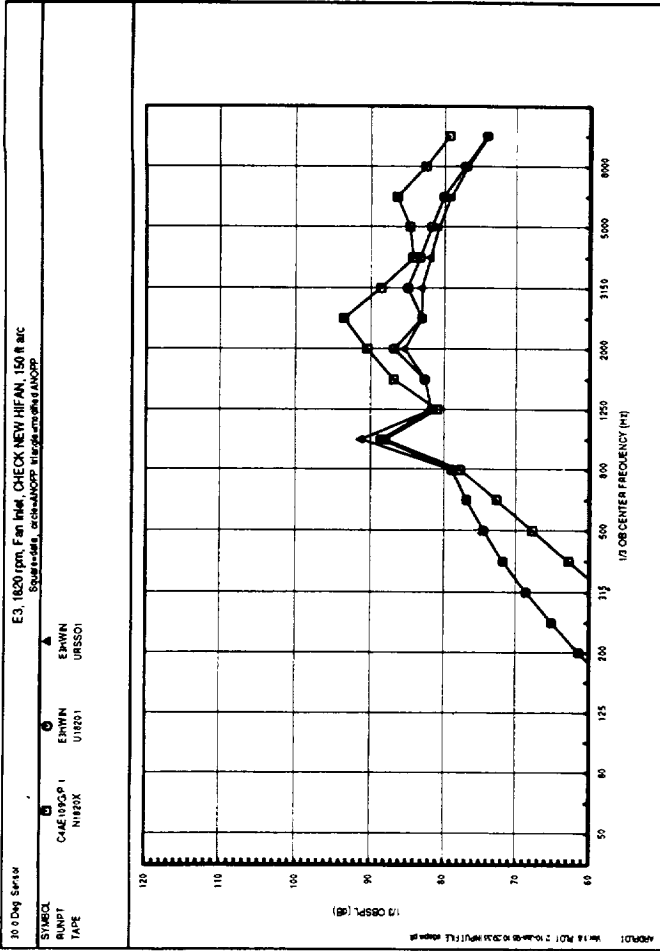
Key to Plots:

squares = total measured engine data
circles = Heidmann method prediction
triangles = modified Heidmann method prediction (see Section 4)



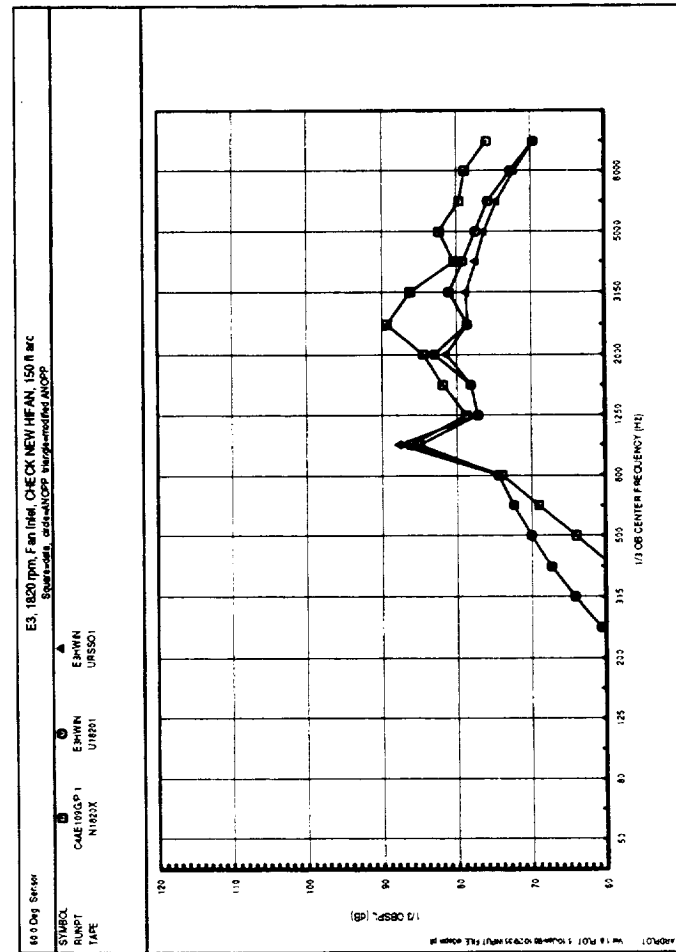
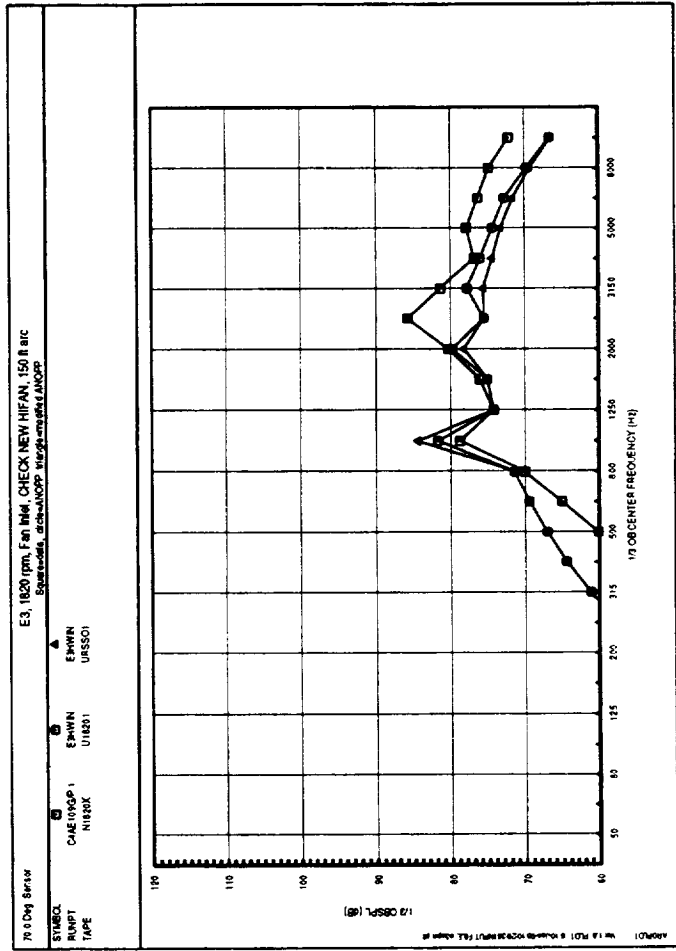






10-20 01/10/96 ma10102024 bdf kontus@c0424 X11 PLOT_1
 EGS LIB 5.1 12/14/95 LEGSREP.XPOST 5.1 12/14/95 on c0424)
 (NO PROG. VER. SPECIFIED)





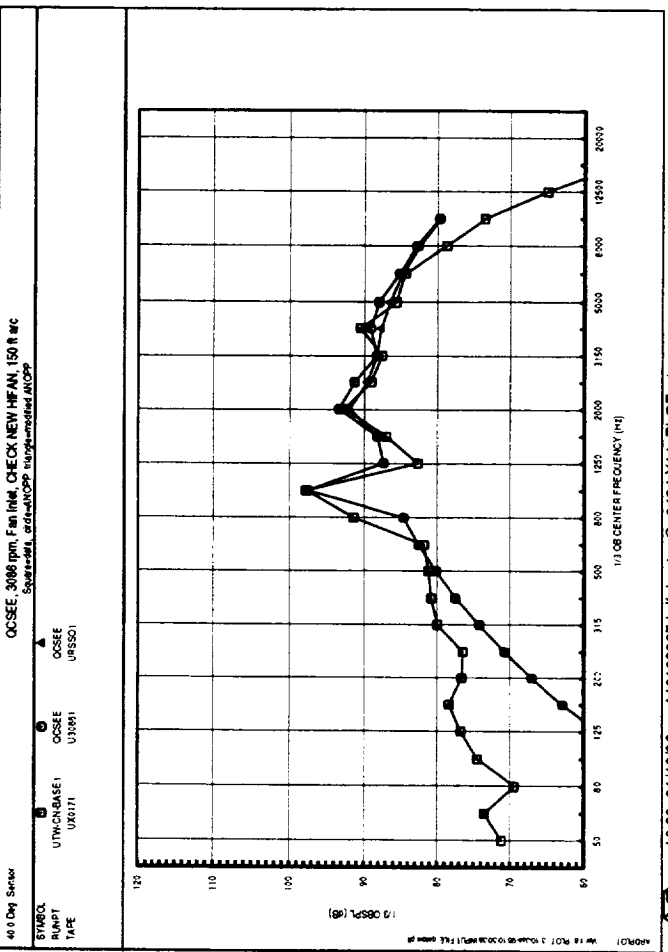
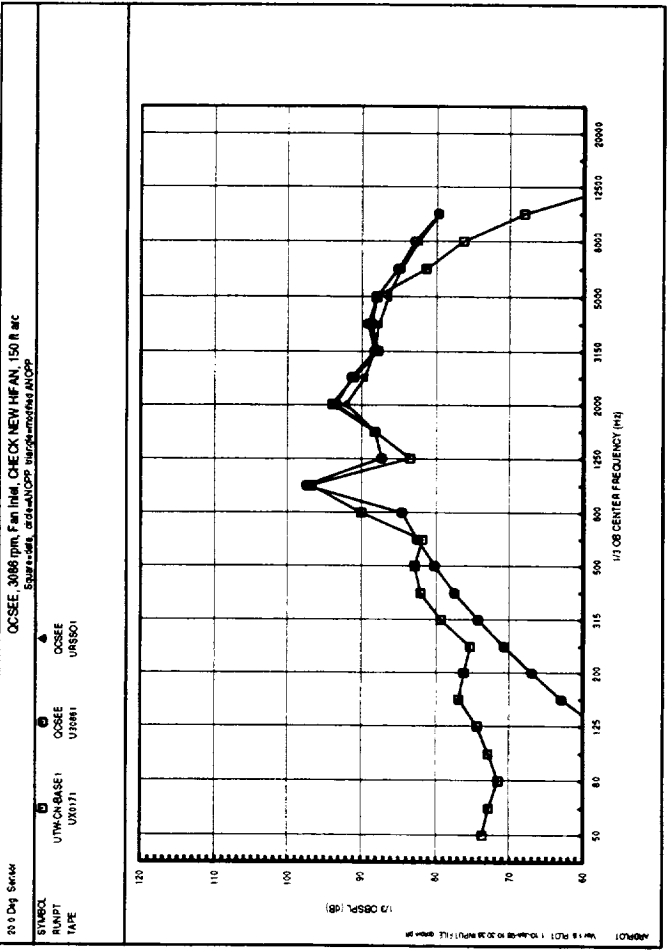
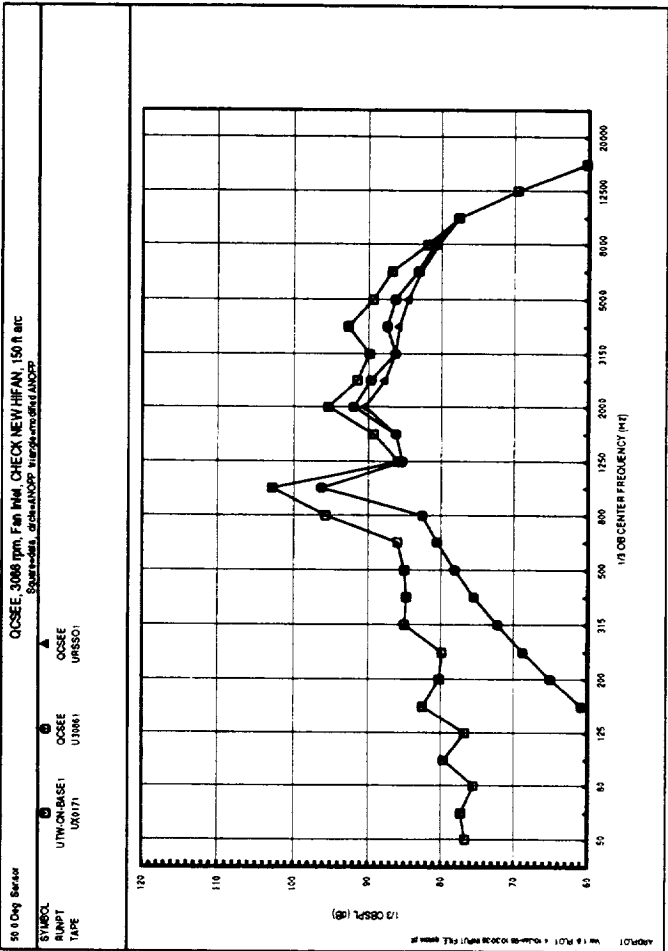
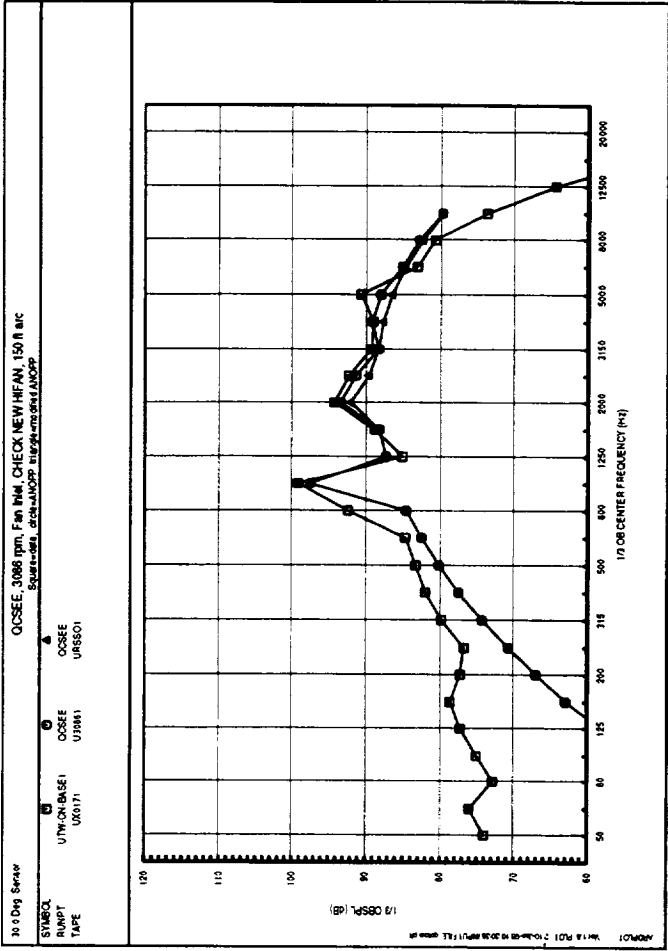
Appendix D
Fan Inlet Noise Spectral Comparisons - QCSEE

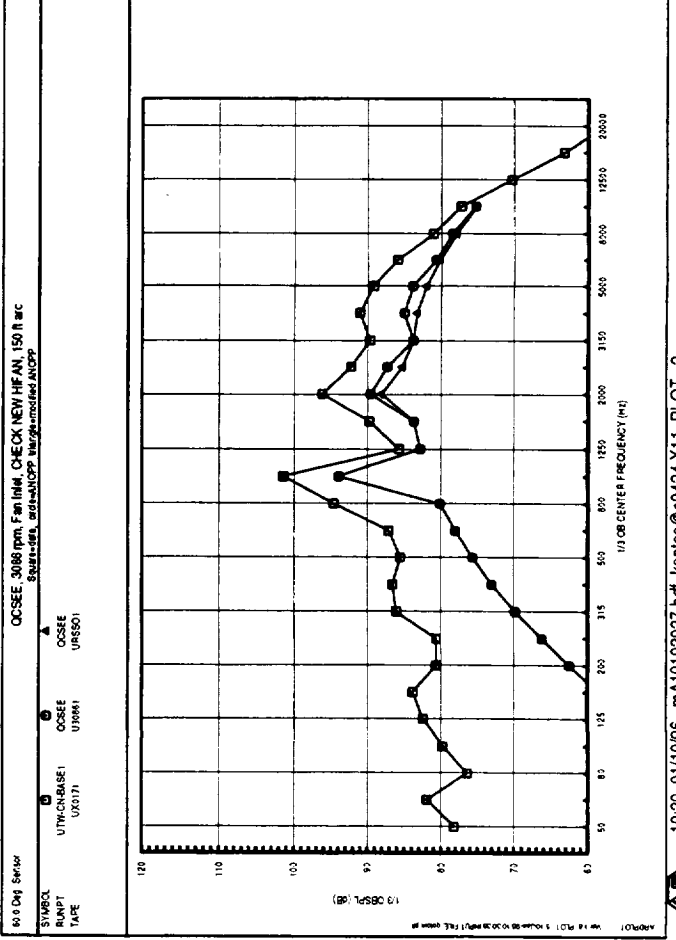
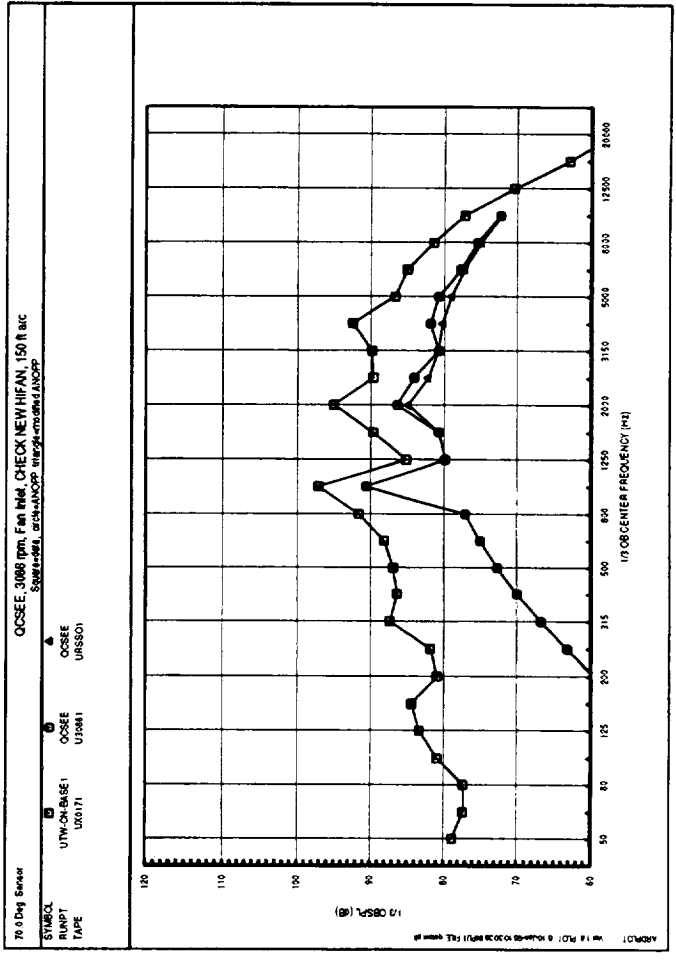
Appendix D Contents

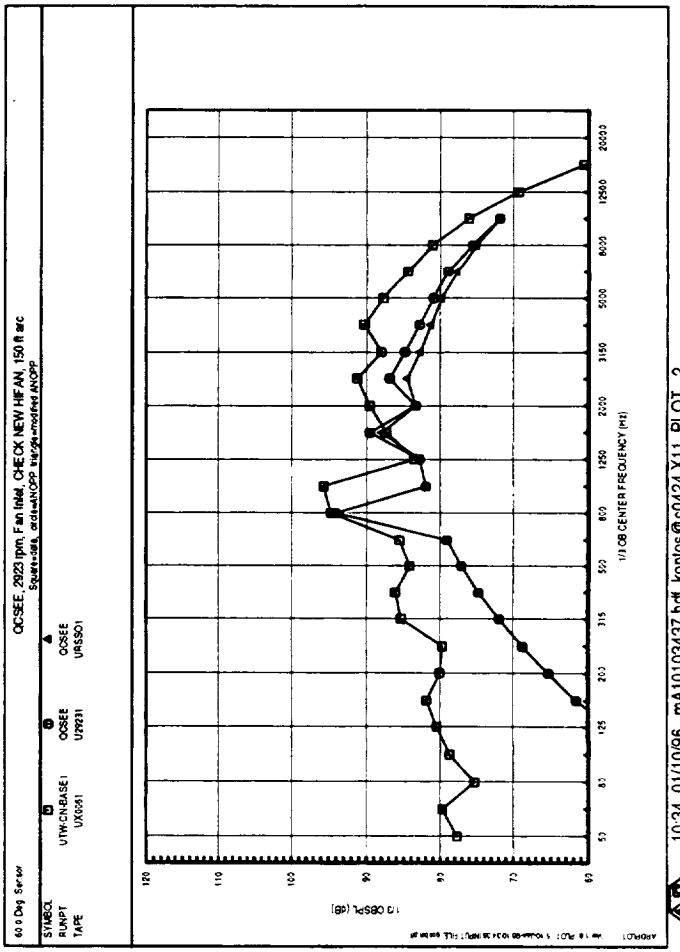
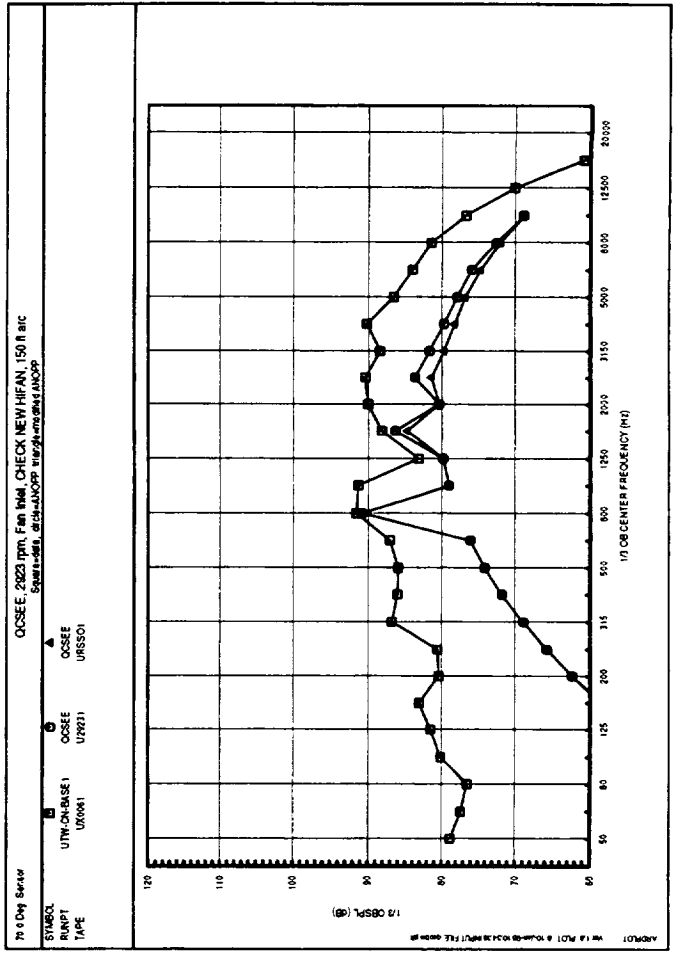
Page	Fan Speed, rpm	Angles, deg
71	3086 (takeoff)	20-50
72	3086 (takeoff)	60-70
73	2931 (cutback)	20-50
74	2931 (cutback)	60-70
75	2759 (approach)	20-50
76	2759 (approach)	60-70

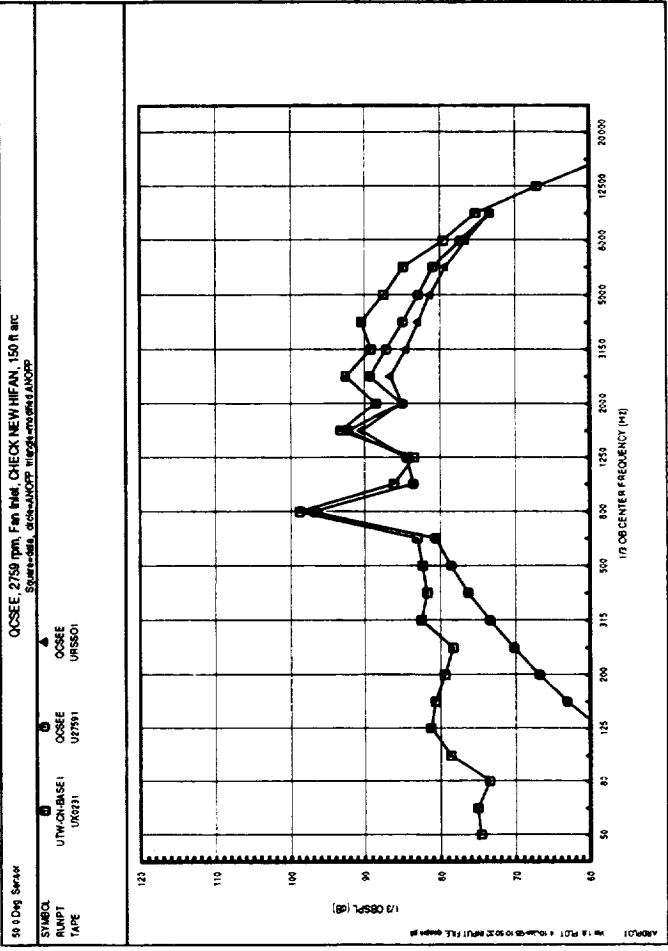
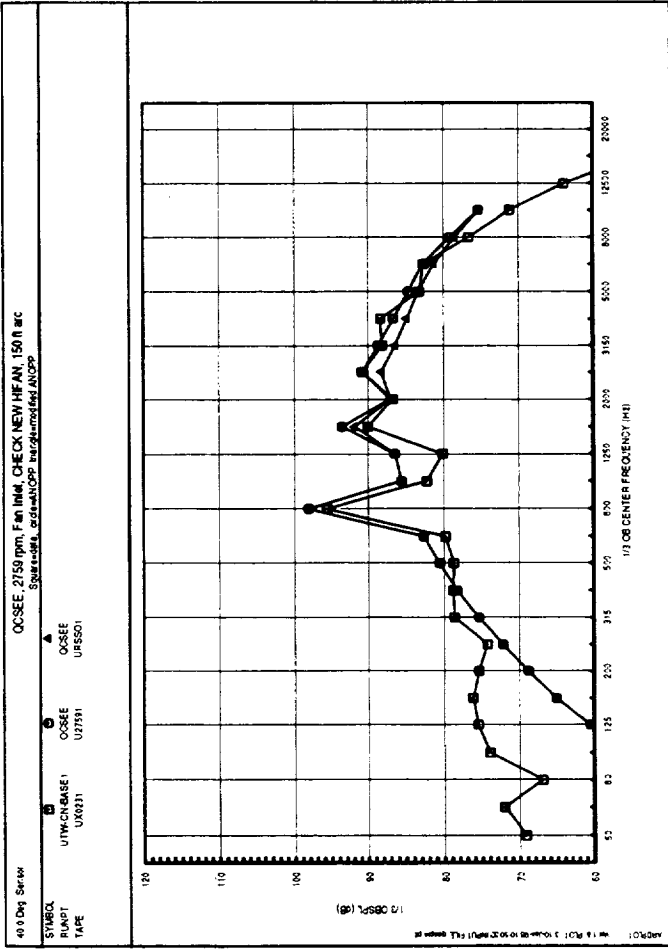
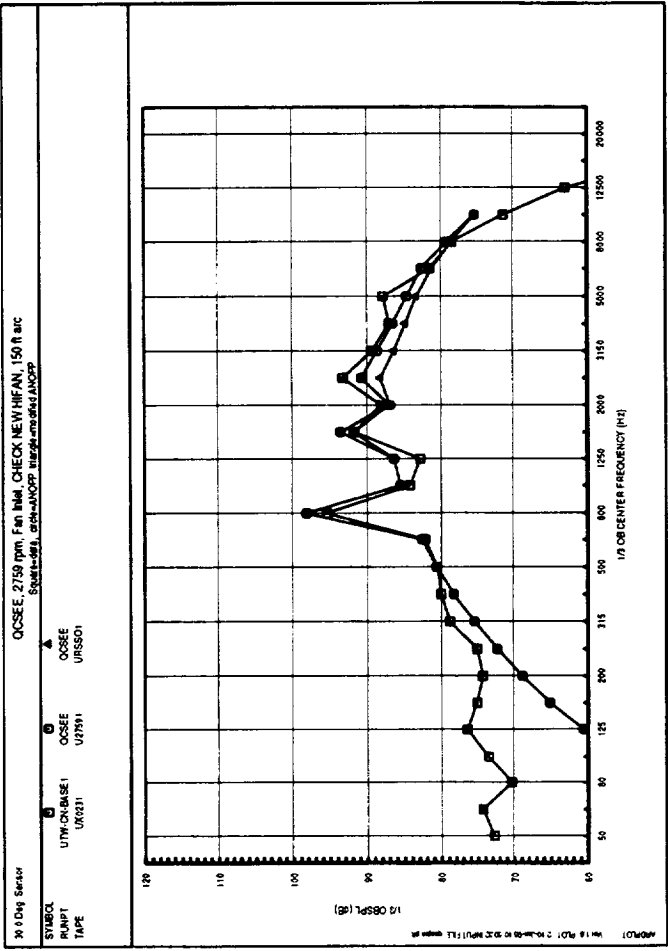
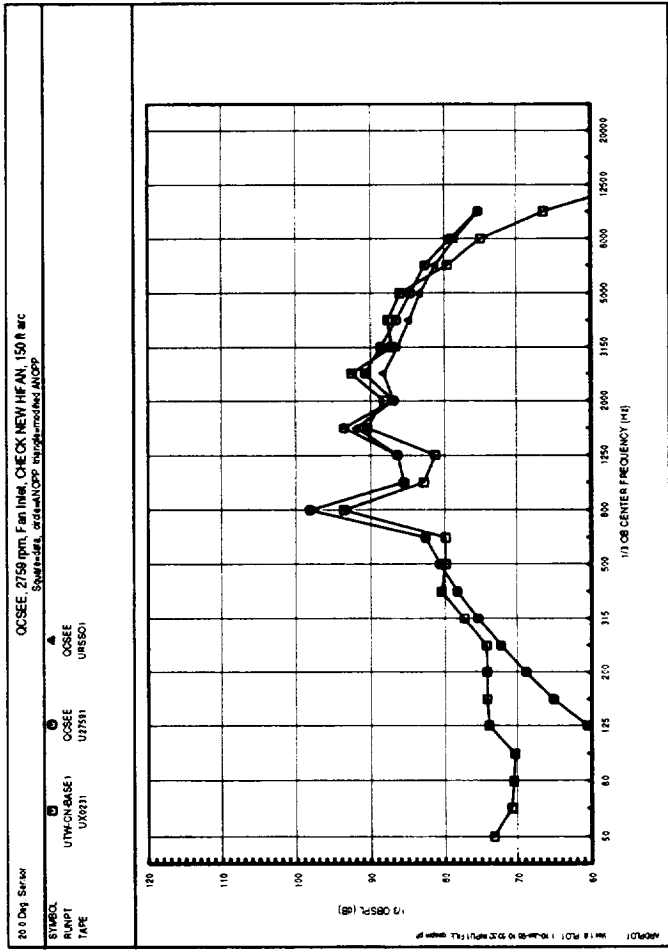
Key to Plots:

squares = total measured engine data
circles = Heidmann method prediction
triangles = modified Heidmann method prediction (see Section 4)

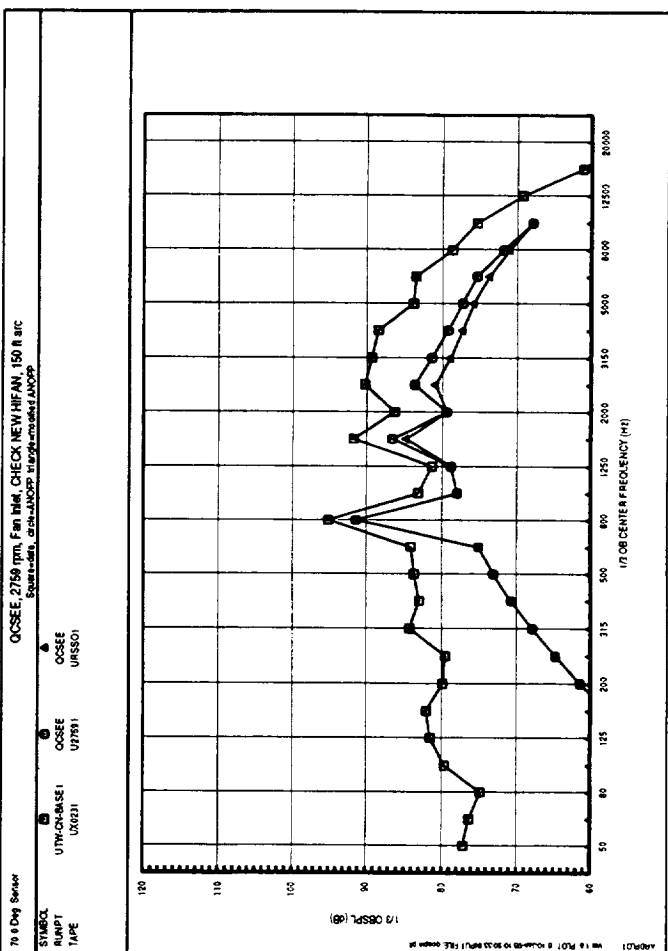
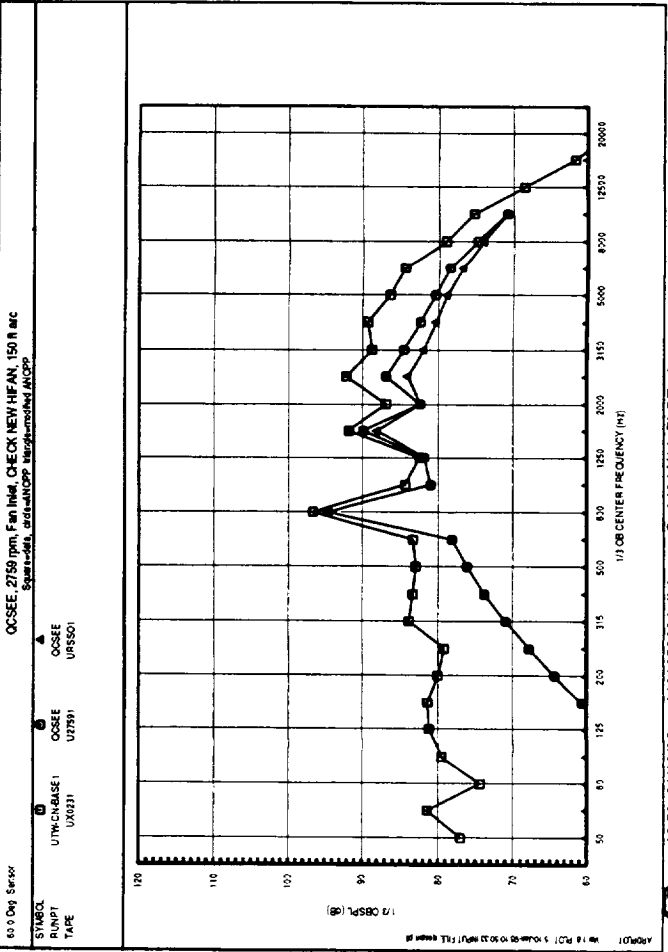








6



10:50 01/10/96 10:50:01.10/96 10:50:01.10/96 10:50:01.10/96 10:50:01.10/96 10:50:01.10/96 10:50:01.10/96 10:50:01.10/96 10:50:01.10/96 10:50:01.10/96
 EGS LIB 5.1 12/14/95 (EGSREP.XPOST 5.1 12/14/95 on c0424)
 (NO PROG. VER. SPECIFIED)



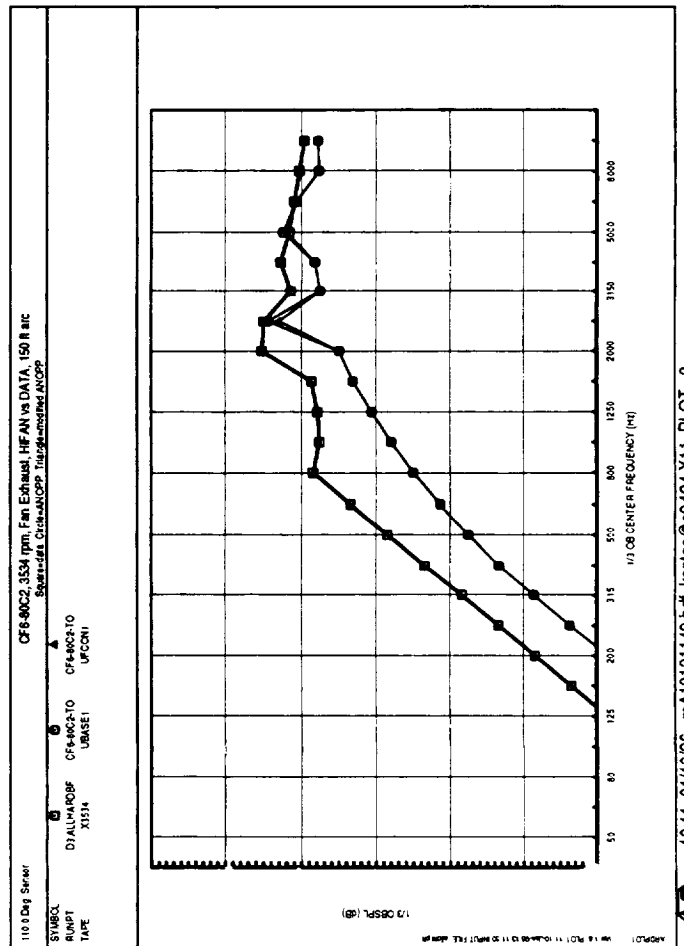
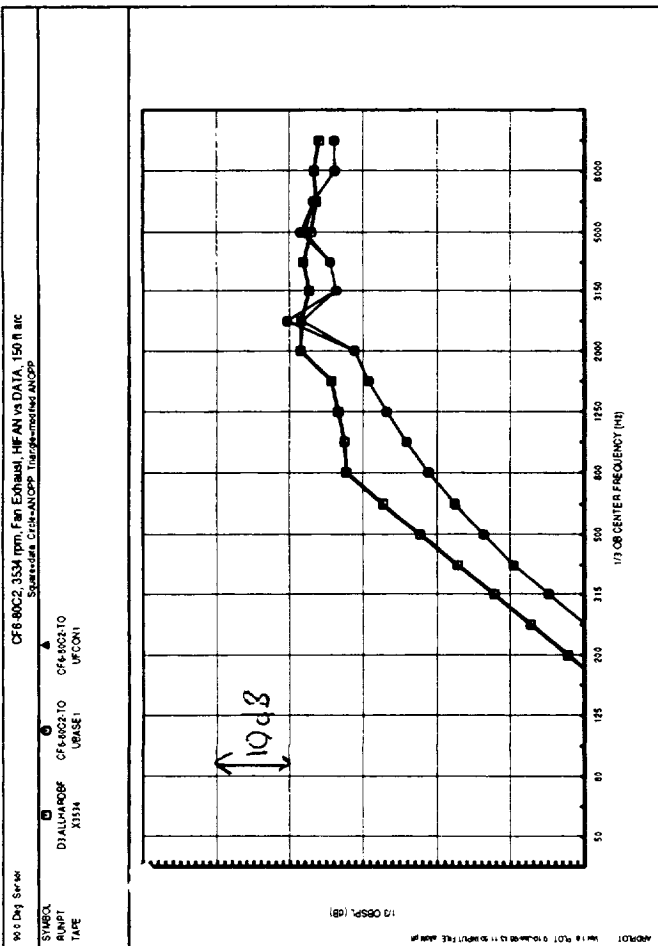
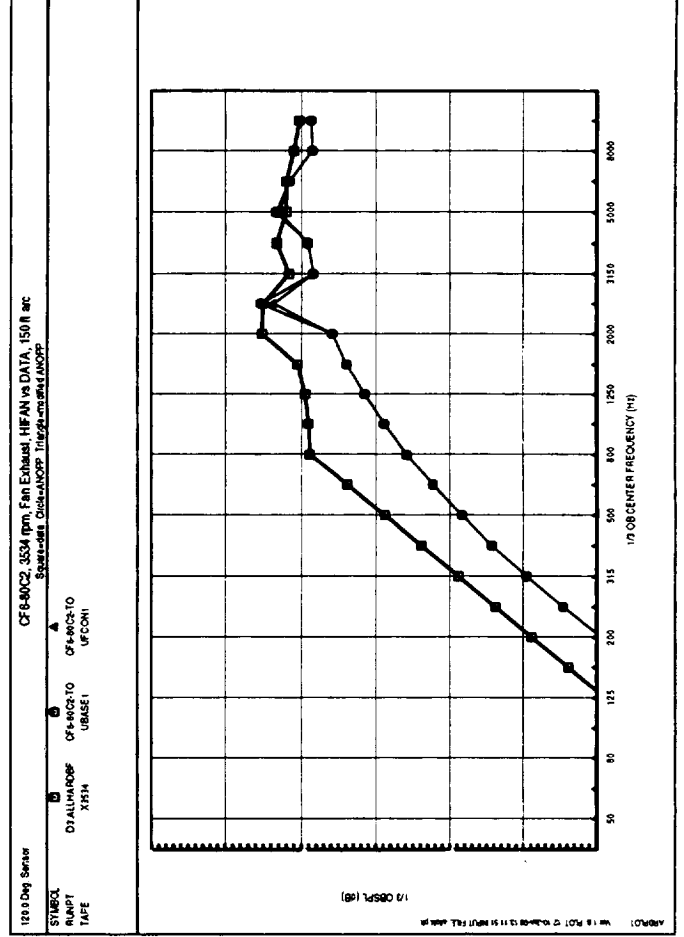
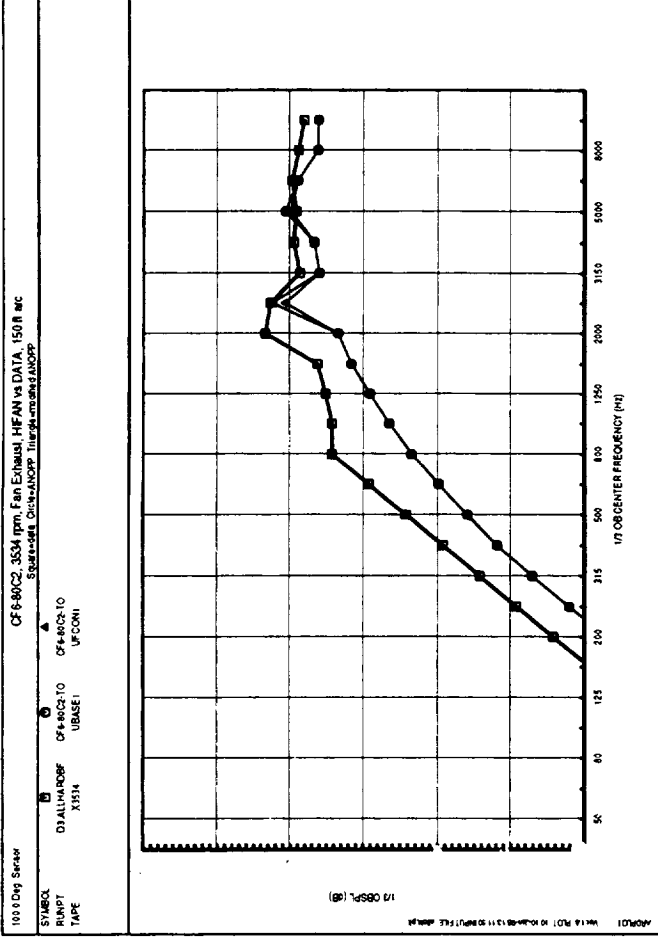
Appendix E
Fan Exhaust Noise Spectral Comparisons - CF6-80C2

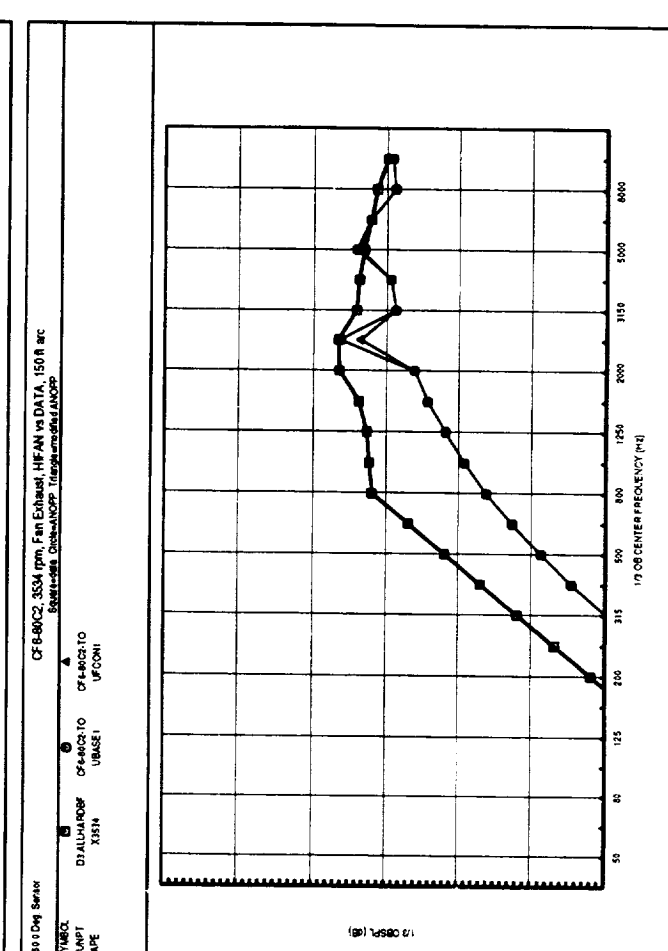
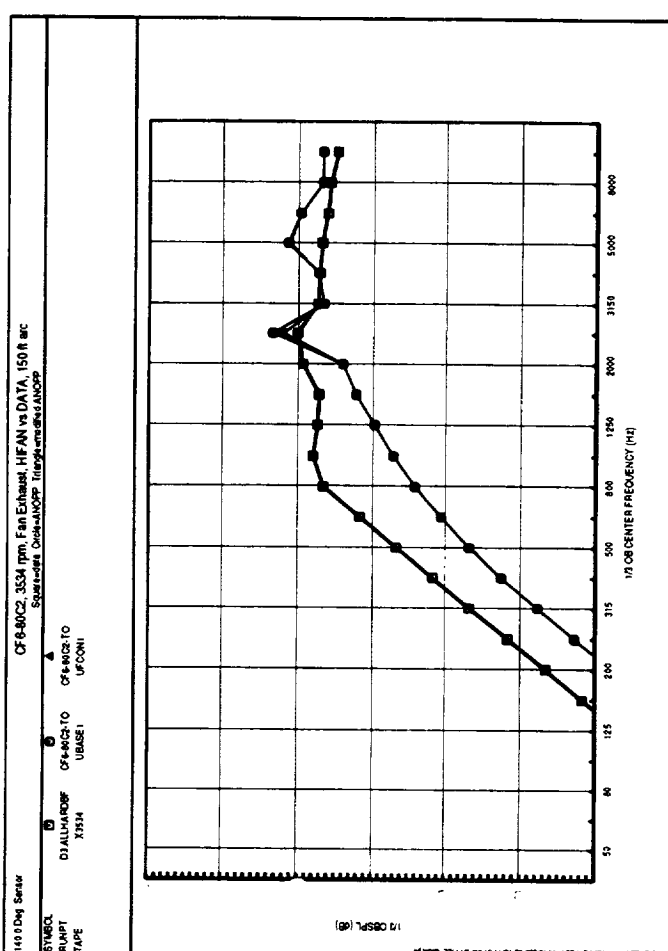
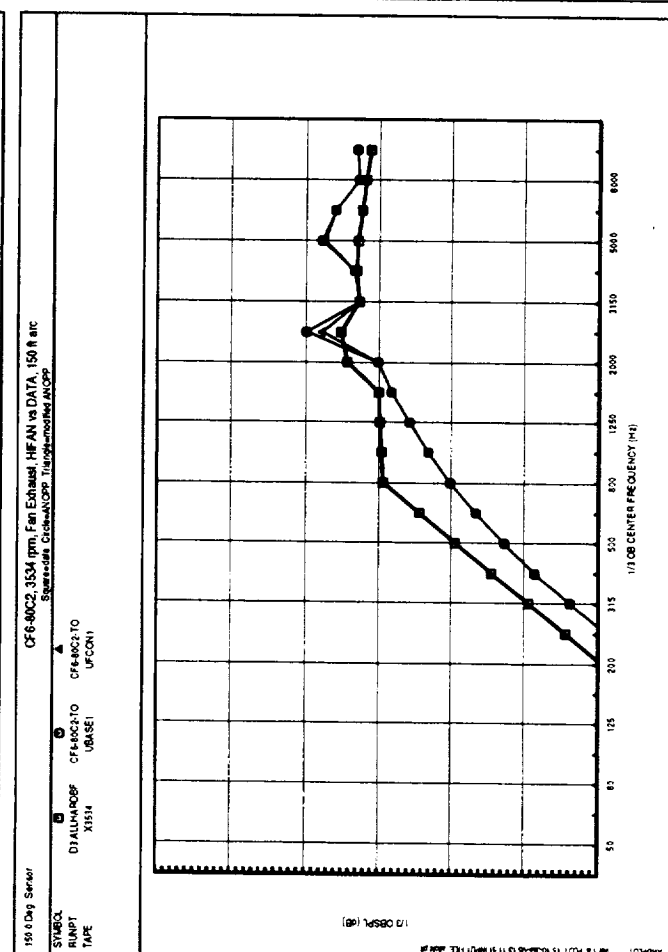
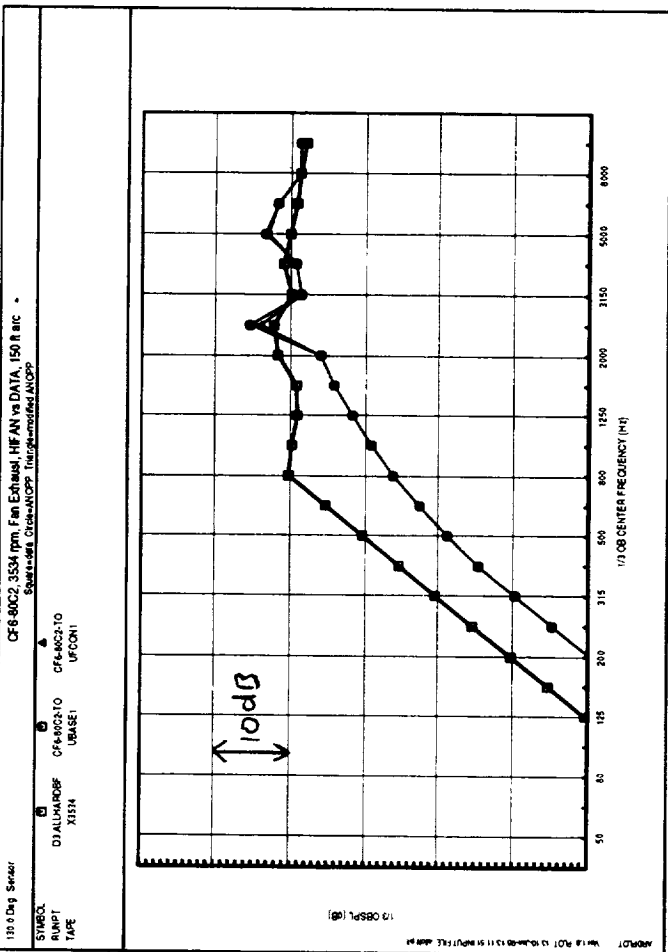
Appendix E Contents

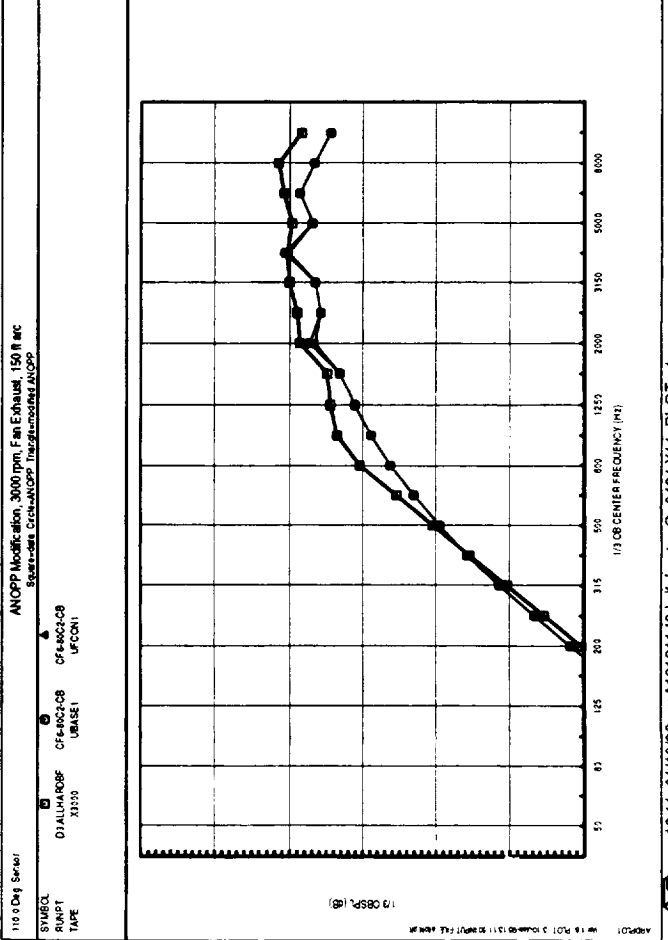
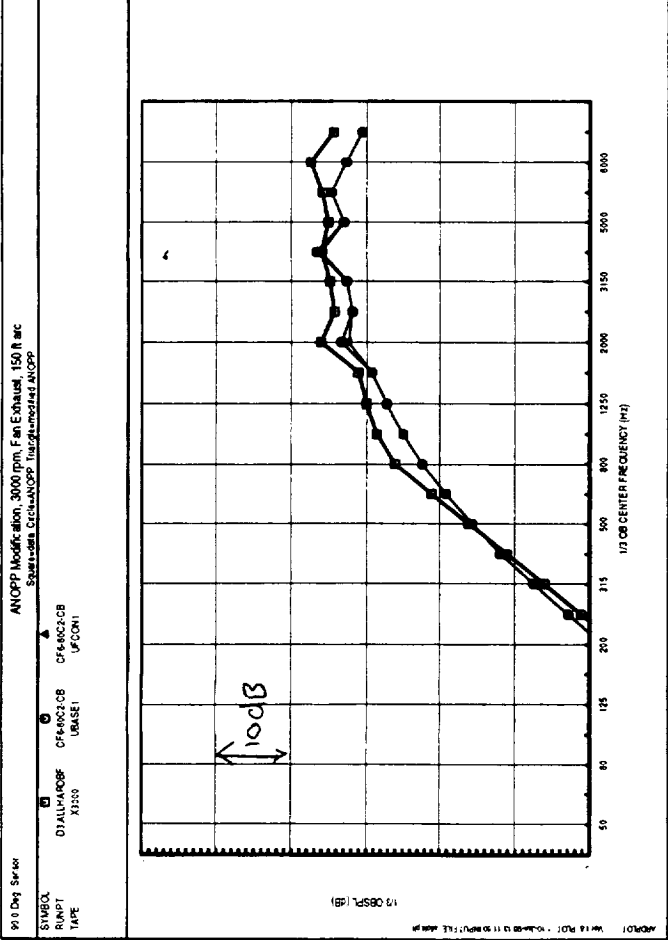
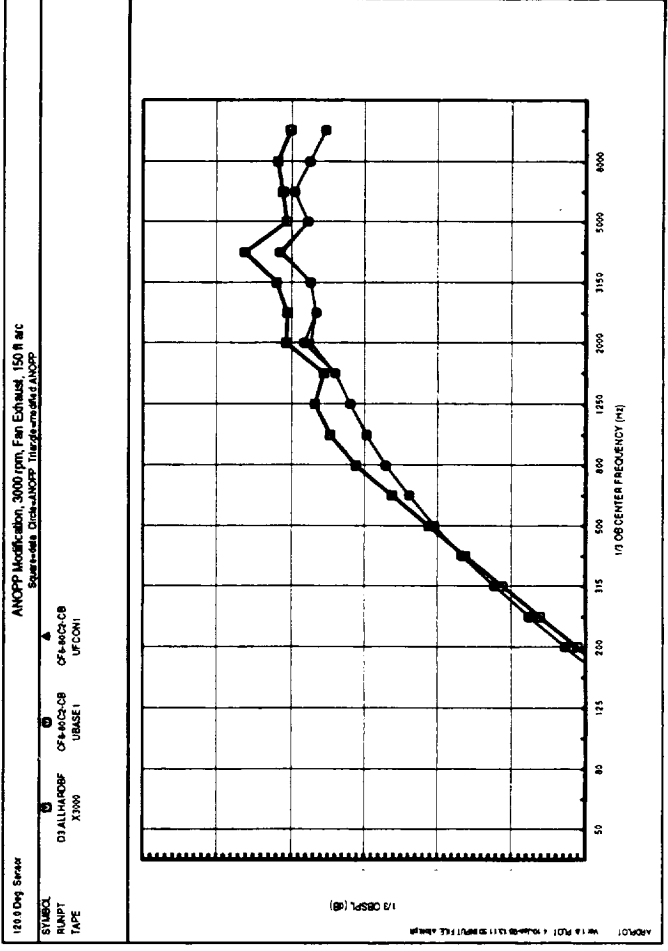
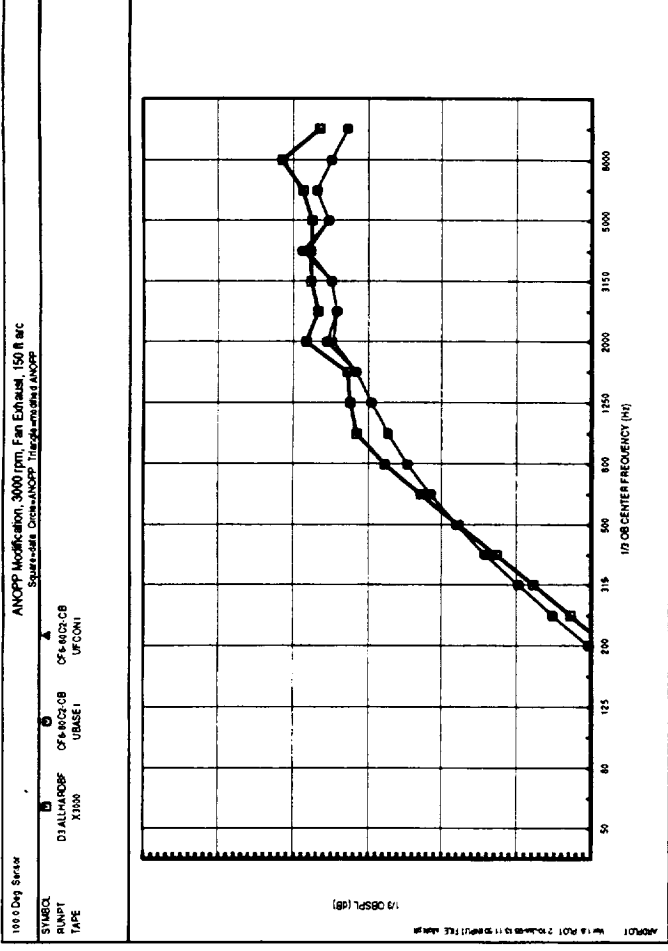
Page	Fan Speed, rpm	Angles, deg
78	3534	90-120
79	3534	130-160
80	3000	90-120
81	3000	130-160
82	2400	90-120
83	2400	130-160
84	3450	90-120
85	3450	130-160
86	3300	90-120
87	3300	130-160
88	3150	90-120
89	3150	130-160
90	2850	90-120
91	2850	130-160
92	2700	90-120
93	2700	130-160
94	2100	90-120
95	2100	130-160
96	1950	90-120
97	1950	130-160
98	1800	90-120
99	1800	130-160
100	1650	90-120
101	1650	130-160

Key to Plots:

- squares = total measured engine data
- circles = Heidmann method prediction
- triangles = modified Heidmann method prediction (see Section 4)

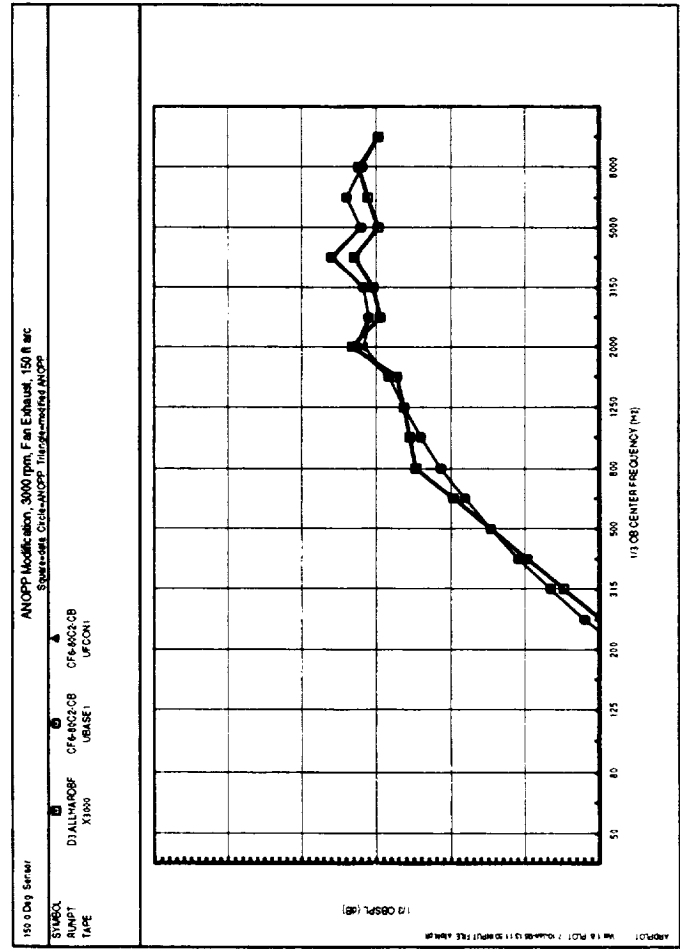
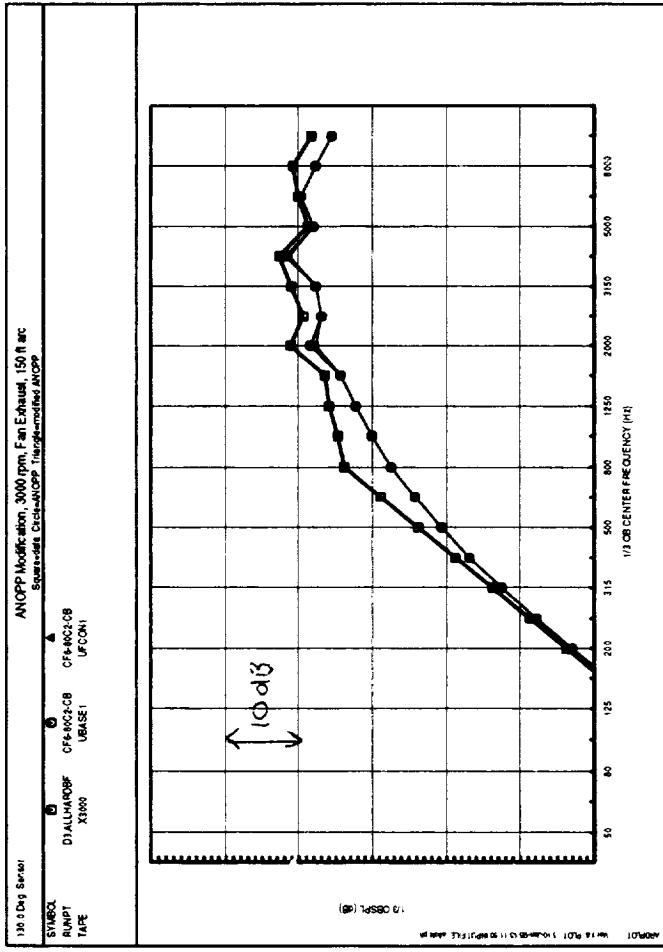
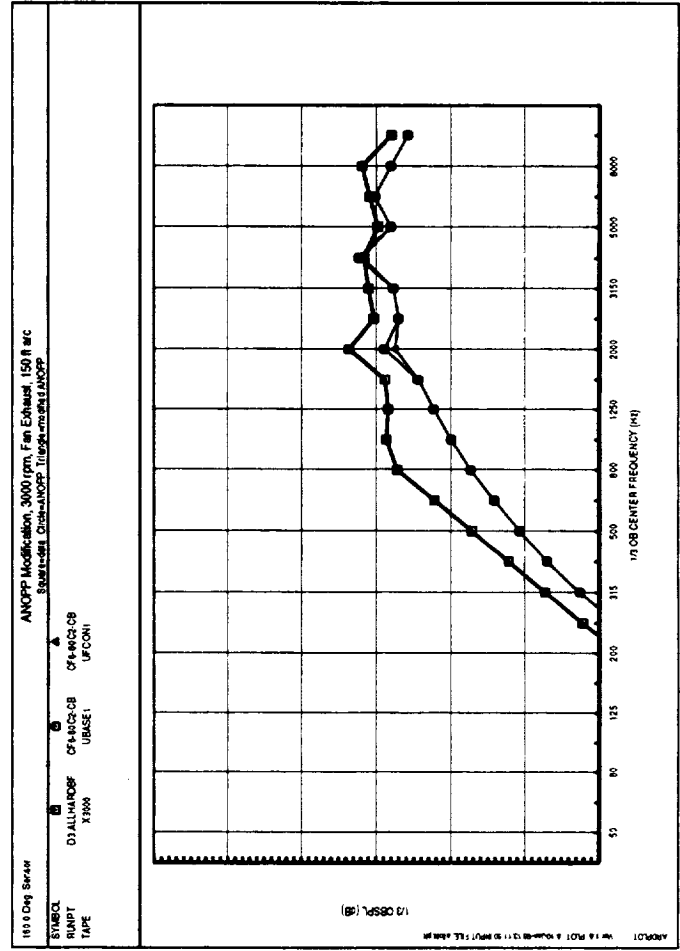
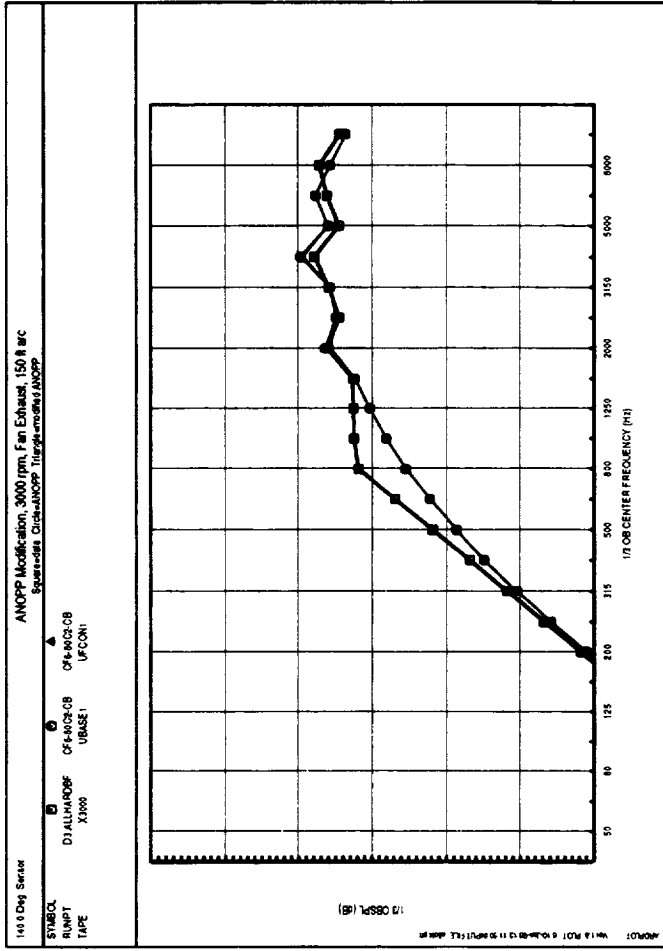


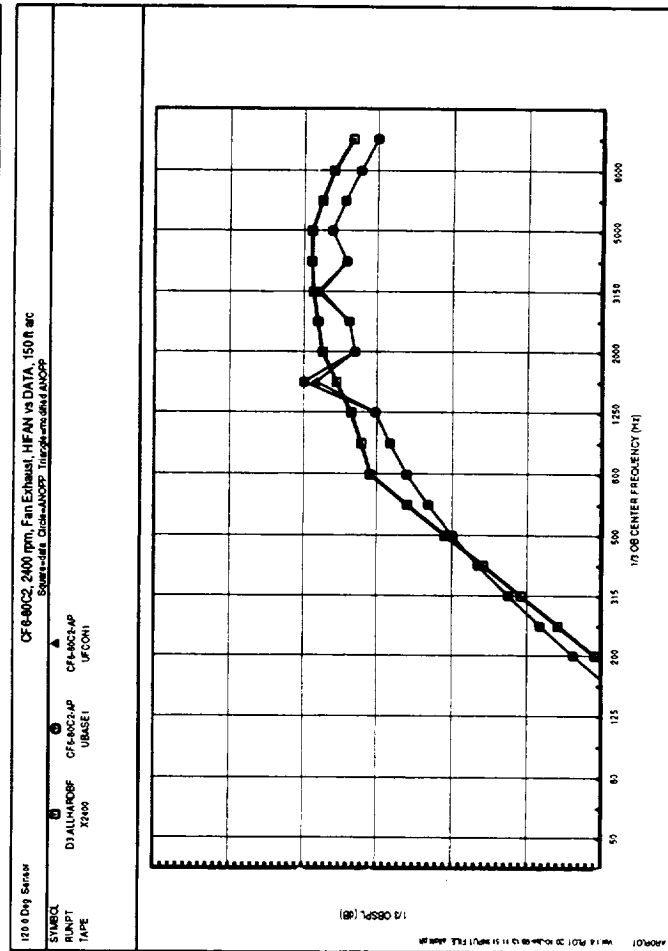
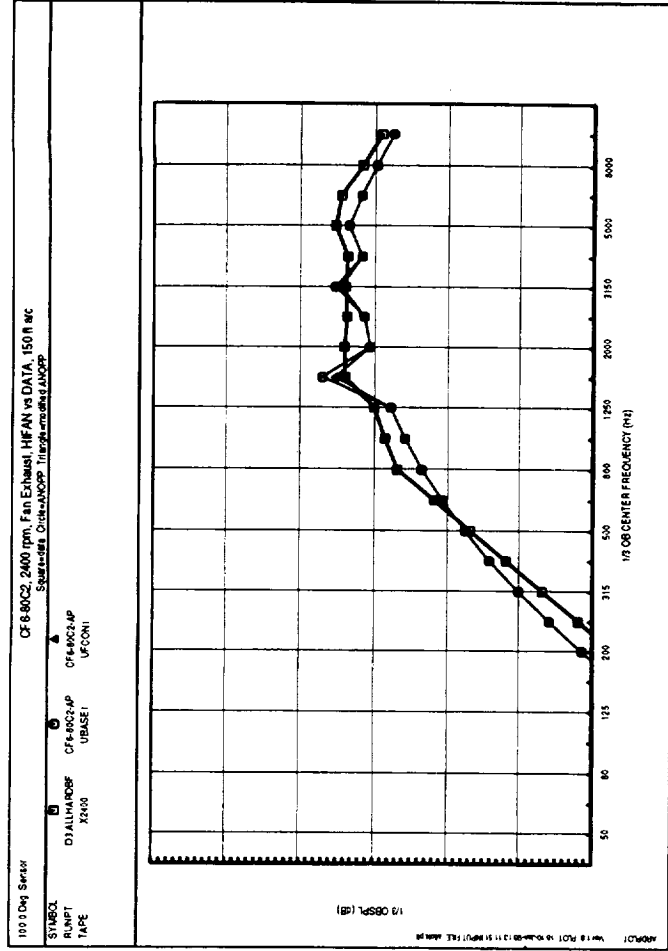
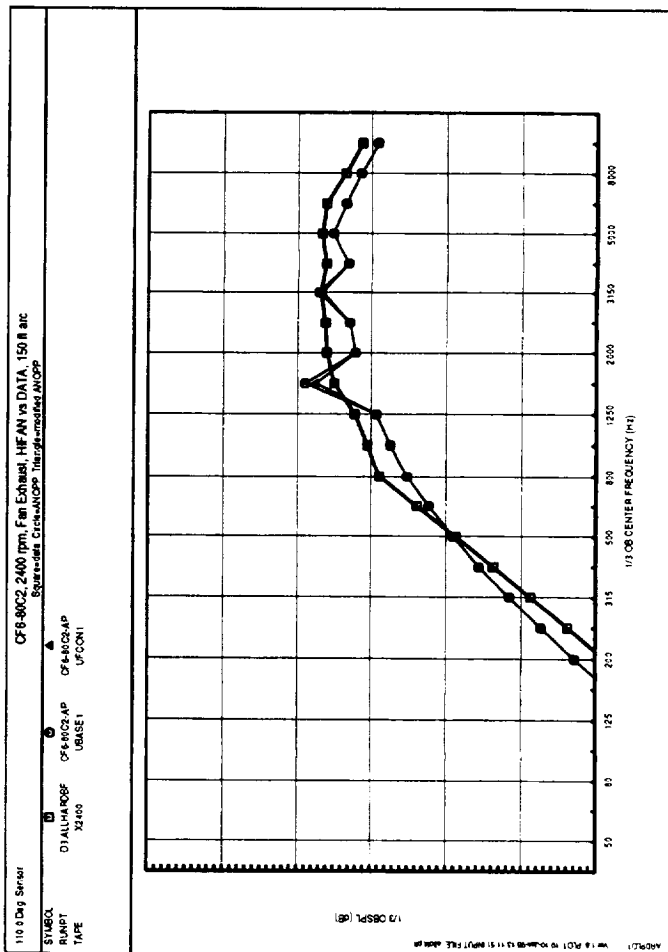
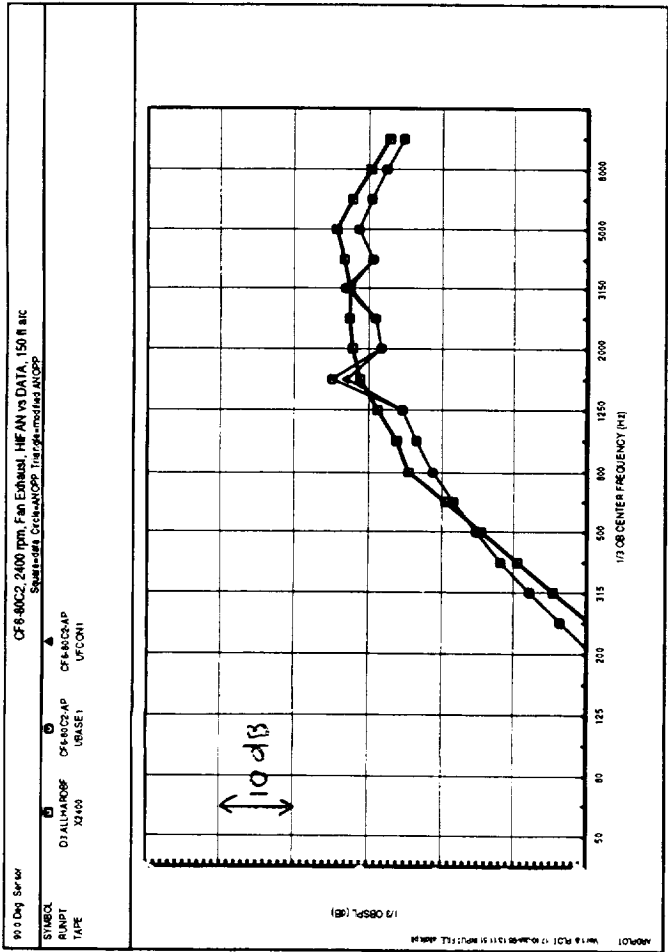


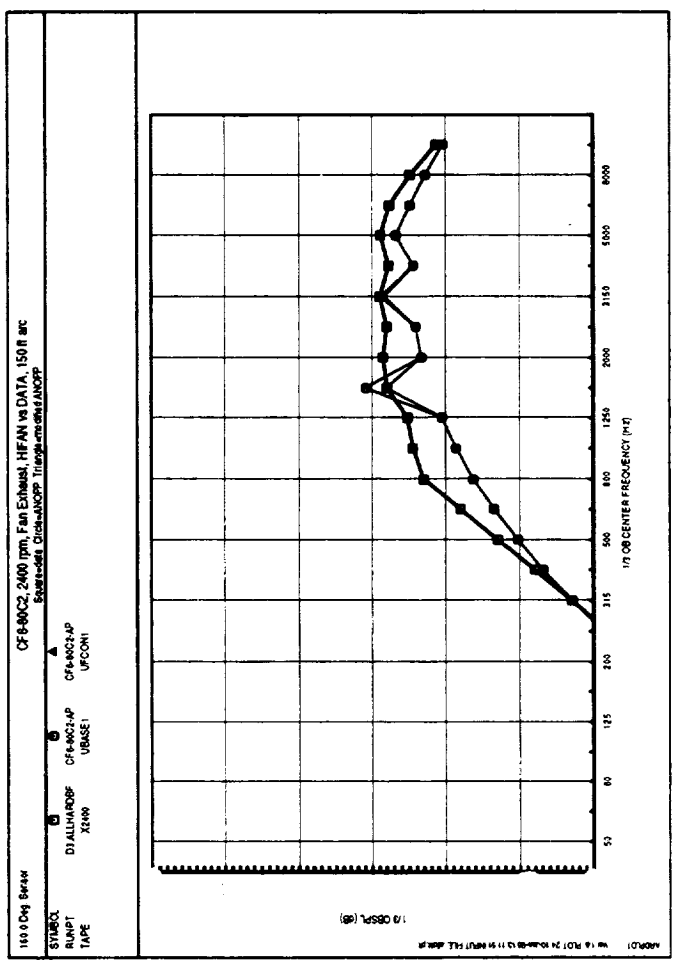
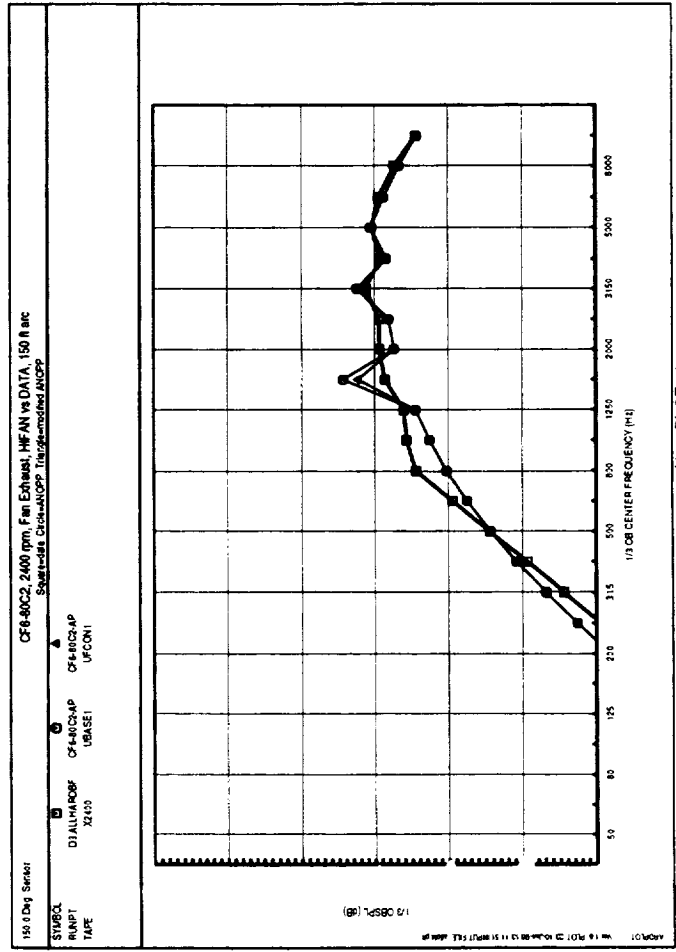
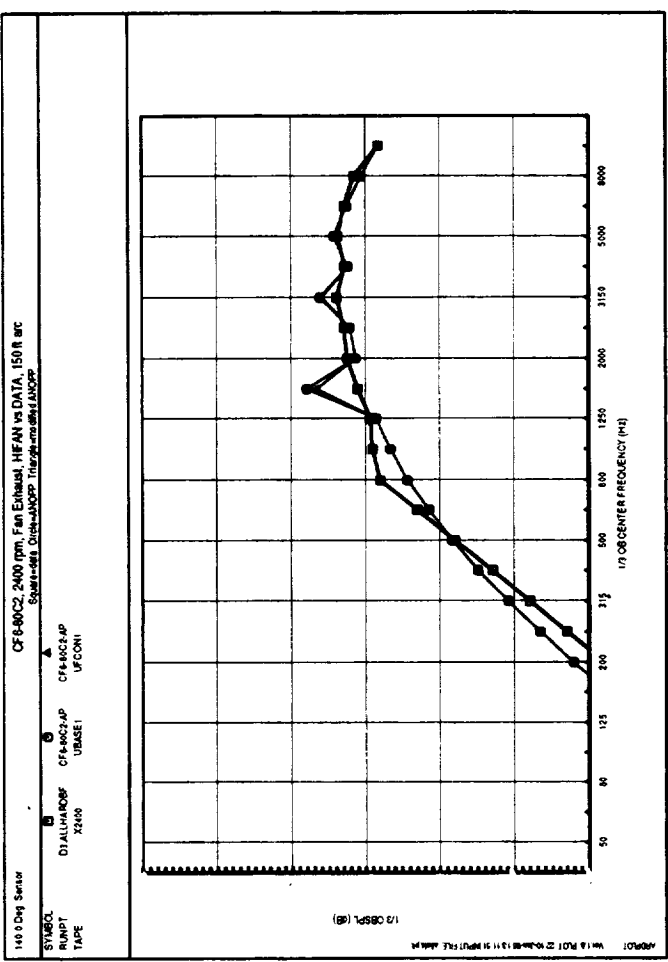
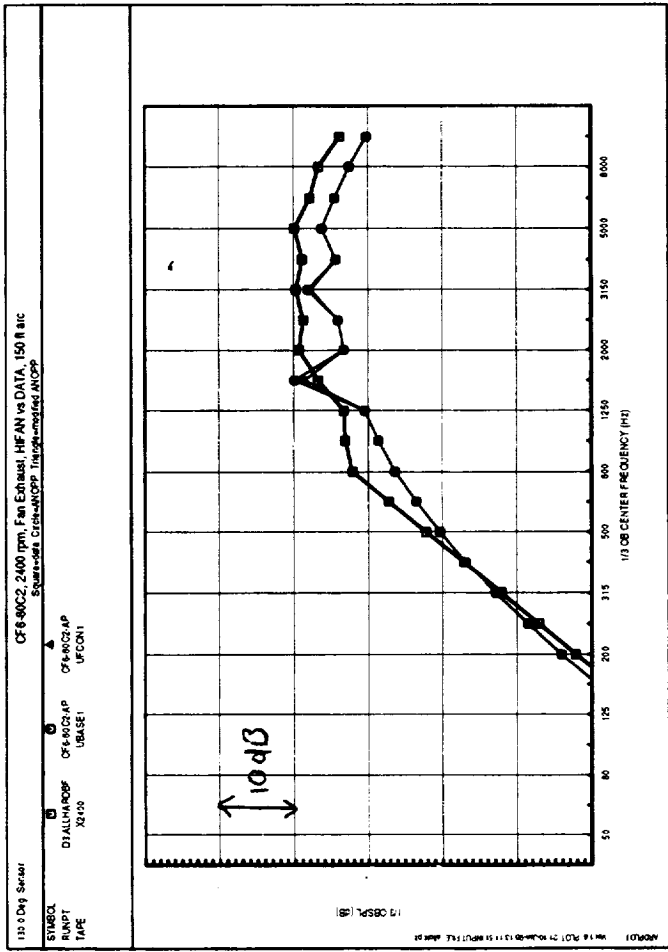


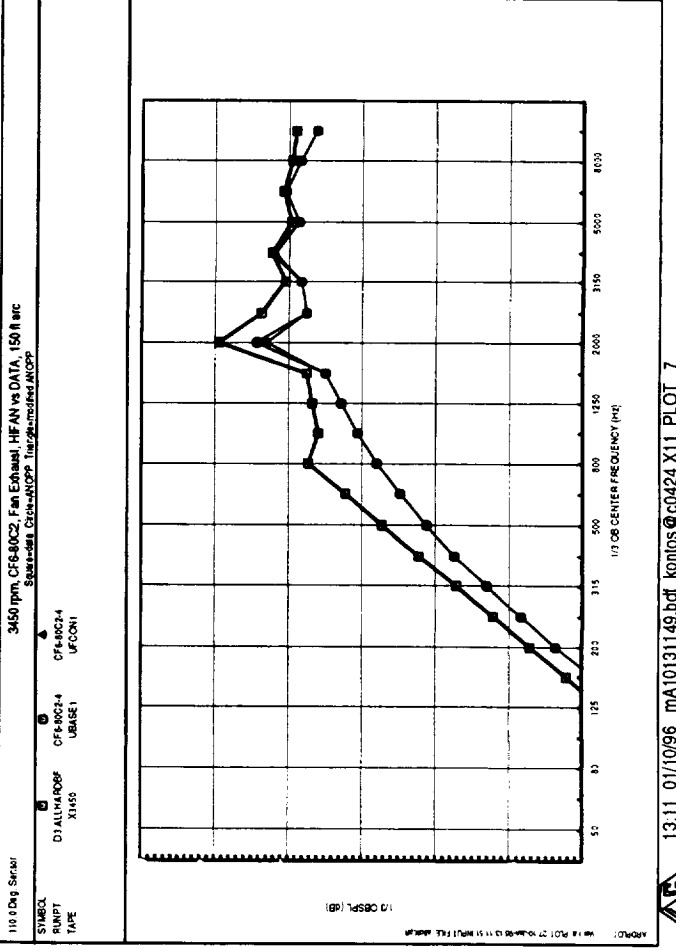
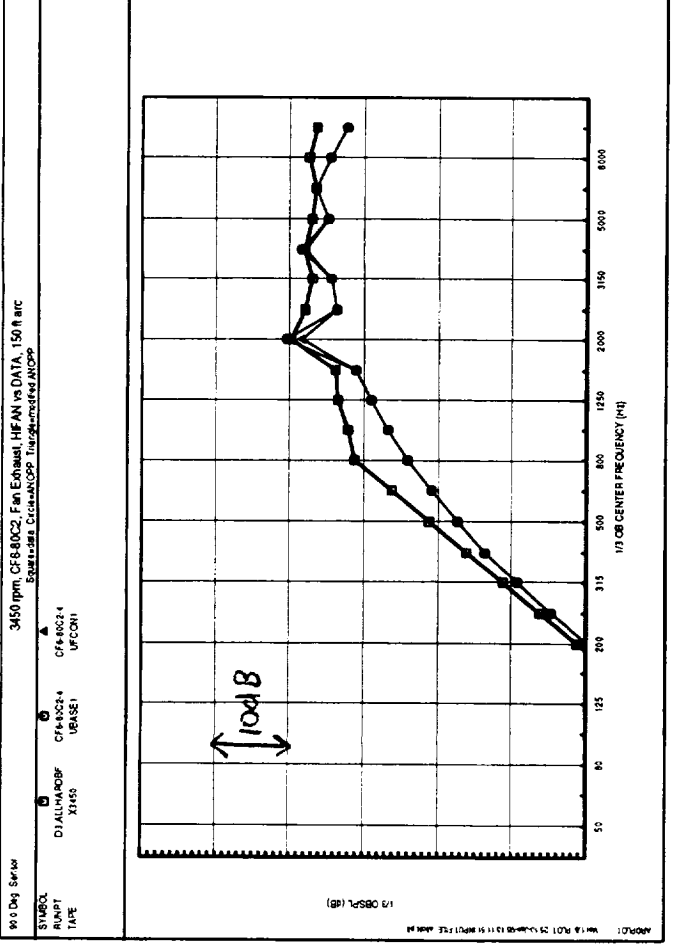
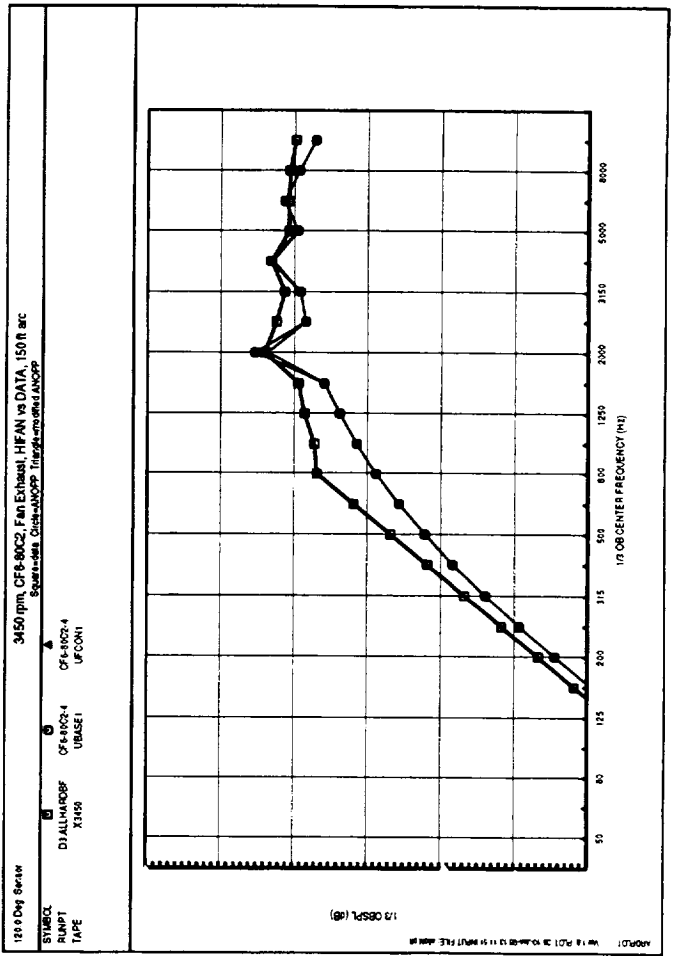
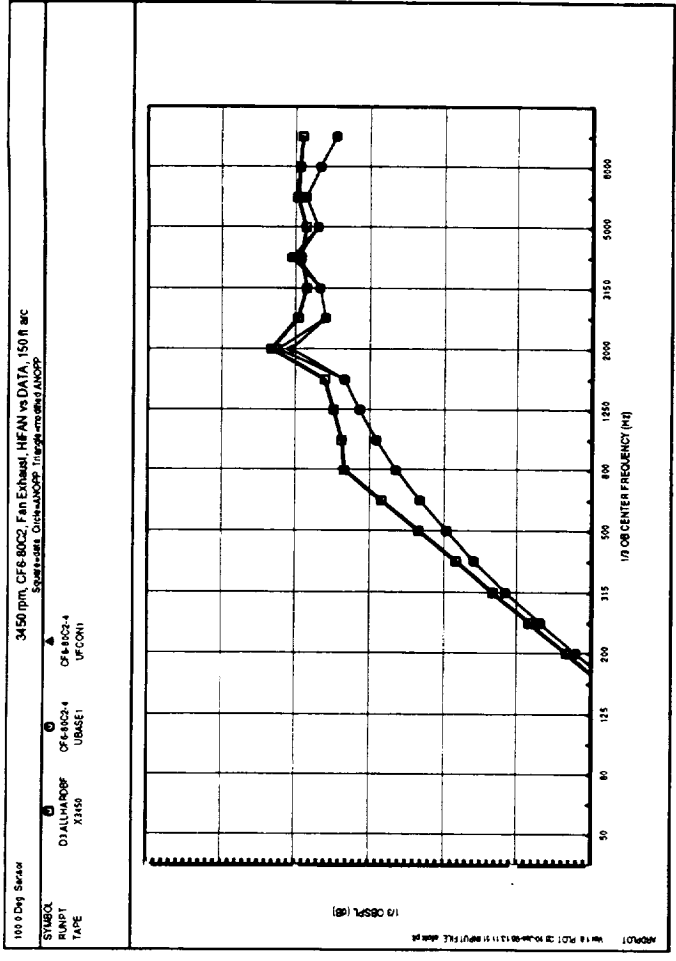
1311 01/10/96 mA10131149 bdf Kontos c0424 X11 PLOT
 EGS LIB 5.1 12/14/95 EGSREP.XPOST 5.1 12/14/95 on c0424
 (NO PROG. VER. SPECIFIED)

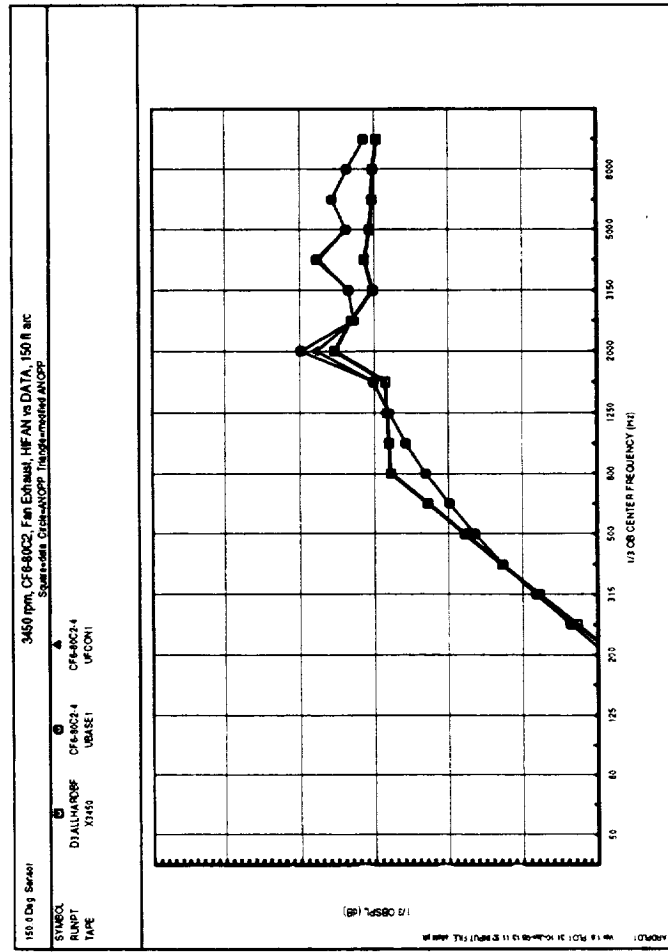
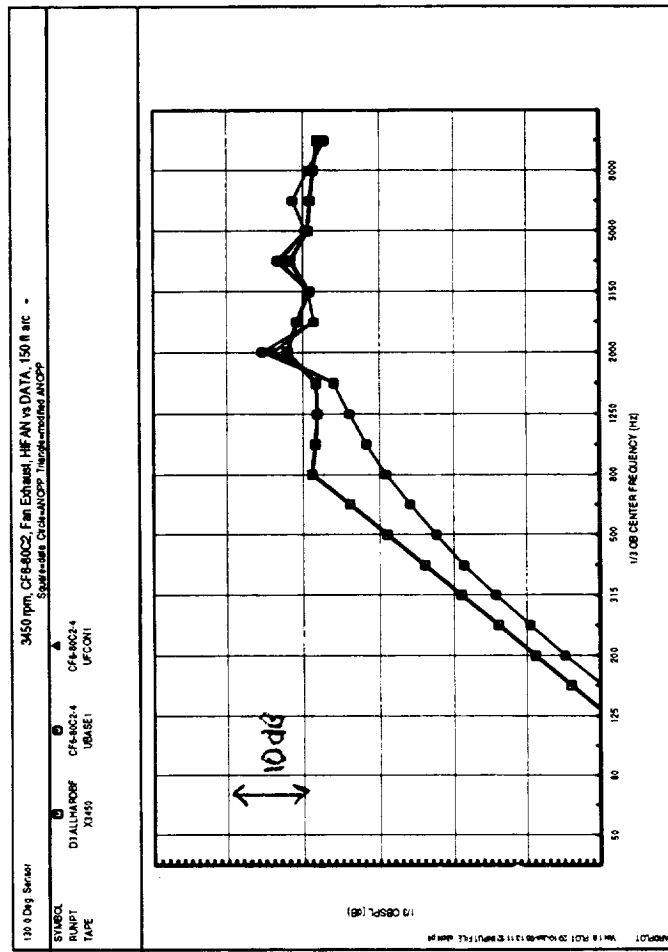
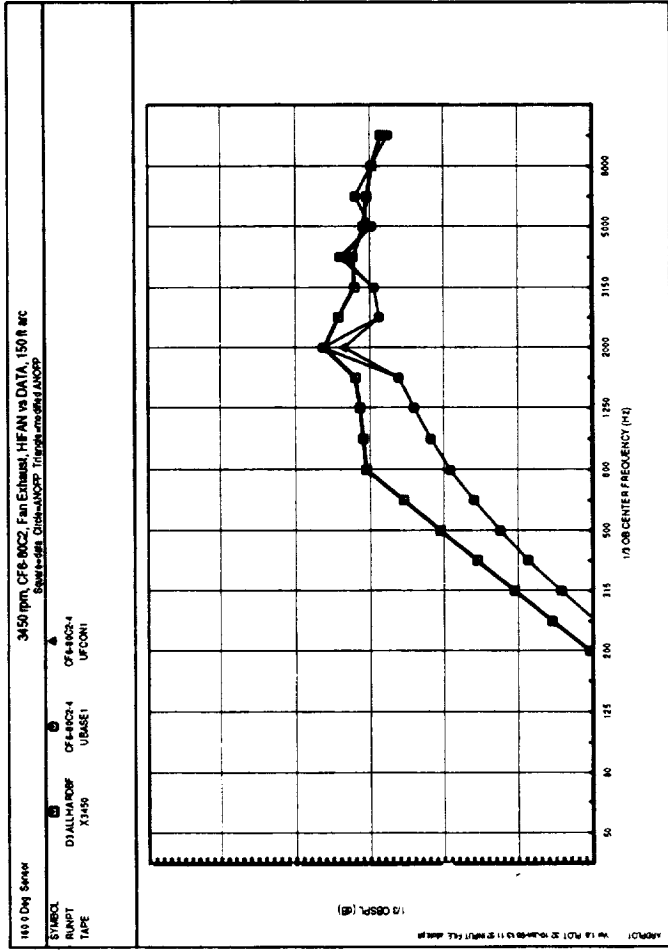
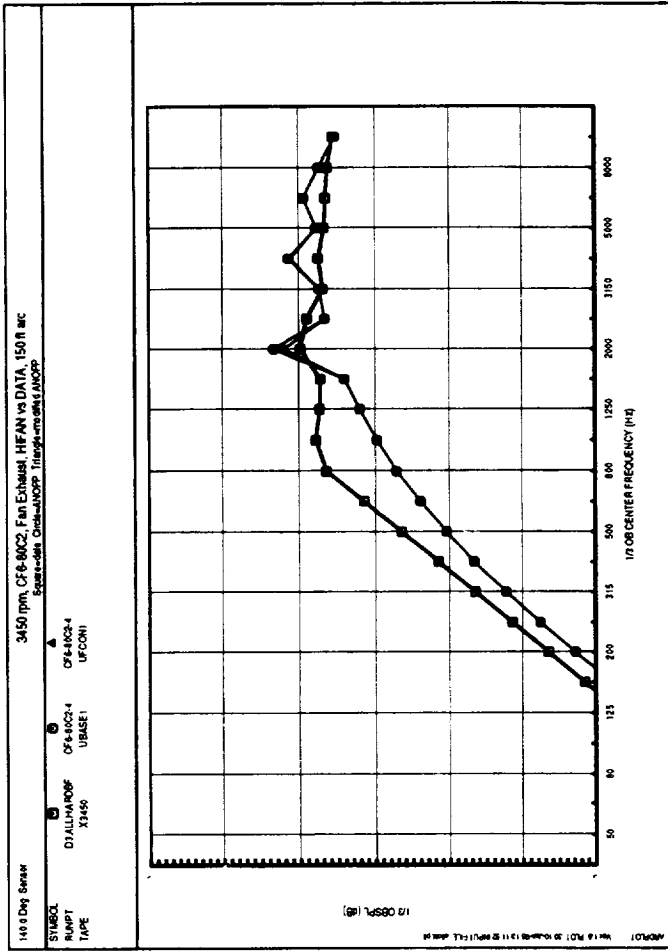


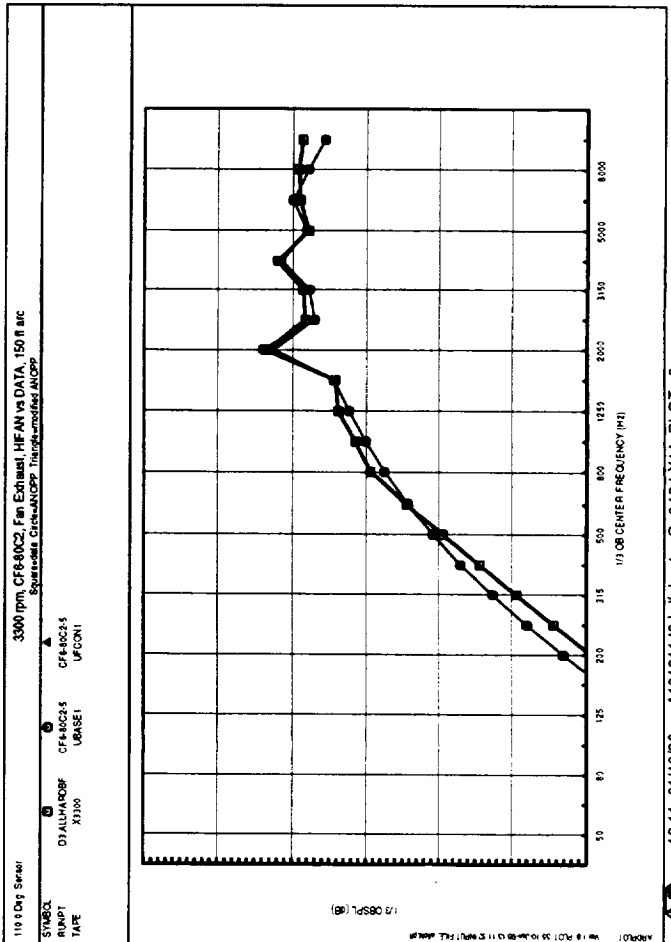
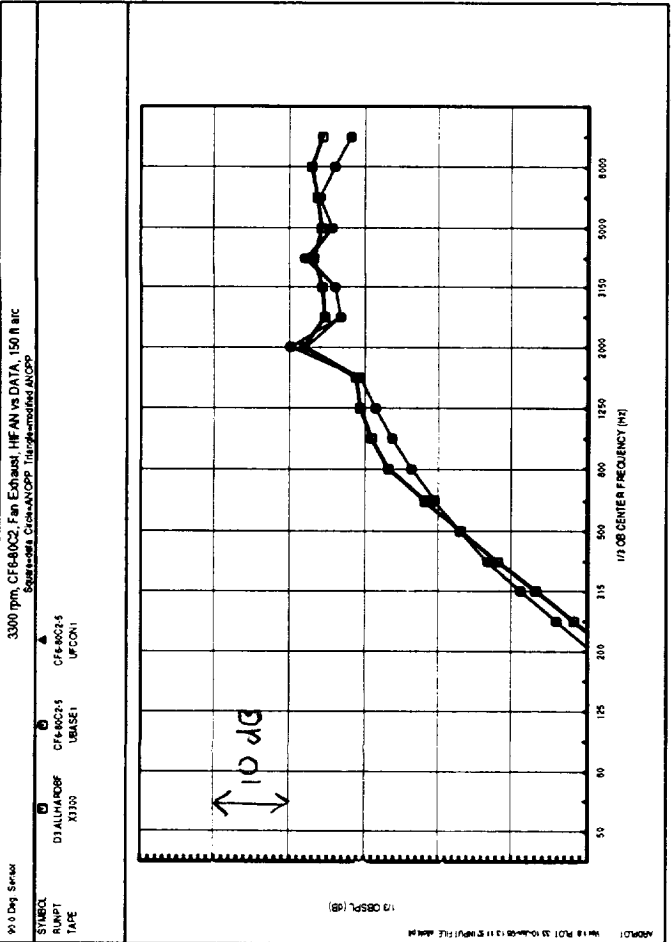
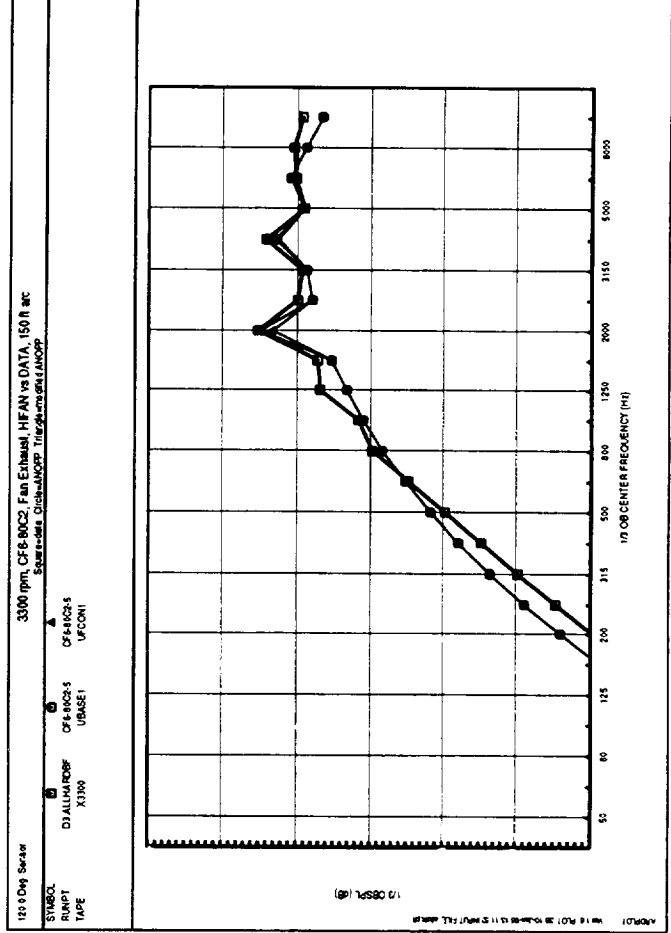
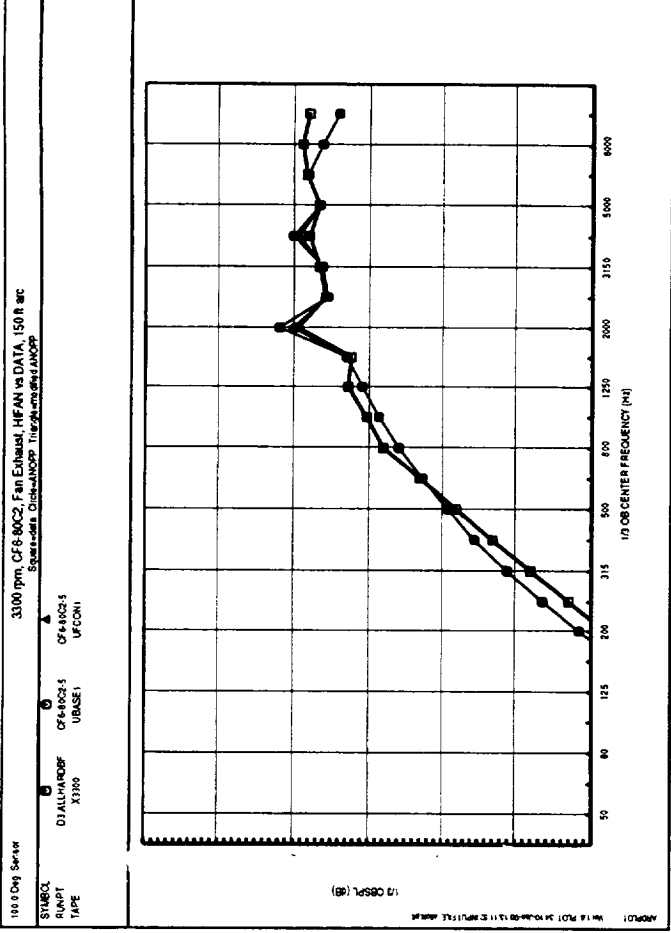


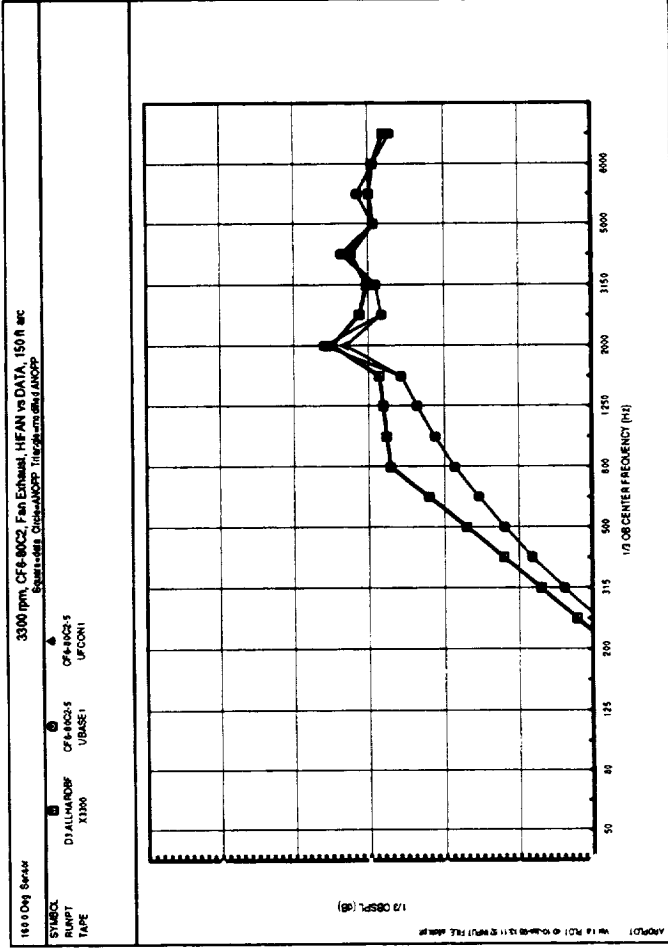
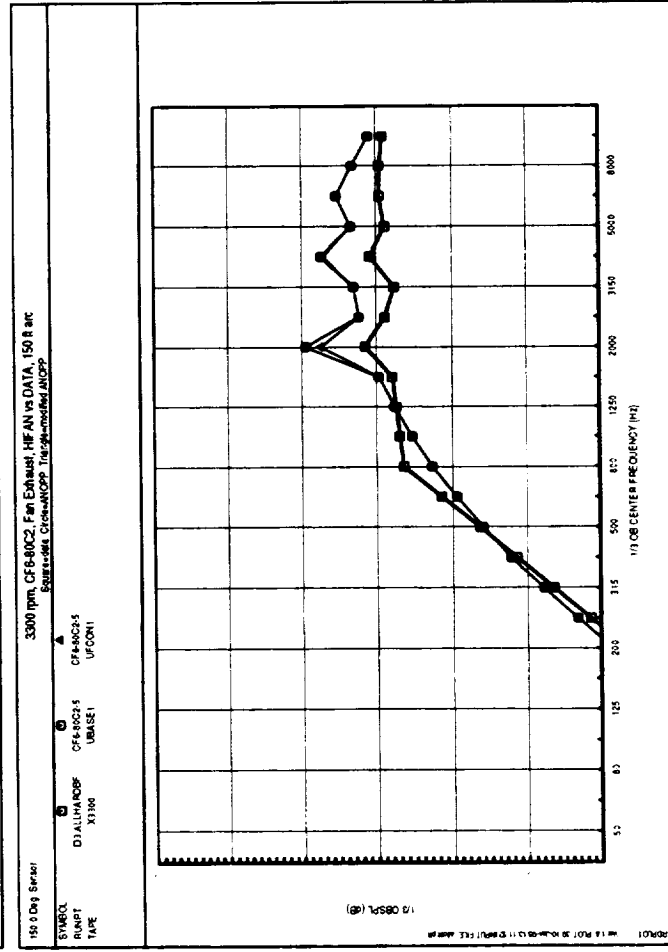
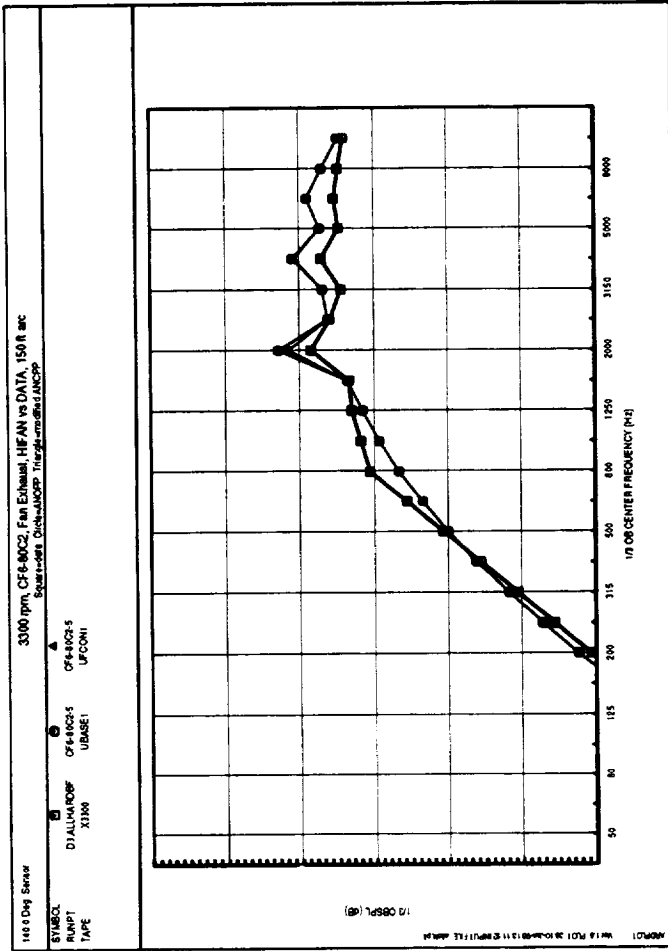
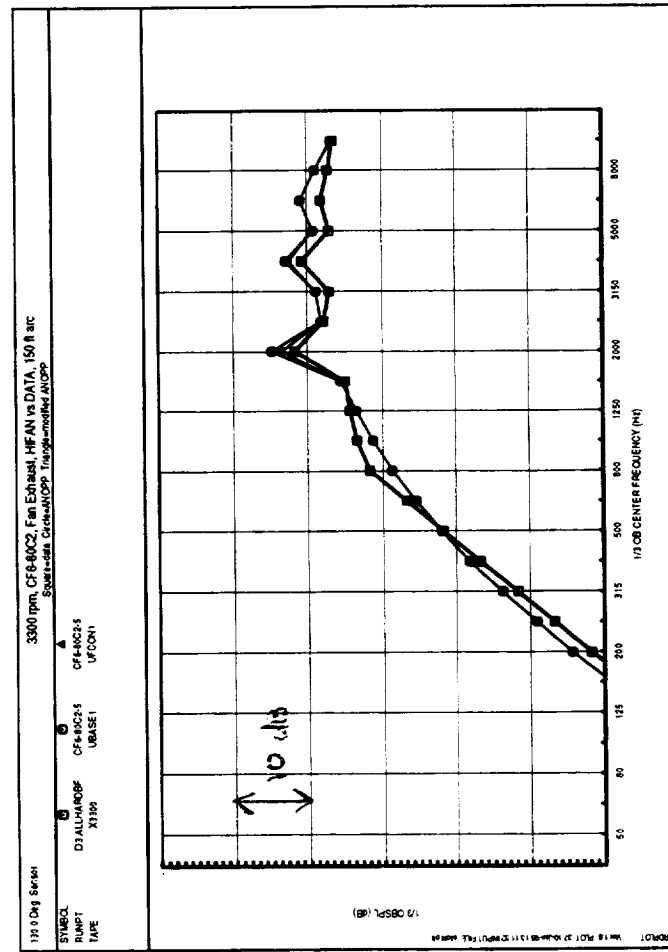


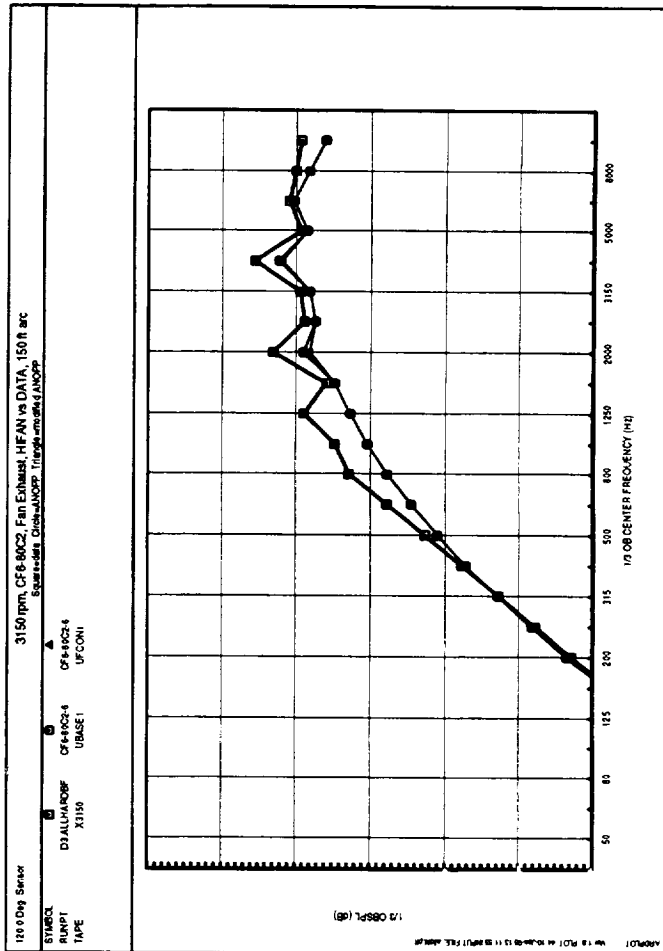
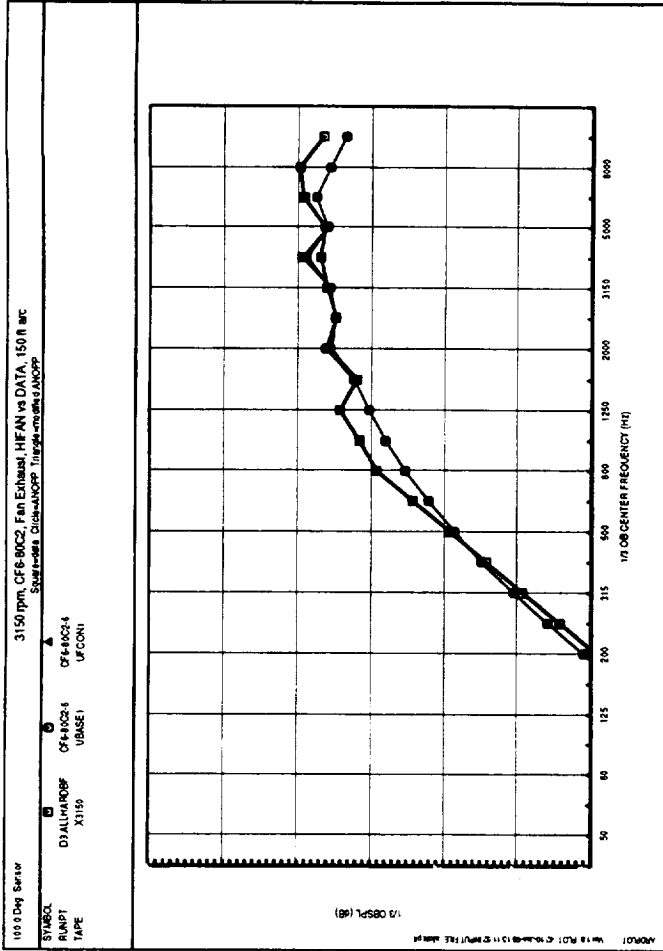
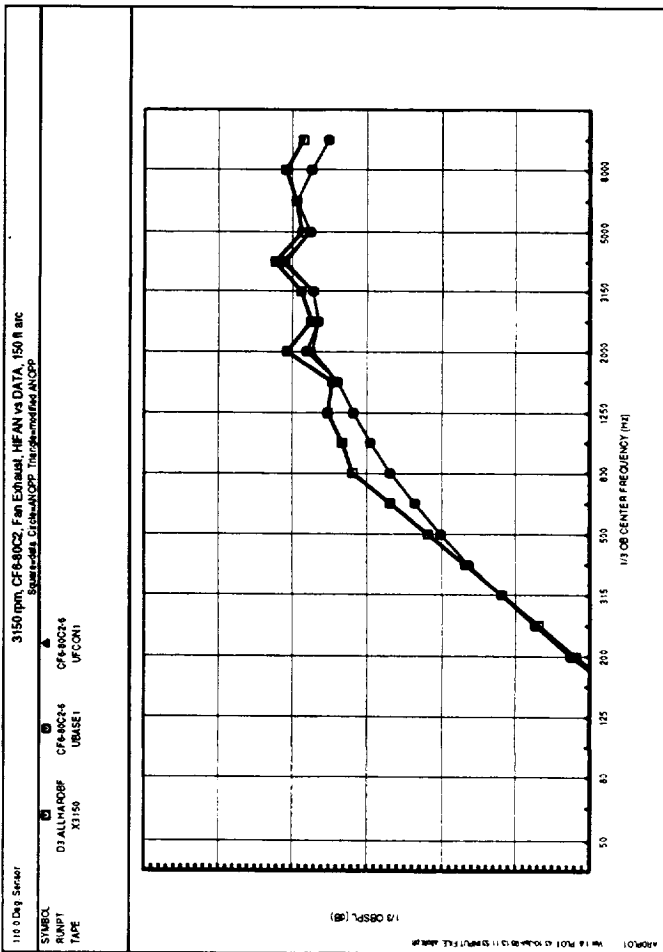
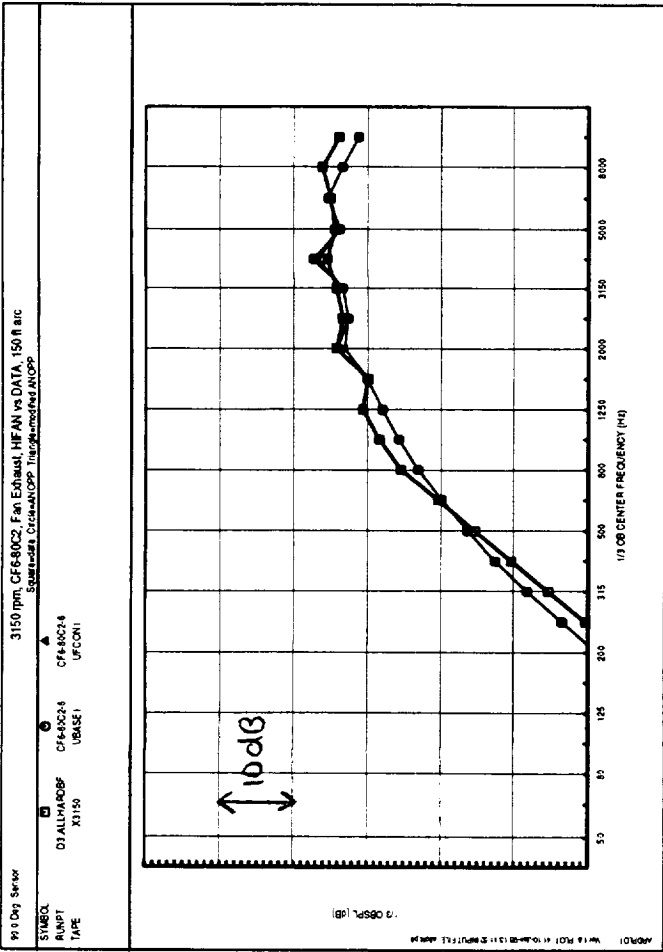


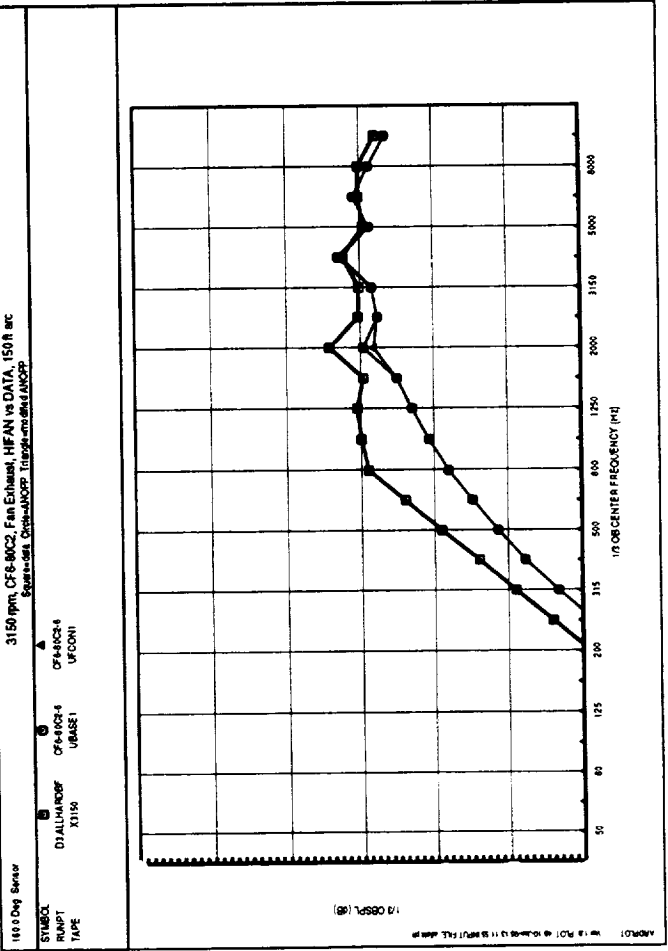
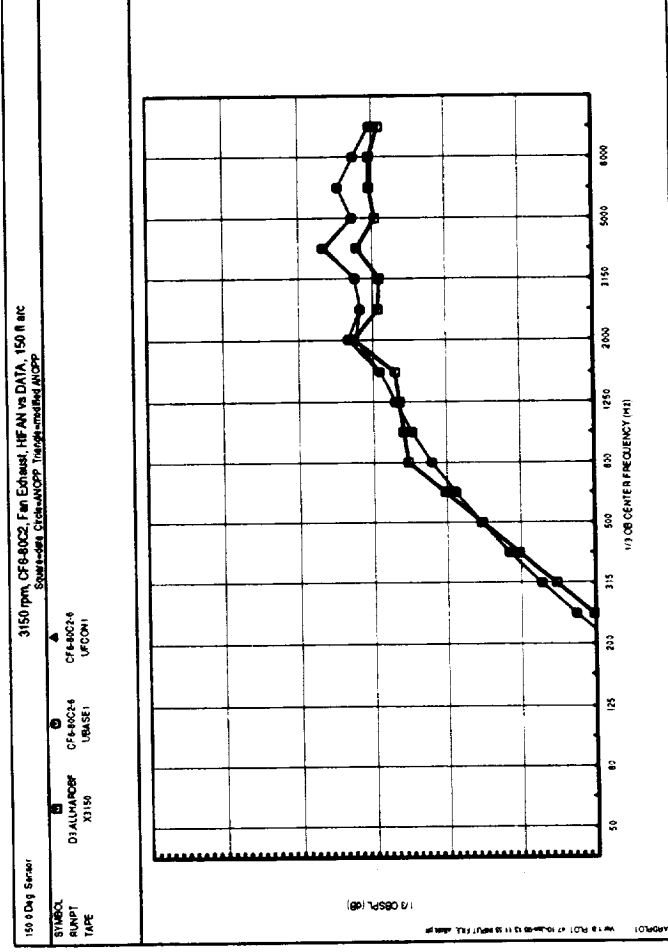
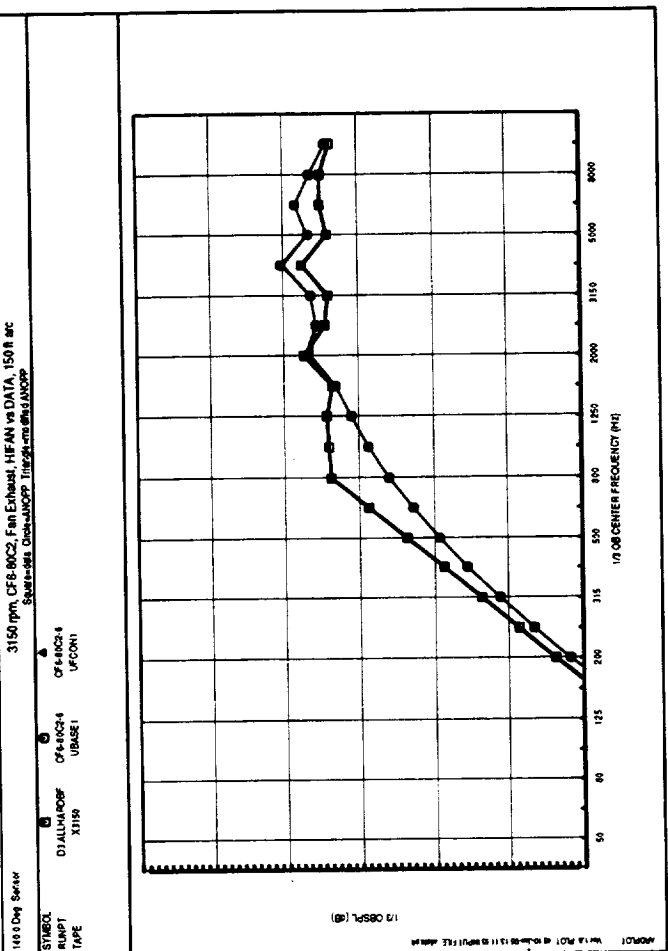
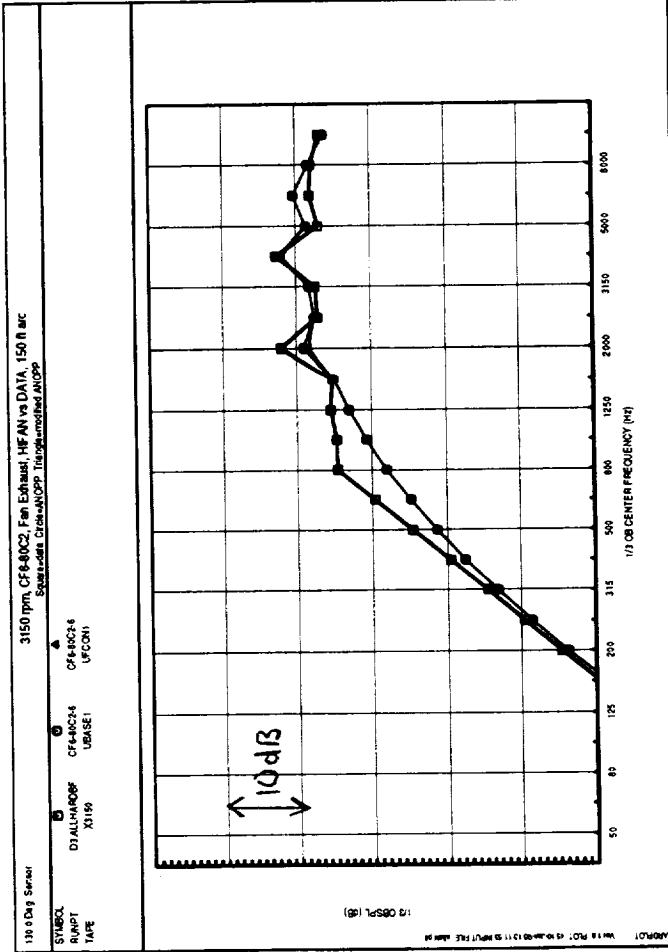


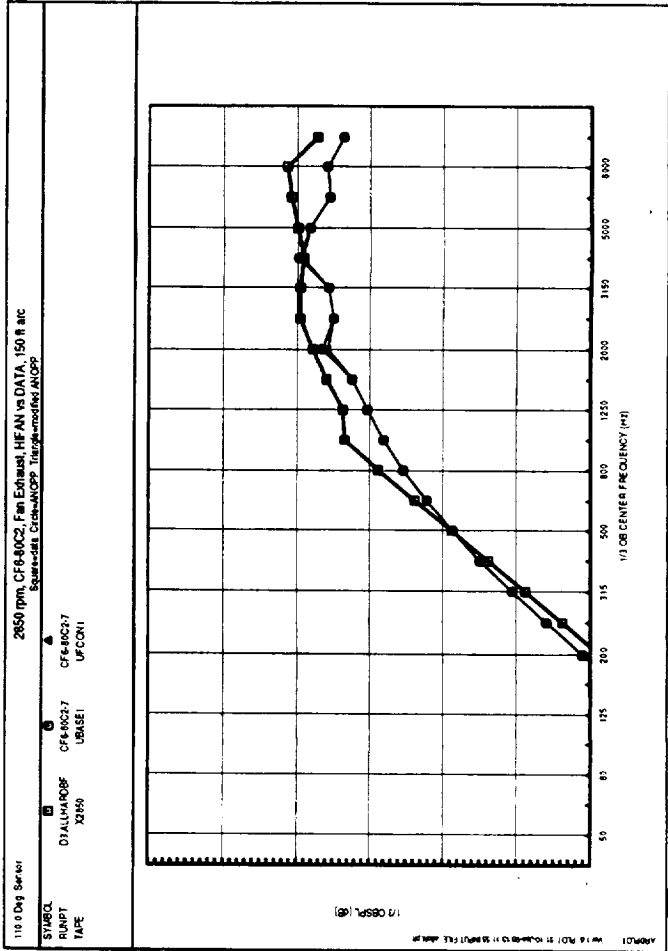
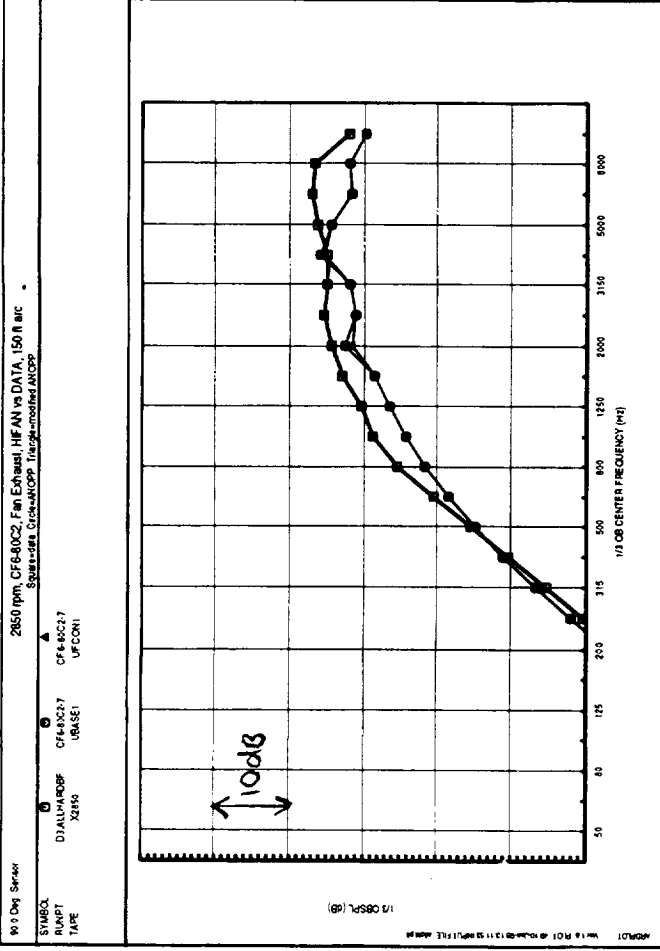
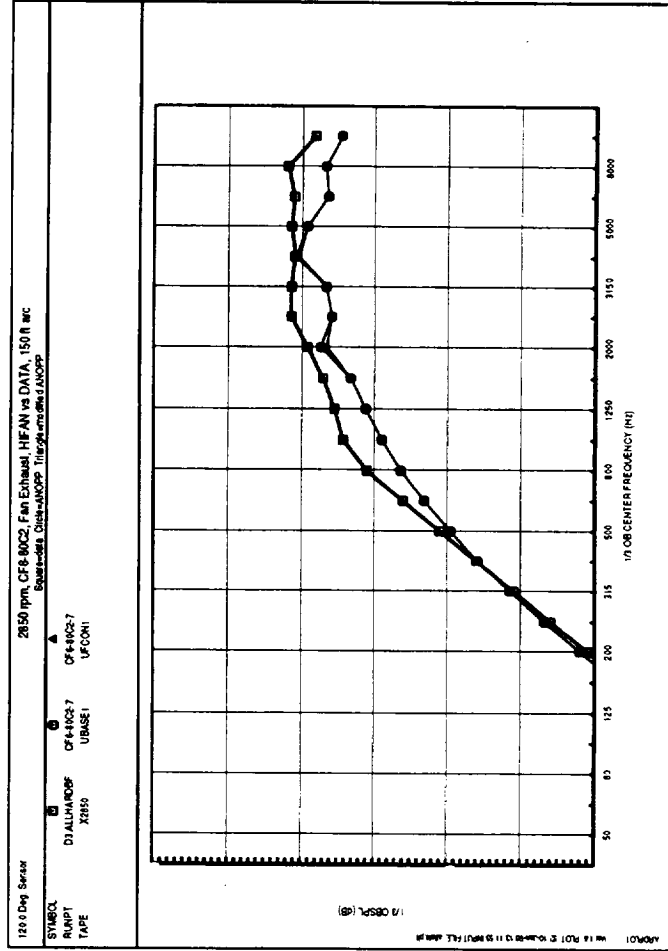
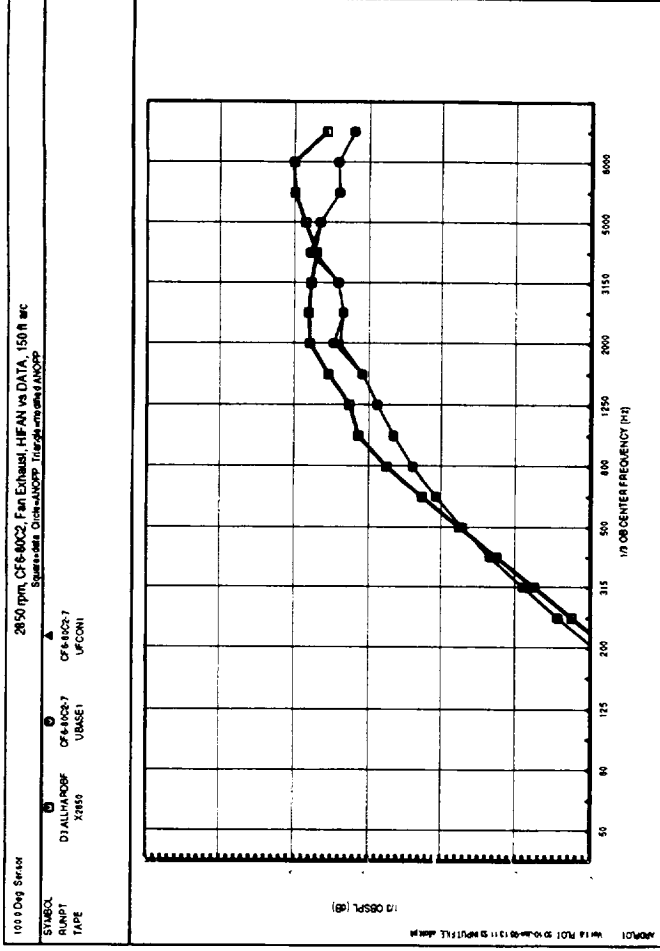


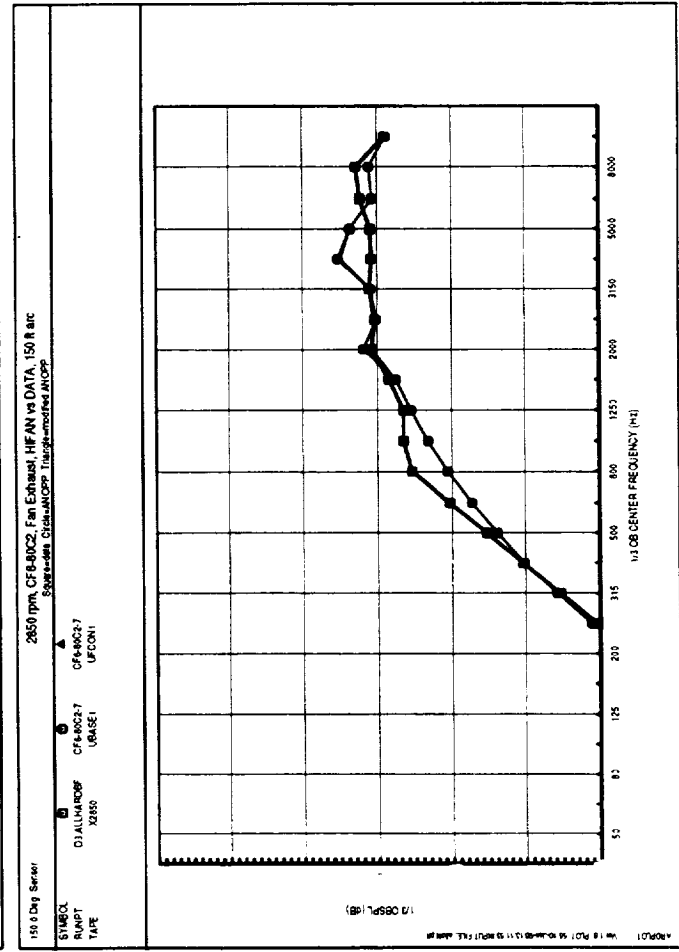
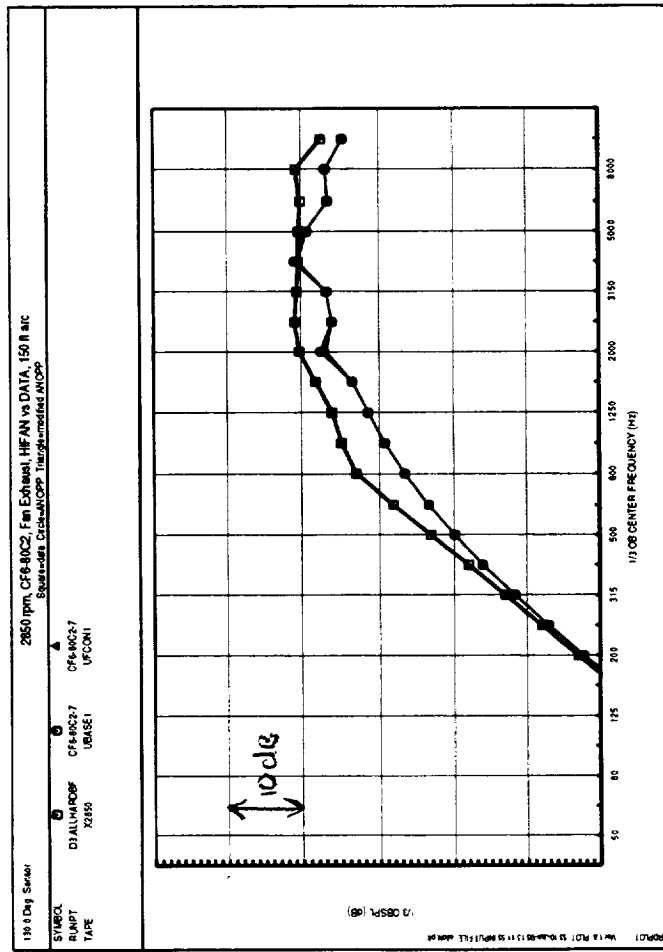
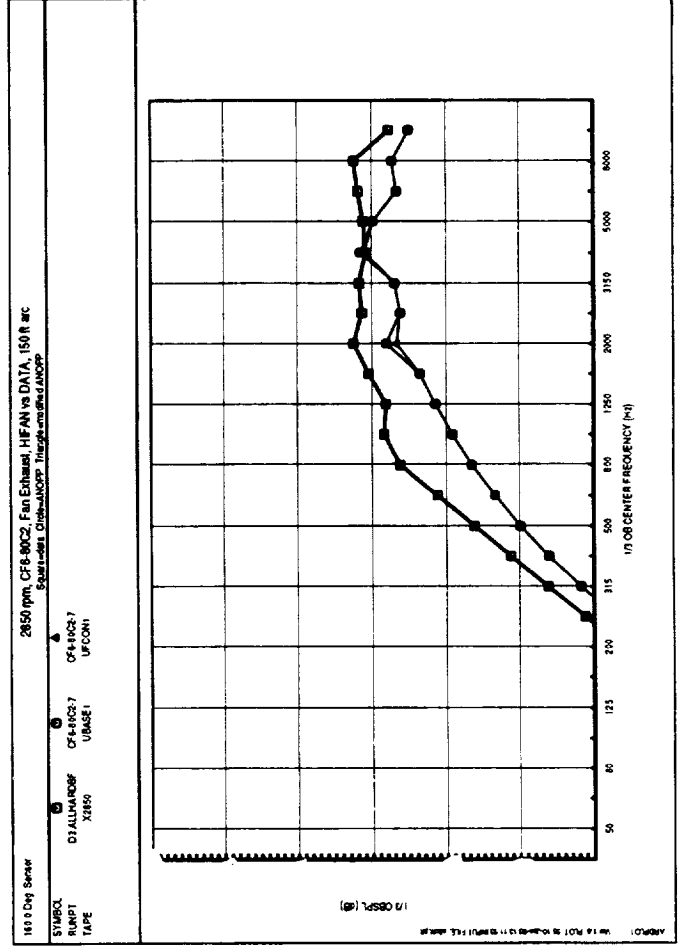
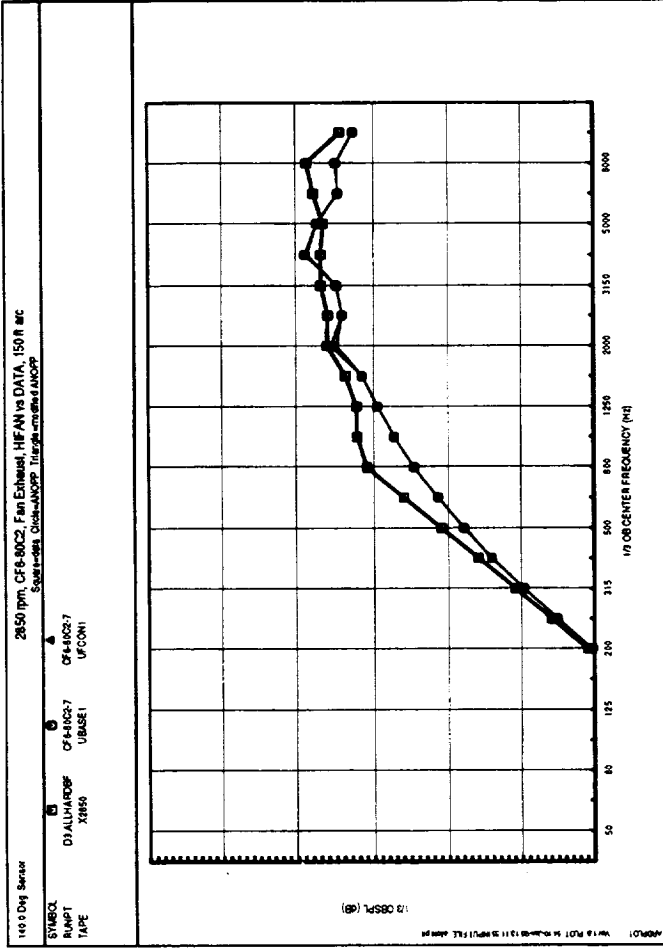


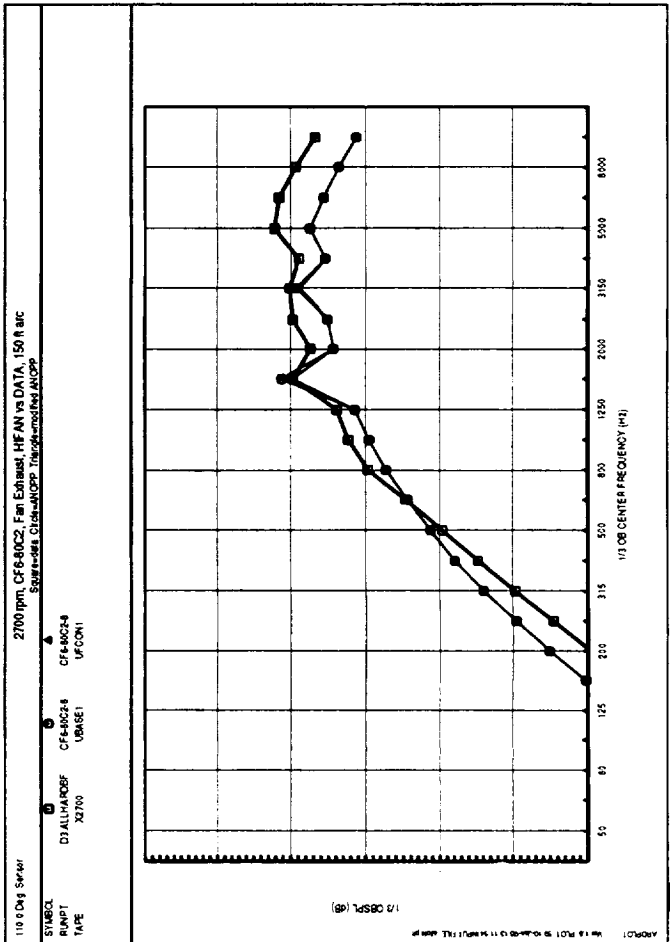
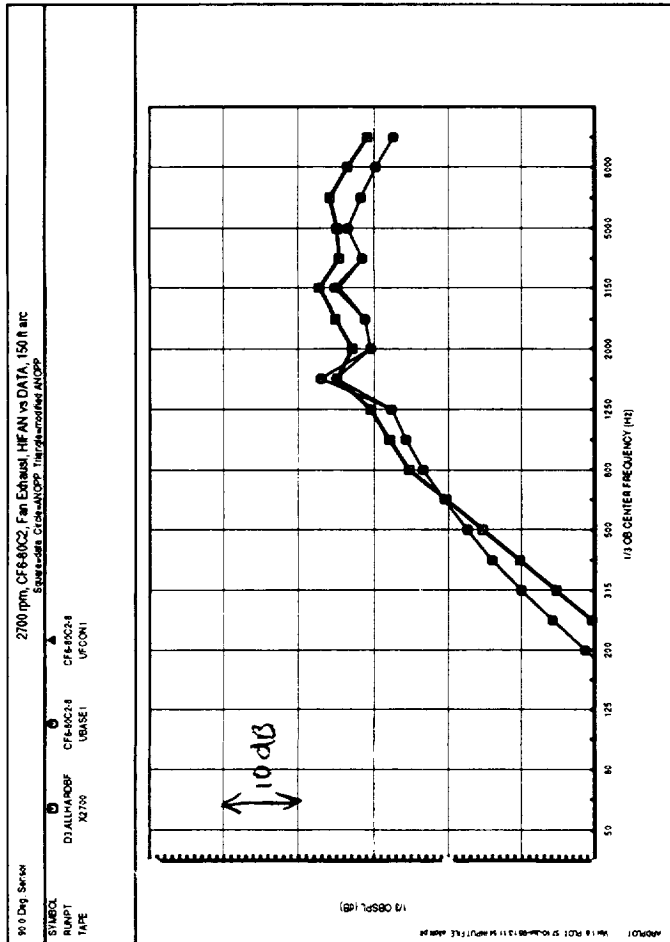
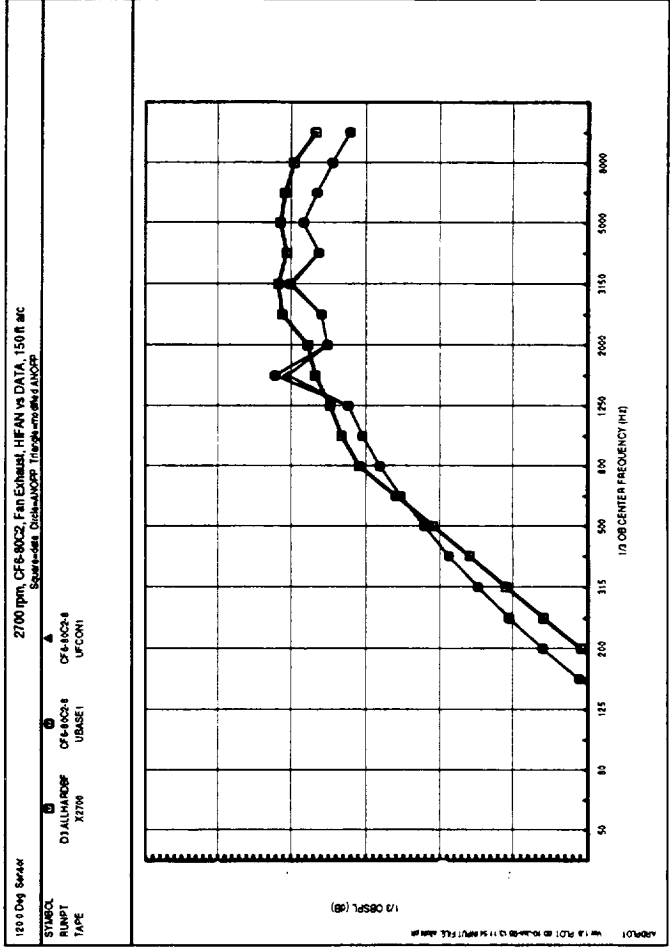
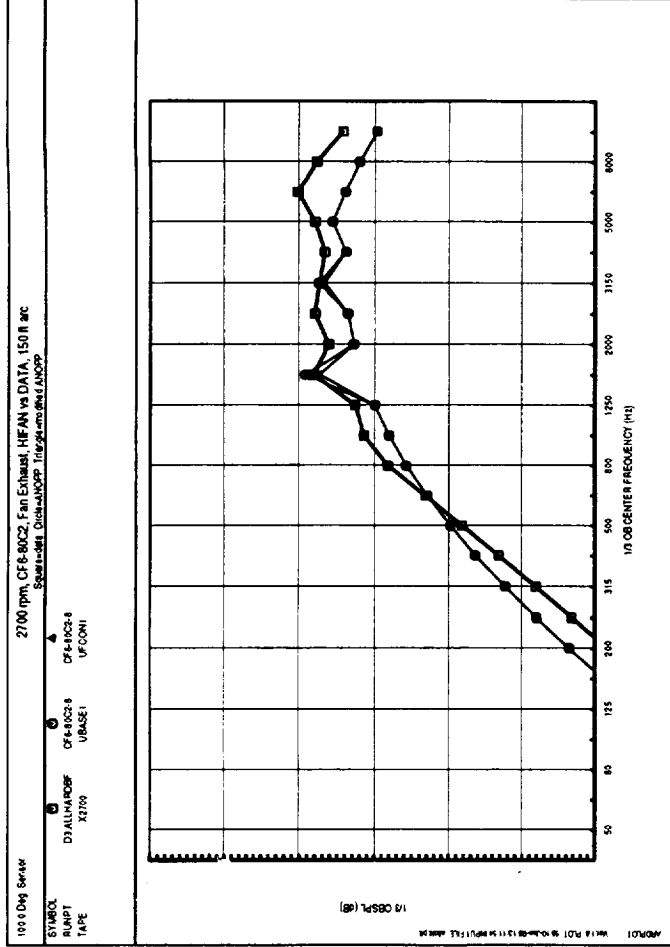


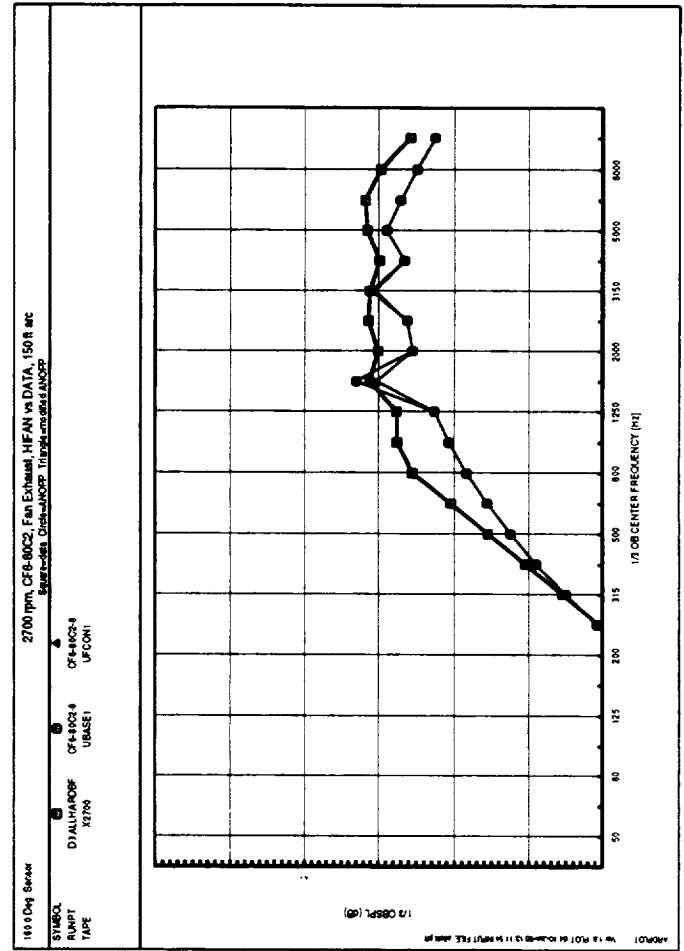
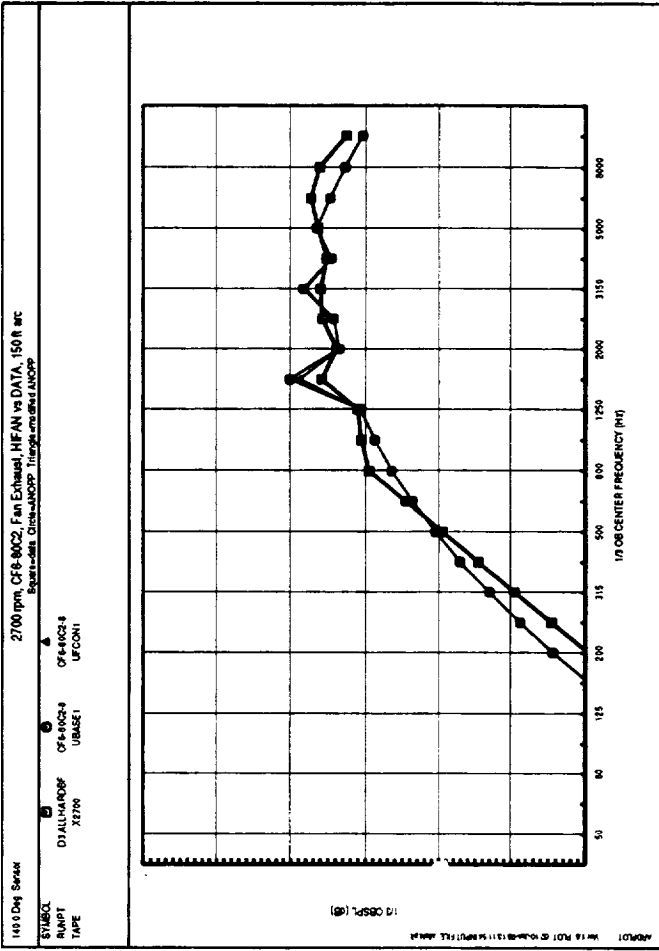
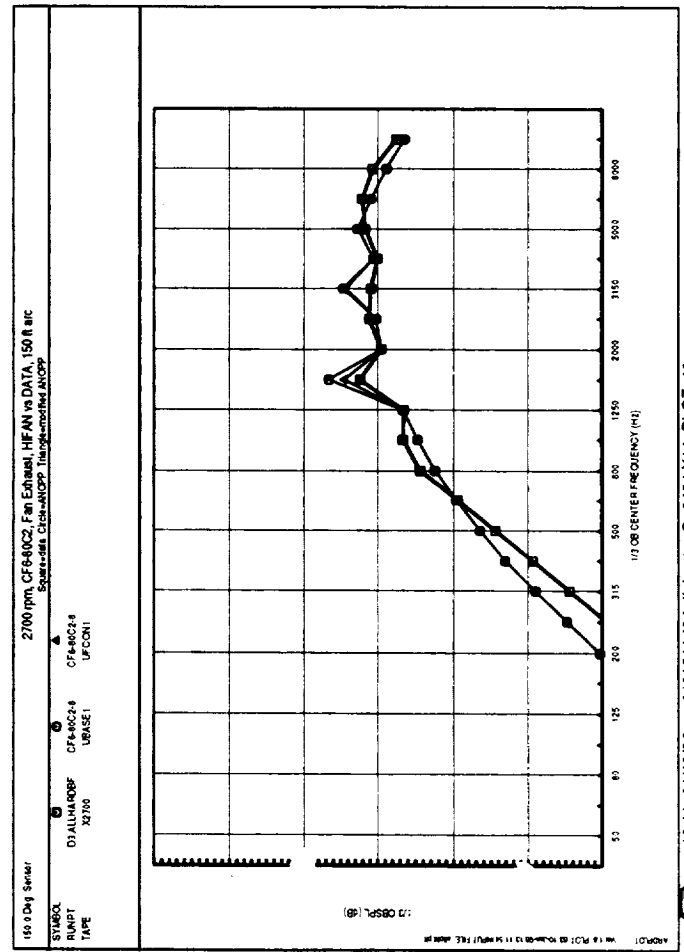
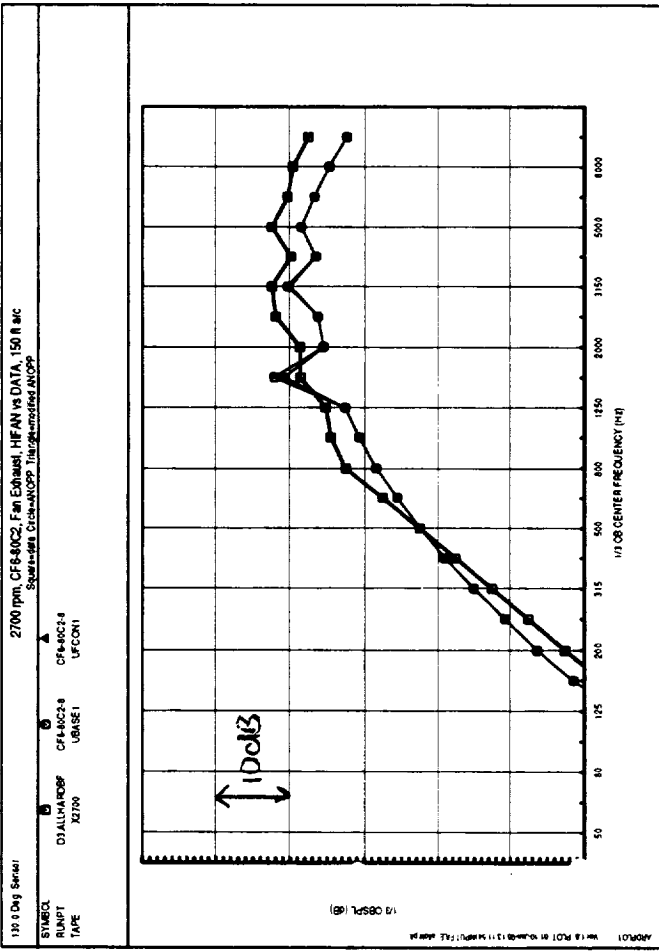


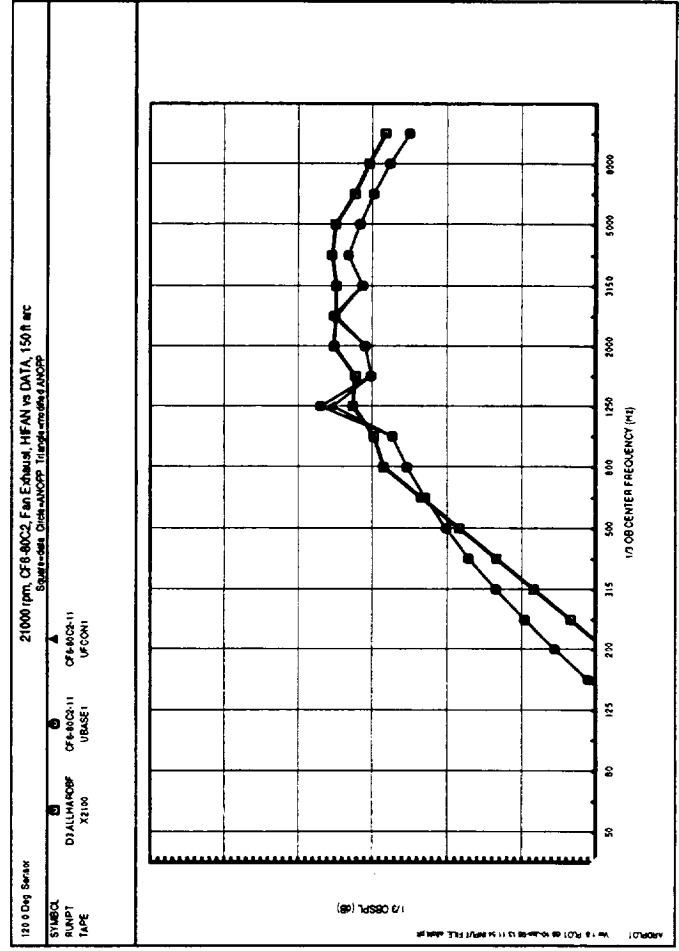
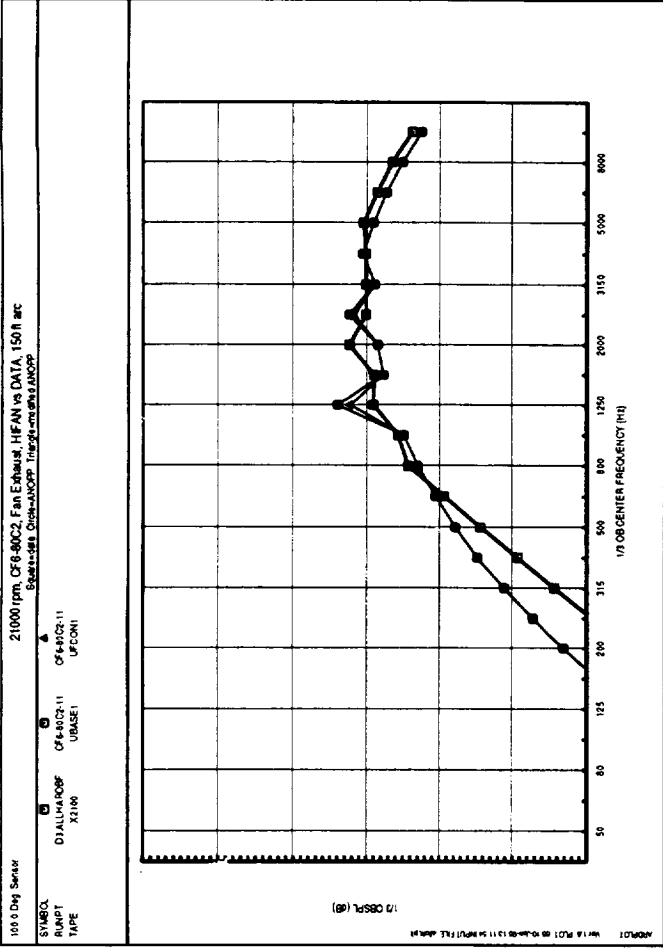
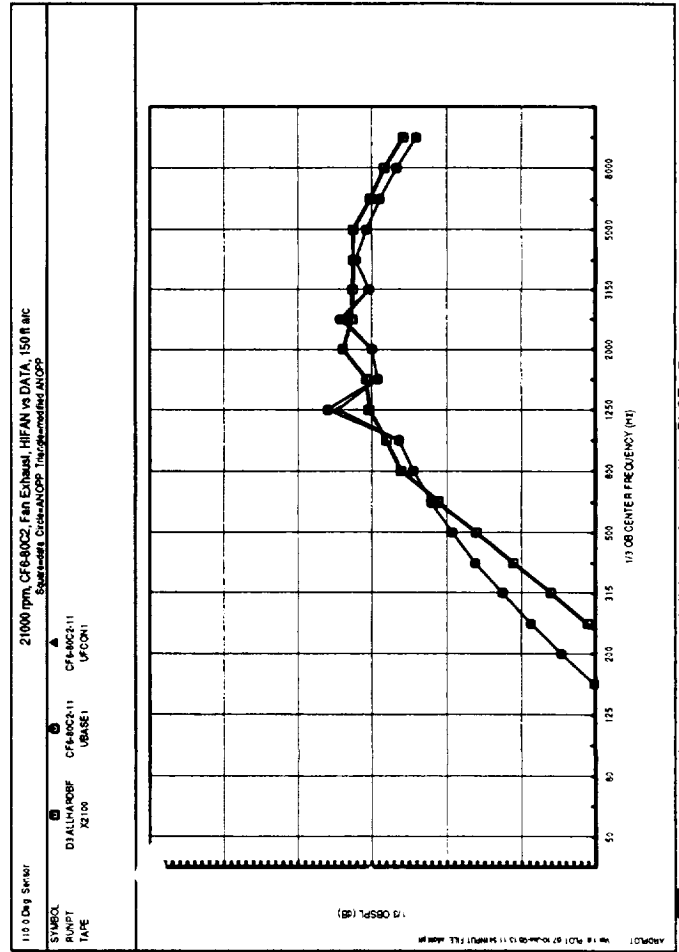
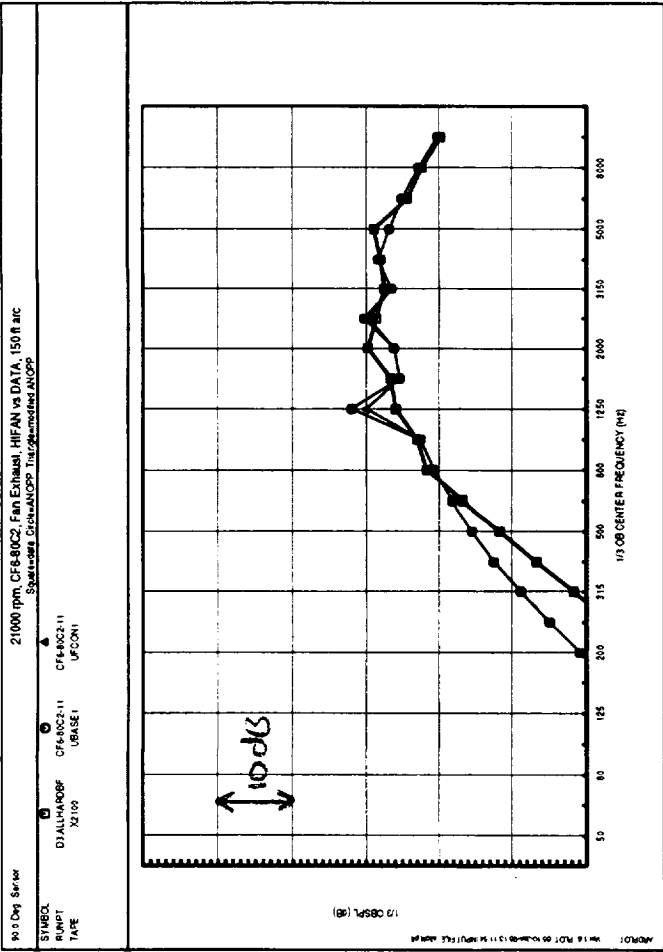


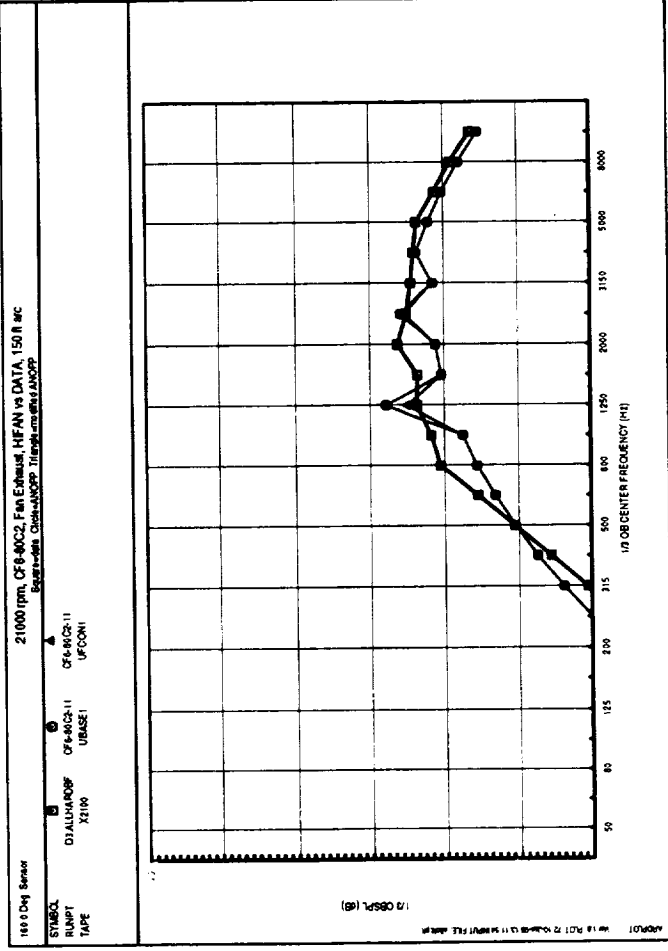
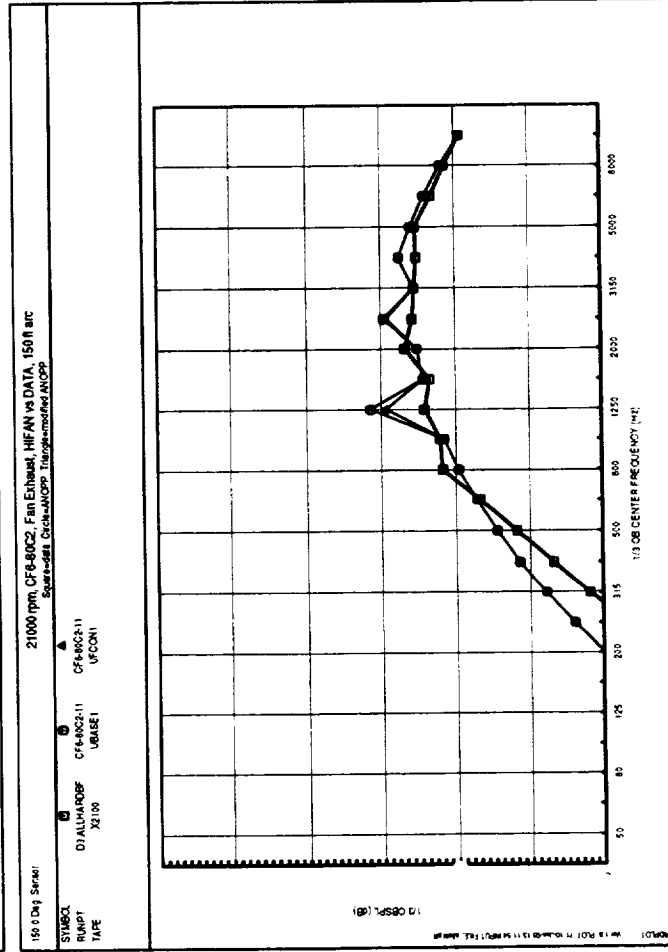
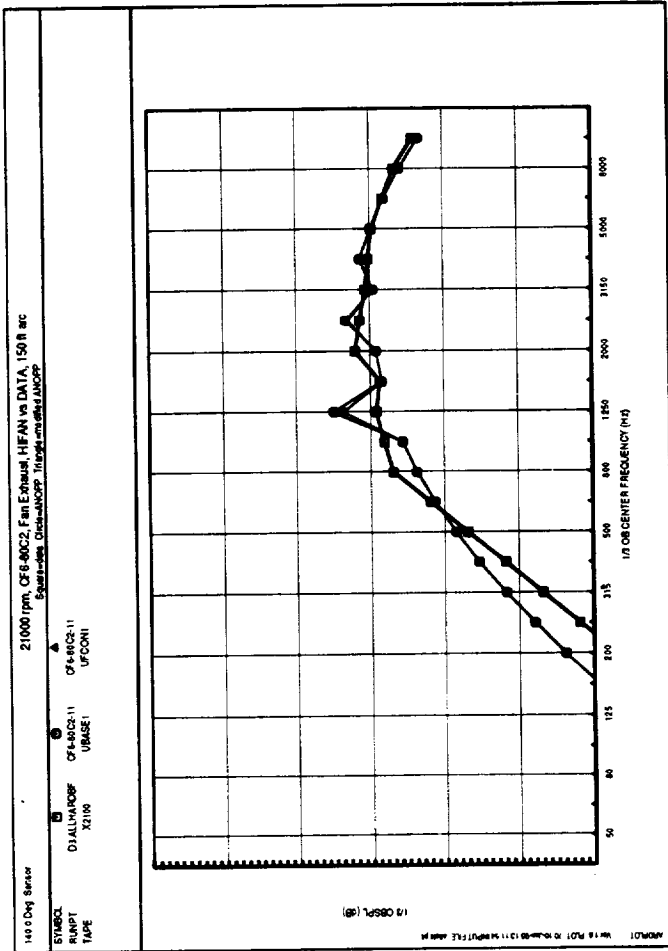
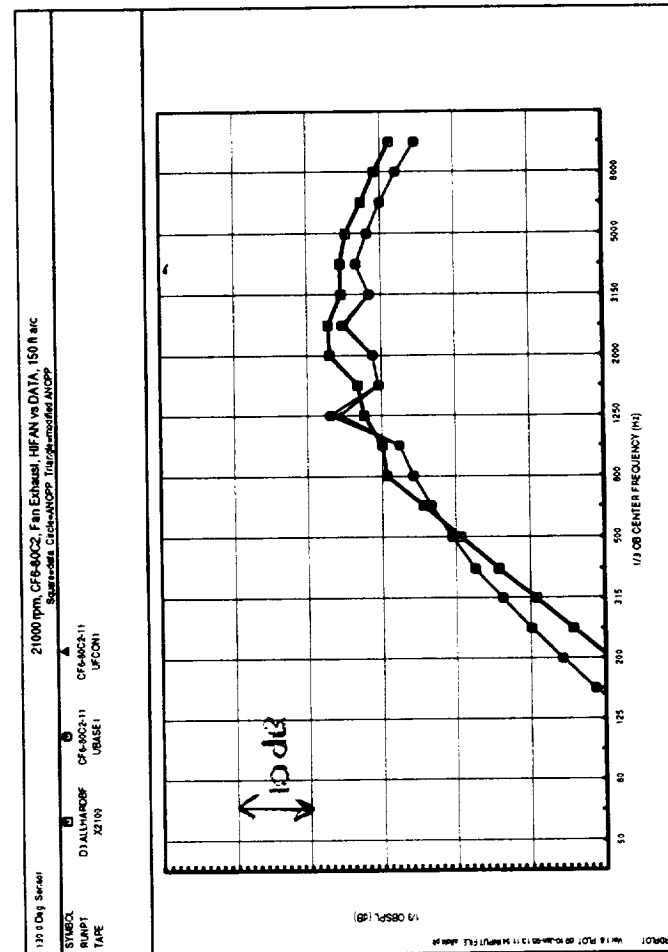






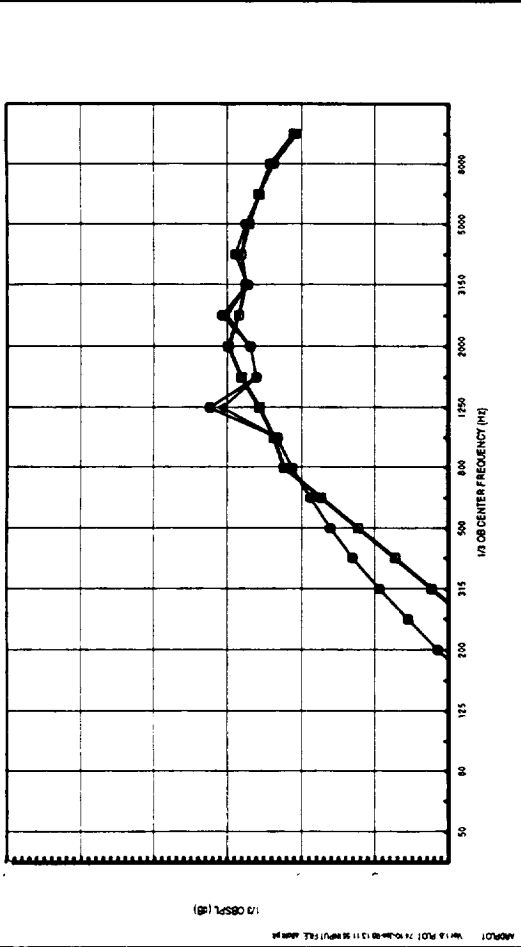






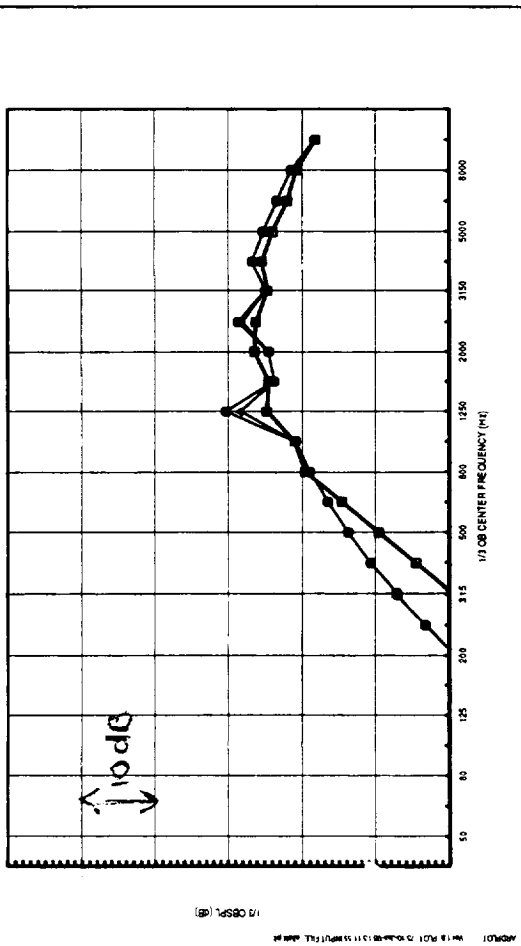
1950 rpm, CF6-90C2, Fan Exhaust, HFAN vs DATA, 150 ft ac
 Square-data Circle-X1950 Triangle-unmodified ANOPP

1000 Day Sensor
 SYMBOL DIALUMHROBF CF6-90C2-12 CF6-90C2-12
 RANPT X1950 UBASE1 UFCOM1
 TAPE



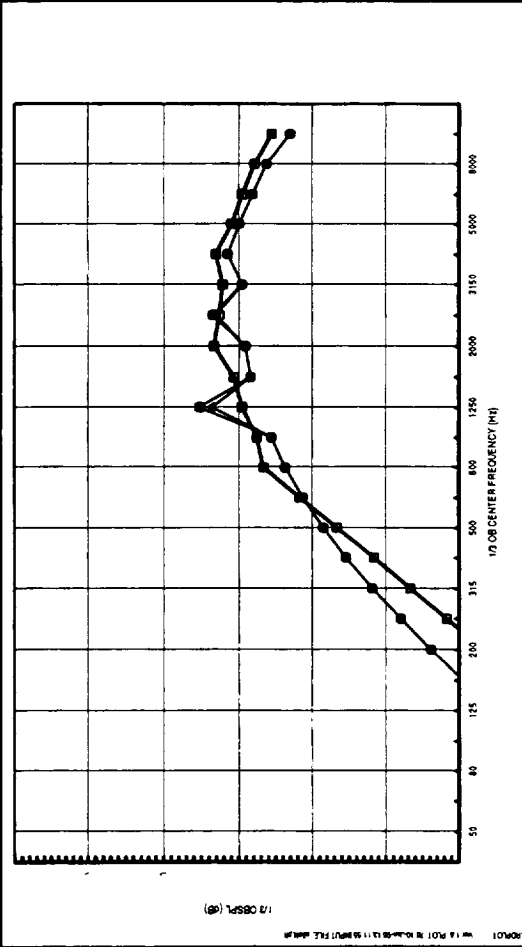
1950 rpm, CF6-90C2, Fan Exhaust, HFAN vs DATA, 150 ft ac
 Square-data Circle-X1950 Triangle-unmodified ANOPP

900 Day Sensor
 SYMBOL DIALUMHROBF CF6-90C2-12 CF6-90C2-12
 RANPT X1950 UBASE1 UFCOM1
 TAPE



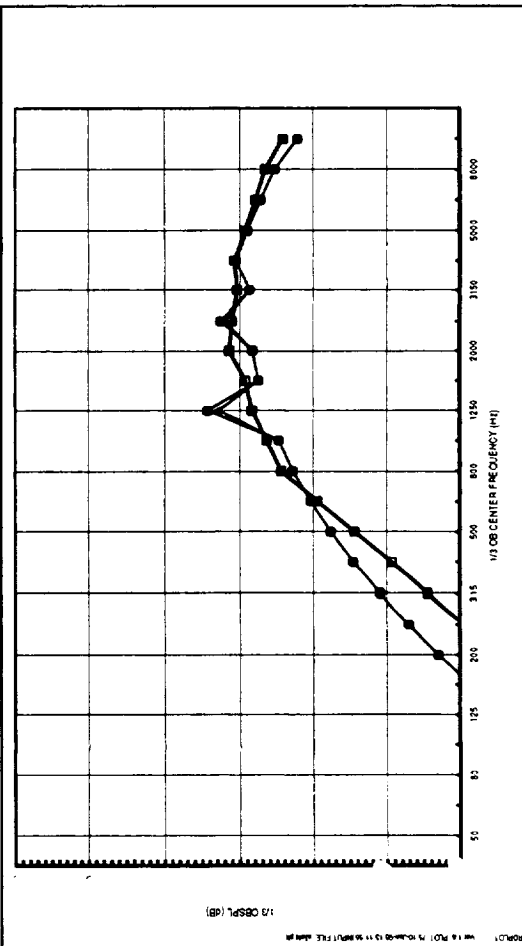
1950 rpm, CF6-90C2, Fan Exhaust, HFAN vs DATA, 150 ft ac
 Square-data Circle-X1950 Triangle-unmodified ANOPP

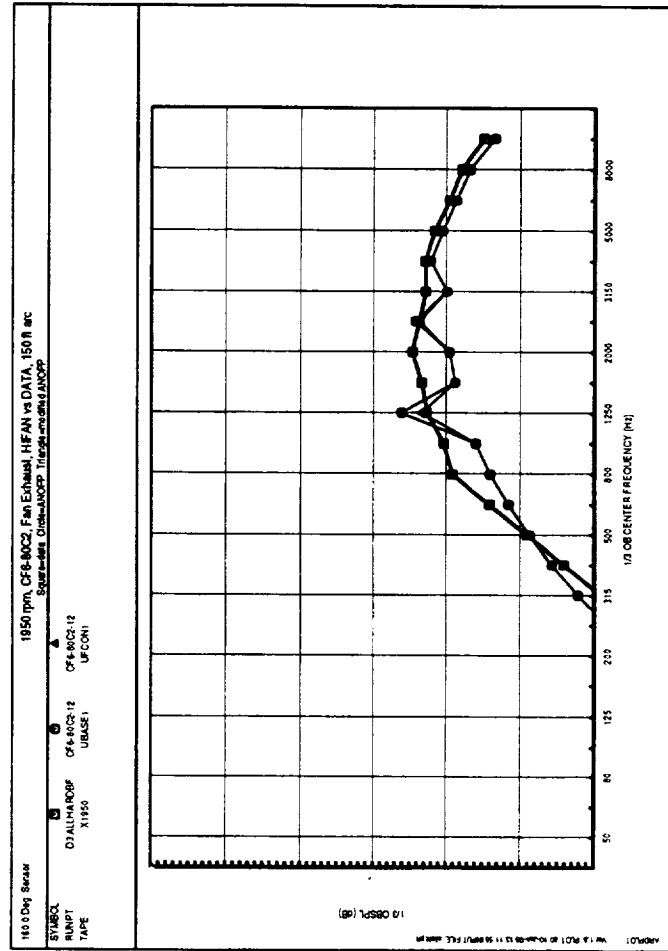
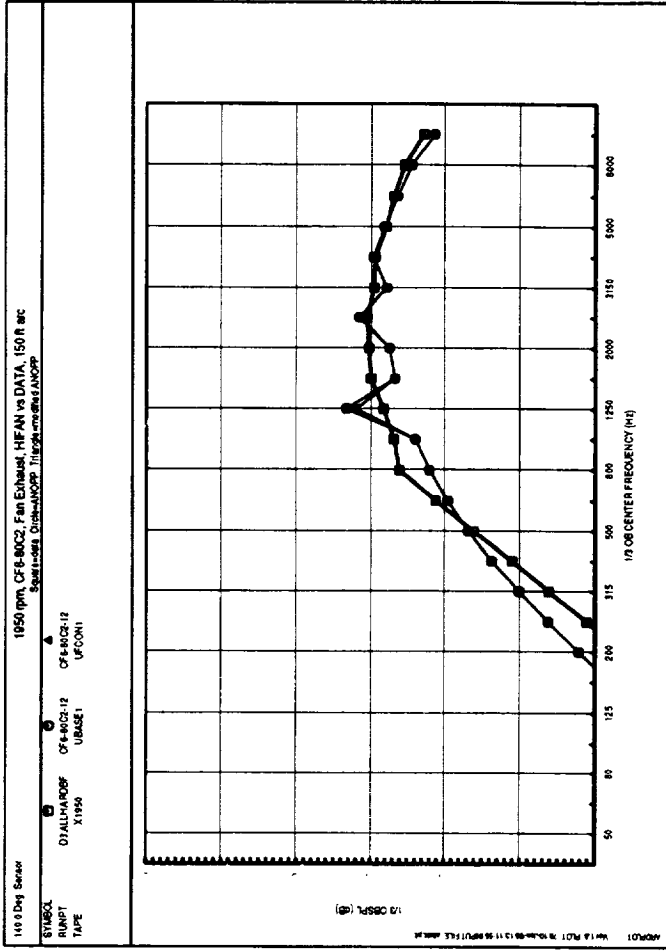
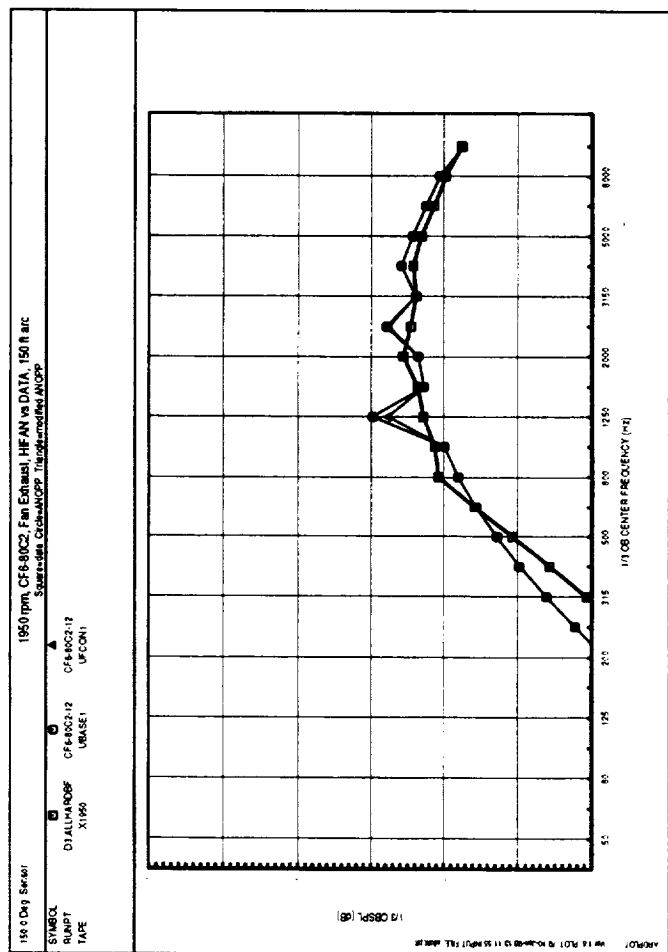
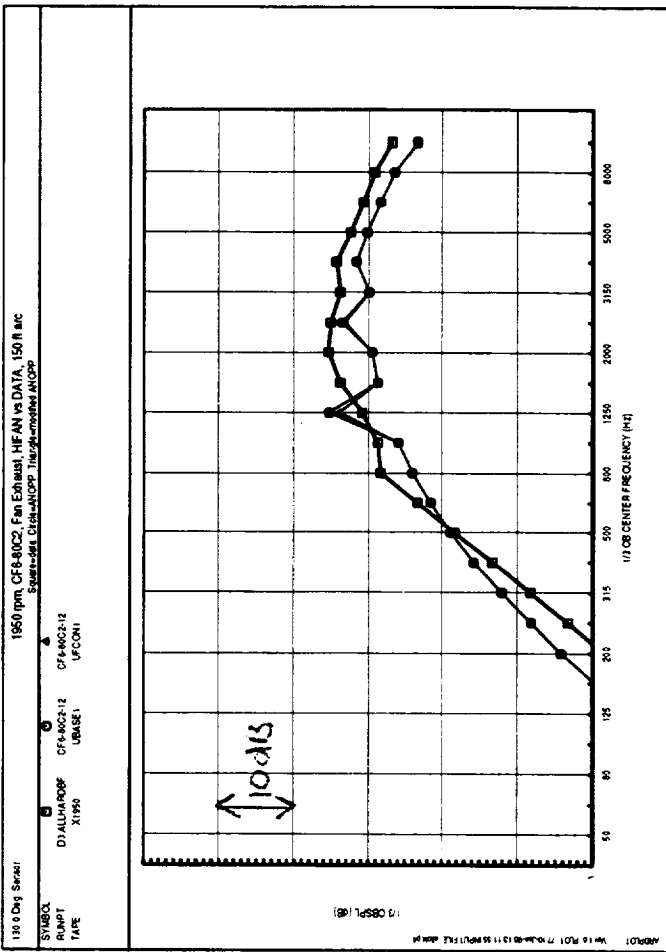
1000 Day Sensor
 SYMBOL DIALUMHROBF CF6-90C2-12 CF6-90C2-12
 RANPT X1950 UBASE1 UFCOM1
 TAPE

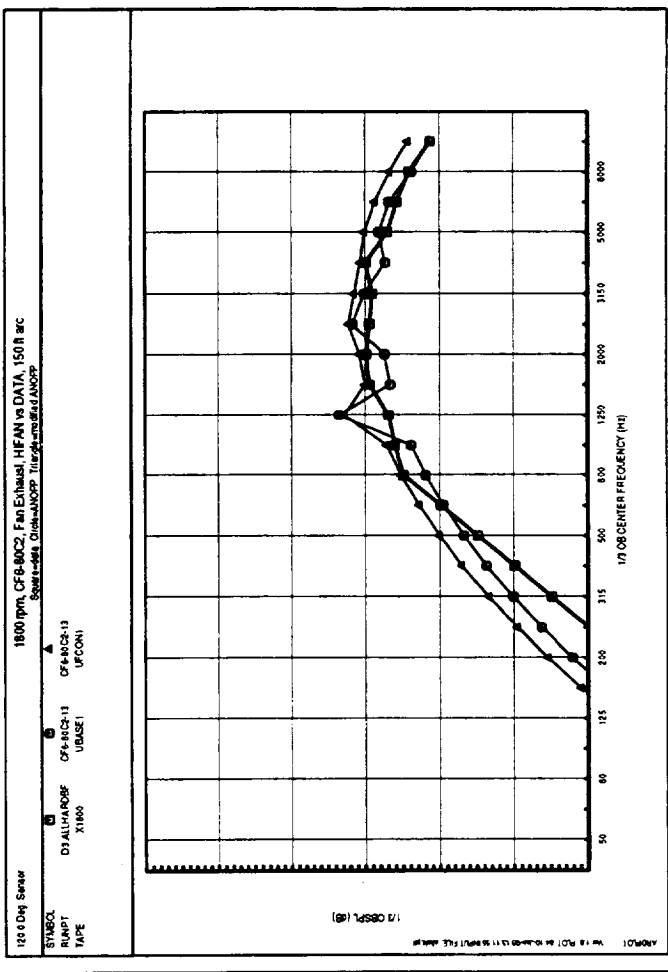
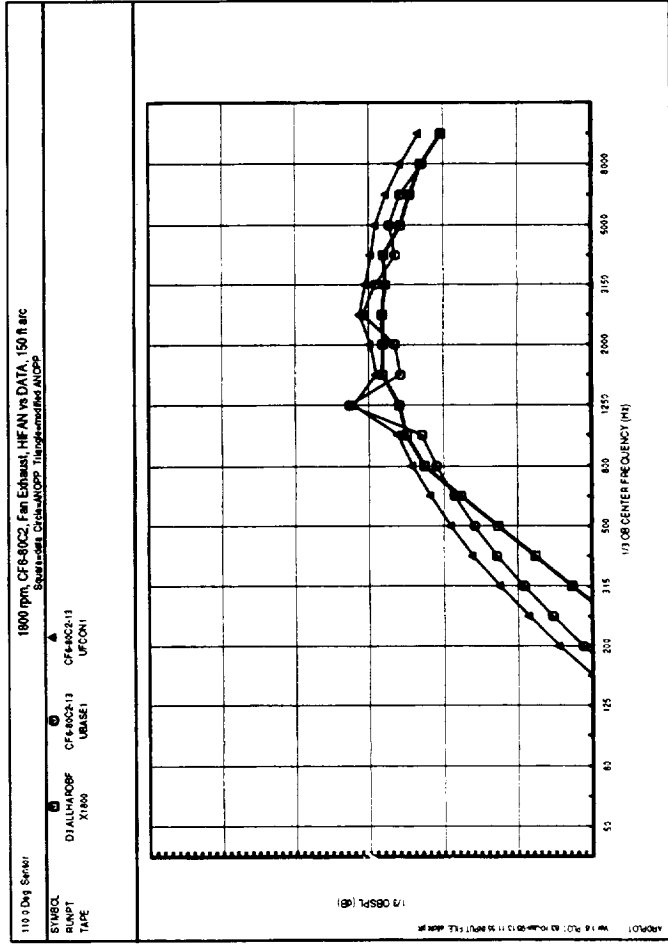
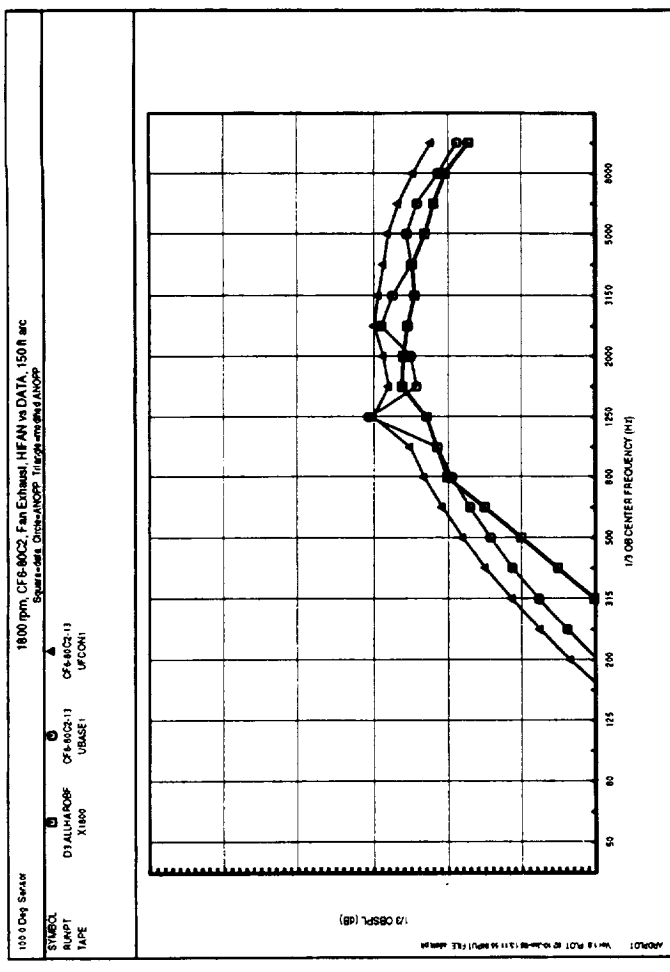
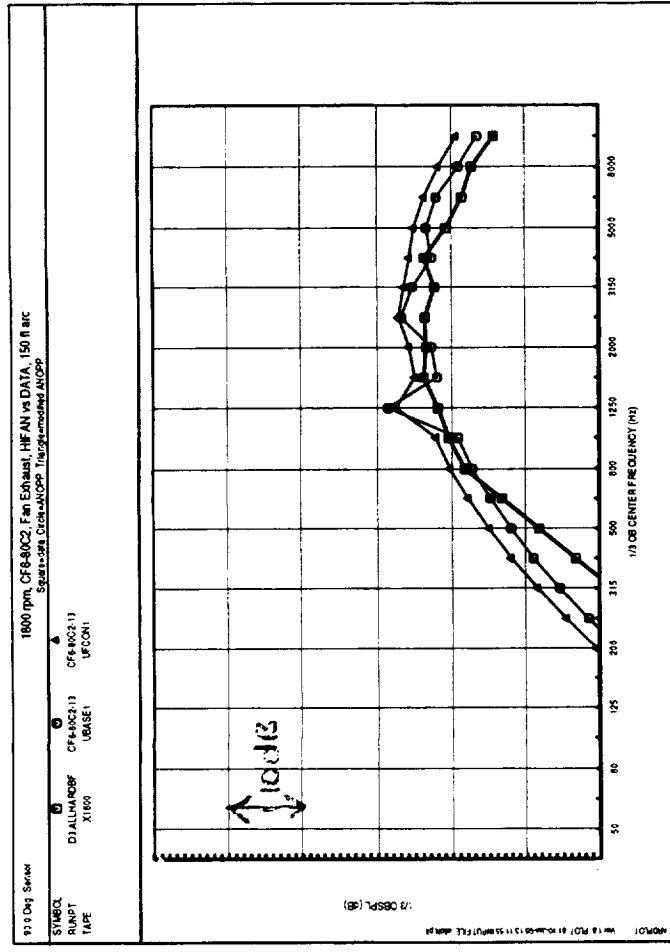


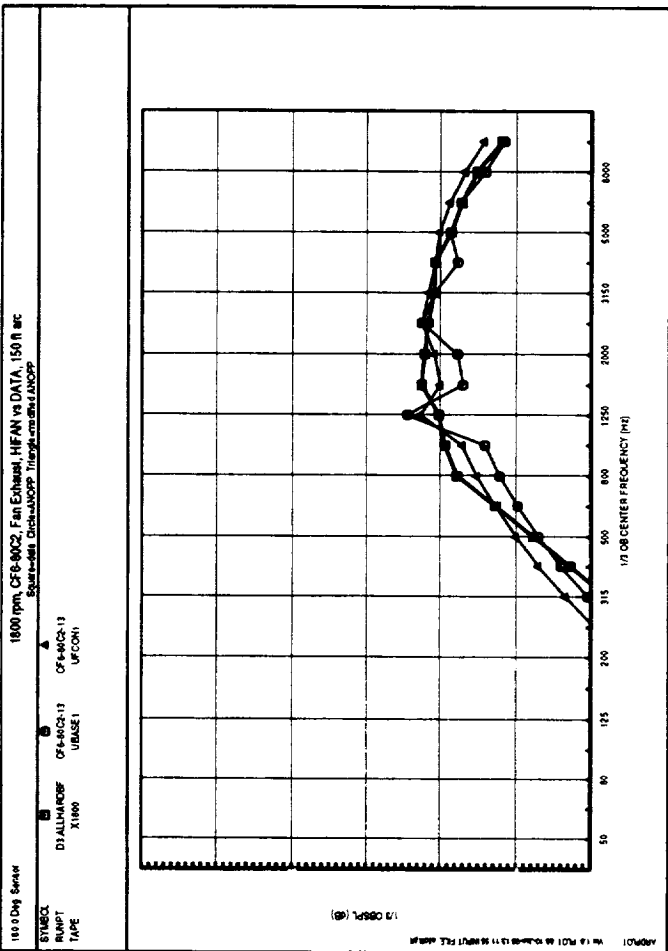
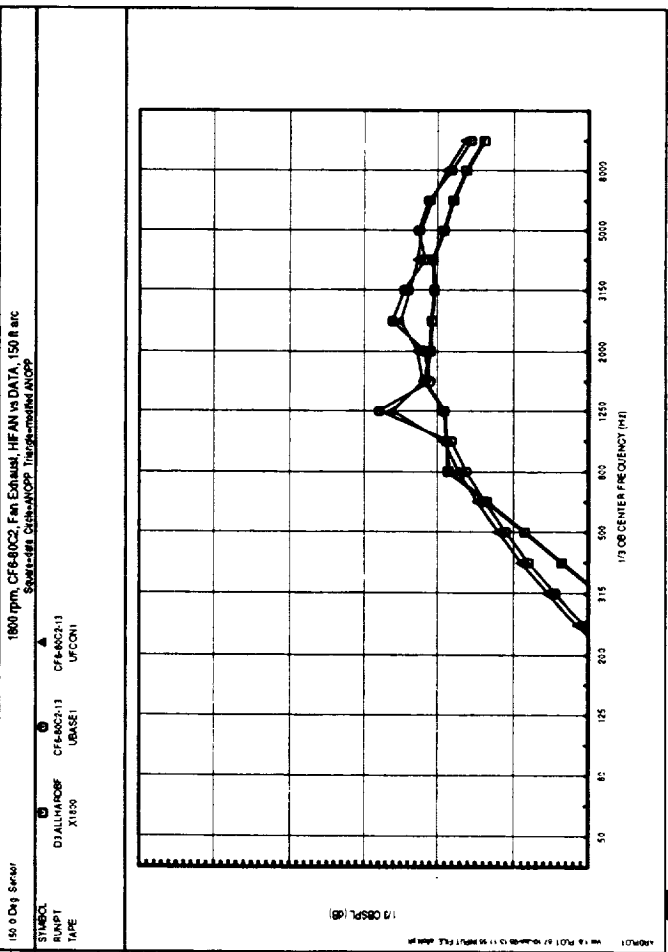
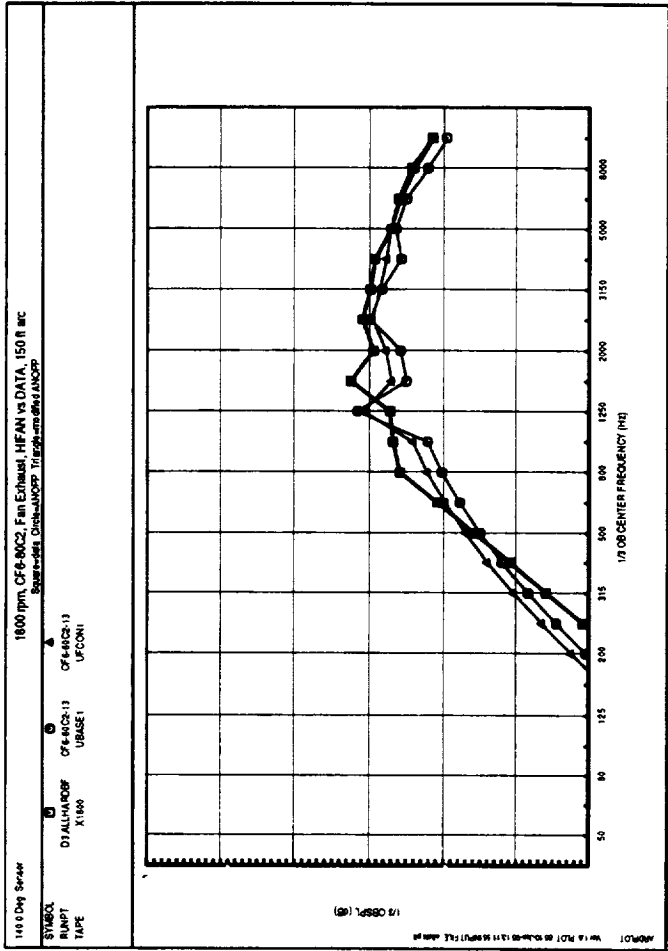
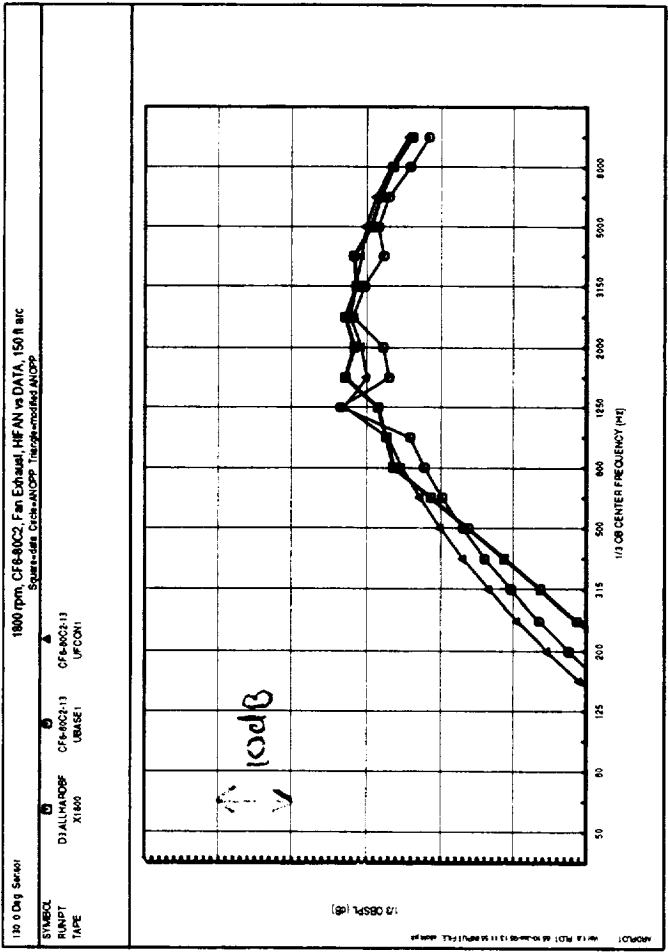
1950 rpm, CF6-90C2, Fan Exhaust, HFAN vs DATA, 150 ft ac
 Square-data Circle-X1950 Triangle-unmodified ANOPP

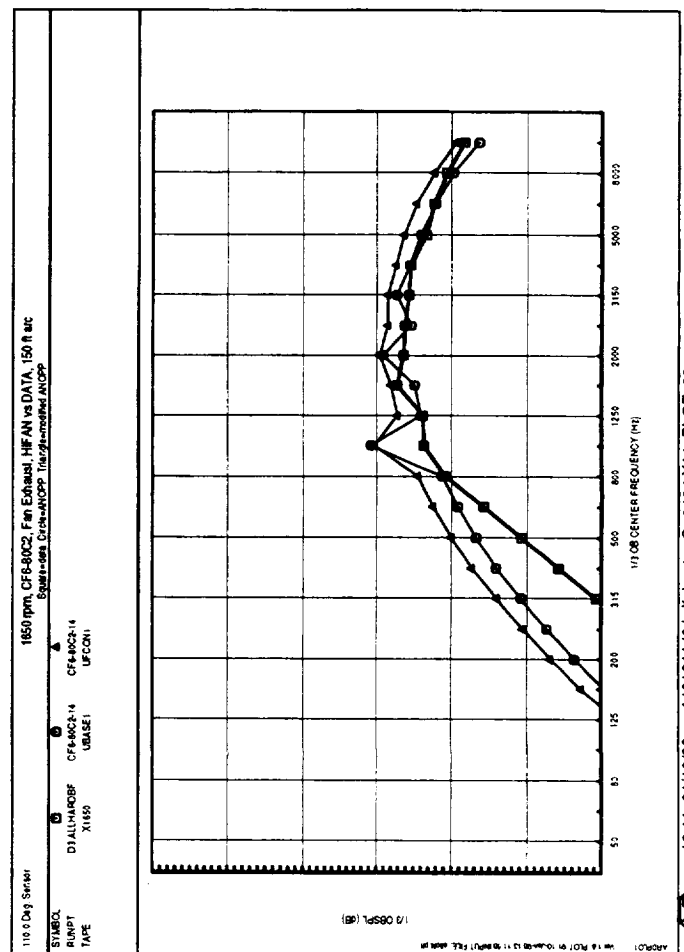
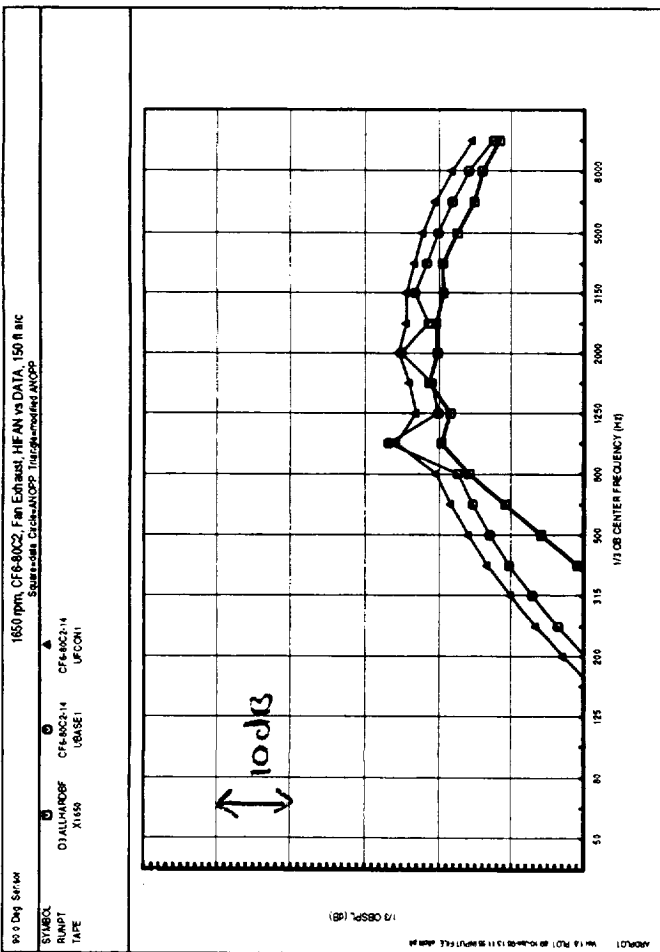
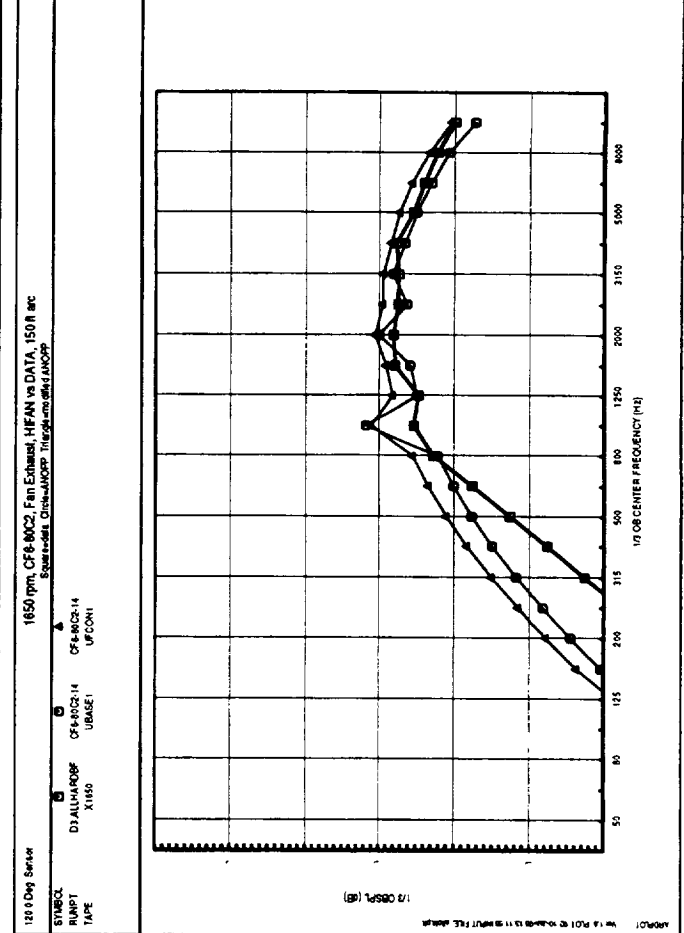
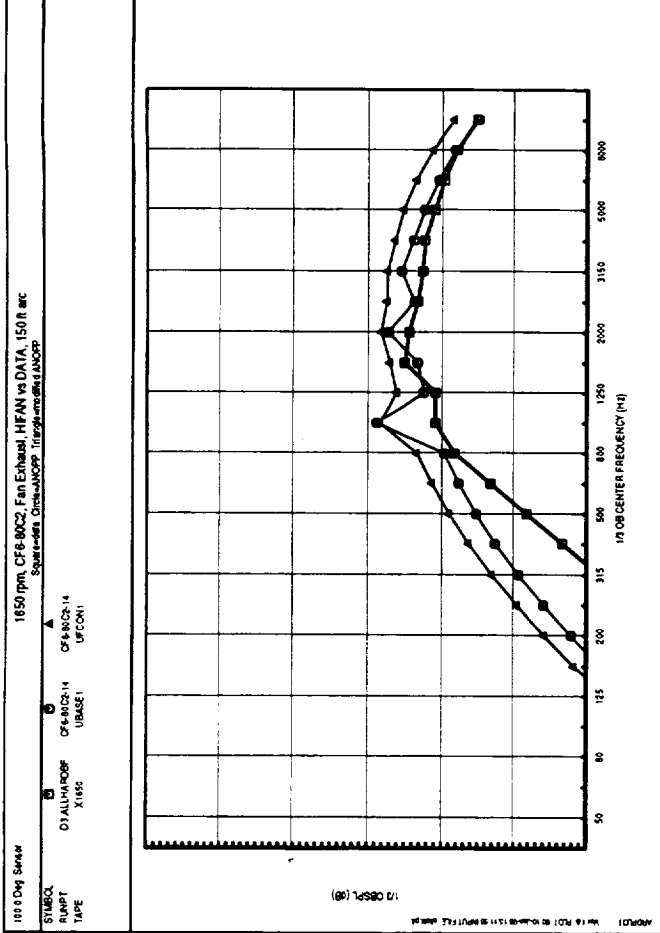
1100 Day Sensor
 SYMBOL DIALUMHROBF CF6-90C2-12 CF6-90C2-12
 RANPT X1950 UBASE1 UFCOM1
 TAPE

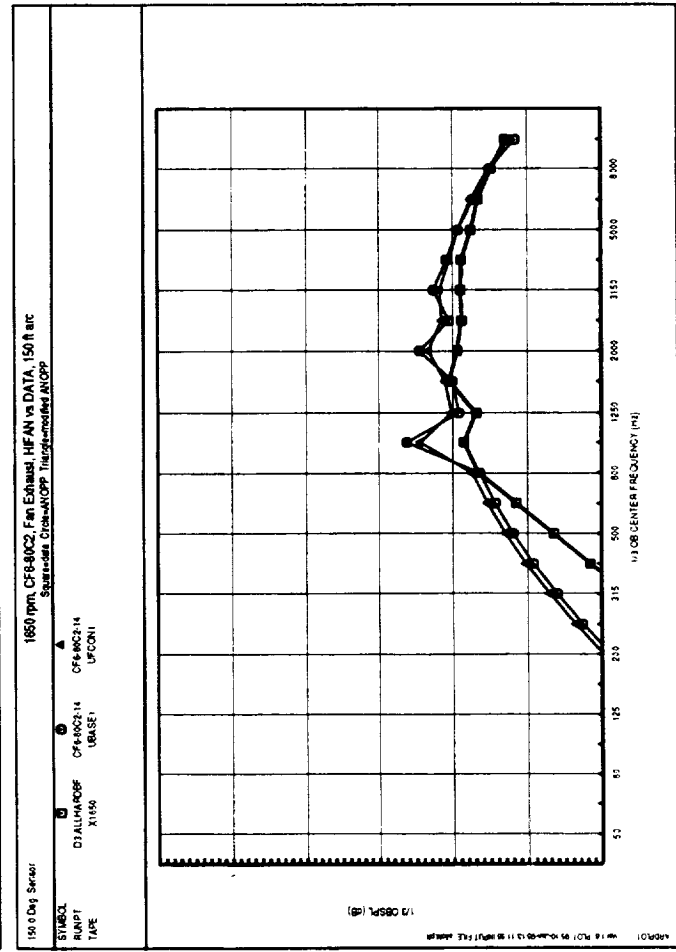
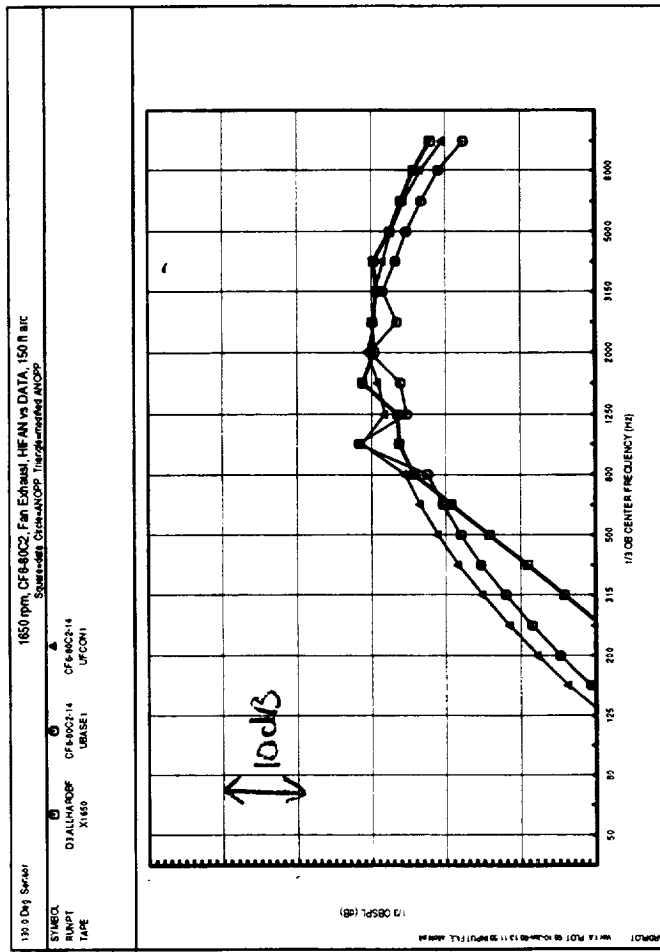
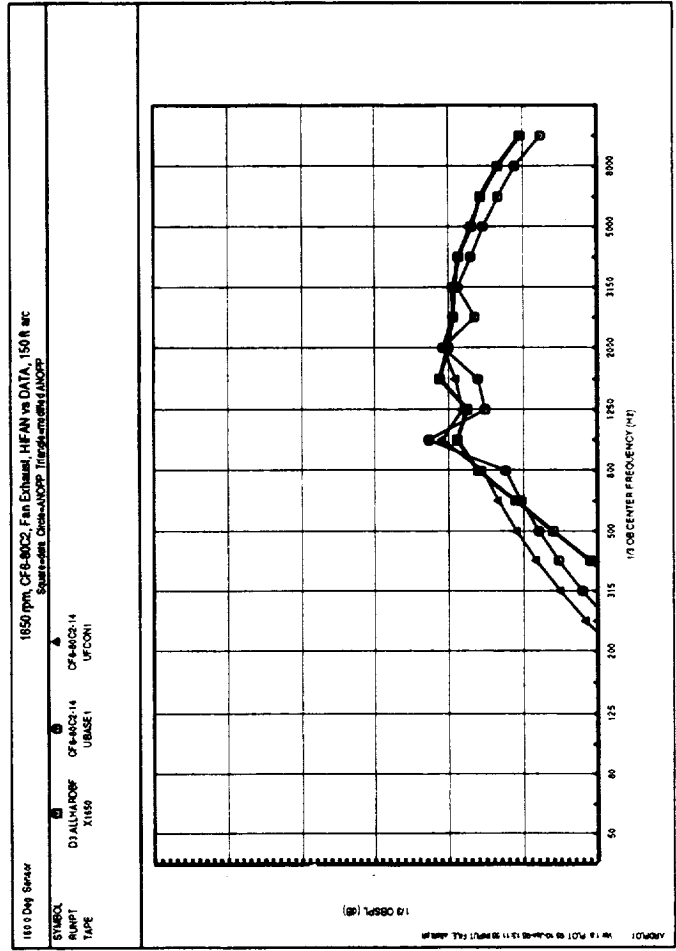
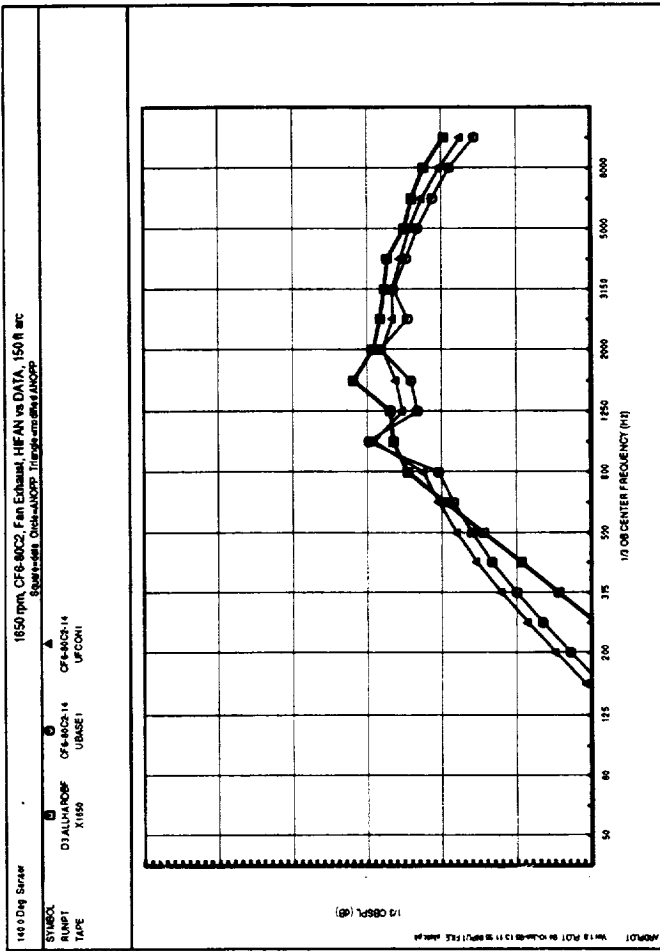












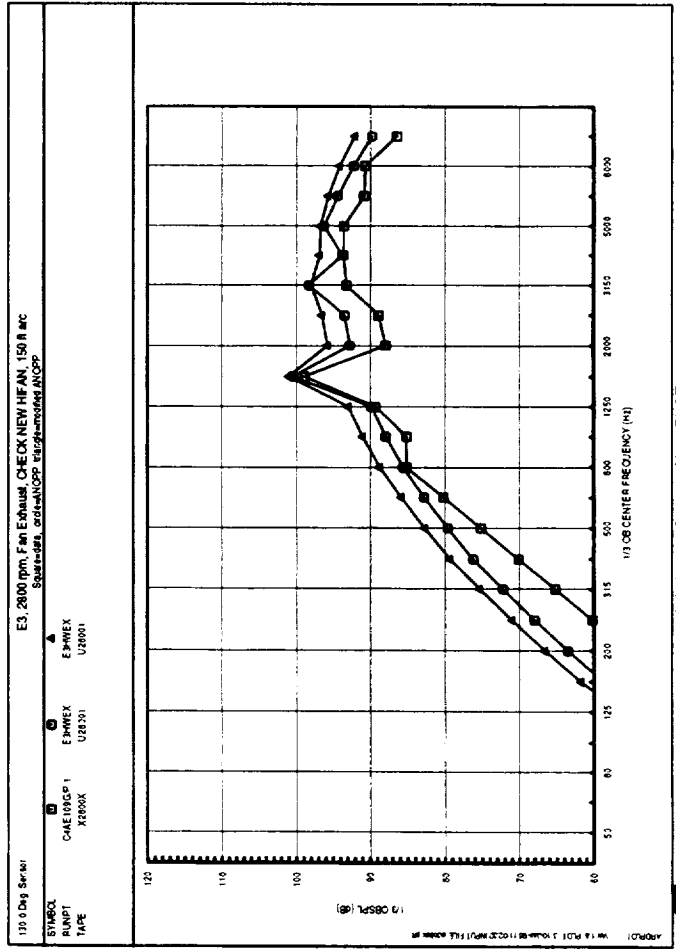
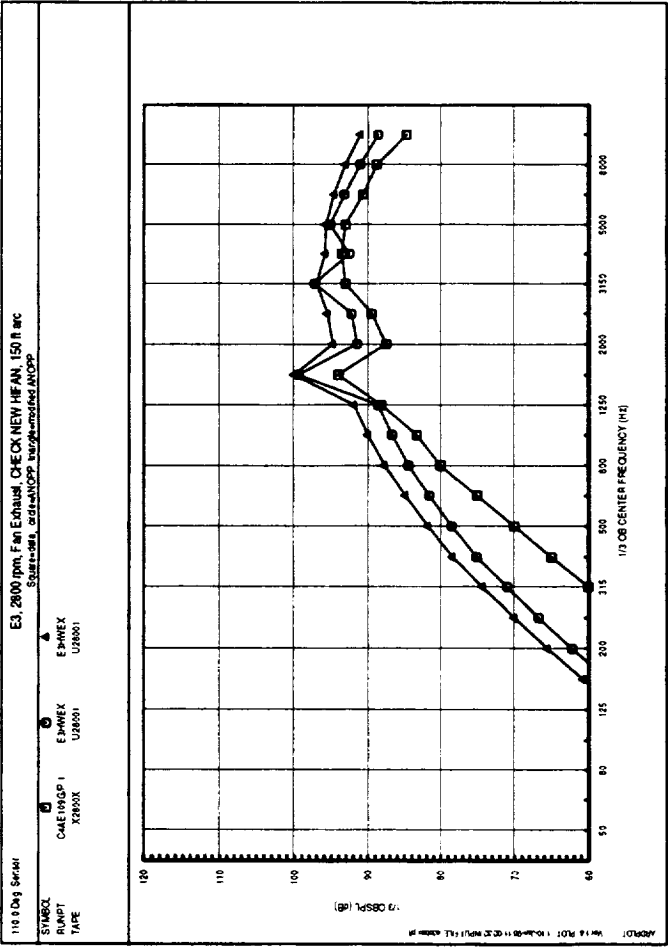
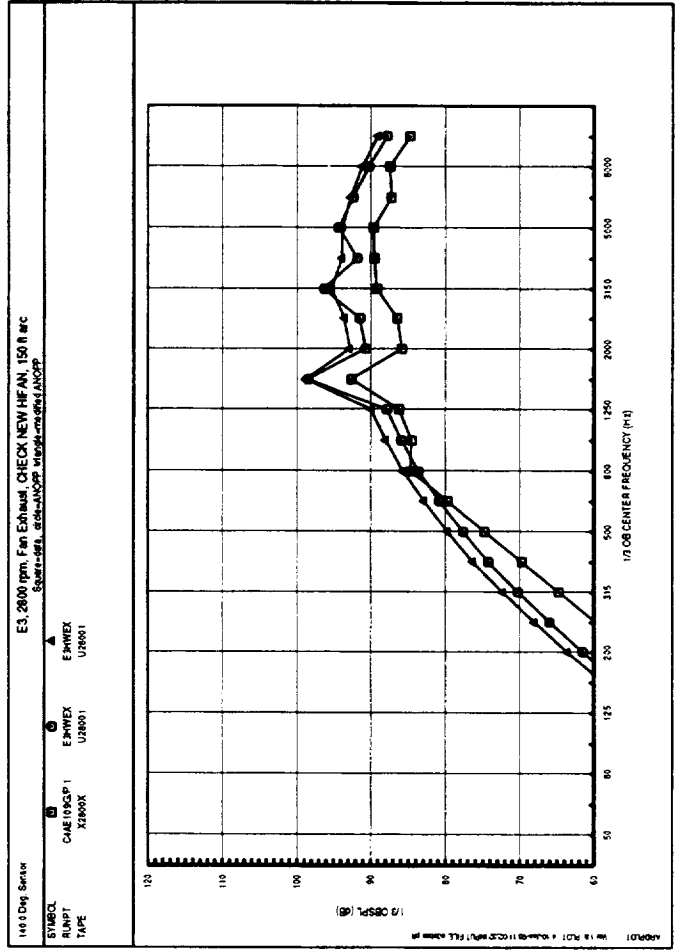
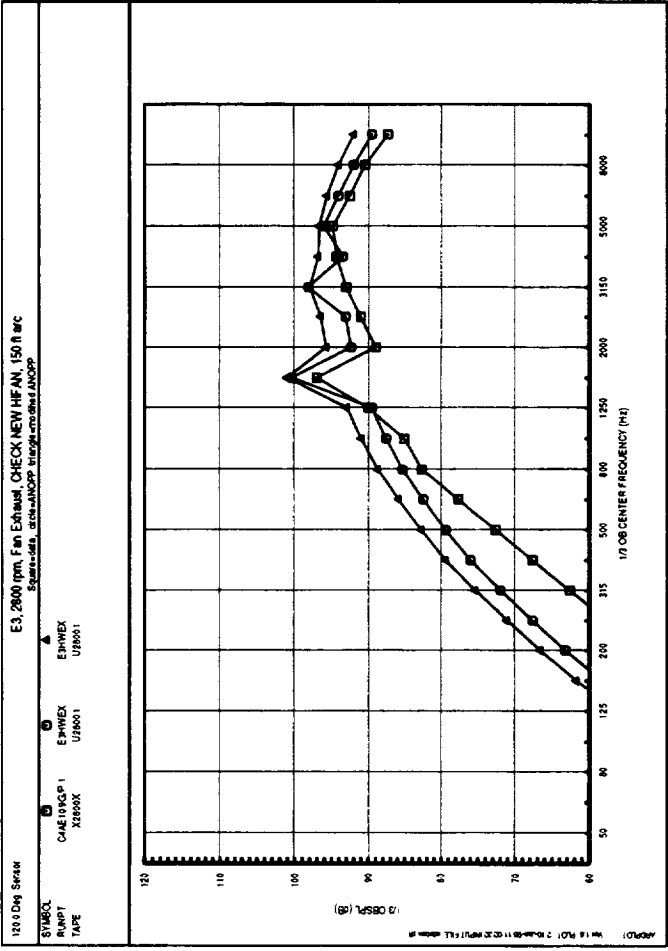
Appendix F
Fan Exhaust Noise Spectral Comparisons - E³

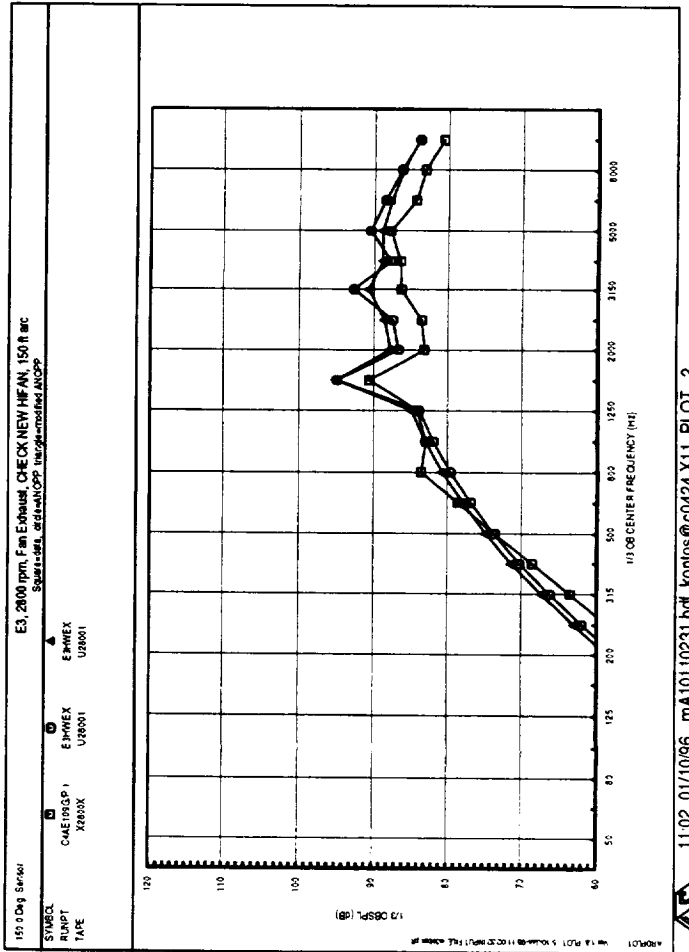
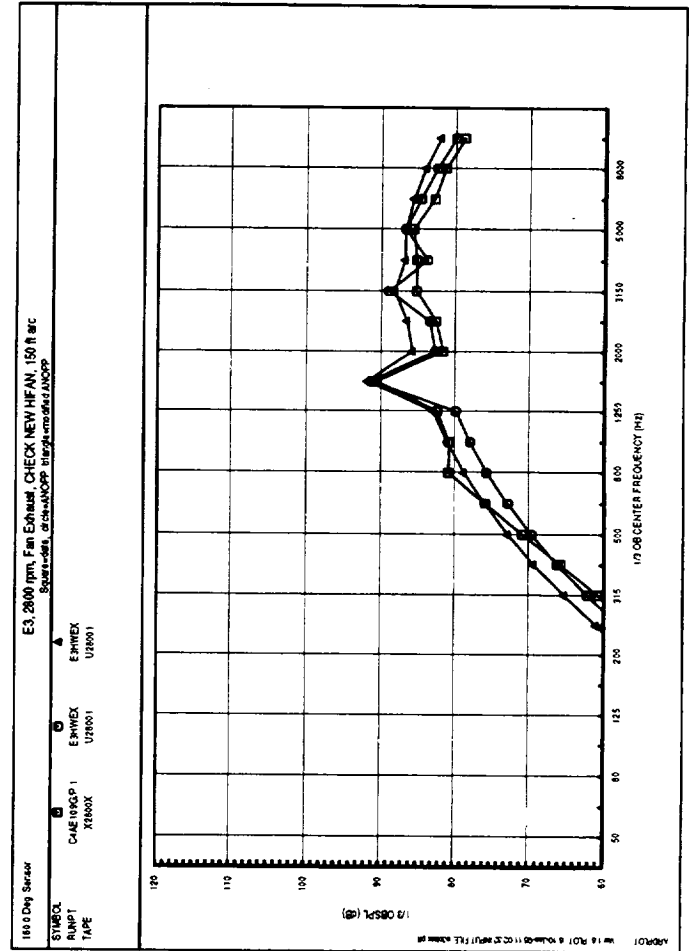
Appendix F Contents

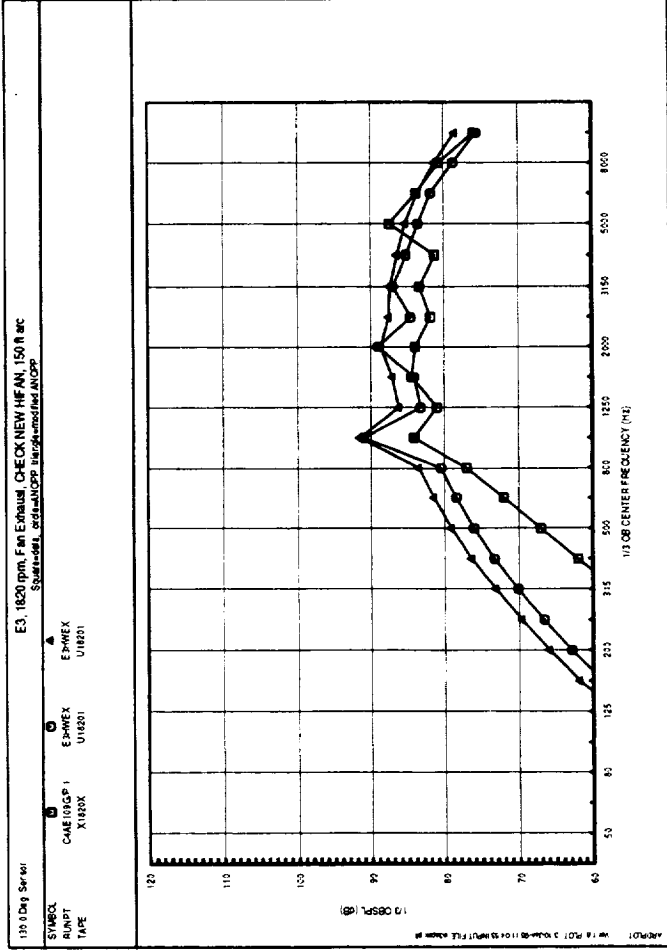
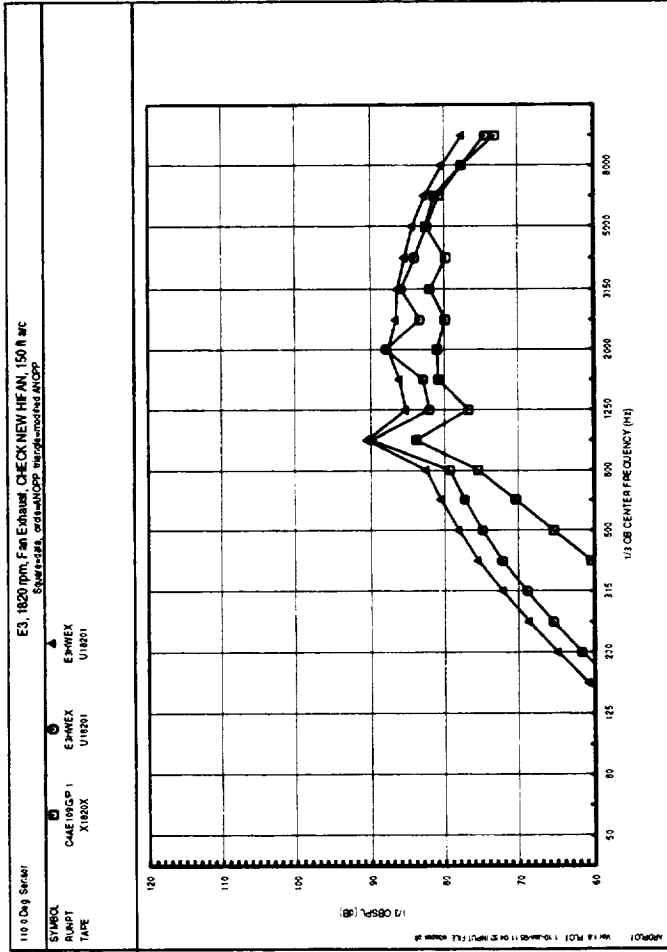
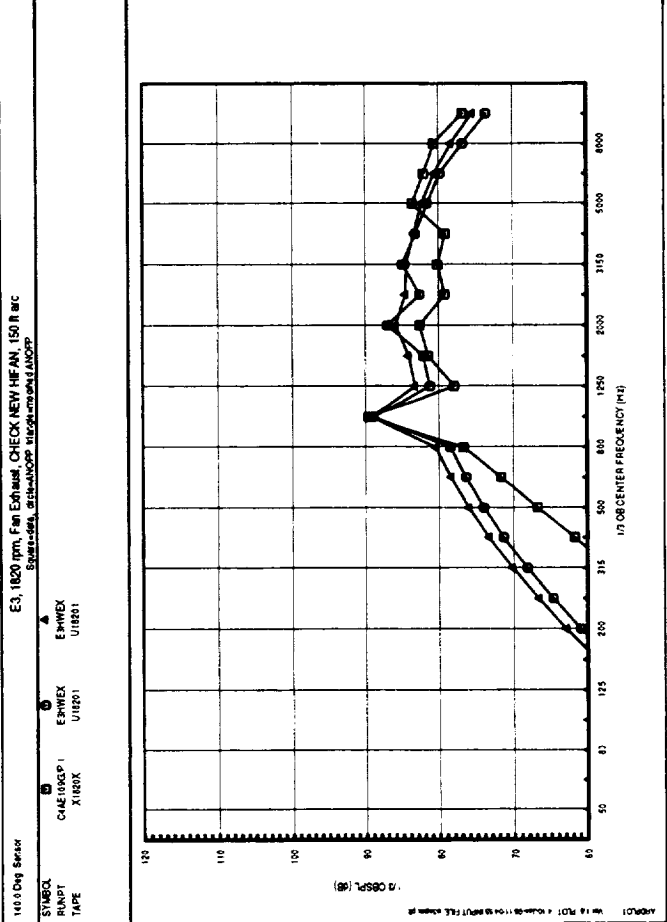
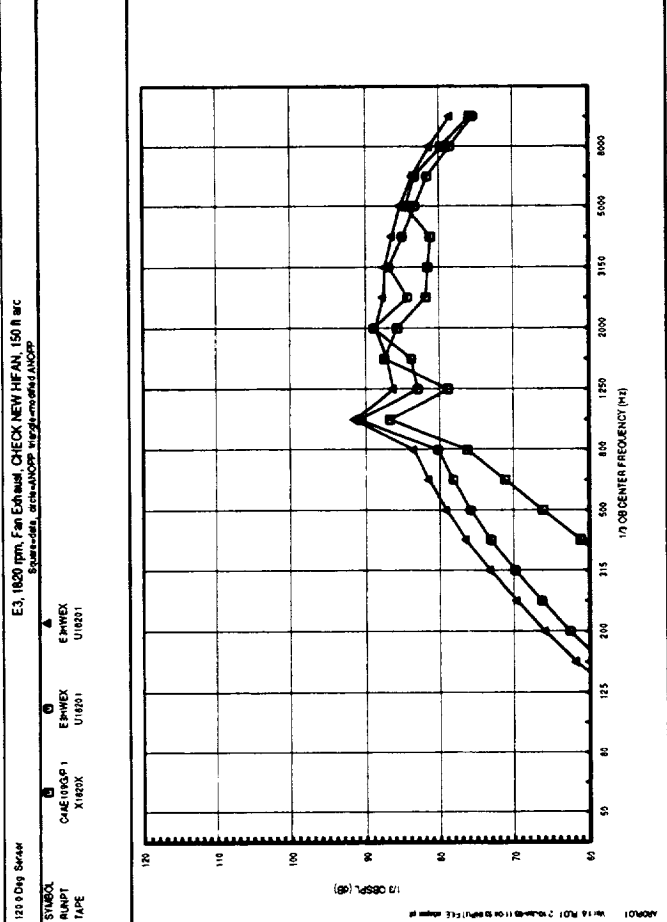
Page	Fan Speed, rpm	Angles, deg
103	3100 (takeoff)	110-140
104	3100 (takeoff)	150-160
105	2800 (cutback)	110-140
106	2800 (cutback)	150-160
107	1820 (approach)	110-140
108	1820 (approach)	150-160

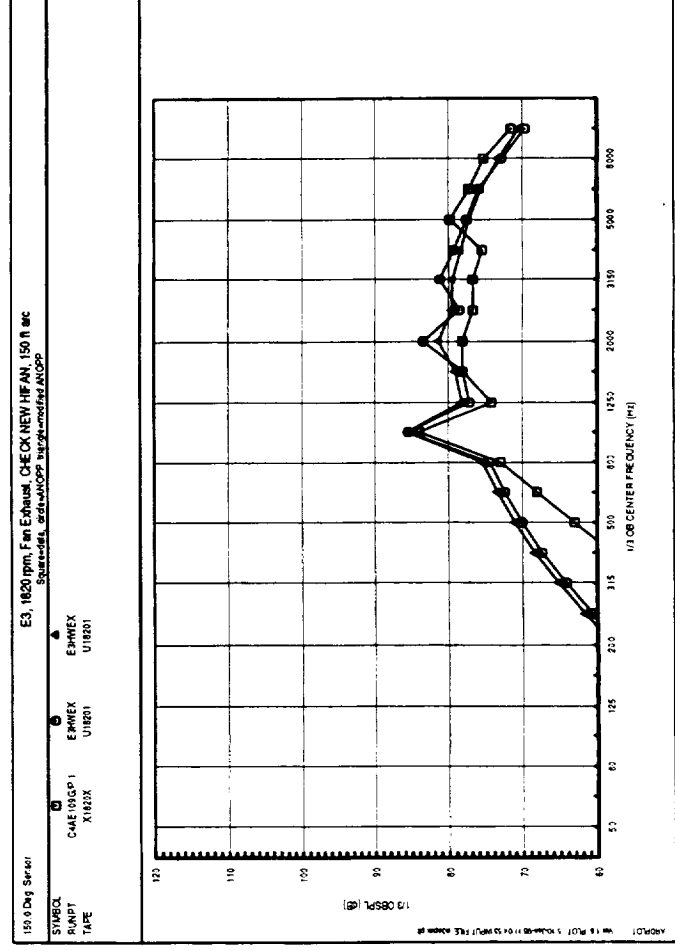
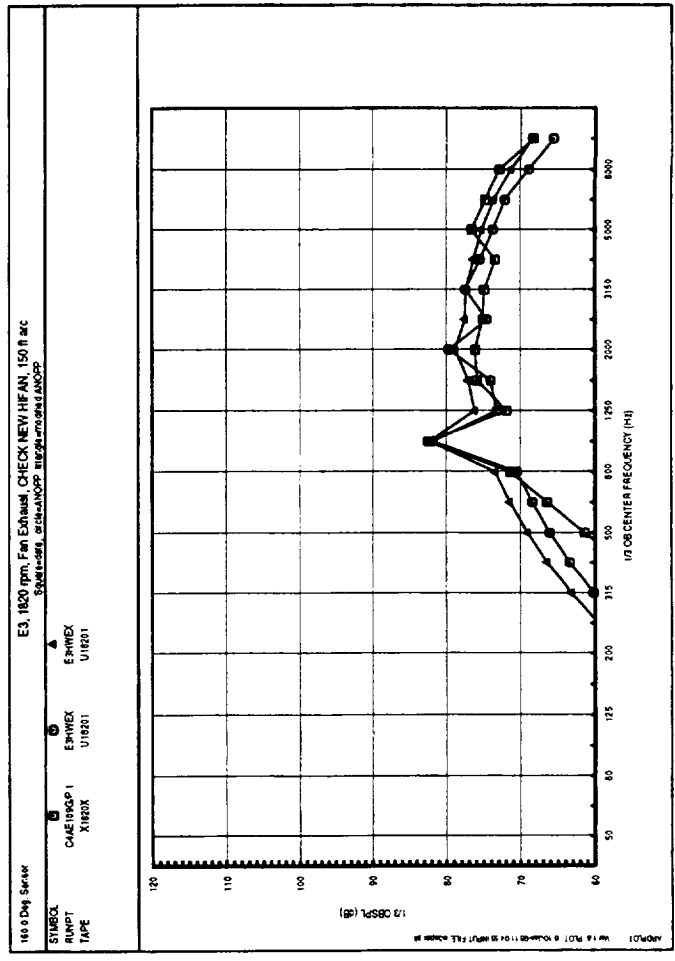
Key to Plots:

- squares = total measured engine data
- circles = Heidmann method prediction
- triangles = modified Heidmann method prediction (see Section 4)









11.04.01/10/95 MA10110452.bcf konlos@c0424.X11 PLOT 2
 EGS LIB 5.1.12/14/95 LECSREP.XPOST 5.1.12/14/95 on c0424
 (NO PROG. VER. SPECIFIED)



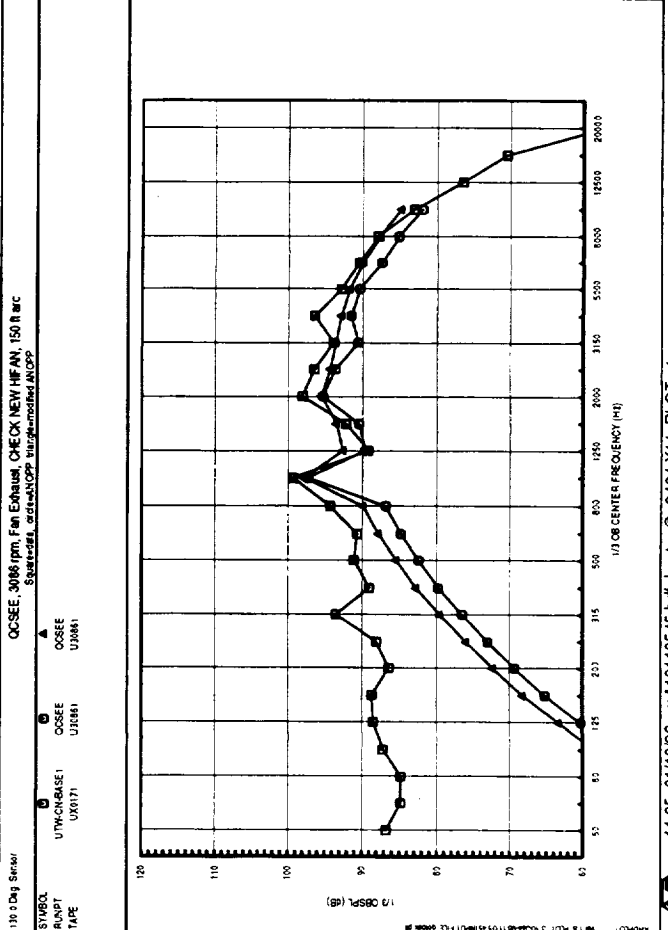
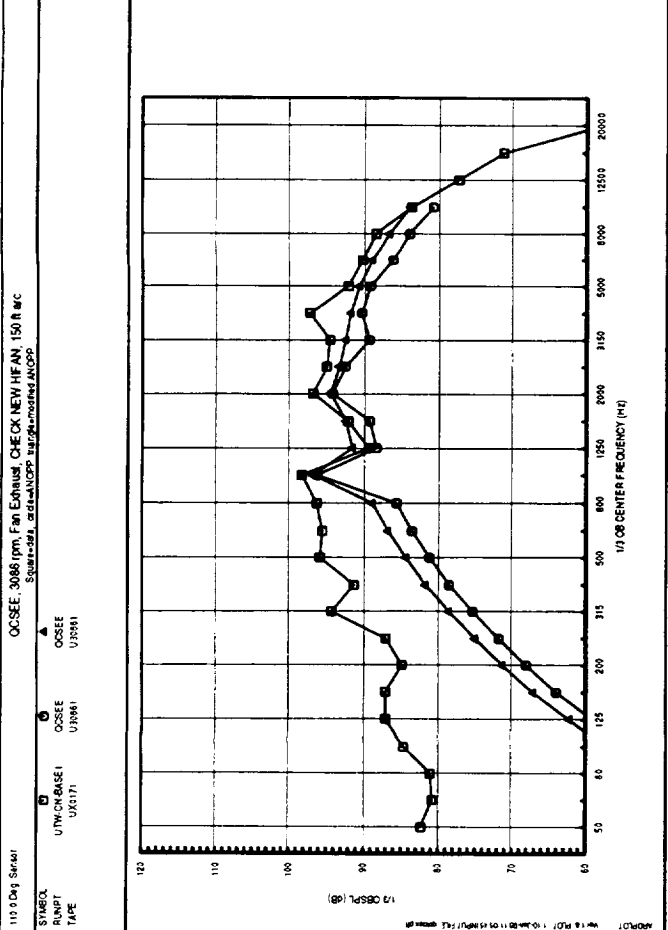
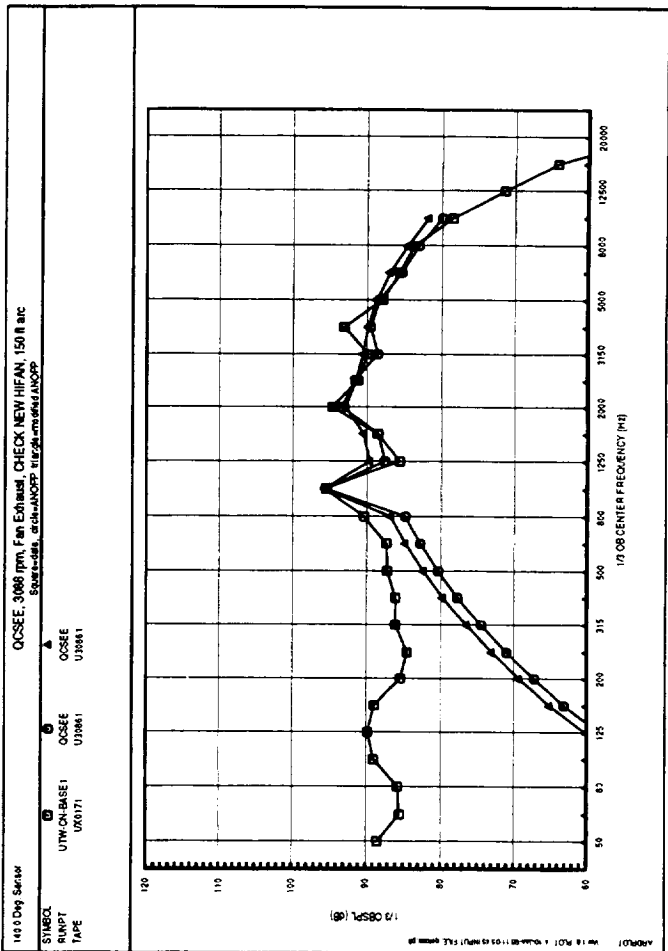
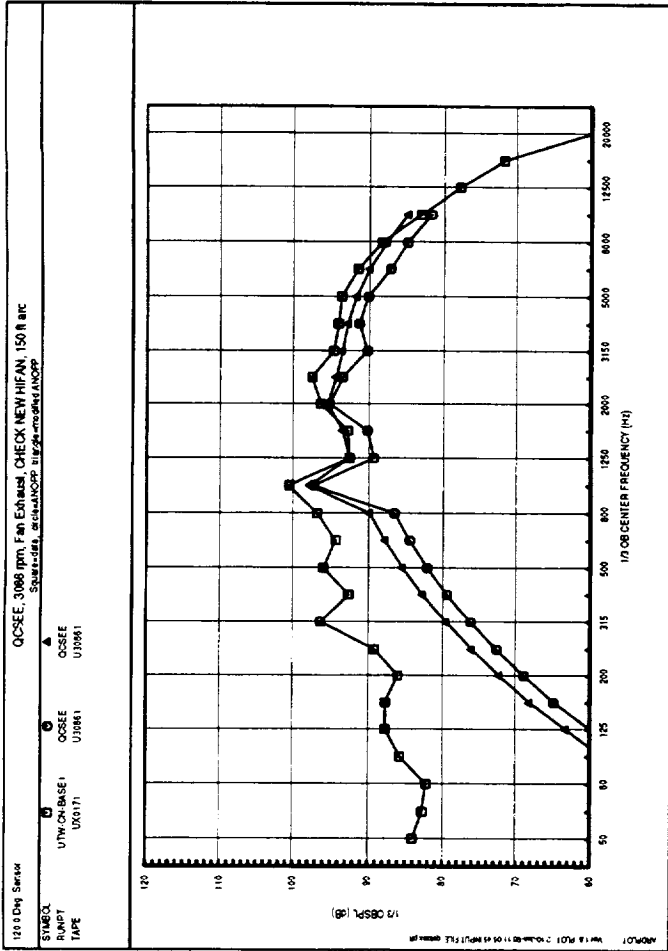
Appendix G
Fan Exhaust Noise Spectral Comparisons - QCSEE

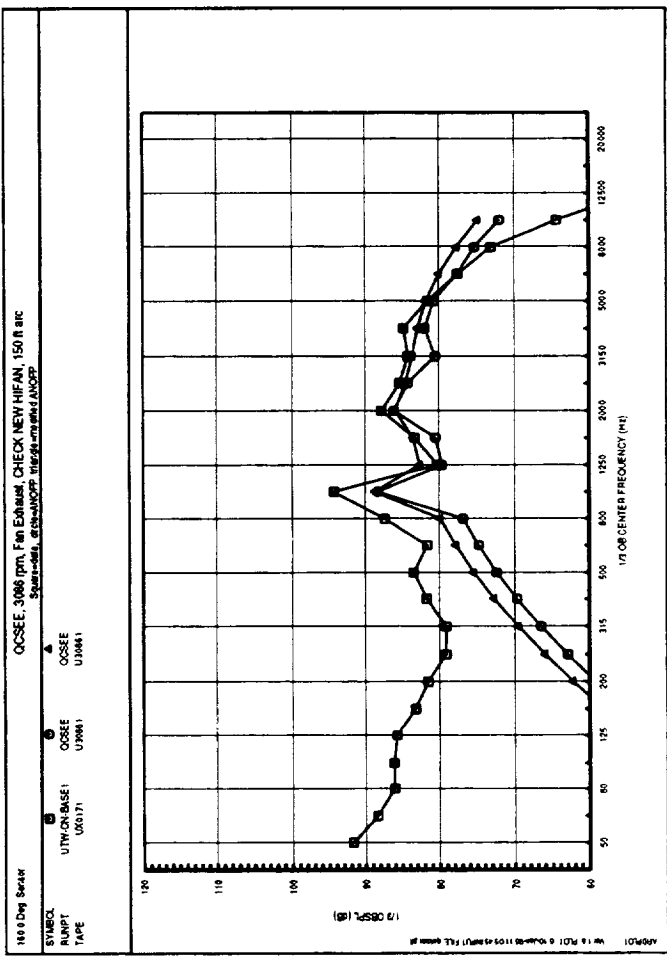
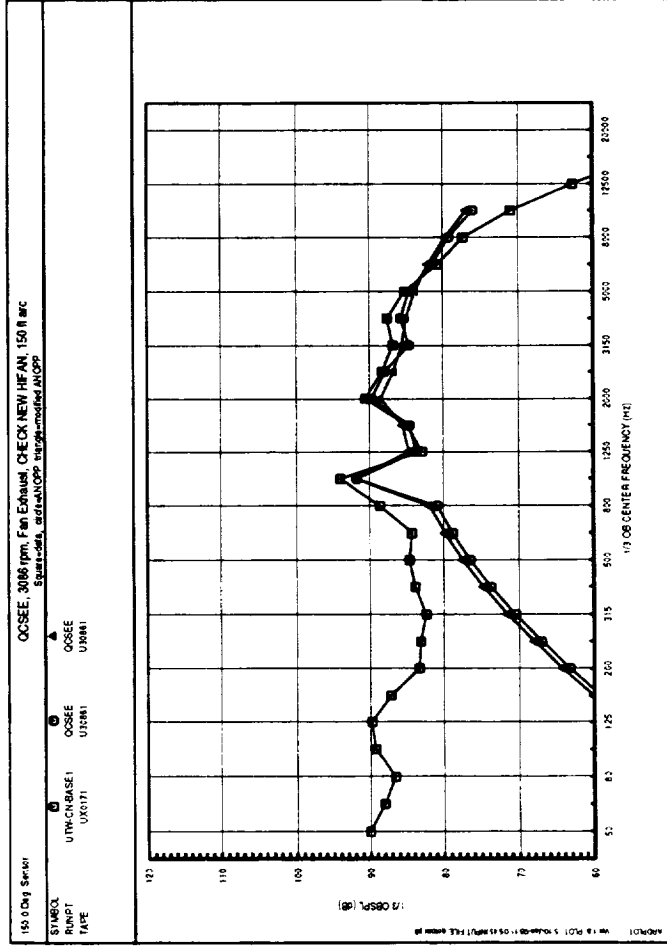
Appendix G Contents

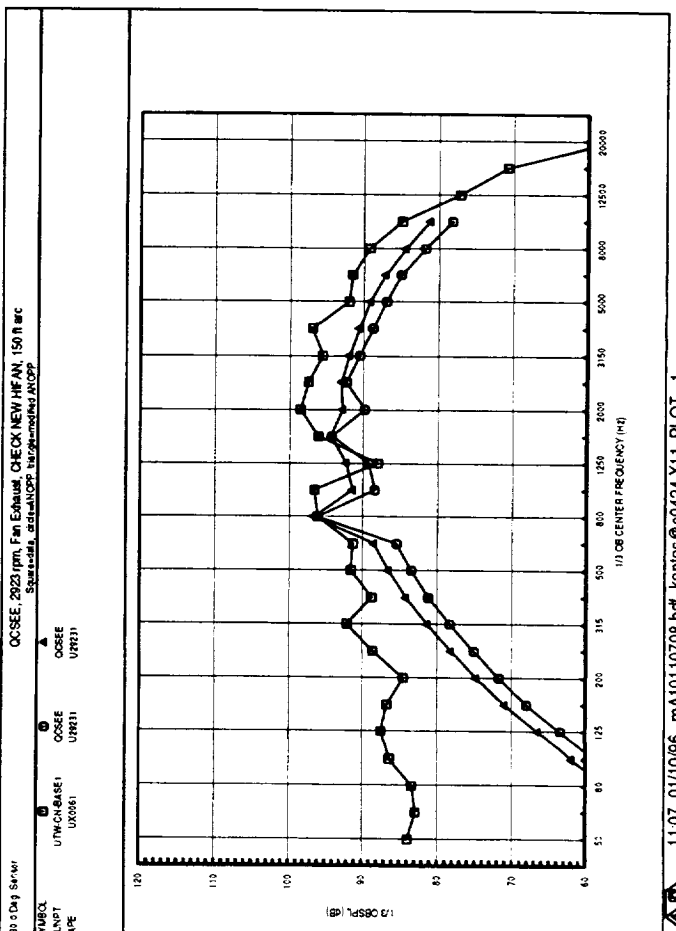
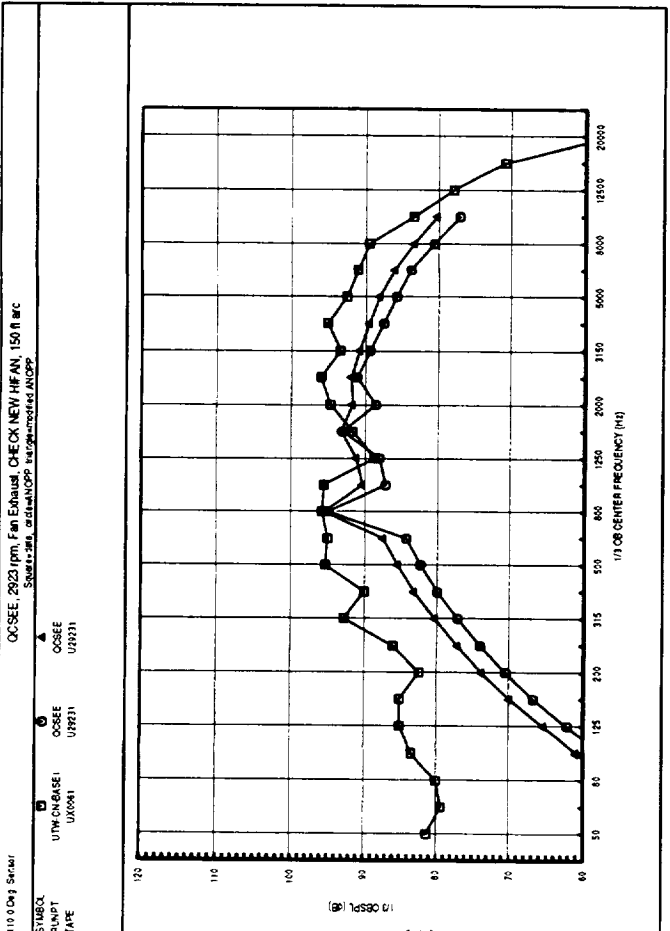
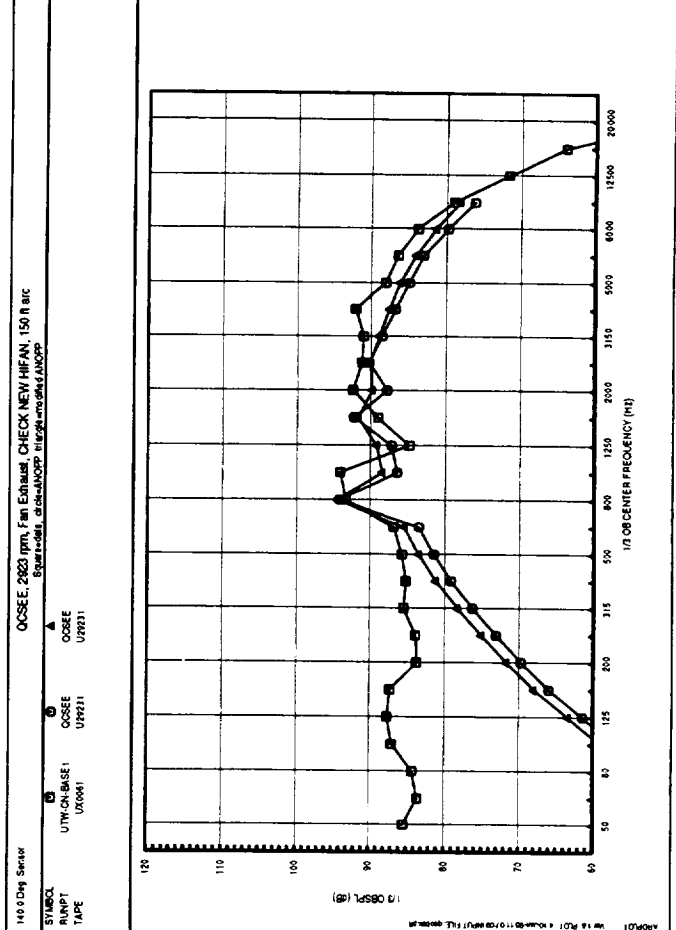
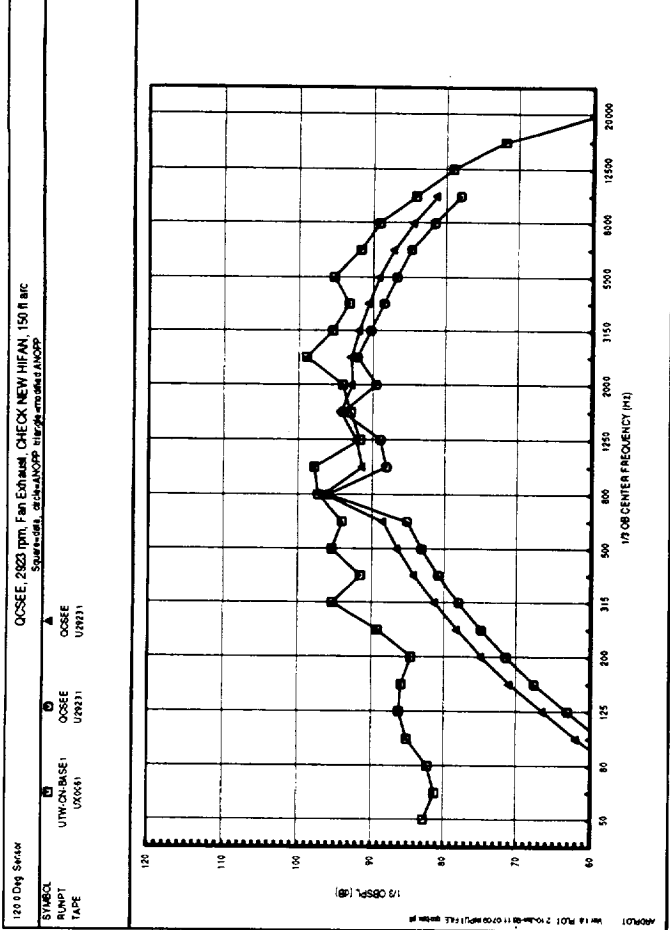
Page	Fan Speed, rpm	Angles, deg
110	3086 (takeoff)	110-140
111	3086 (takeoff)	150-160
112	2923 (cutback)	110-140
113	2923 (cutback)	150-160
114	2759 (approach)	110-140
115	2759 (approach)	150-160

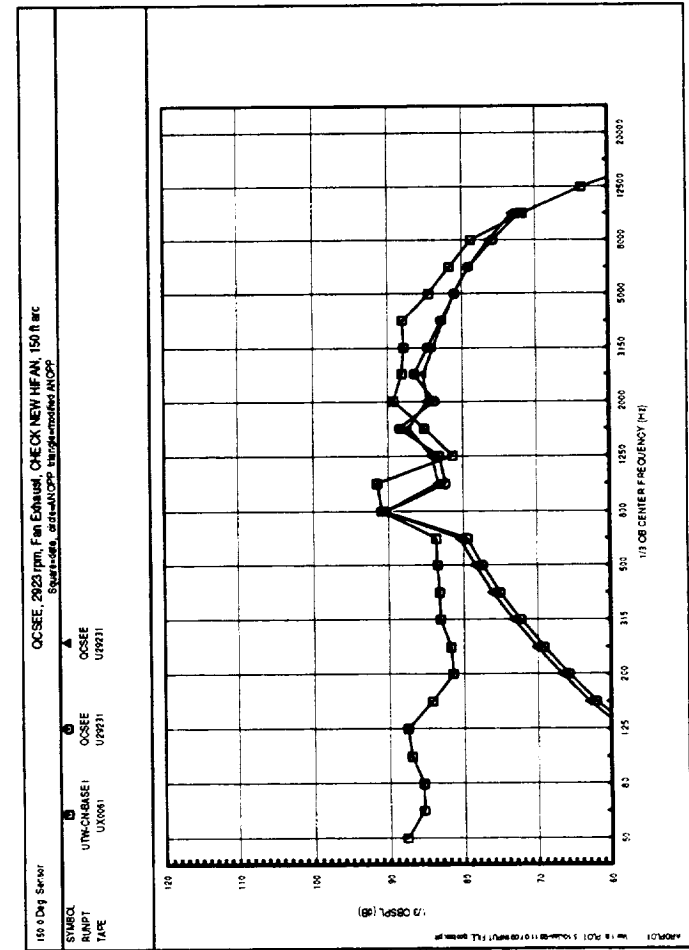
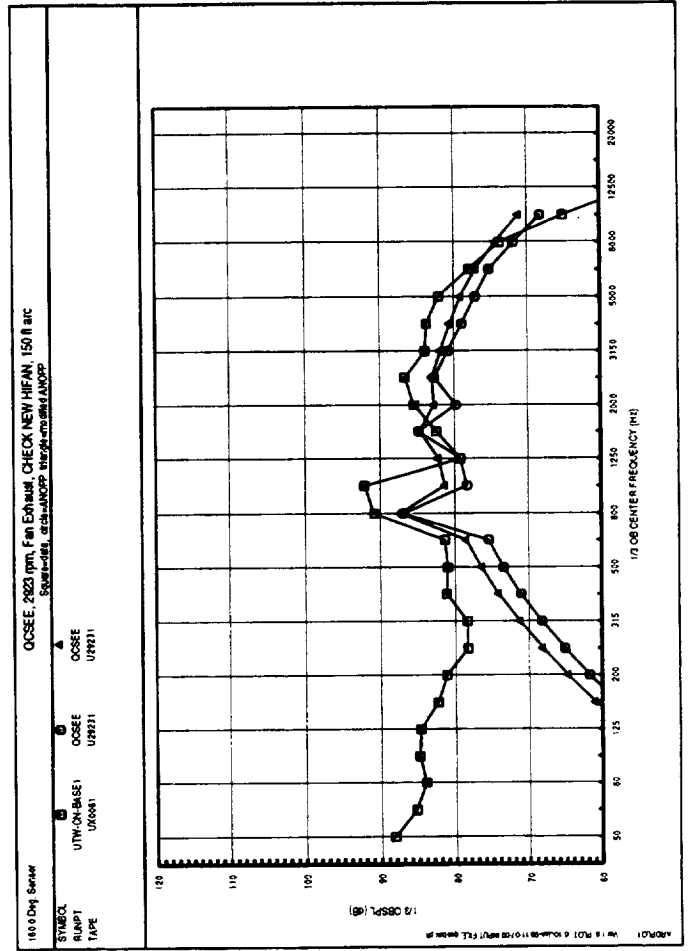
Key to Plots:

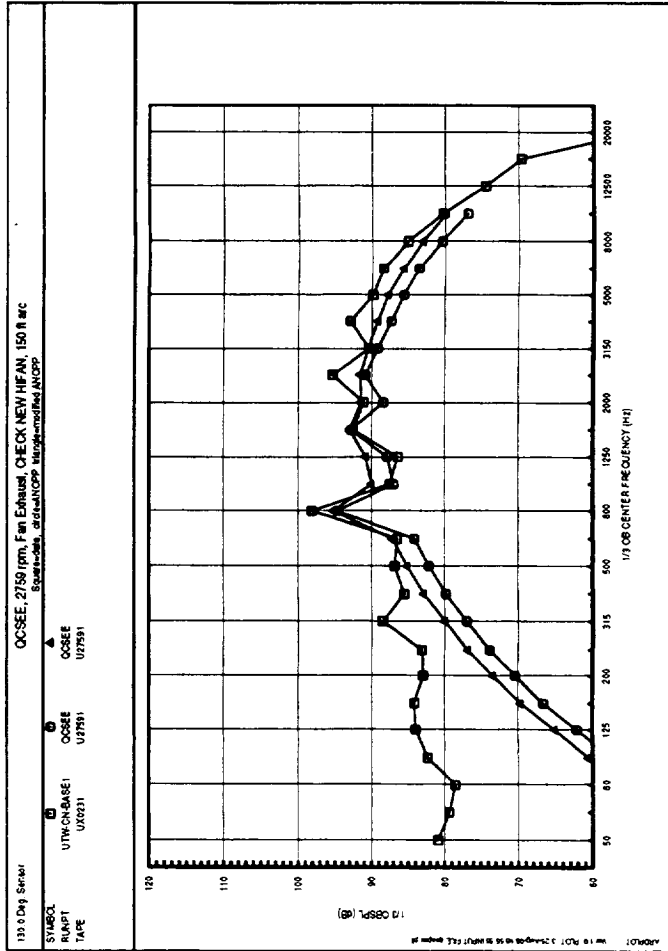
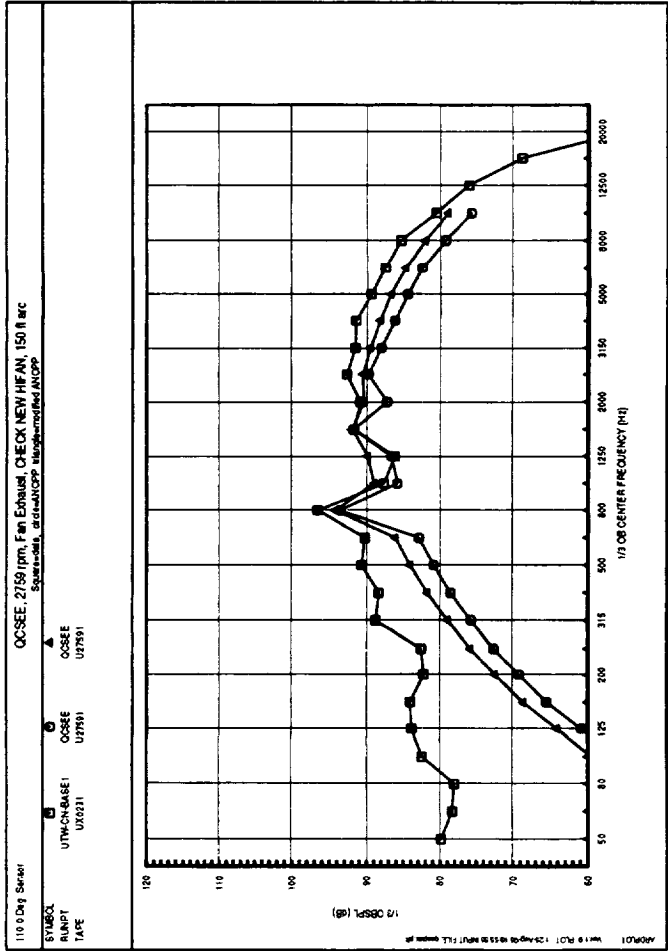
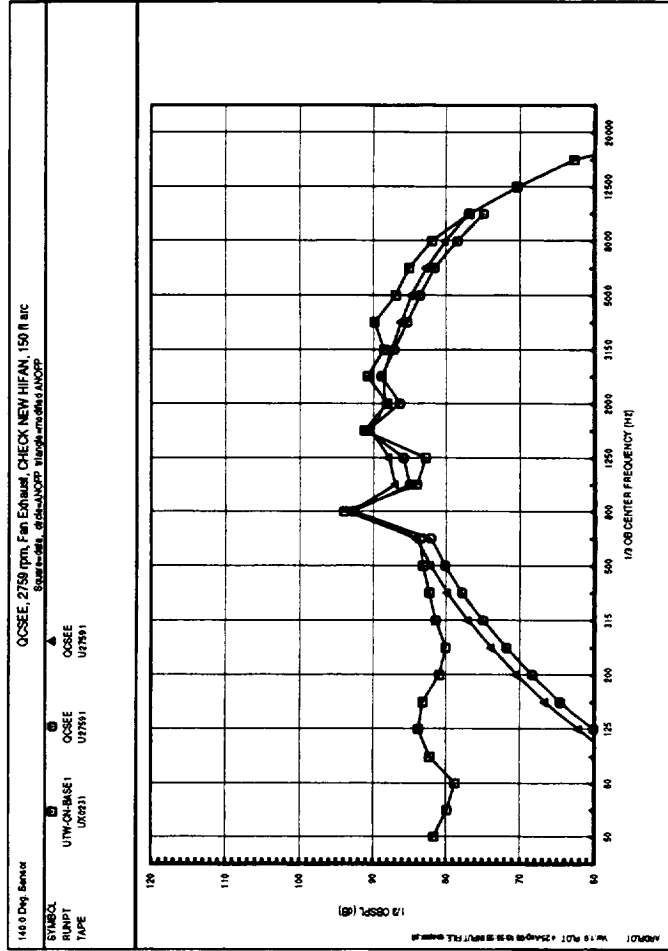
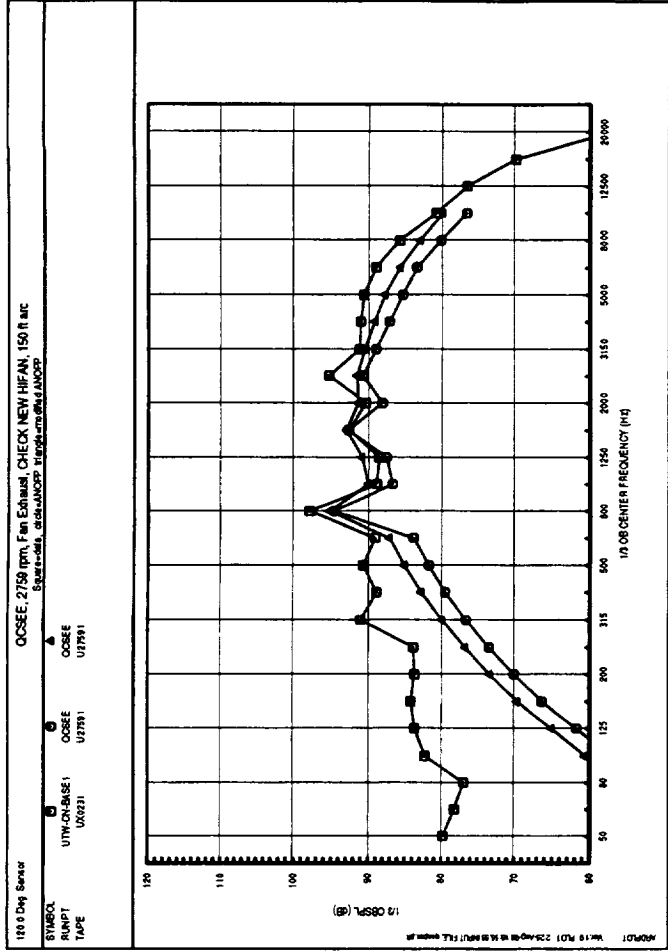
squares = total measured engine data
circles = Heidmann method prediction
triangles = modified Heidmann method prediction (see Section 4)











Appendix H
Jet Noise Spectral Comparison, 150 degrees

Appendix H Contents

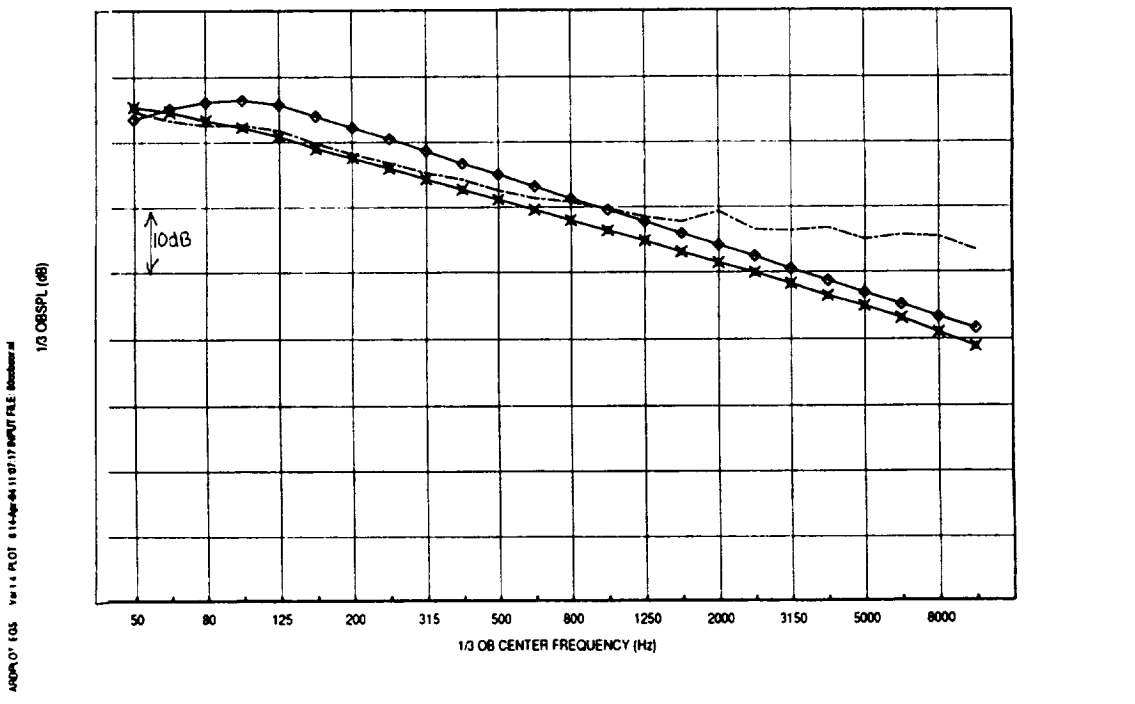
Page	Engine	Condition
117	CF6-80C2	cutback
117	CF6-80C2	approach
118	E ³	cutback
118	E ³	approach
119	QCSEE	cutback
119	QCSEE	approach

Key to Plots:

dashed line = total measured engine data
 X = GE jet noise
 diamonds = ANOPP jet noise (STNJET) prediction

150.0 Deg. Sensor

ANOPP versus JTFXFN PREDICTION CFR JET, 150 FT ARC, CLIMB CONDITION

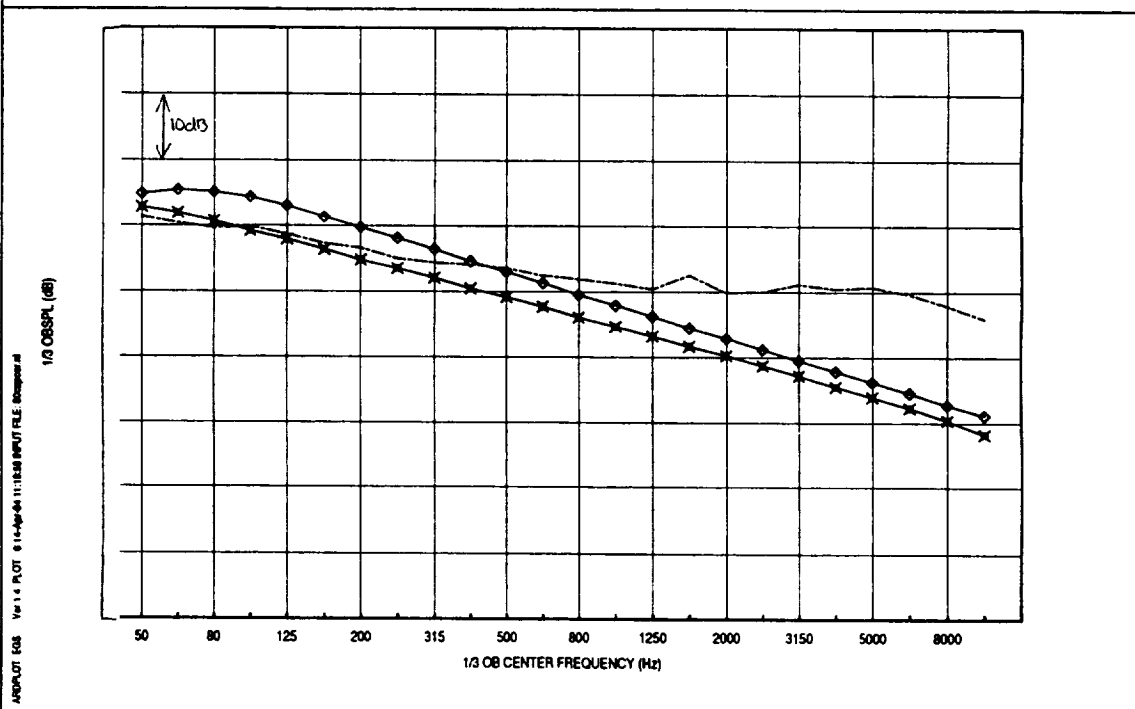


ANOPPLOT EGS Ver 1.4 PLOT 8 14-Apr-84 11:07:33 INPUT FILE: ANOPPLOT.M

11 07 04/1494 MD14110683 bnf c0242 X11 PLOT 3
EGS 1.0 4 SJ 04/08/84 (EGSREP XCPST 4 SJ 04/08/84 on c0424)
(NO PROG VER SPECIFIED)

150.0 Deg. Sensor

ANOPP versus JTFXFN PREDICTION CFR JET, 150 FT ARC, APPROACH CONDITION

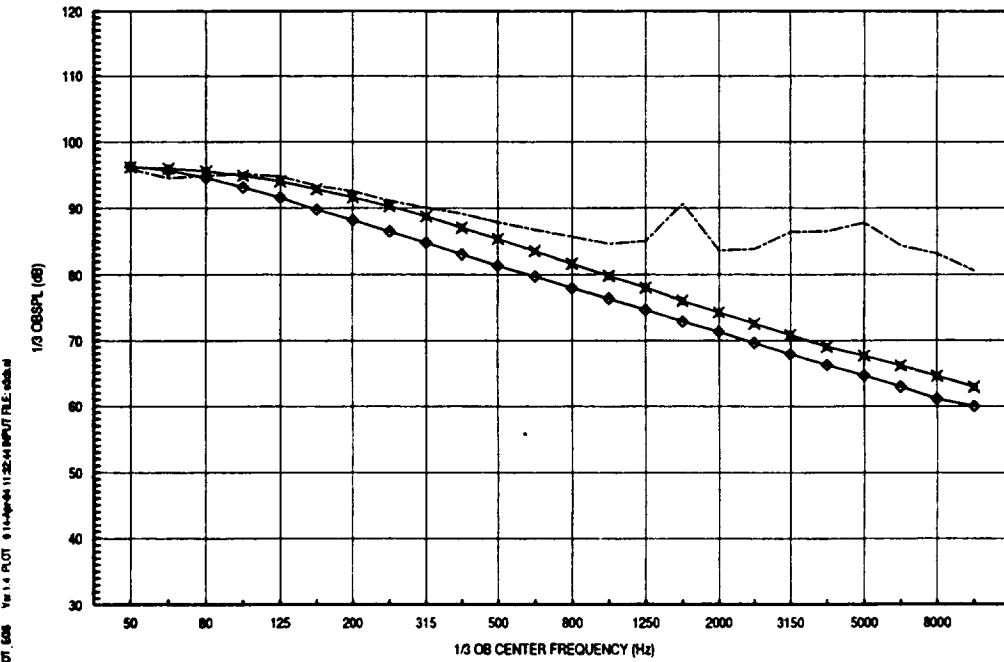


ANOPPLOT EGS Ver 1.4 PLOT 8 14-Apr-84 11:08:08 INPUT FILE: ANOPPLOT.M

11 08 04/1494 MD14110683 bnf c0242 X11 PLOT 3
EGS 1.0 4 SJ 04/08/84 (EGSREP XCPST 4 SJ 04/08/84 on c0424)
(NO PROG VER SPECIFIED)

150.0 Deg. Sensor

ANOPP versus JTFXFN PREDICTION
E3 JET, 150 FT ARC, CUTBACK CONDITION

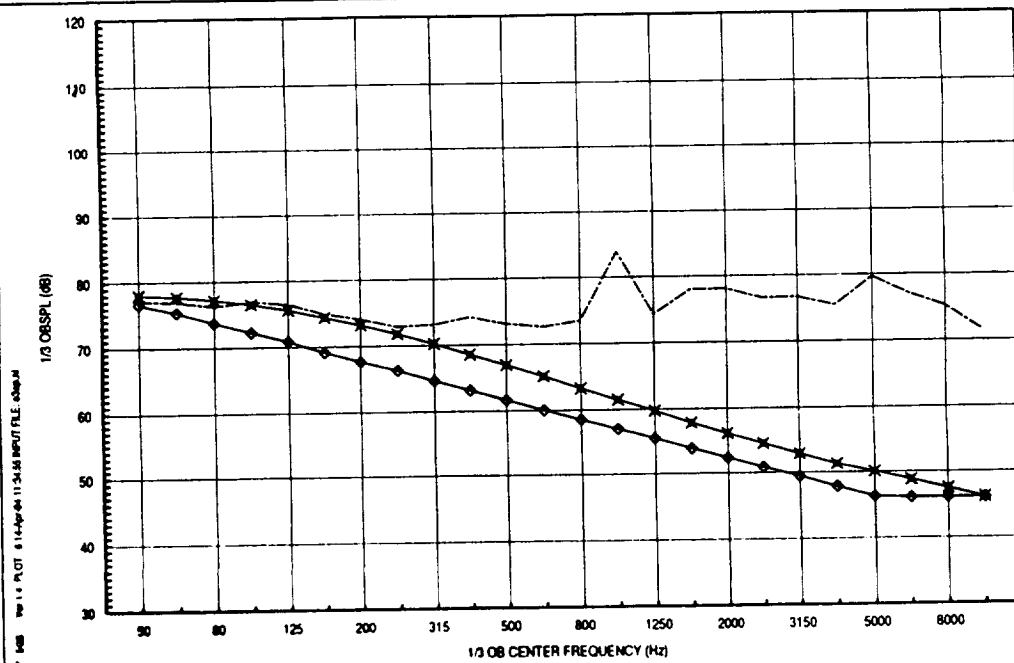


ANOPPLOT (dB) Ver 1.1.4 PLOT 8 11-14-94 11:25:44 INPUT FILE: sdb.m

11 32 04/14/94 m01411323 301 c024 Y11 PLOT 4
EGS LB 4 SJ 0408/94 (EGSREP XCPST 4 SJ 0408/94 on c0424)
NO PROG VER SPECIFIED

150.0 Deg. Sensor

ANOPP versus JTFXFN PREDICTION
E3 JET, 150 FT ARC, APPROACH CONDITION

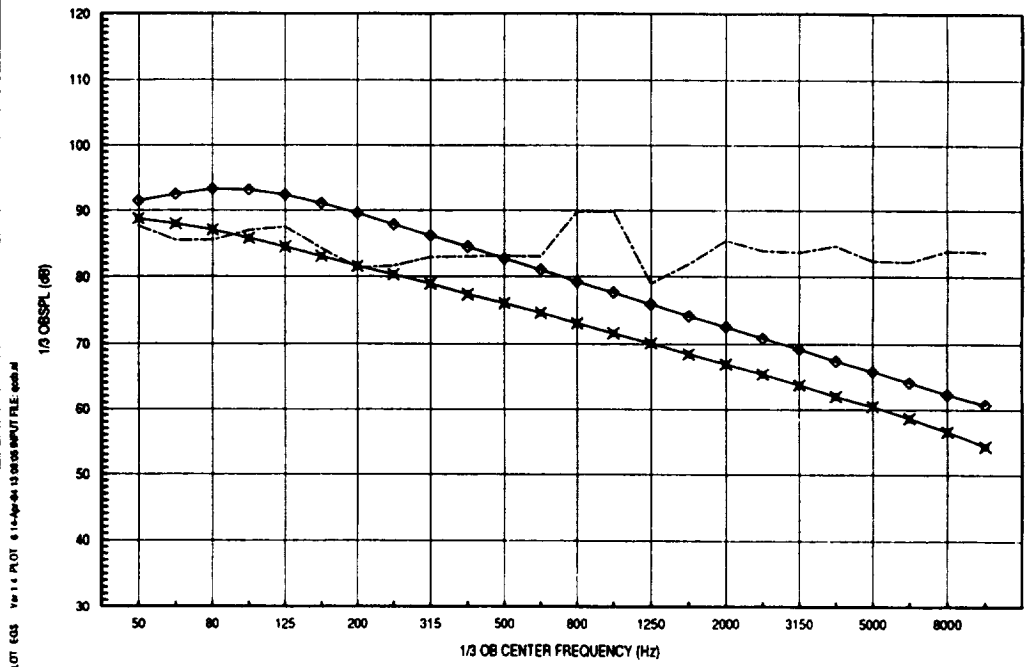


ANOPPLOT (dB) Ver 1.1.4 PLOT 8 11-14-94 11:25:55 INPUT FILE: sdb.m

11 34 04/14/94 m01411323 301 c024 Y11 PLOT 4
EGS LB 4 SJ 0408/94 (EGSREP XCPST 4 SJ 0408/94 on c0424)
NO PROG VER SPECIFIED

150.0 Deg. Sensor

ANOPP versus JTFXFN PREDICTION
QCSEE JET, 150 FT ARC, CUTBACK CONDITION

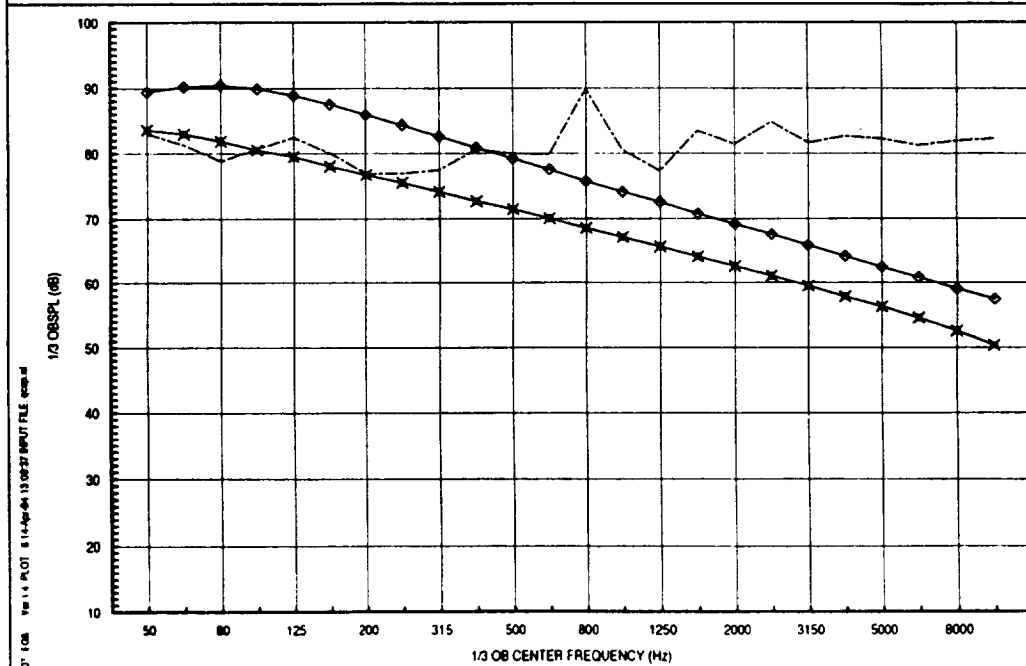


ANOPPLOT.EGS Ver 1.4 PLOT 6 14-Apr-84 13:08:05 INPUT FILE: egs.in

13 08 04/14/84 M014130633 bnf c0424 X11 PLOT 6
EGS LB 4 SJ 04/08/84 (EGSREP XCPOST 4 SJ 04/08/84 on c0424)
(NO PROG VER SPECIFIED)

150.0 Deg. Sensor

ANOPP versus JTFXFN PREDICTION
QCSEE JET, 150 FT ARC, APPROACH CONDITION



ANOPPLOT.EGS Ver 1.4 PLOT 6 14-Apr-84 13:08:27 INPUT FILE: egs.in

13 08 04/14/84 M014130633 bnf c0424 X11 PLOT 6
EGS LB 4 SJ 04/08/84 (EGSREP XCPOST 4 SJ 04/08/84 on c0424)
(NO PROG VER SPECIFIED)

Appendix I
Combustor Noise Spectral Comparisons, 120 degrees

Appendix I Contents

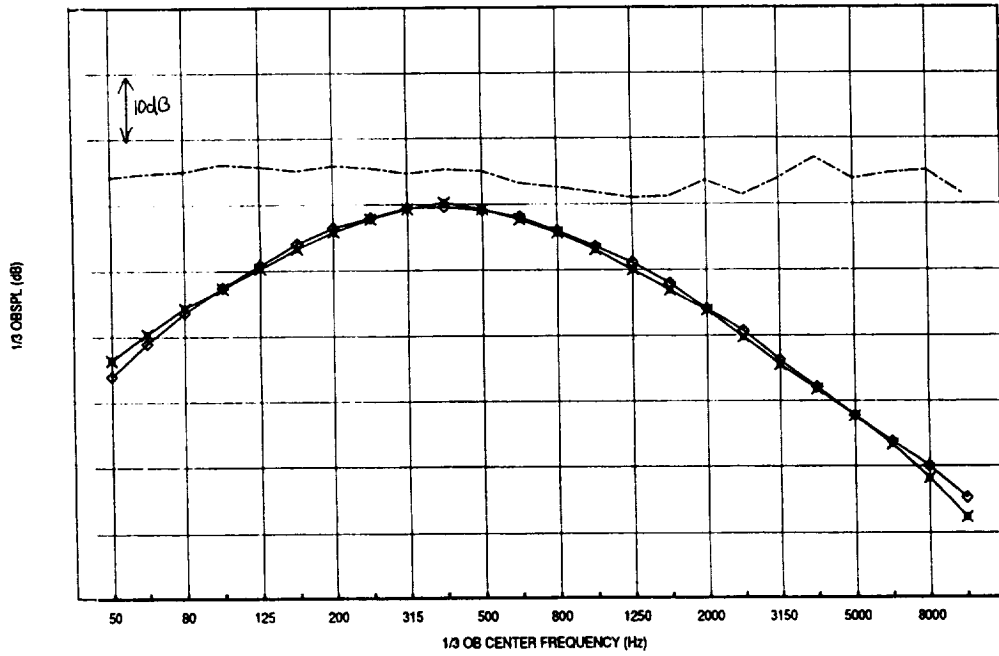
Page	Engine	Condition
121	CF6-80C2	cutback
121	CF6-80C2	approach
122	E ³	cutback
122	E ³	approach
123	QCSEE	cutback
123	QCSEE	approach

Key to Plots:

dashed line = total measured engine data
X or filled square = GE combustor noise
diamonds or open square = ANOPP combustor noise (GECOR) prediction

120.0 Deg Sensor

ANOPP versus JTFXFN PREDICTION
CF6 COMBUSTOR, 150 FT ARC, CUTBACK CONDITION



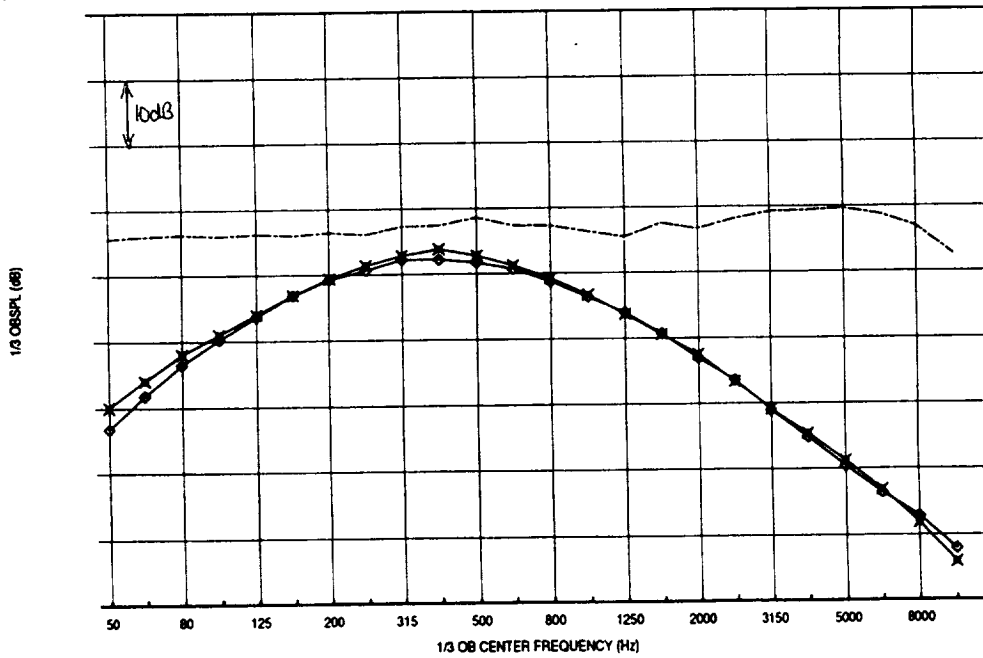
ANOPP OT EGS Ver 1.8 PLOT 3 28-Apr-94 08:53:59 INPUT FILE: B0000004.M



08 33 04/28/94 m02000361 b0 c0424 X11 PLOT 3
EGS 1.8 4 SJ 04/08/94 (EGSREP ACPOST 4 SJ 04/08/94 on c0424)

120.0 Deg Sensor

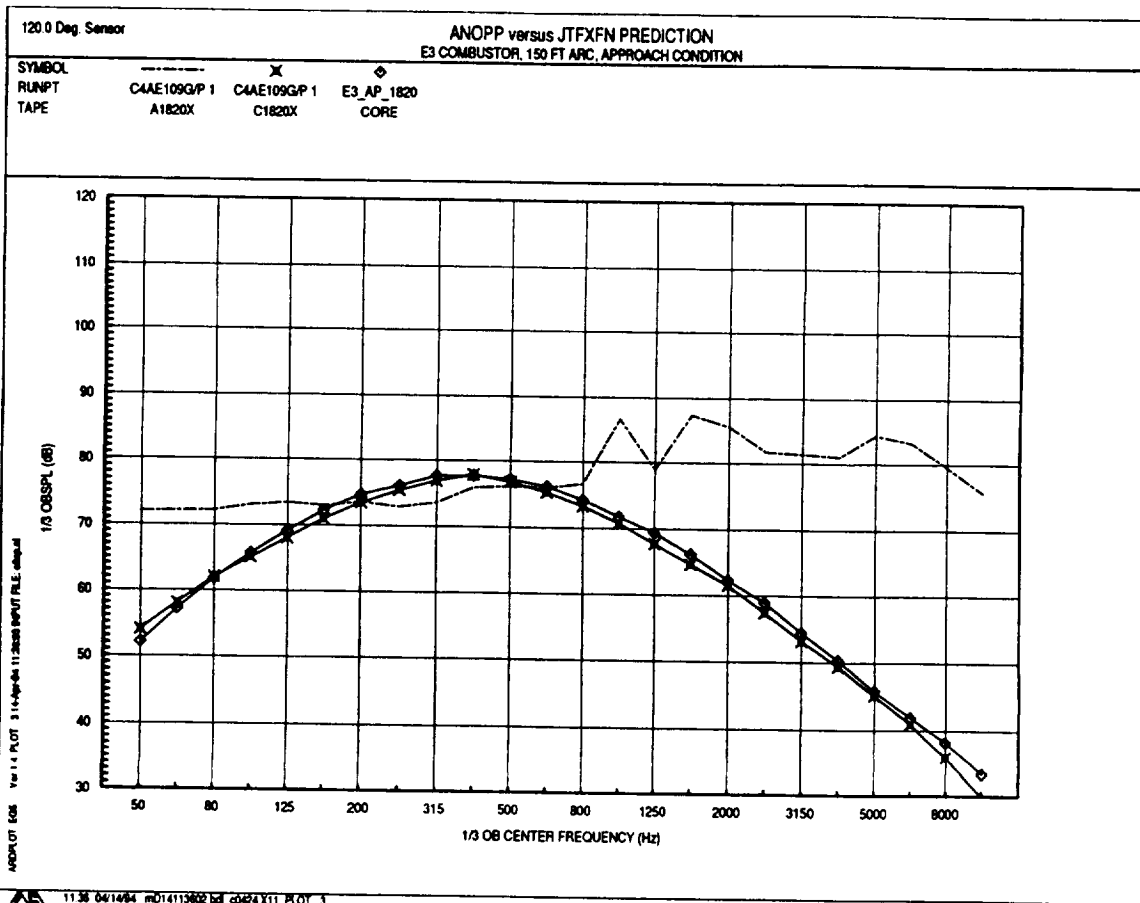
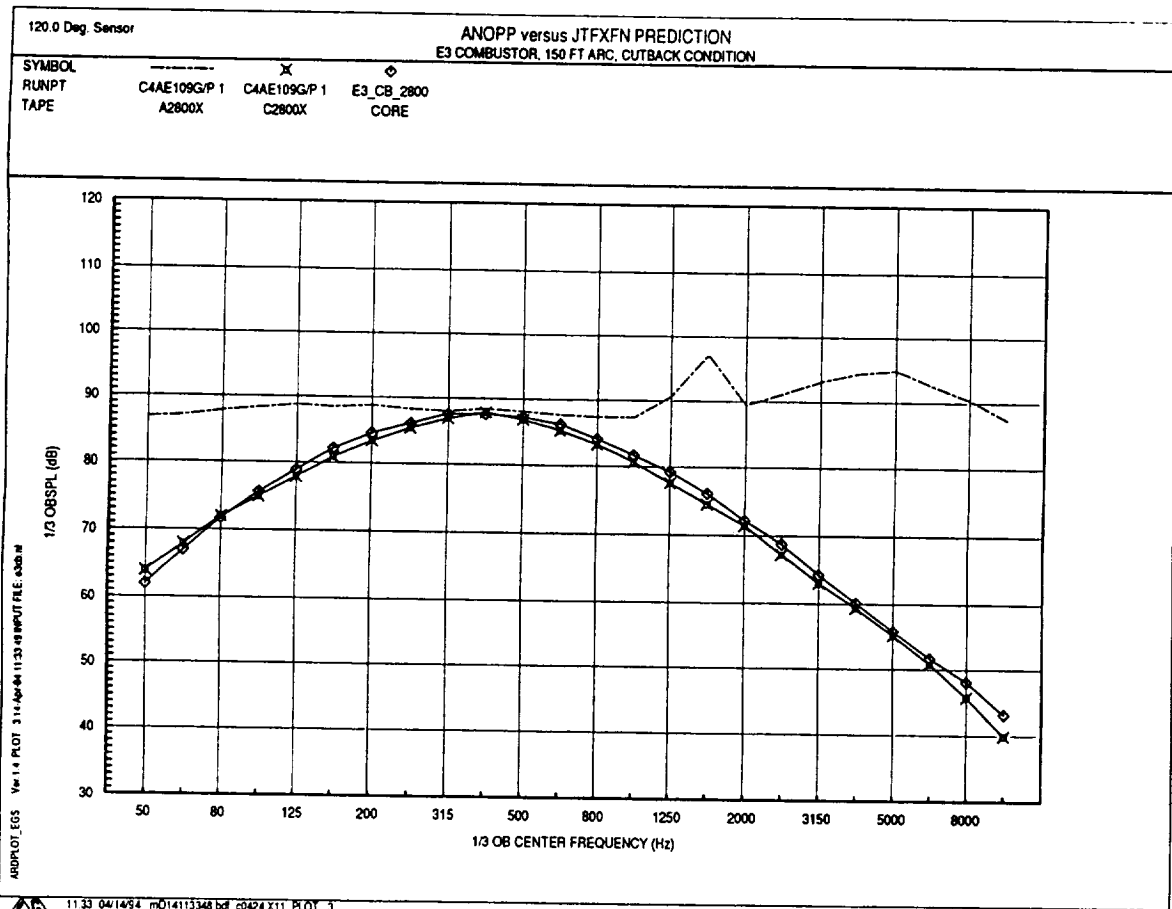
ANOPP versus JTFXFN PREDICTION
CF6 COMBUSTOR, 150 FT ARC, APPROACH CONDITION



ANOPP OT EGS Ver 1.8 PLOT 3 14-Apr-94 11:28:54 INPUT FILE: B0000004.M

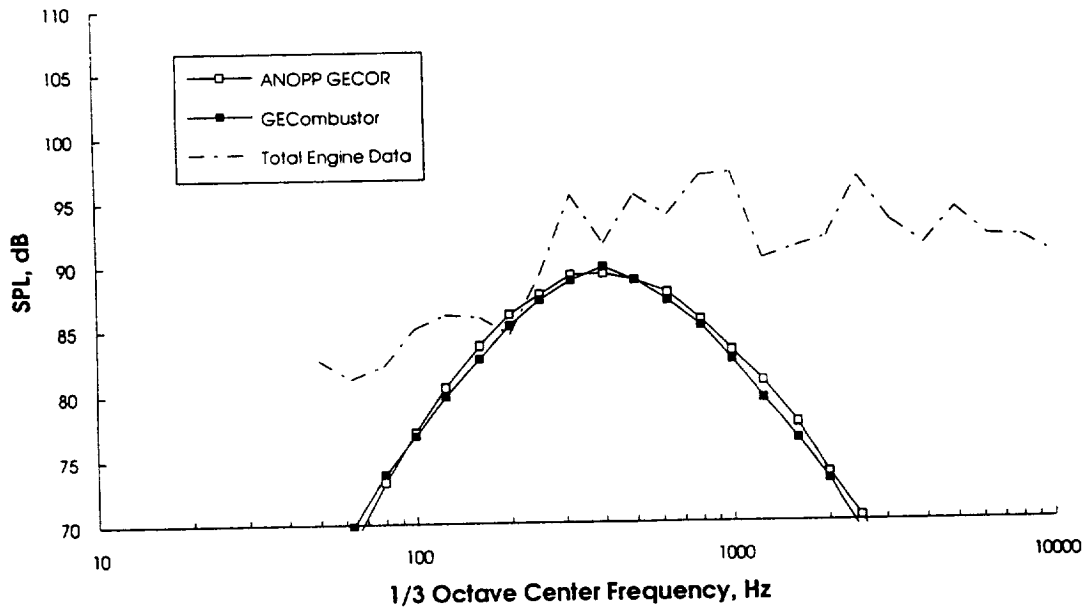


11 20 04/14/94 m01411205 b0 c0424 X11 PLOT 3
EGS 1.8 4 SJ 04/08/94 (EGSREP ACPOST 4 SJ 04/08/94 on c0424)
(NO PROG VER SPECIFIED)



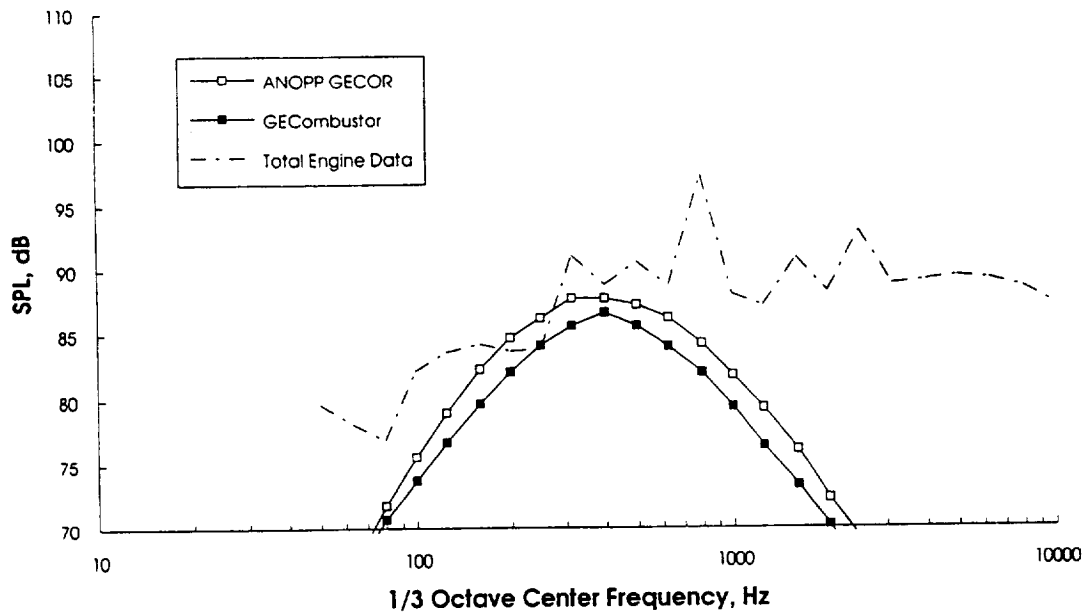
Task 24 ANOPP Assessment: Combustor Noise

QCSEE, Cutback, 150 ft arc, 120 deg



Task 24 ANOPP Assessment: Combustor Noise

QCSEE, Approach, 150 ft arc, 120 deg



Appendix J
Turbine Noise Spectral Comparisons, 120 degrees

Appendix J Contents

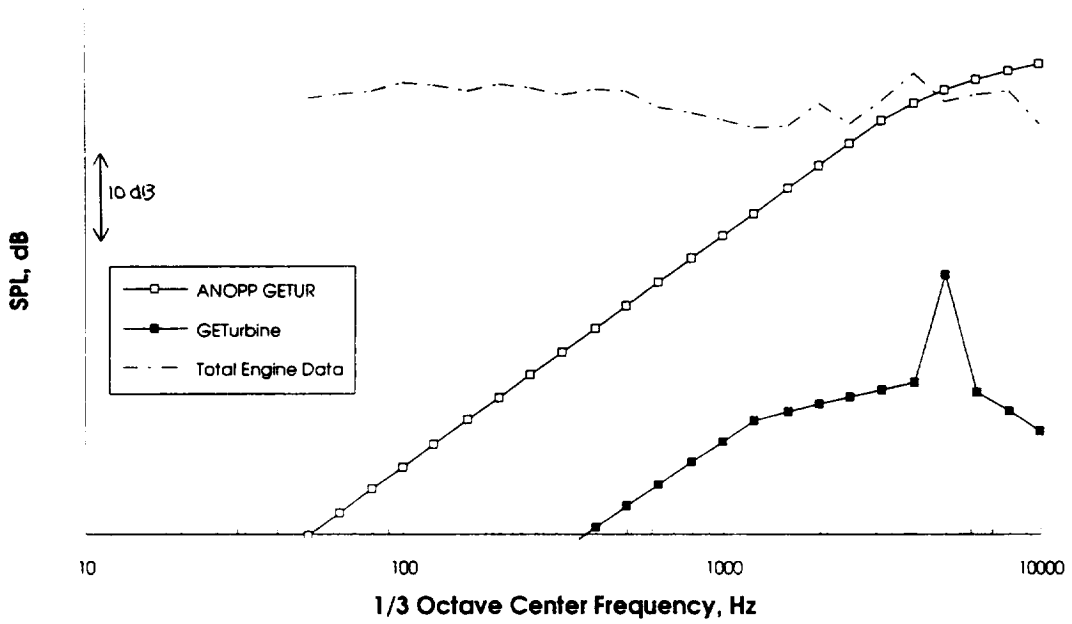
Page	Engine	Condition
125	CF6-80C2	cutback
125	CF6-80C2	approach
126	E ³	cutback
126	E ³	approach
127	QCSEE	cutback
127	QCSEE	approach

Key to Plots:

dashed line = total measured engine data
filled squares = GE turbine noise
open squares = ANOPP turbine noise (GETUR) prediction

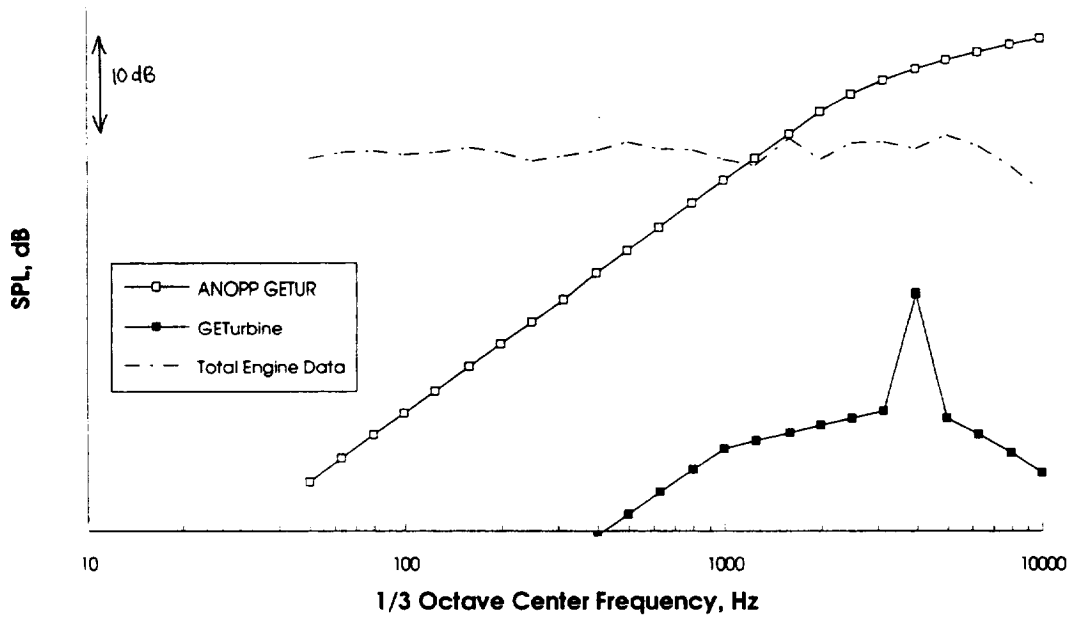
Task 24 ANOPP Assessment: Turbine Noise

CF6-80C2, Cutback, 150 ft arc, 120 deg



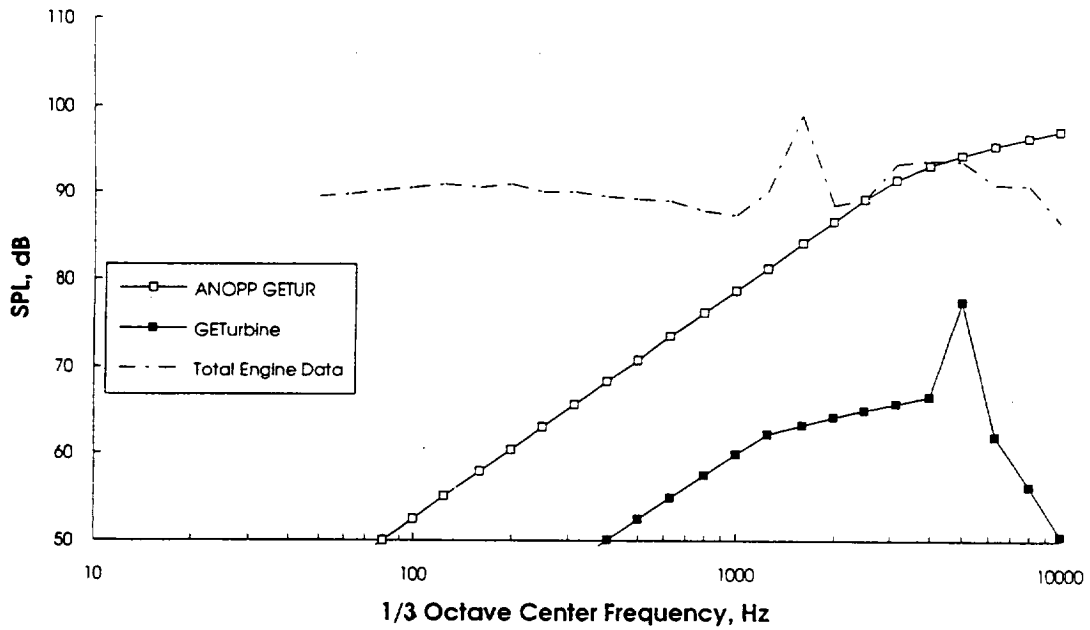
Task 24 ANOPP Assessment: Turbine Noise

CF6-80C2, Approach, 150 ft arc, 120 deg



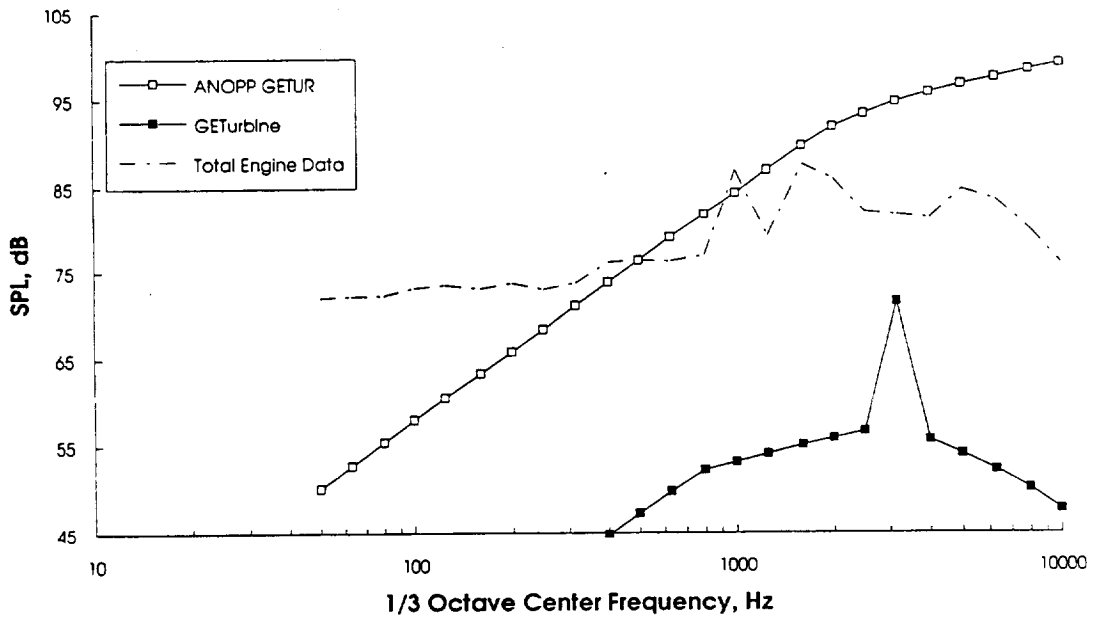
Task 24 ANOPP Assessment: Turbine Noise

E3, Cutback, 150 ft arc, 120 deg



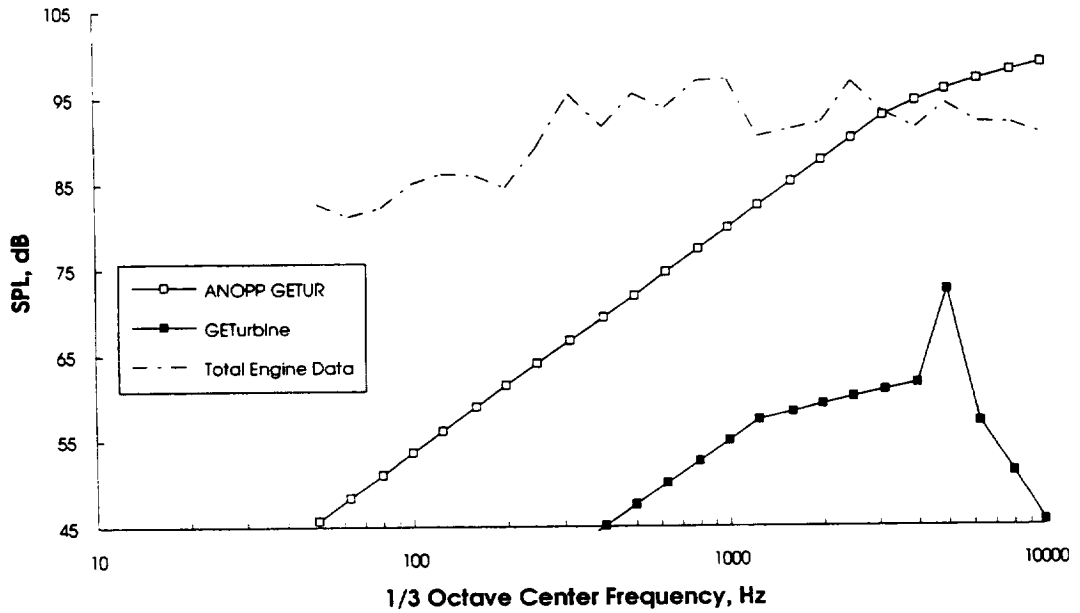
Task 24 ANOPP Assessment: Turbine Noise

E3, Approach, 150 ft arc, 120 deg



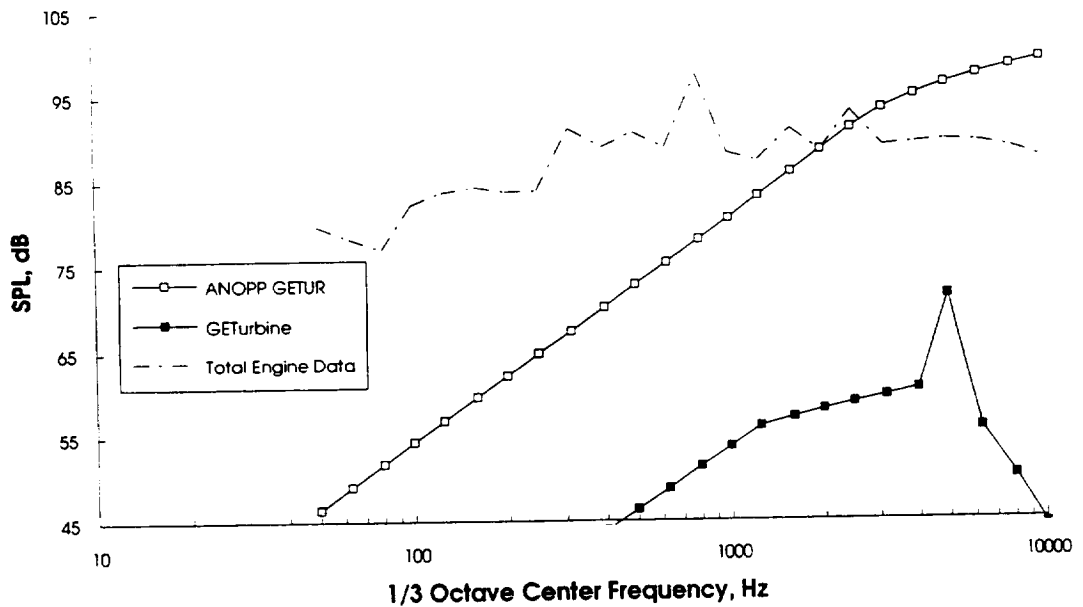
Task 24 ANOPP Assessment: Turbine Noise

QCSEE, Cutback, 150 ft arc, 120 deg



Task 24 ANOPP Assessment: Turbine Noise

QCSEE, Approach, 150 ft arc, 120 deg



Appendix K
Directivity, CF6-80C2 and QCSEE

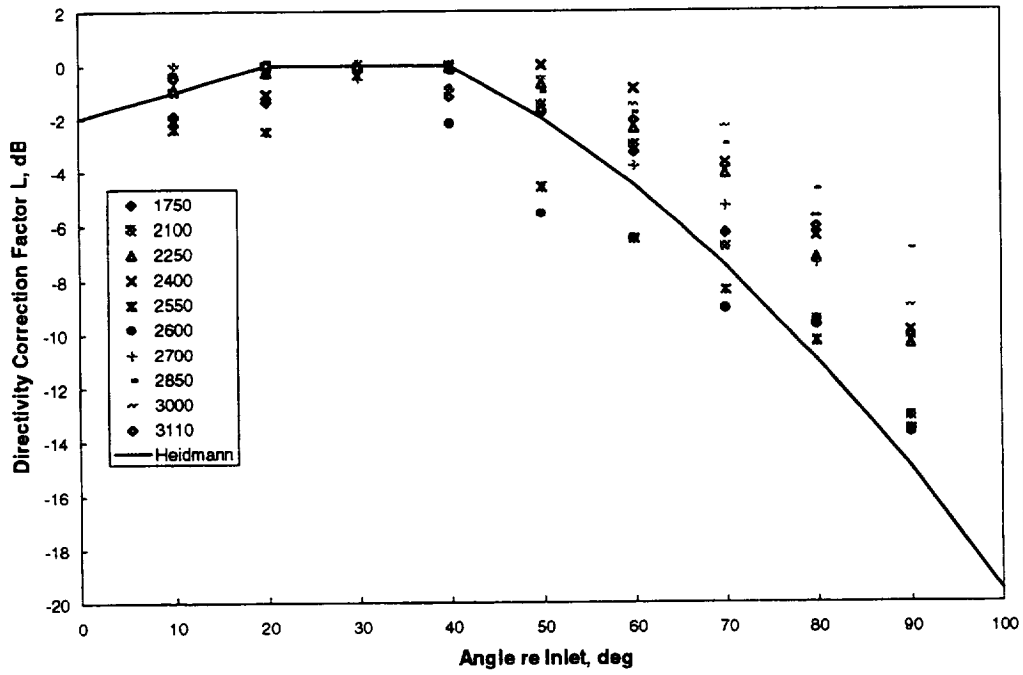
Appendix K Contents

Page	Noise Component	Engine
129	Fan Inlet Broadband	CF6-80C2
129	Fan Inlet Broadband	QCSEE
130	Fan Inlet Tone	CF6-80C2
130	Fan Inlet Tone	QCSEE
131	Fan Exhaust Broadband	CF6-80C2
131	Fan Exhaust Broadband	QCSEE
132	Fan Exhaust Tone	CF6-80C2
132	Fan Exhaust Tone	QCSEE

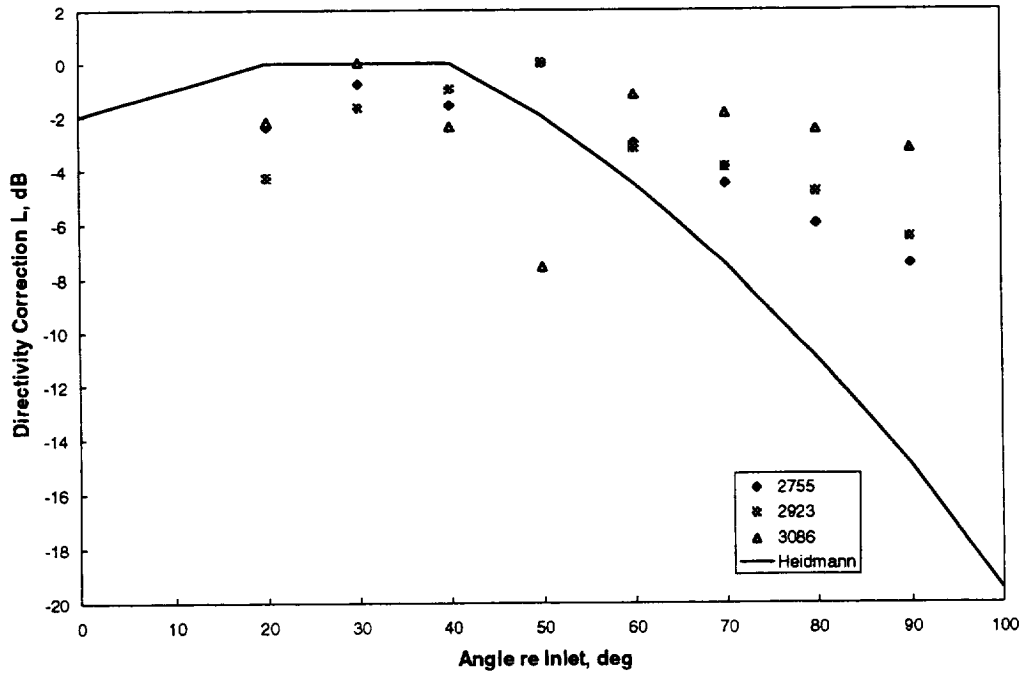
Key to Plots:

all symbols = total measured engine data, all speeds
 solid line = Heidmann method

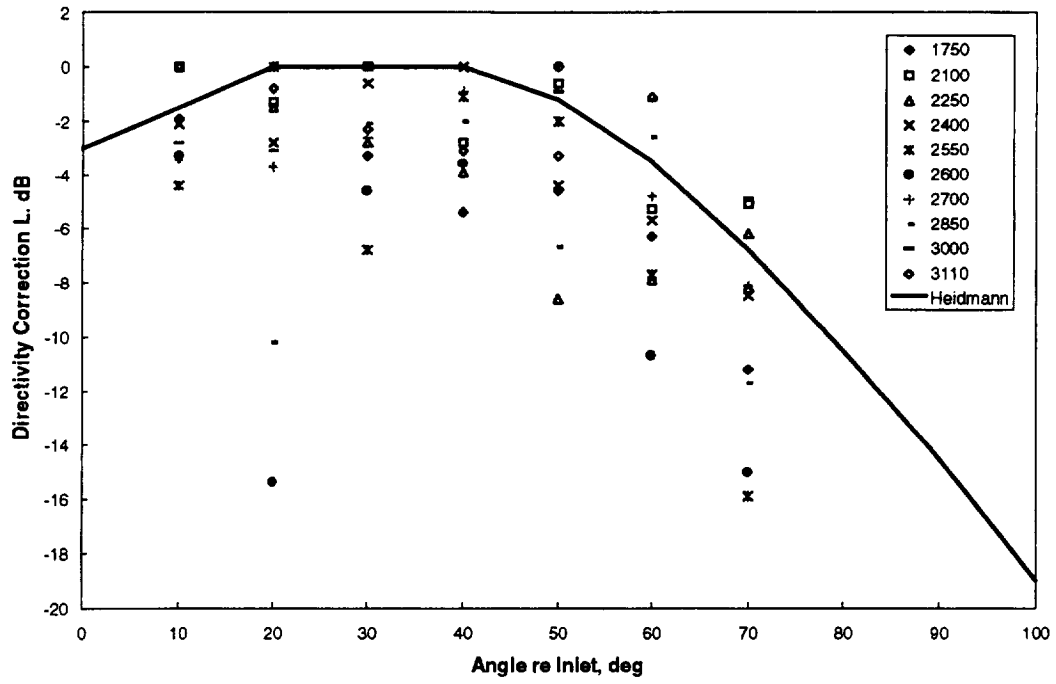
Fan Inlet Broadband Directivity Correction, CF6-80C2



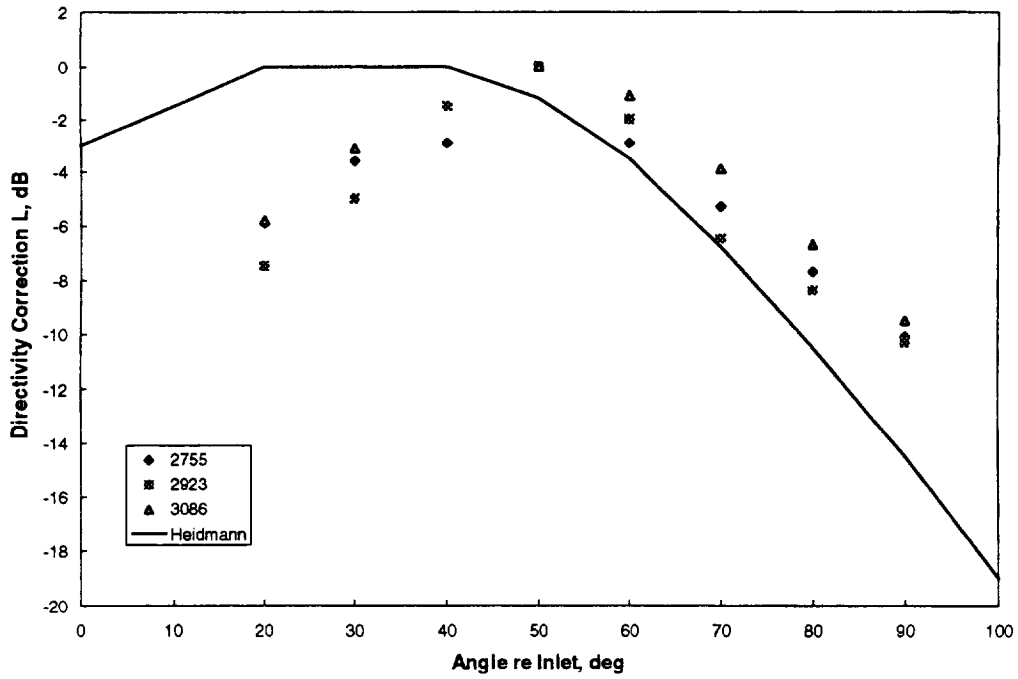
Fan Inlet Broadband Directivity Correction, QCSEE



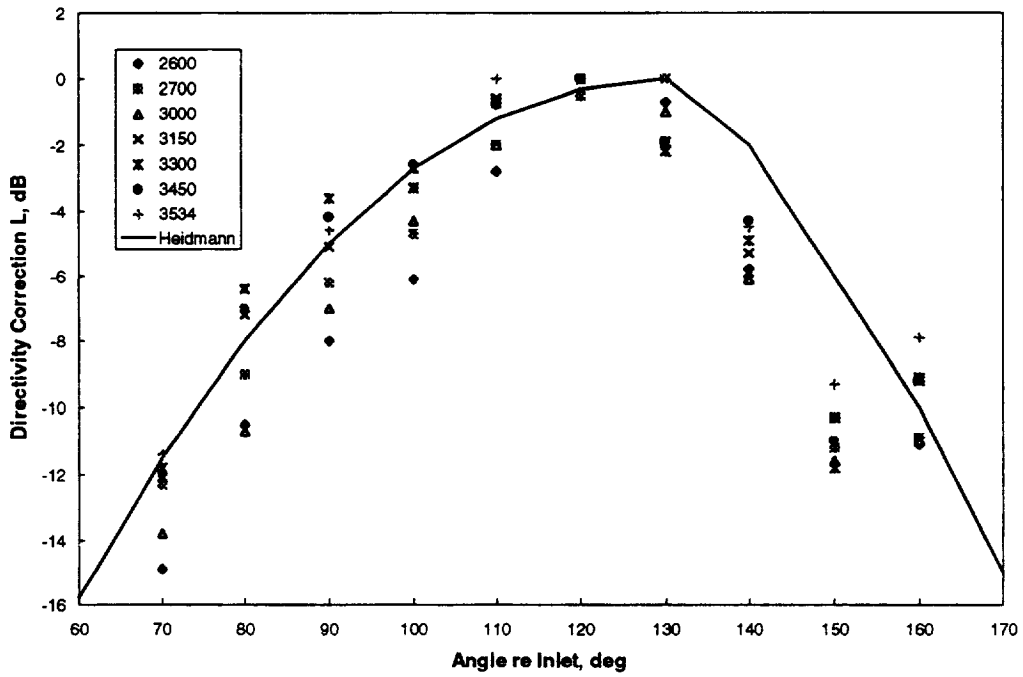
Fan Inlet Tone Directivity Correction, CF6-80C2



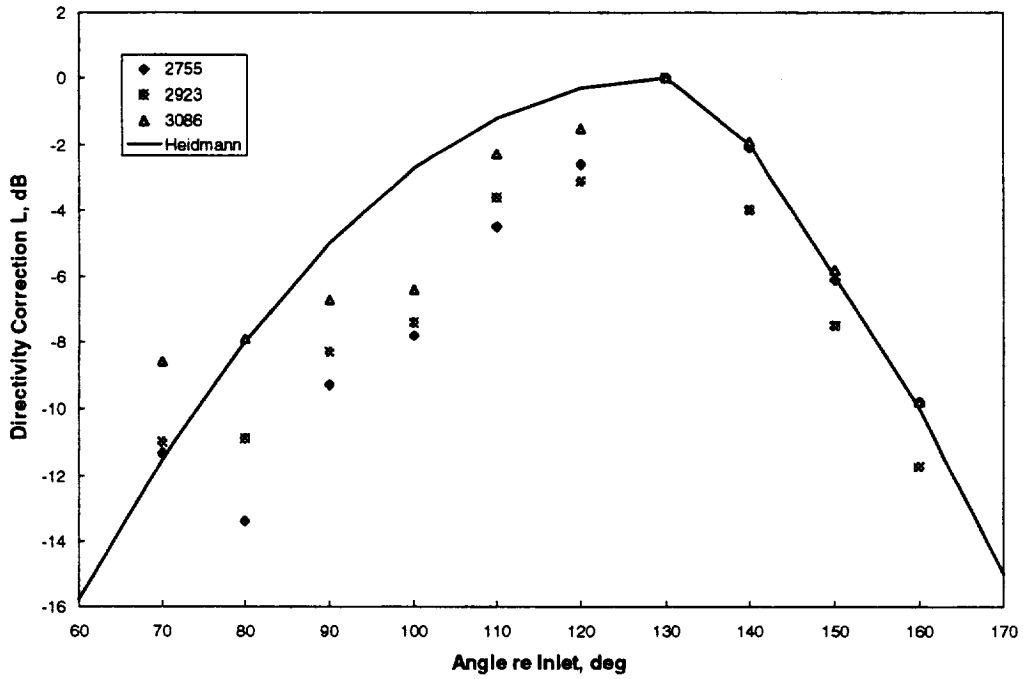
Fan Inlet Tone Directivity Correction, QCSEE



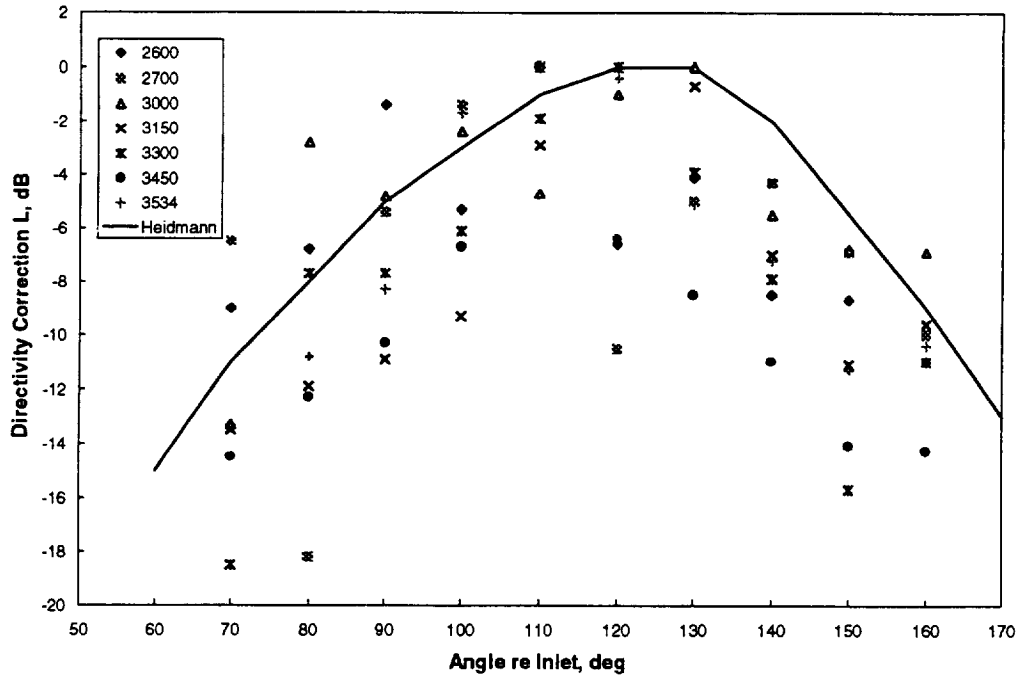
Fan Exhaust Broadband Directivity Correction, CF6-80C2



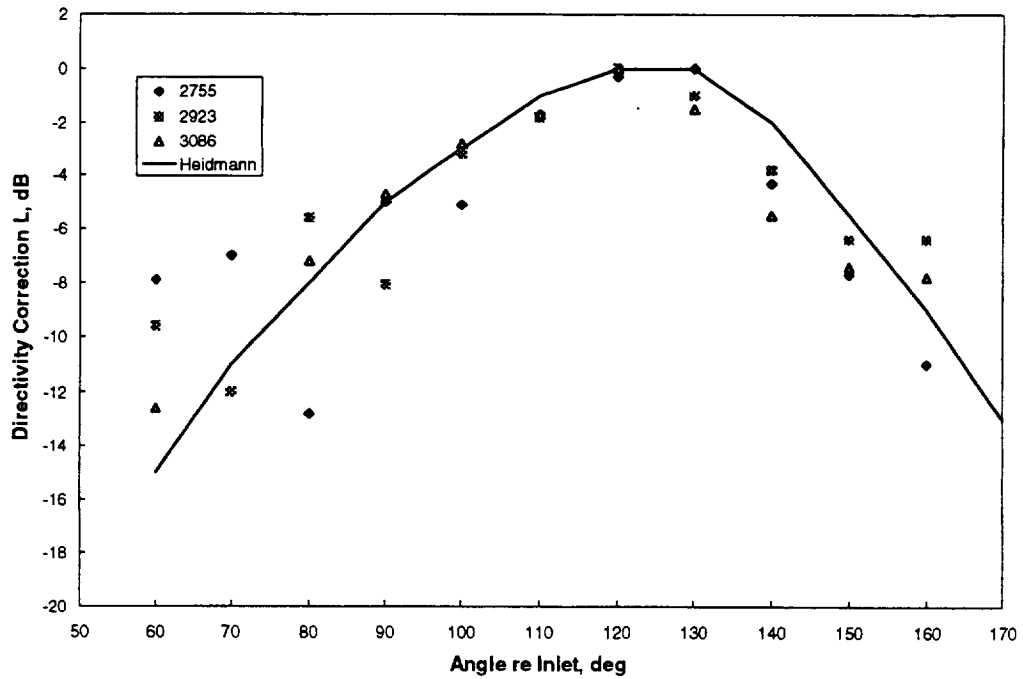
Fan Exhaust Broadband Directivity Correction, QCSEE



Fan Exhaust Tone Directivity Correction, CF6-80C2



Fan Exhaust Tone Directivity Correction, QCSEE



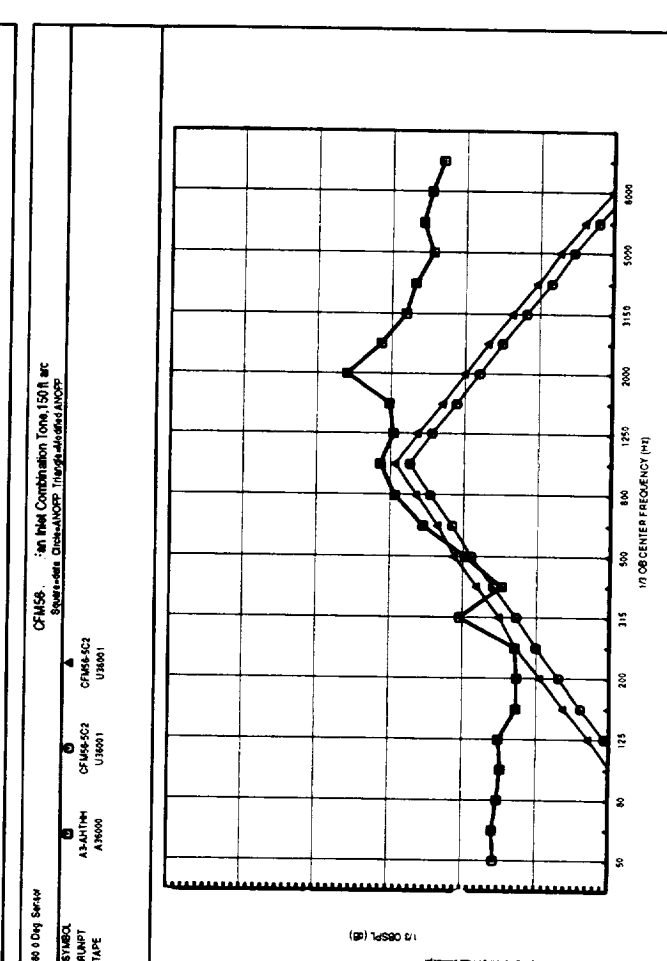
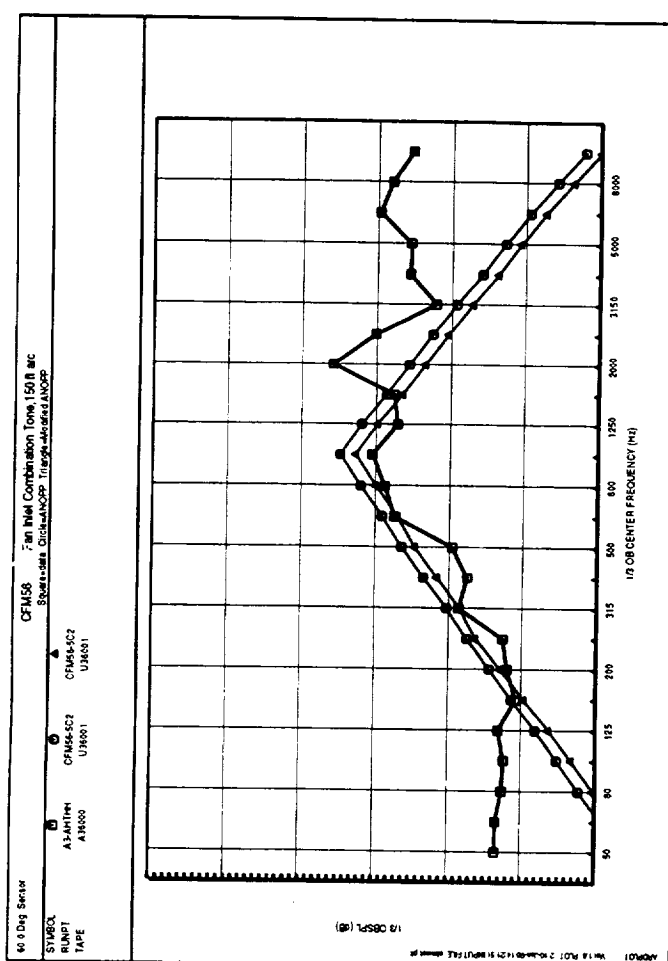
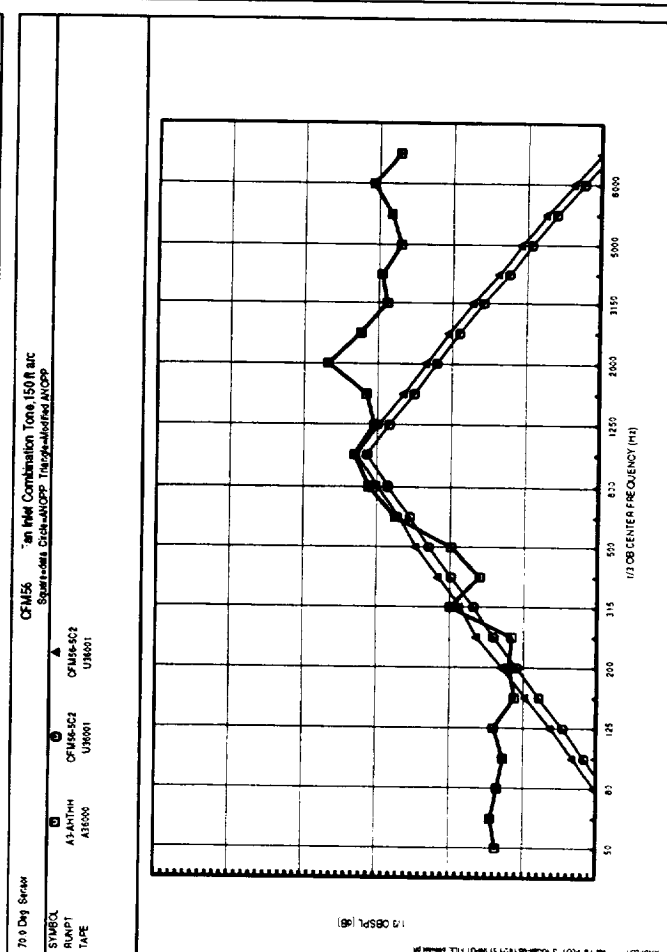
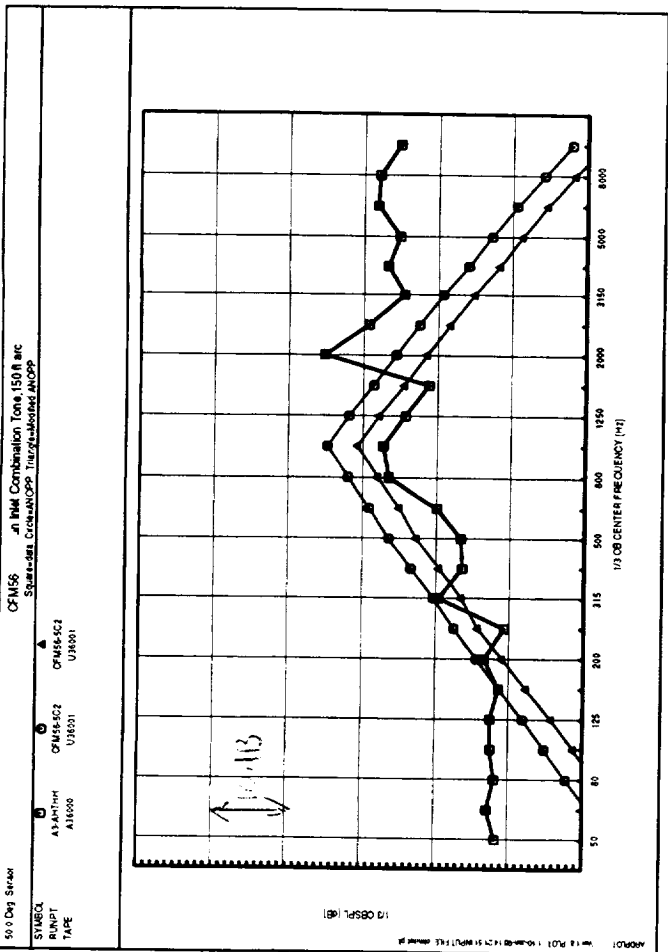
Appendix L
Combination Tone Noise Spectra - CFM56

Appendix L Contents

Page	Fan Speed, rpm	Angles
134	3600	50-80
135	3900	50-80
136	4050	50-80
137	4150	50-80
138	4250	50-80
139	4350	50-80
140	4450	50-80
141	4550	50-80

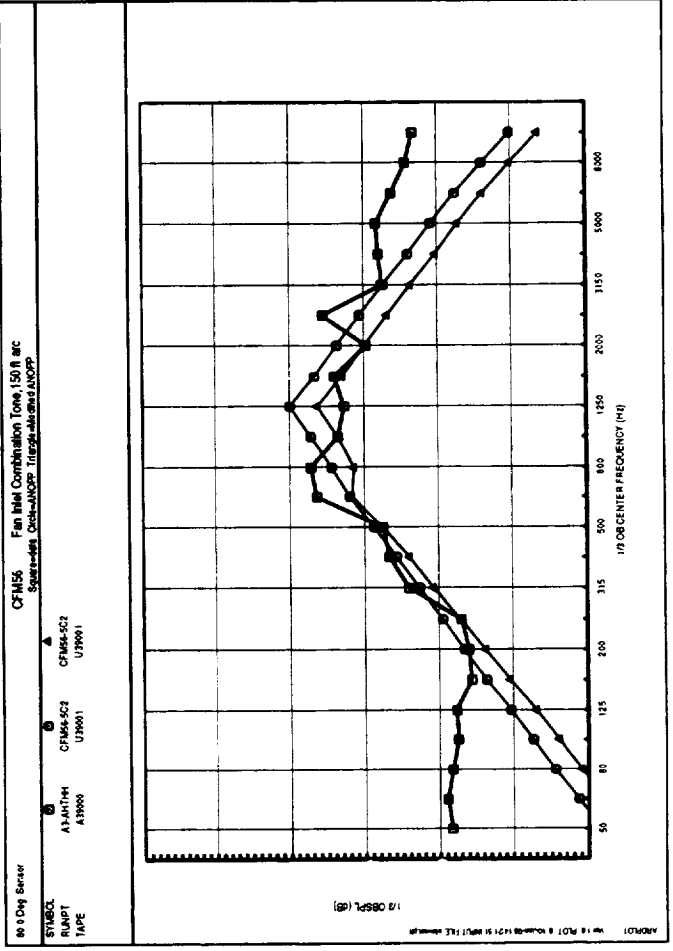
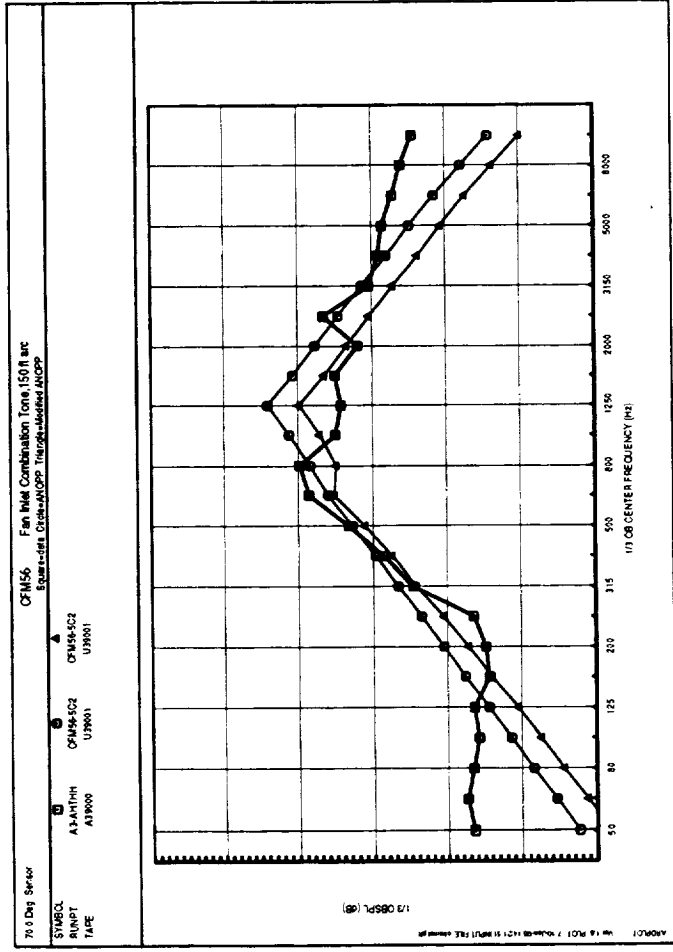
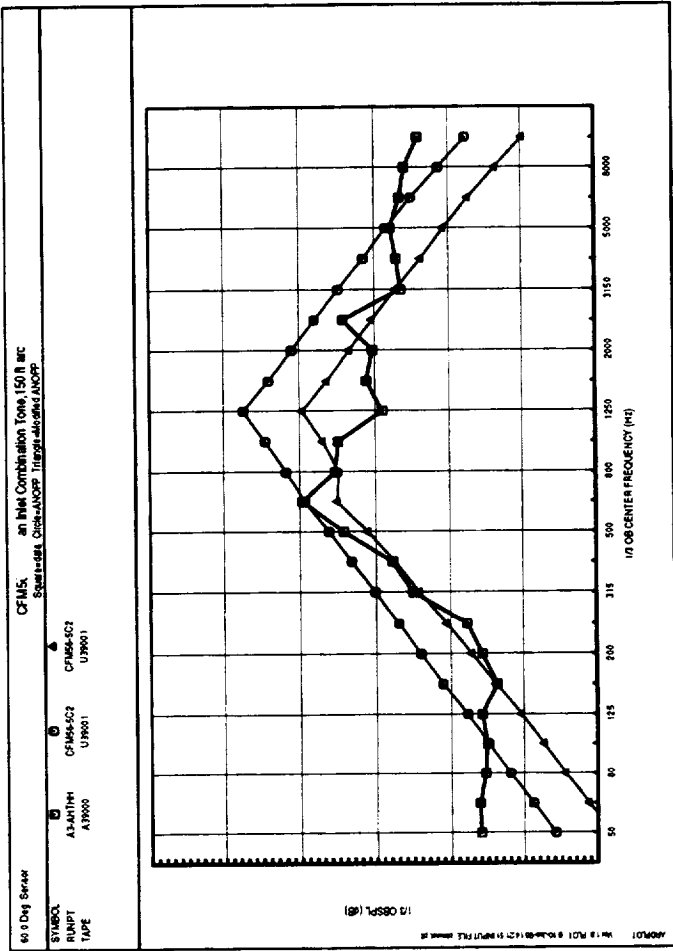
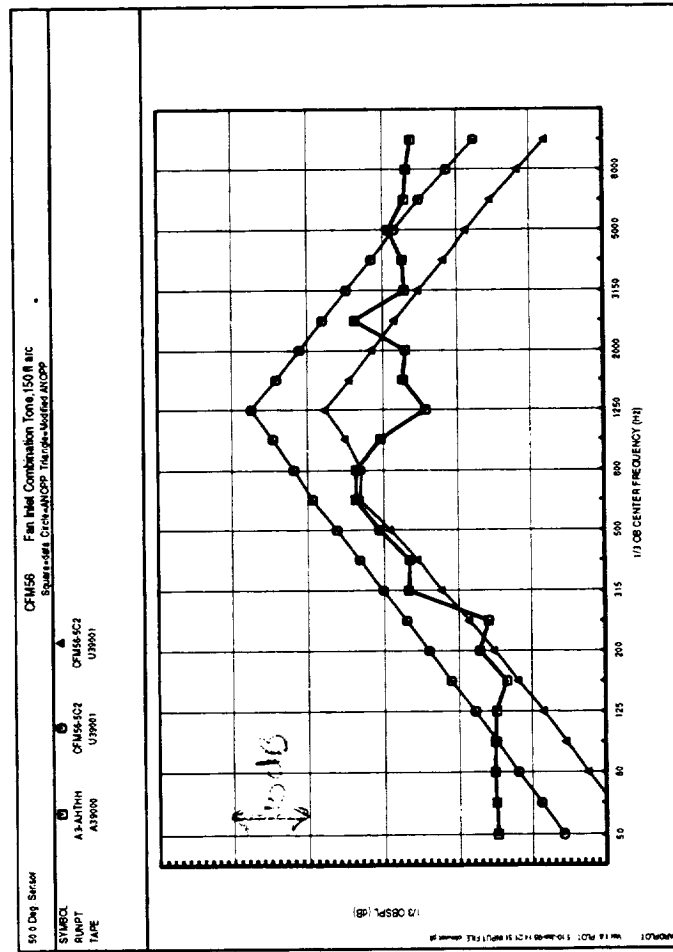
Key to Plots:

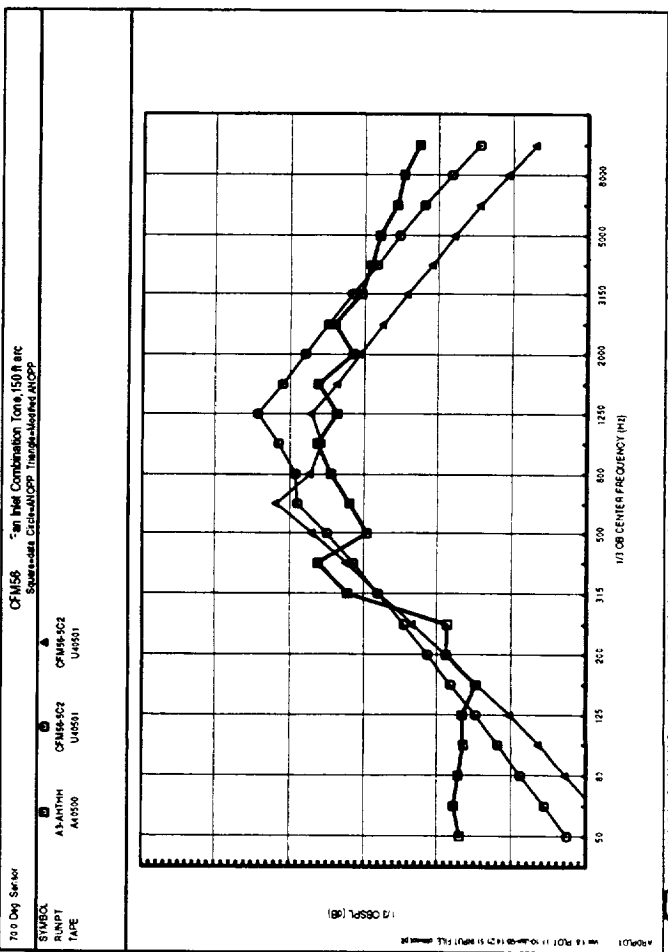
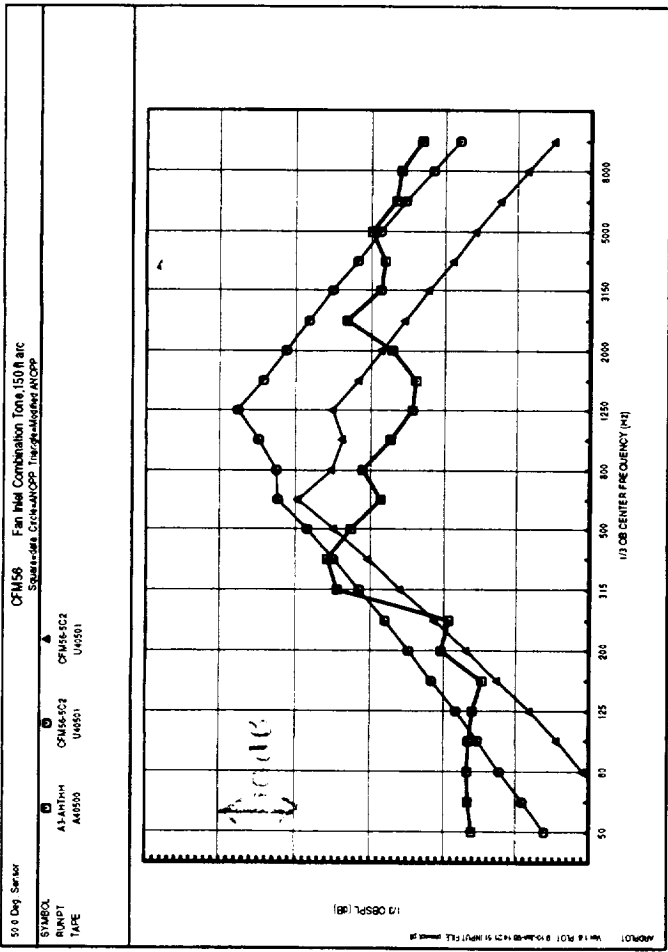
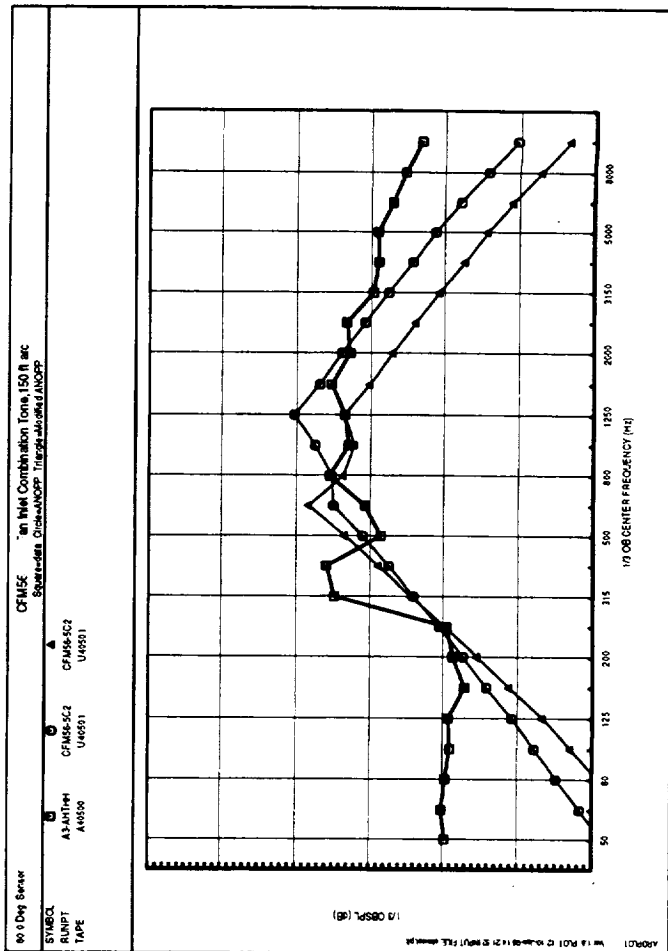
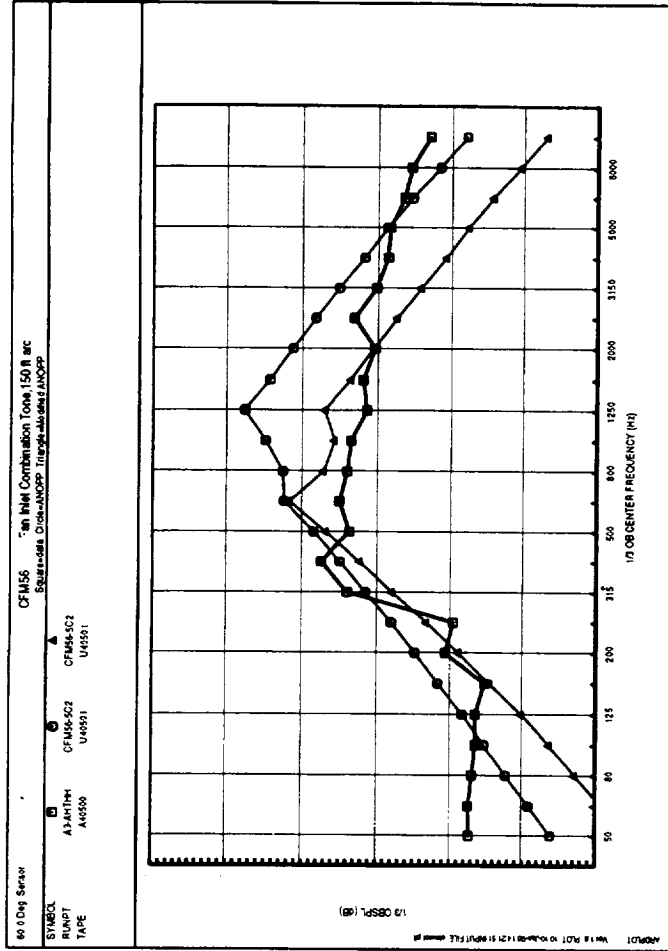
squares = total measured engine data
circles = Heidmann method
triangles = modified Heidmann method

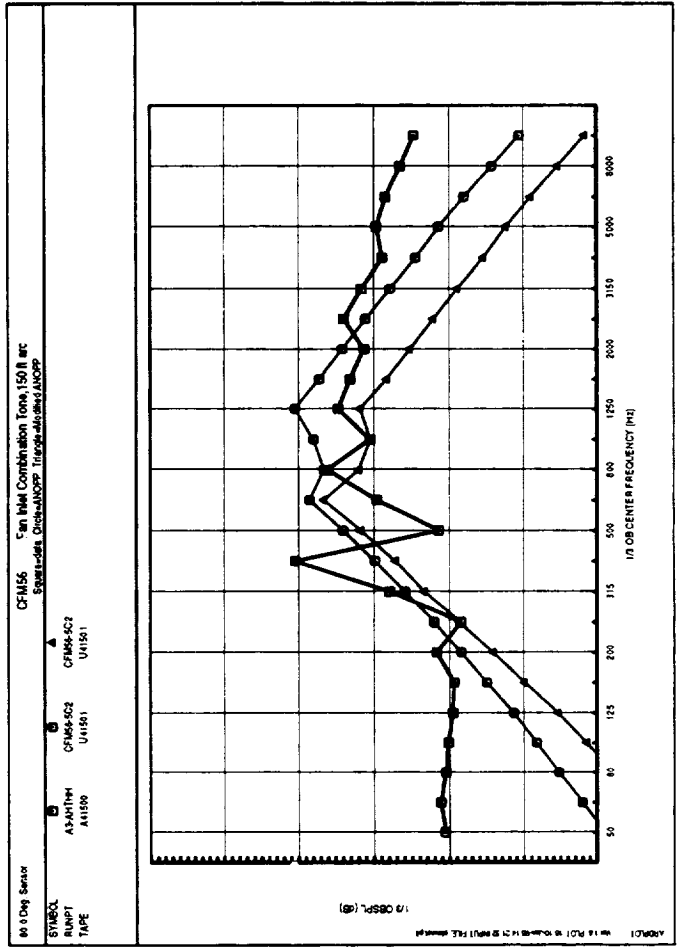
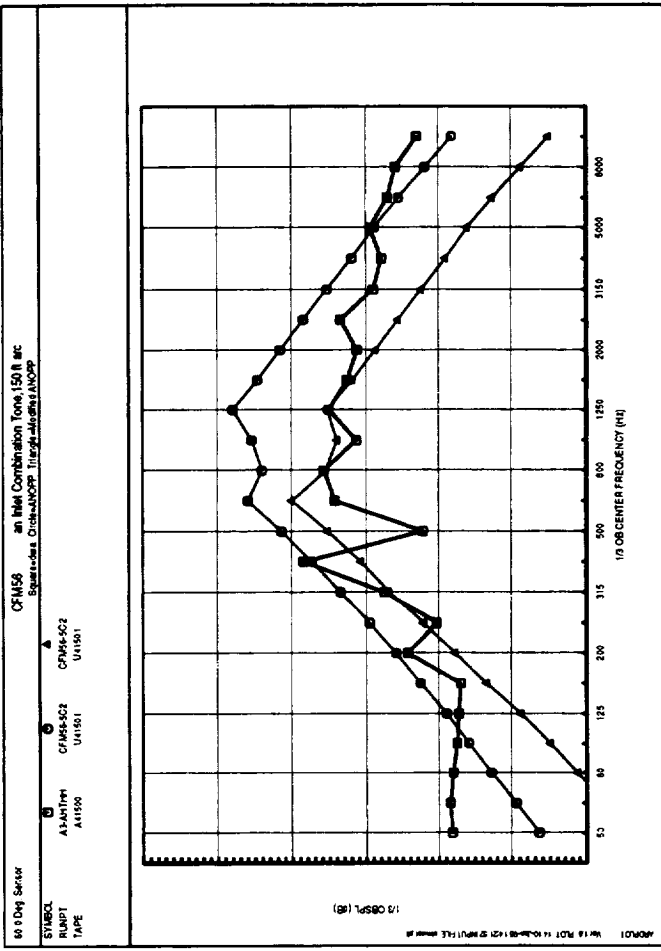
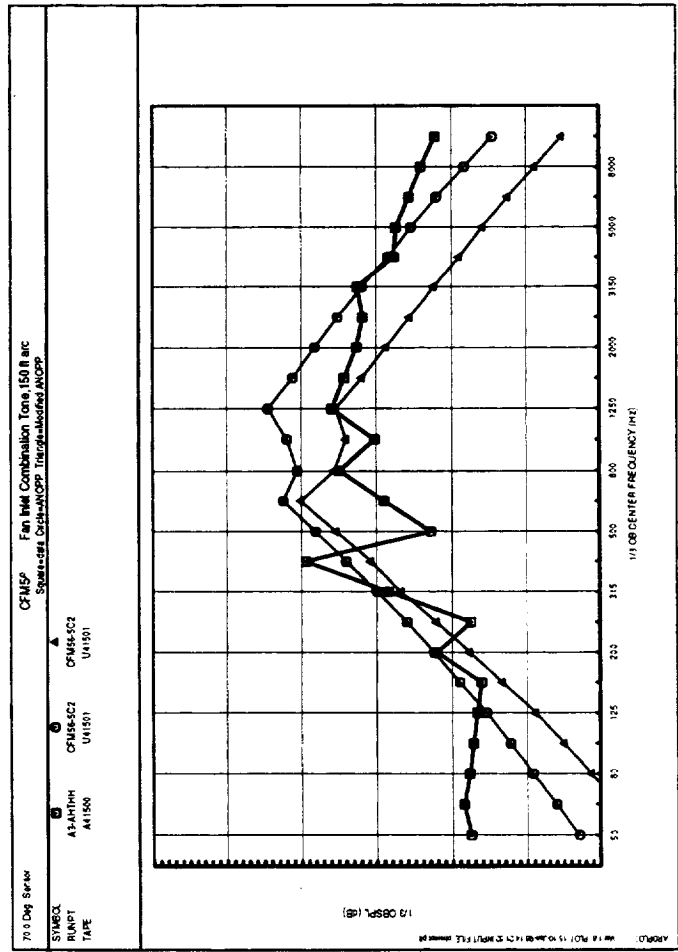
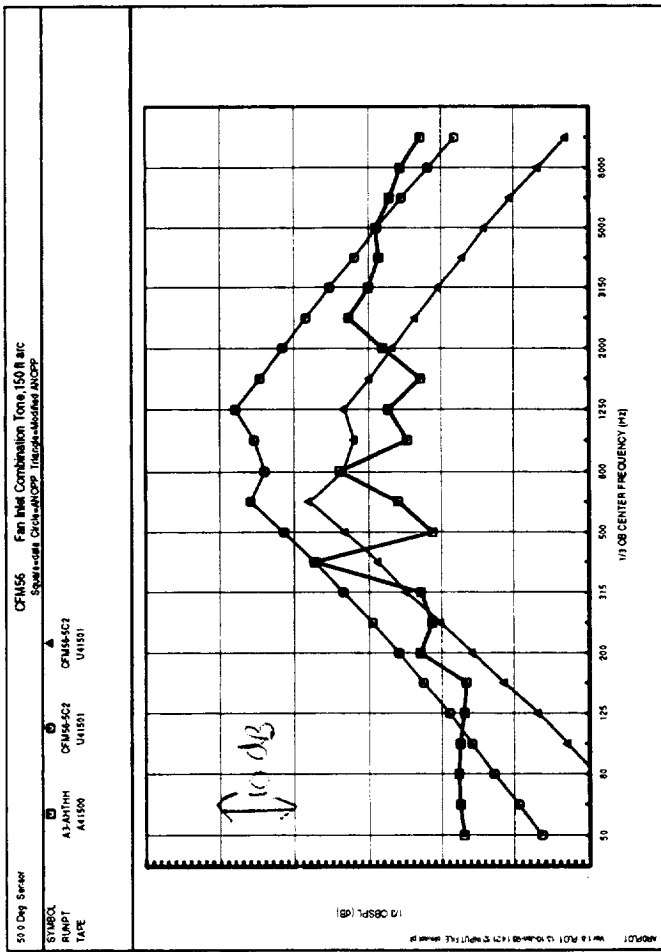


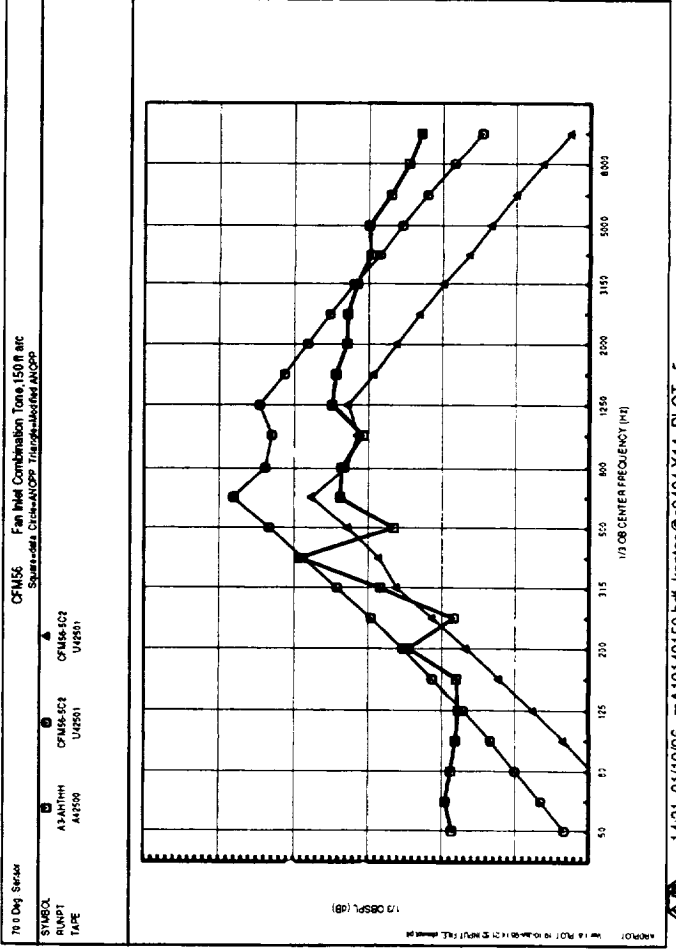
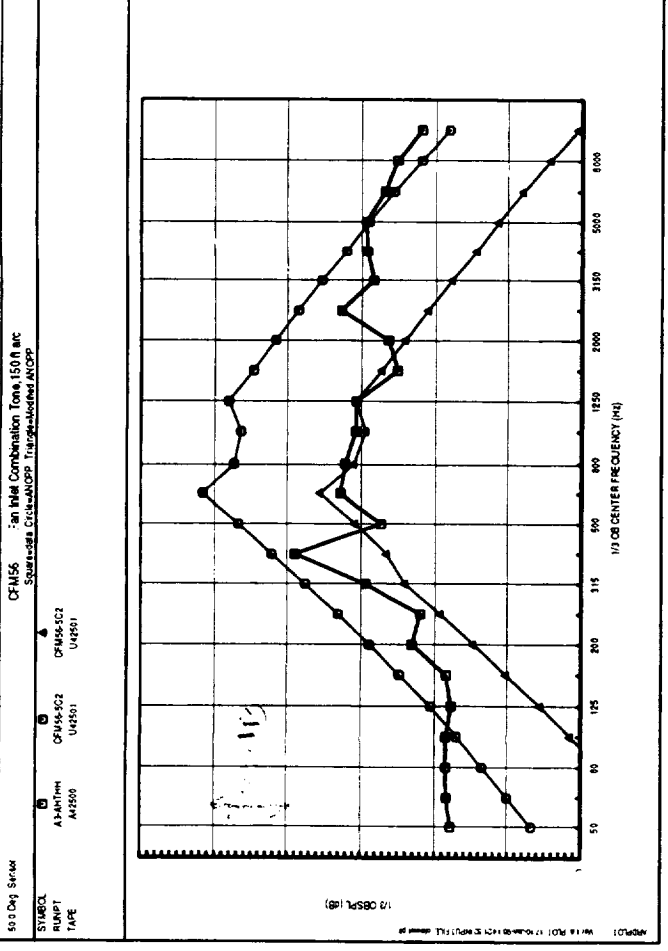
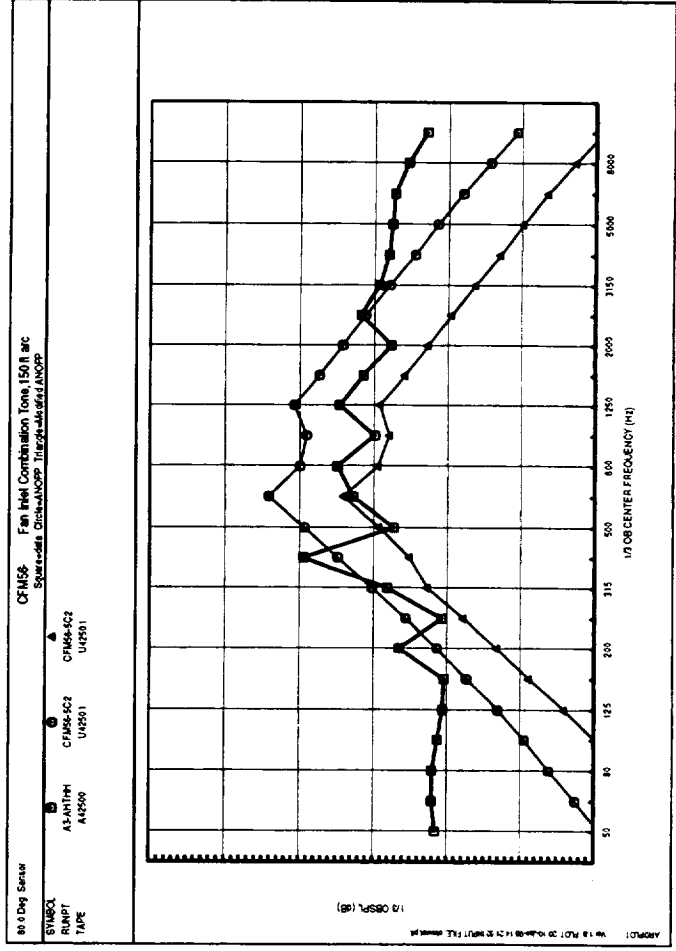
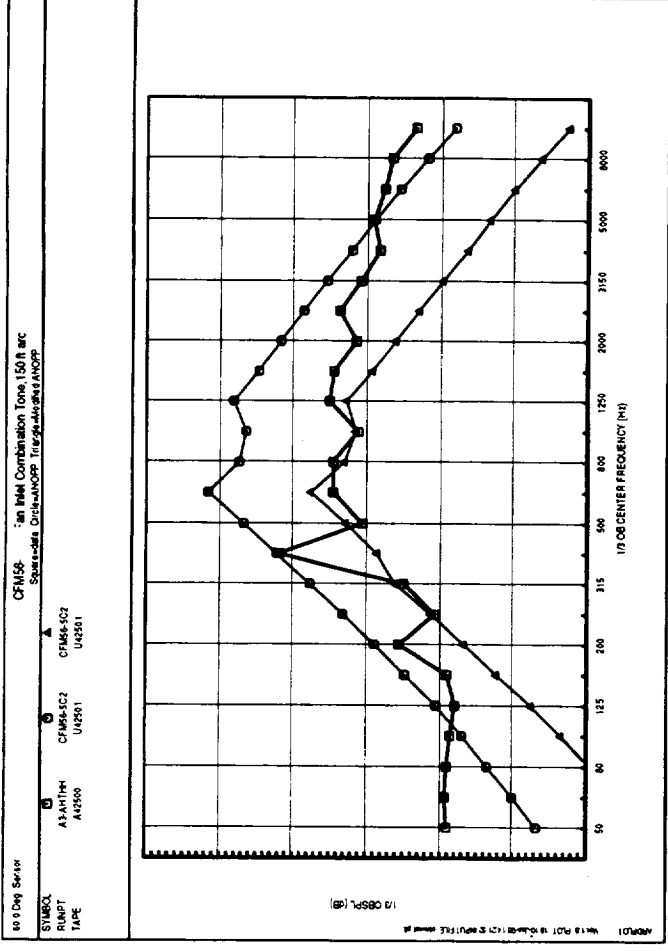
1421 01/10/96 ma10142150.pdf kordos@c0424 X11 PLOT 1
EGS LIB 5.1 12/14/95 (EGSREP.XPOST 5.1 12/14/95 on c0424)
(NO PROG. VER. SPECIFIED)

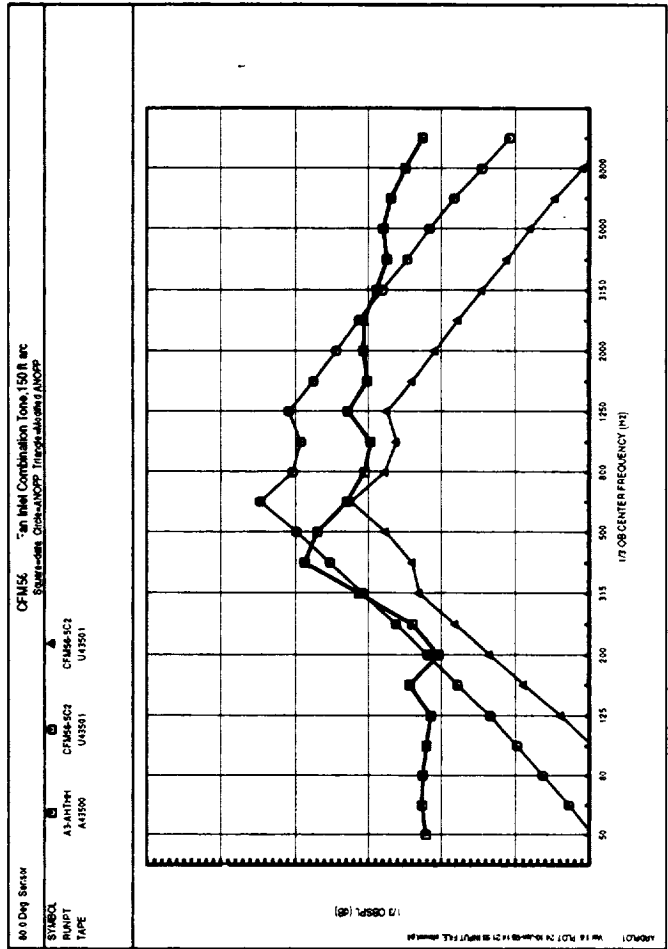
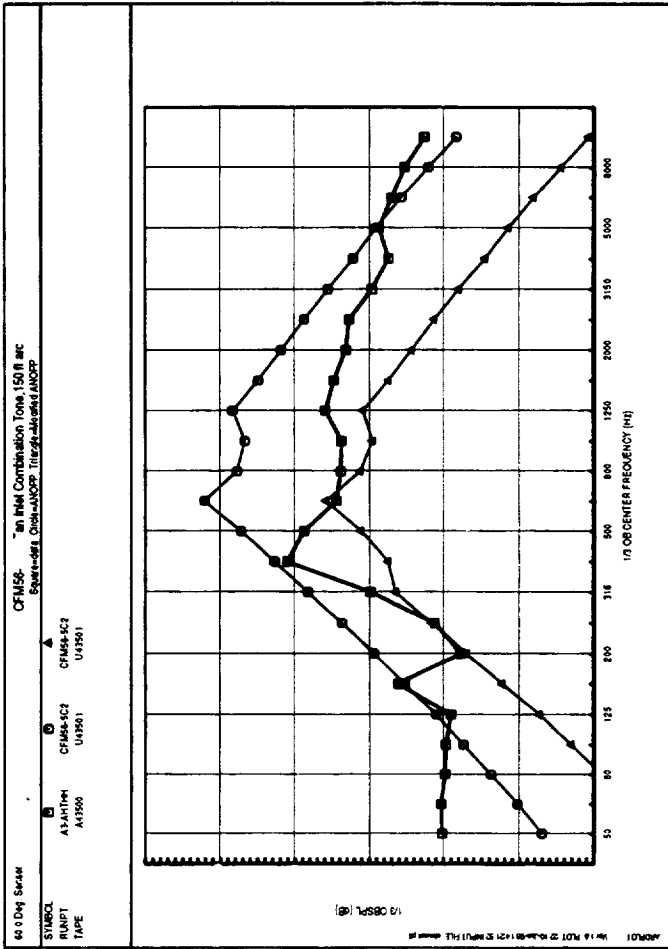
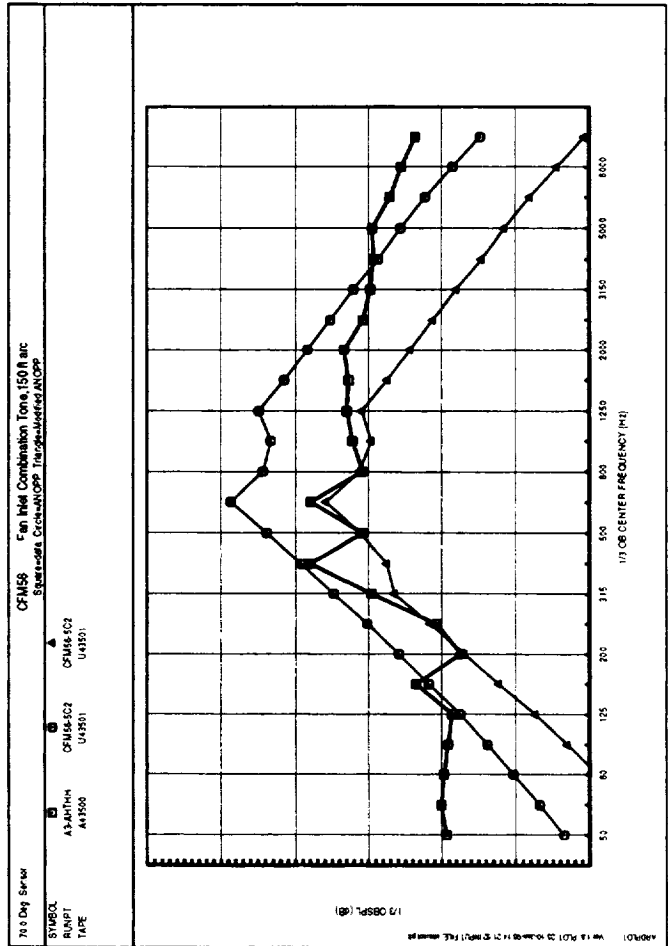
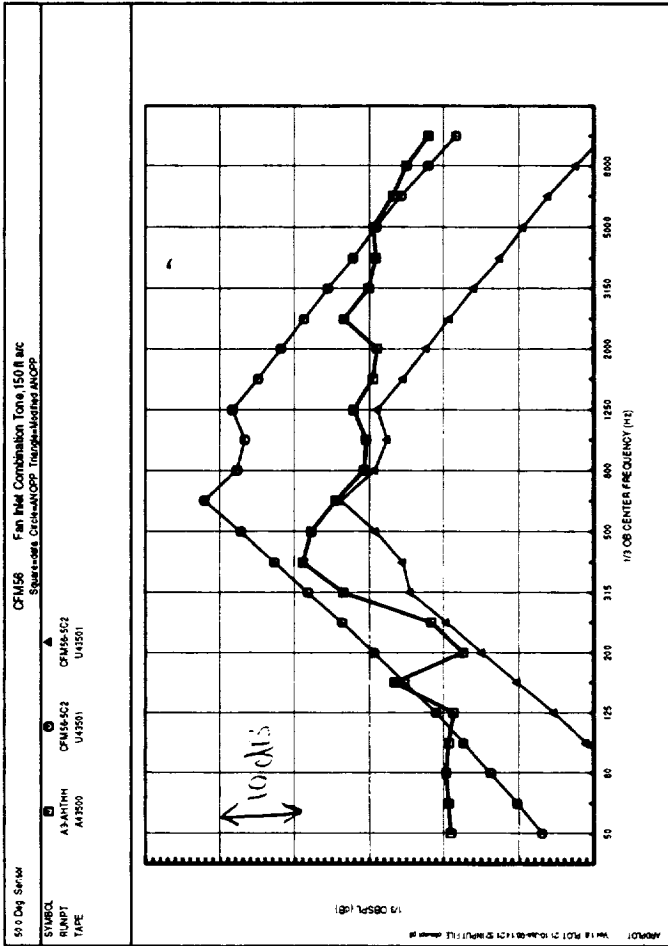










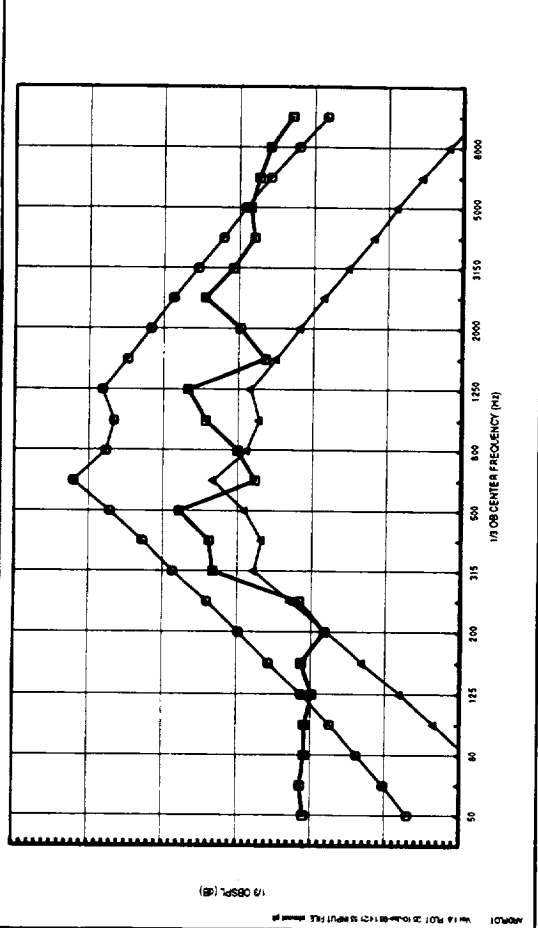


130

90 Deg Sensor

CFM56 Fan Inlet Combination Tone, 150 ft arc
 Square-Root Correction, Triangular Arc

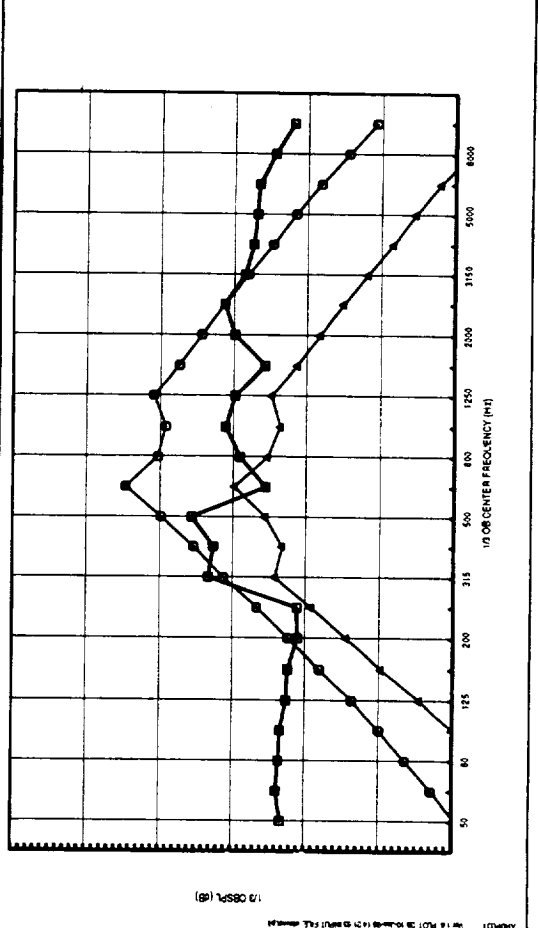
SYMBOL: ▲
 RUNPT: A3-ANTHM CFM56-5C2 U44501
 TAPE: A44500 U44501



90 Deg Sensor

CFM56 Fan Inlet Combination Tone, 150 ft arc
 Square-Root Correction, Triangular Arc

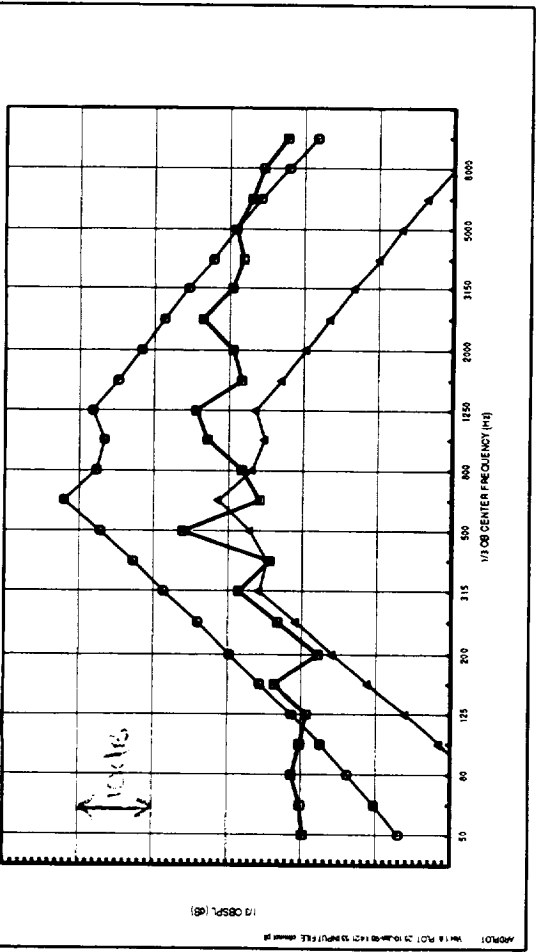
SYMBOL: ▲
 RUNPT: A3-ANTHM CFM56-5C2 U44501
 TAPE: A44500 U44501



90 Deg Sensor

CFM56 Fan Inlet Combination Tone, 150 ft arc
 Square-Root Correction, Triangular Arc

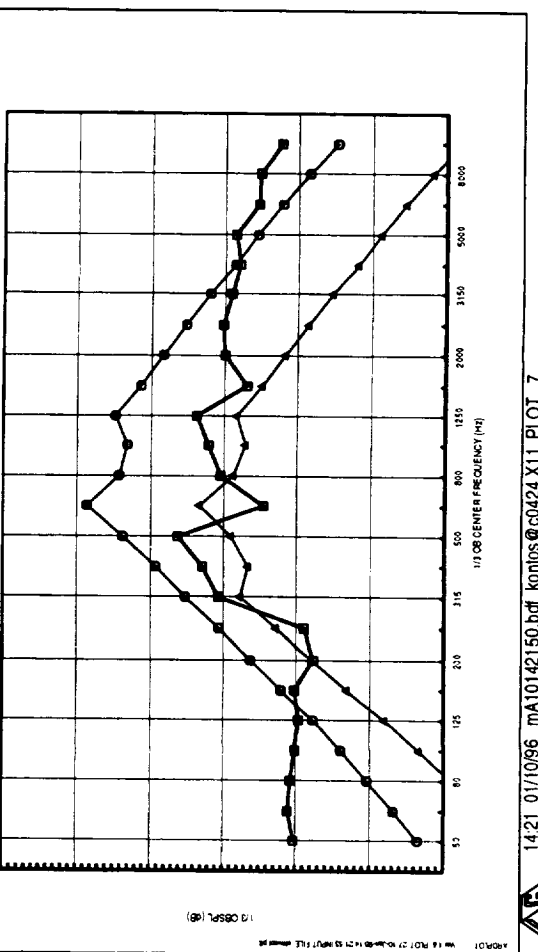
SYMBOL: ▲
 RUNPT: A3-ANTHM CFM56-5C2 U44501
 TAPE: A44500 U44501



90 Deg Sensor

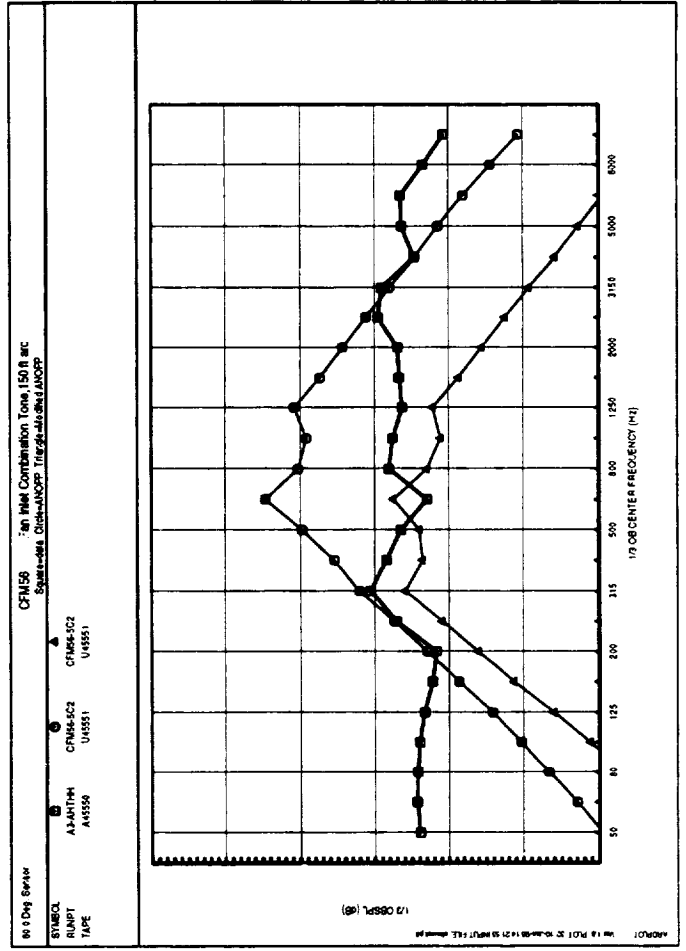
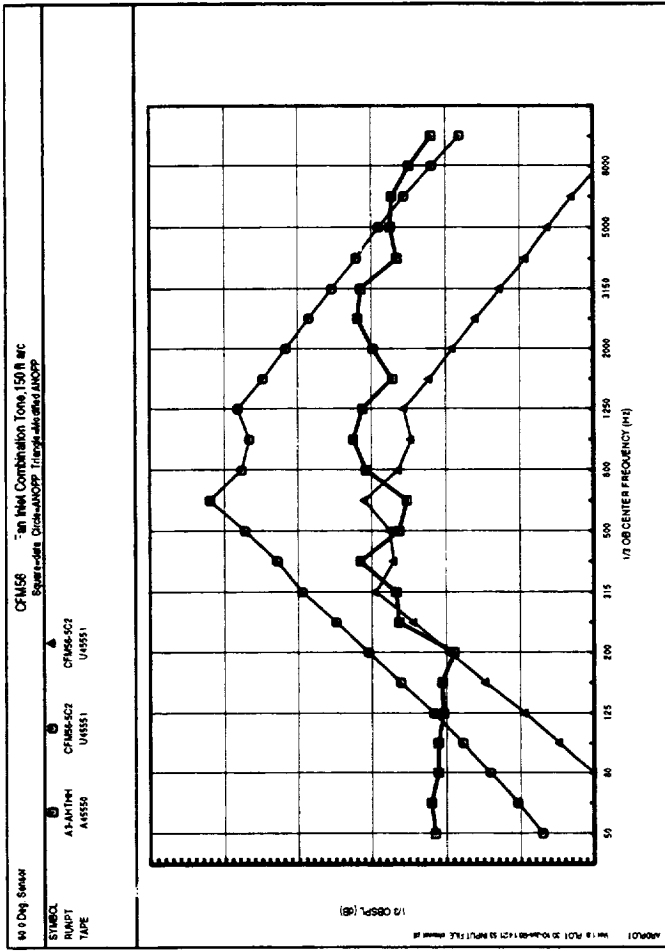
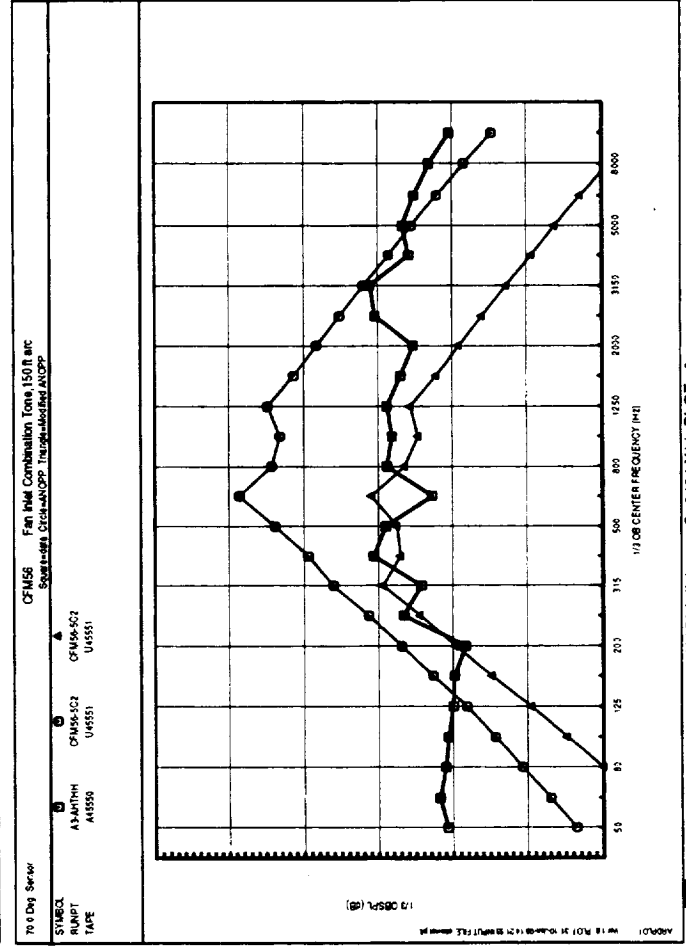
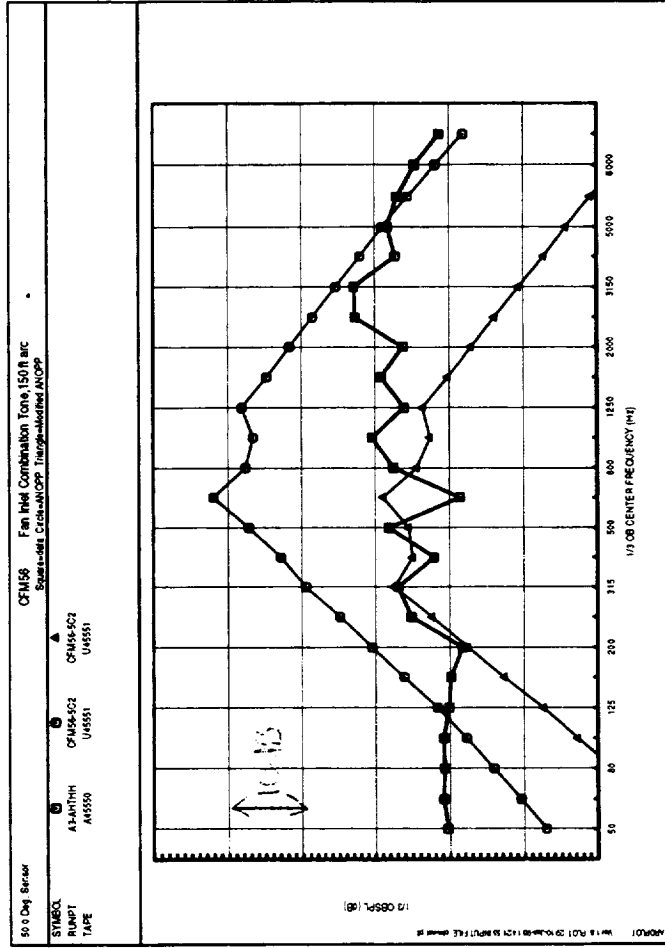
CFM56 Fan Inlet Combination Tone, 150 ft arc
 Square-Root Correction, Triangular Arc

SYMBOL: ▲
 RUNPT: A3-ANTHM CFM56-5C2 U44501
 TAPE: A44500 U44501



1421 01/10/96 MA10102150.pdf, Kontos @ 60424 X11 PLOT_7
 EGS LIB 3.1 12/14/95 JESSREP.XPOST 5.1 12/14/95 on 60424
 (NO PROG. VER. SPECIFIED)





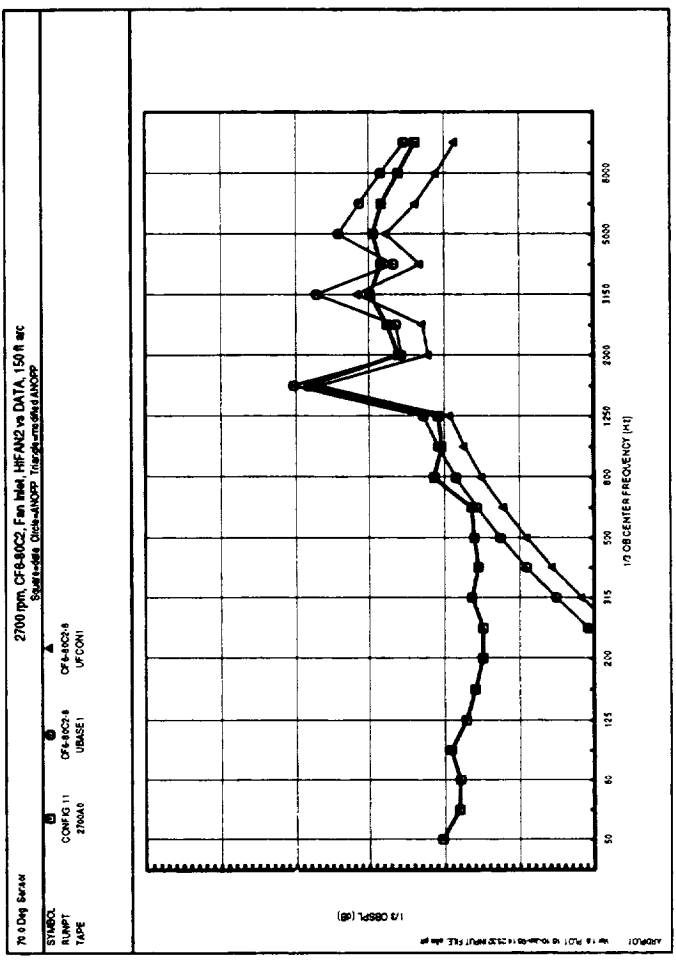
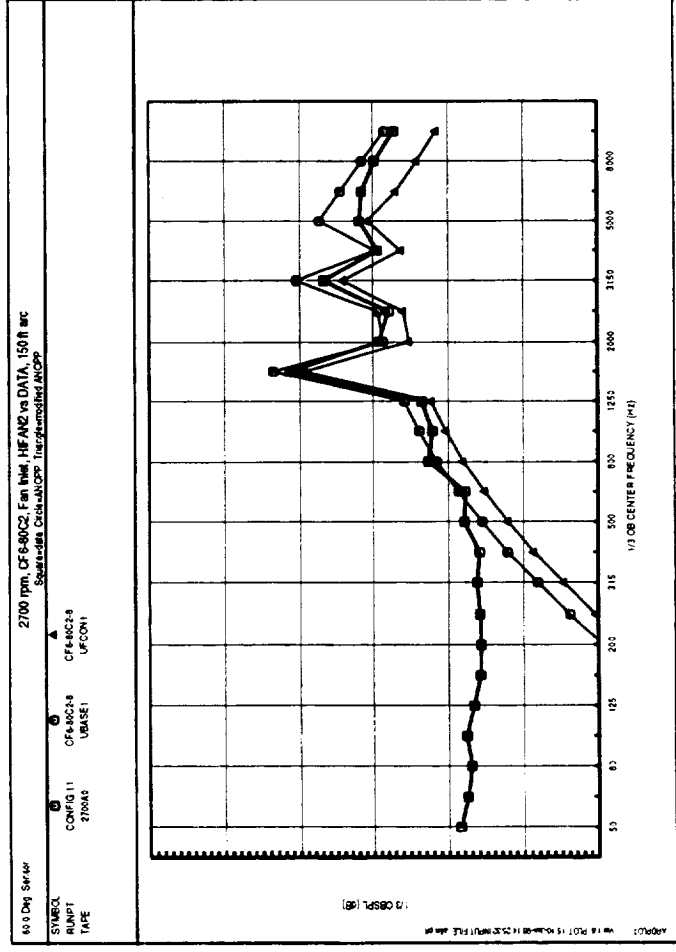
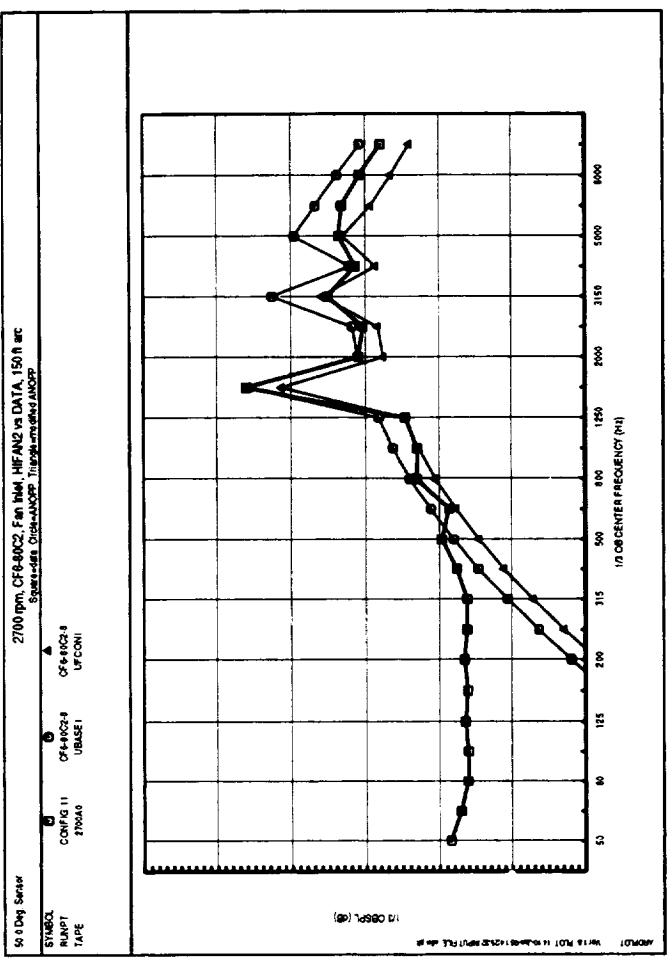
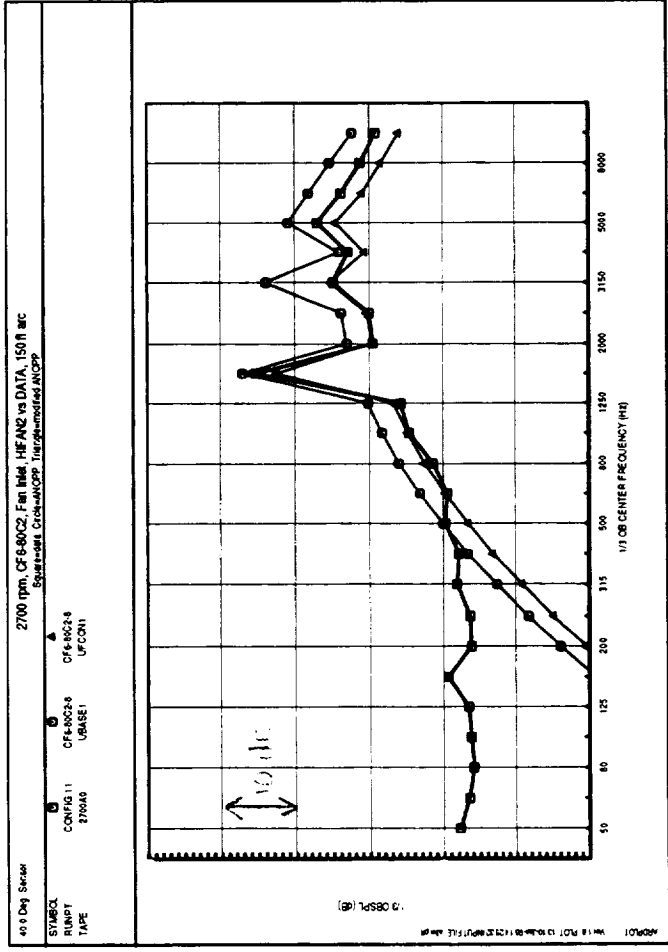
Appendix M
Combination Tone Noise Spectra - CF6-80C2

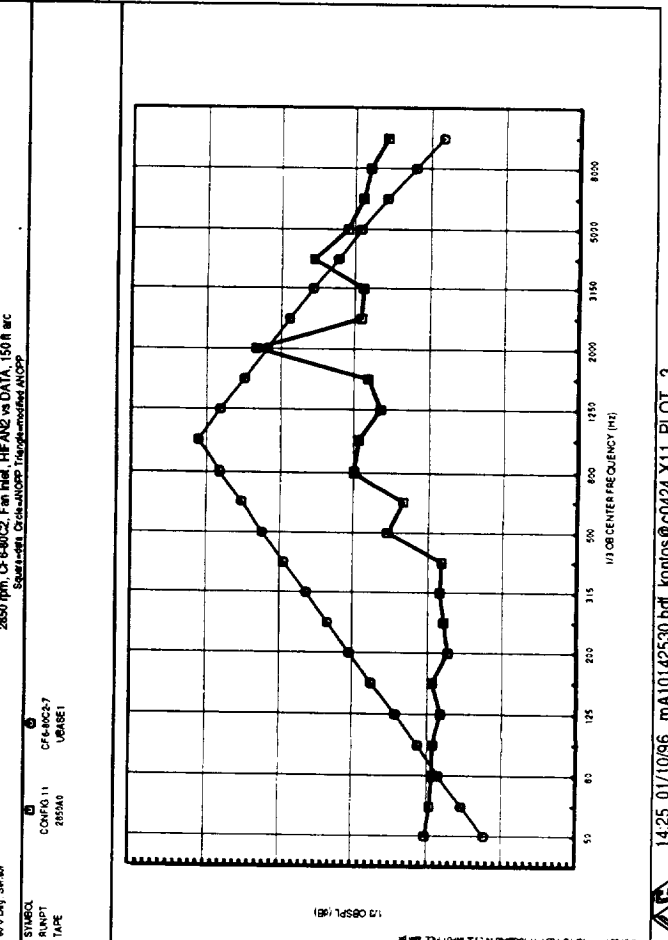
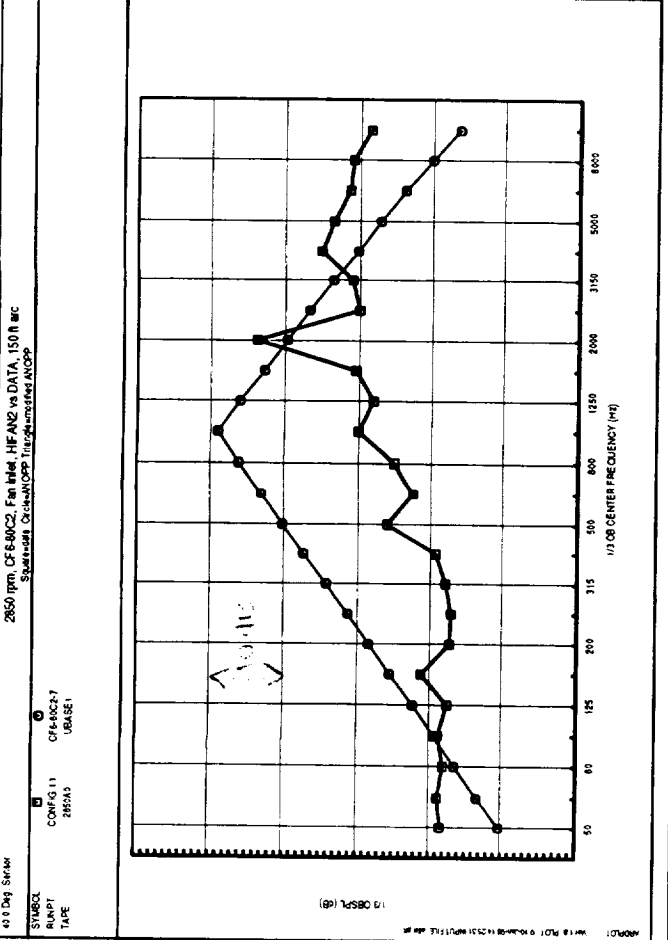
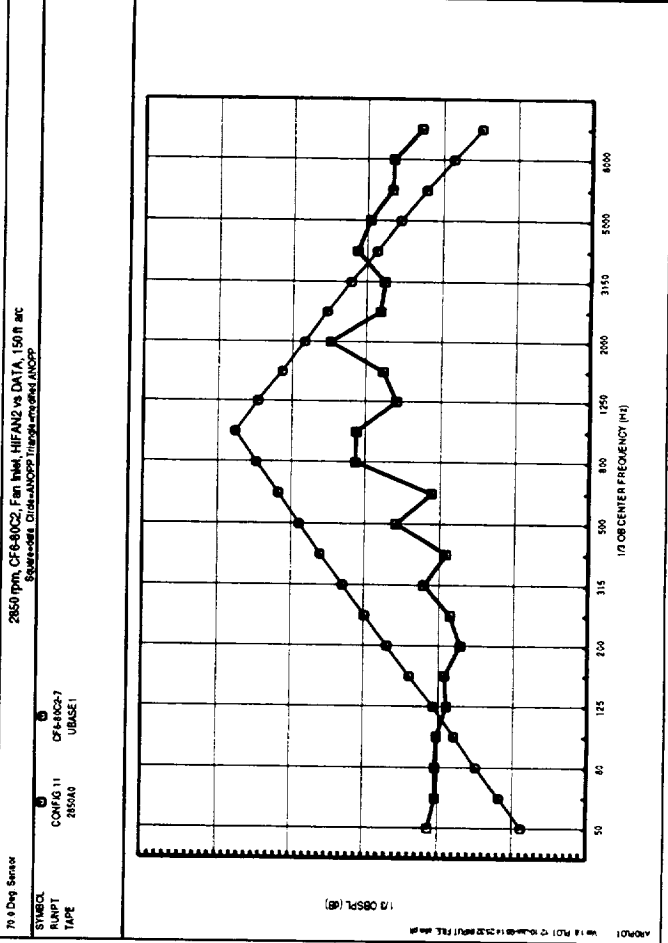
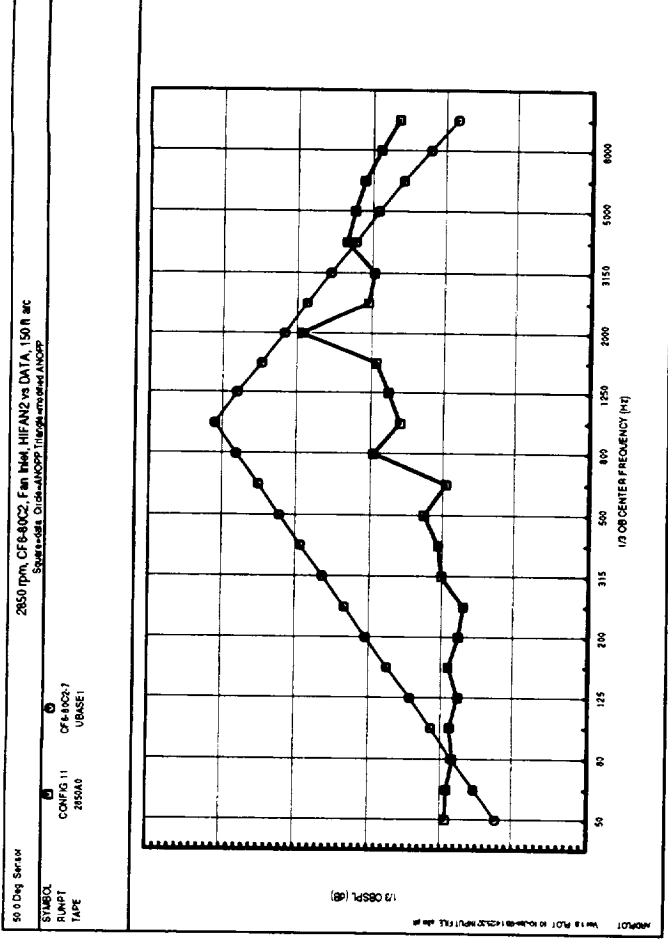
Appendix M Contents

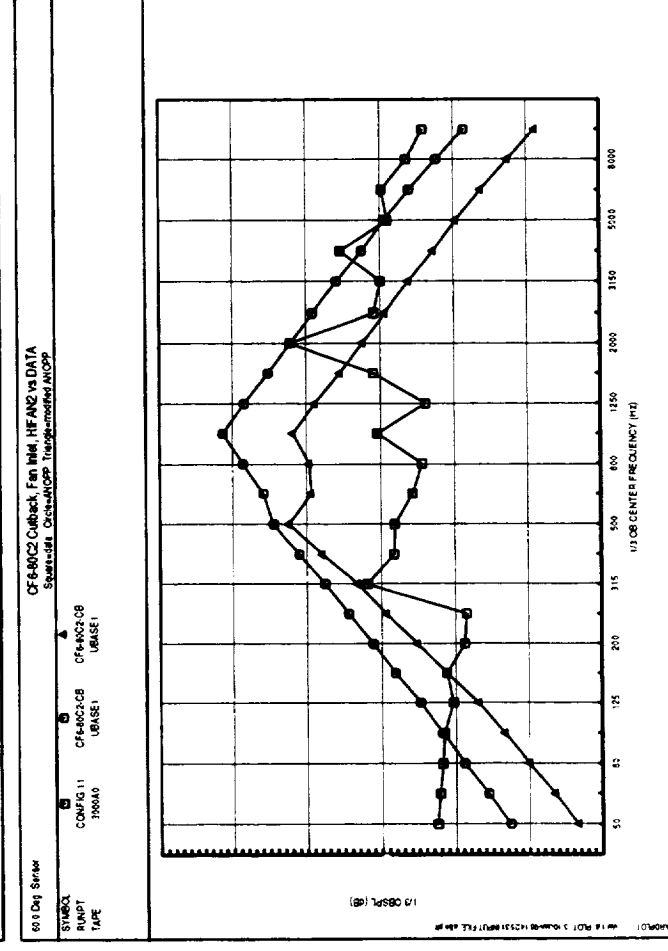
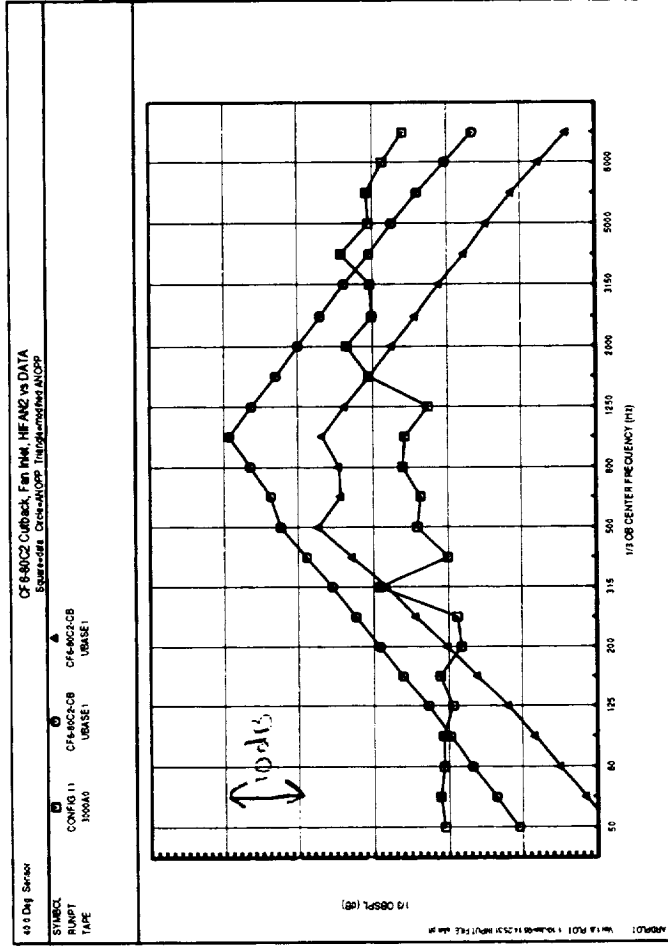
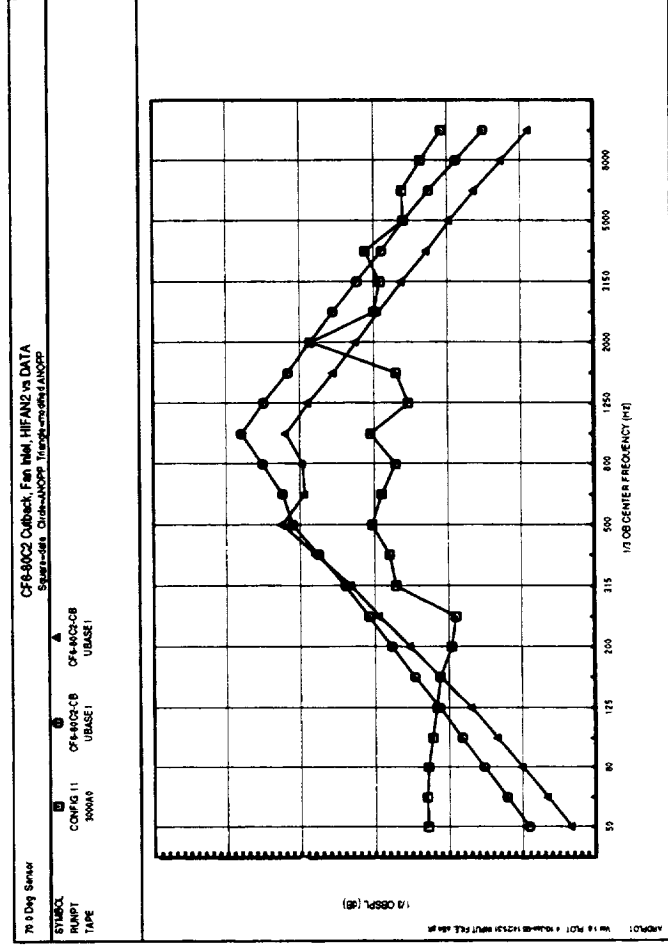
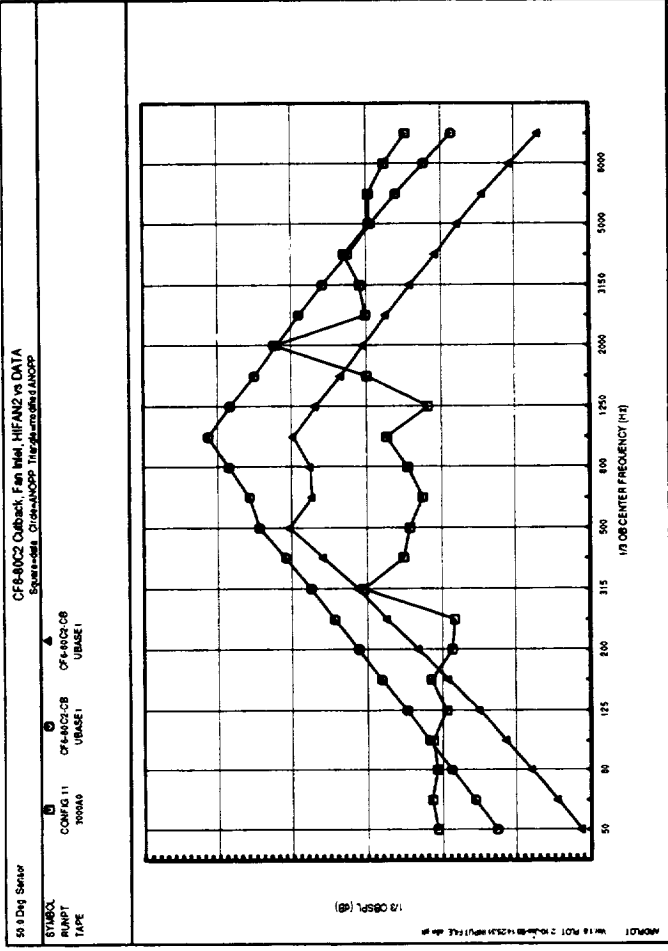
Page	Fan Speed, rpm	Angles
143	2700	40-70
144	2850	40-70
145	3000	40-70
146	3110	40-70

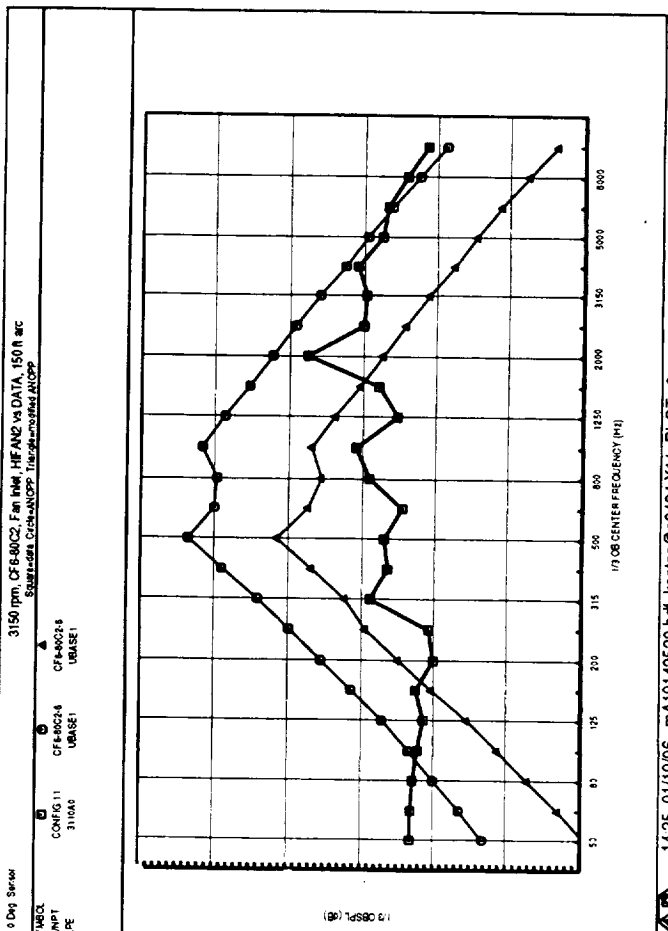
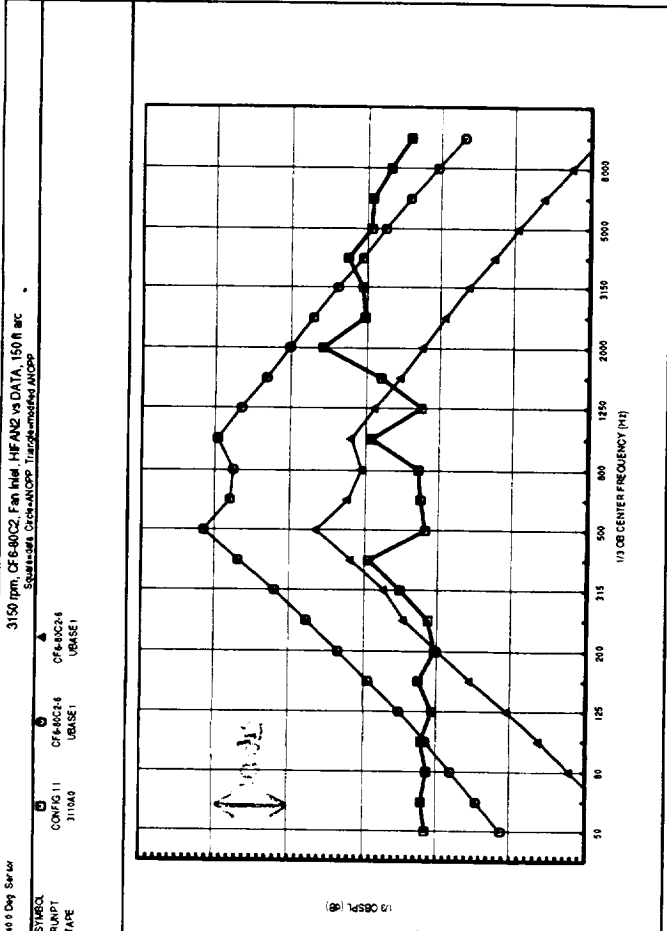
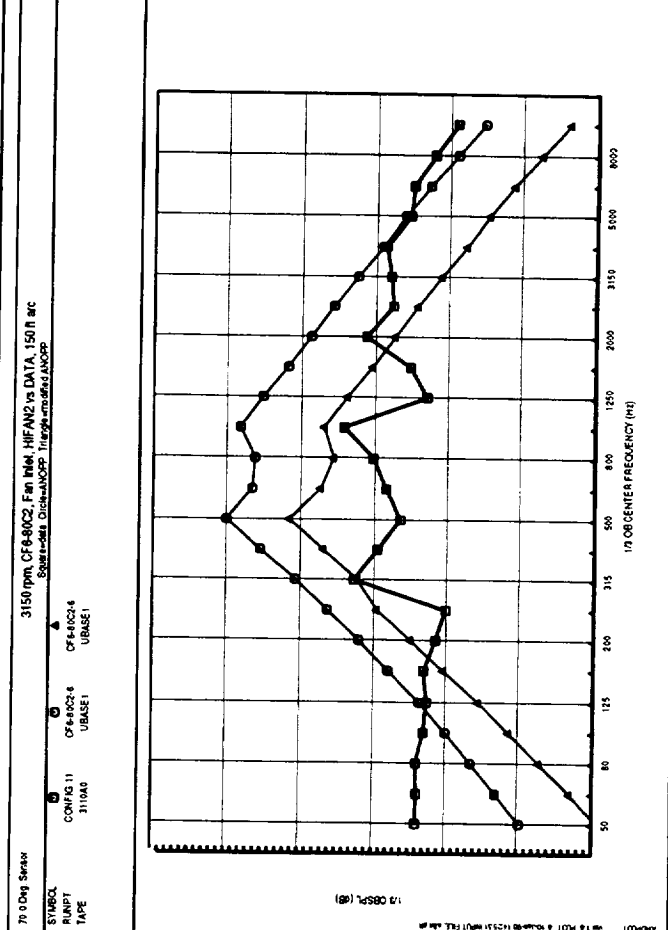
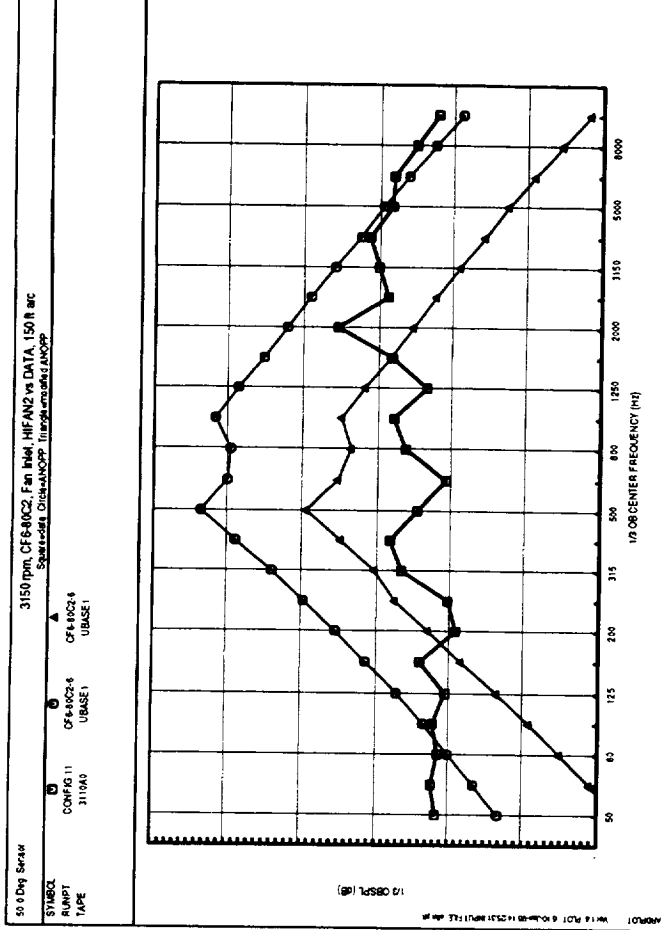
Key to Plots:

squares = total measured engine data
circles = Heidmann method
triangles = modified Heidmann method









14.95.01/10/96 MA10142520.pdf konios@c0424.X11 PLOT 2
 EGS JIB 5.1 12/14/95 LESS REP.XPOST 5.1 12/14/95 on c0424
 (NO PROG. VER. SPECIFIED)



6.0 References

Gillian, Ronnie: Aircraft Noise Prediction Program User's Manual, NASA TM 84486, 1982.

Heidmann, Marcus F., and Feiler, C. E.: Noise Comparisons From Full-Scale Fan Tests at NASA Lewis Research Center, AIAA 73-1017, October 1973.

Heidmann, Marcus F.: Interim Prediction Method for Fan and Compressor Source Noise, NASA TM X-71763, 1979.

Lavin, S. P., and Ho, P.: NASA Energy Efficient Engine Acoustic Technology Report, Contract NAS3-20643, GE Aircraft Engines, 1978.

Stimpert, Dale L.: Quiet Clean Short-Haul Experimental Engine (QCSEE) Under the Wing (UTW) Composite Nacelle Test Report, Vol. II -- Acoustic Performance, NASA CR-159472, 1979.

REPORT DOCUMENTATION PAGE

Form Approved
OMB No. 0704-0188

Public reporting burden for this collection of information is estimated to average 1 hour per response, including the time for reviewing instructions, searching existing data sources, gathering and maintaining the data needed, and completing and reviewing the collection of information. Send comments regarding this burden estimate or any other aspect of this collection of information, including suggestions for reducing this burden, to Washington Headquarters Services, Directorate for Information Operations and Reports, 1215 Jefferson Davis Highway, Suite 1204, Arlington, VA 22202-4302, and to the Office of Management and Budget, Paperwork Reduction Project (0704-0188), Washington, DC 20503.

1. AGENCY USE ONLY (Leave blank)	2. REPORT DATE August 1996	3. REPORT TYPE AND DATES COVERED Final Contractor Report	
4. TITLE AND SUBTITLE Improved NASA-ANOPP Noise Prediction Computer Code for Advanced Subsonic Propulsion Systems		5. FUNDING NUMBERS WU-538-08-11 C-NAS3-26617 Task Order 24	
6. AUTHOR(S) Karen Kontos, Bangalore Janardan, and Philip Gliebe		7. PERFORMING ORGANIZATION NAME(S) AND ADDRESS(ES) GE Aircraft Engines P.O. Box 156301 Cincinnati, Ohio 45215-6301	
8. PERFORMING ORGANIZATION REPORT NUMBER E-9710		9. SPONSORING/MONITORING AGENCY NAME(S) AND ADDRESS(ES) National Aeronautics and Space Administration Lewis Research Center Cleveland, Ohio 44135-3191	
10. SPONSORING/MONITORING AGENCY REPORT NUMBER NASA CR-195480		11. SUPPLEMENTARY NOTES Project Manager, Jeffrey J. Berton, Acropulsion Analysis Office, organization code 2430, (216) 977-7031.	
12a. DISTRIBUTION/AVAILABILITY STATEMENT Unclassified - Unlimited Subject Category 07 This publication is available from the NASA Center for Aerospace Information, (301) 621-0390.		12b. DISTRIBUTION CODE	
13. ABSTRACT (Maximum 200 words) Recent experience using ANOPP to predict turbofan engine flyover noise suggests that it over-predicts overall EPNL by a significant amount. An improvement in this prediction method is desired for system optimization and assessment studies of advanced UHB engines. An assessment of the ANOPP fan inlet, fan exhaust, jet, combustor, and turbine noise prediction methods is made using static engine component noise data from the CF6-80C2, E ³ , and QCSEE turbofan engines. It is shown that the ANOPP prediction results are generally higher than the measured GE data, and that the inlet noise prediction method (Heidmann method) is the most significant source of this overprediction. Fan noise spectral comparisons show that improvements to the fan tone, broadband, and combination tone noise models are required to yield results that more closely simulate the GE data. Suggested changes that yield improved fan noise predictions but preserve the Heidmann model structure are identified and described. These changes are based on the sets of engine data mentioned, as well as some CFM56 engine data that was used to expand the combination tone noise database. It should be noted that the recommended changes are based on an analysis of engines that are limited to single stage fans with design tip relative mach numbers greater than one.			
14. SUBJECT TERMS ANOPP, Heidmann Method, Engine Noise Prediction		15. NUMBER OF PAGES 147	
17. SECURITY CLASSIFICATION OF REPORT Unclassified		16. PRICE CODE A08	
18. SECURITY CLASSIFICATION OF THIS PAGE Unclassified	19. SECURITY CLASSIFICATION OF ABSTRACT Unclassified	20. LIMITATION OF ABSTRACT	